Evidence for Higgs boson decay to muons

Result submitted to JHEP and available in ***arXiv.2009.04363***

Raffaele Gerosa

University of California San Diego (UCSD)

On behalf of the CMS Collaboration

HEP seminar at Imperial College, Department of Physics

Higgs boson measurements began in 2012

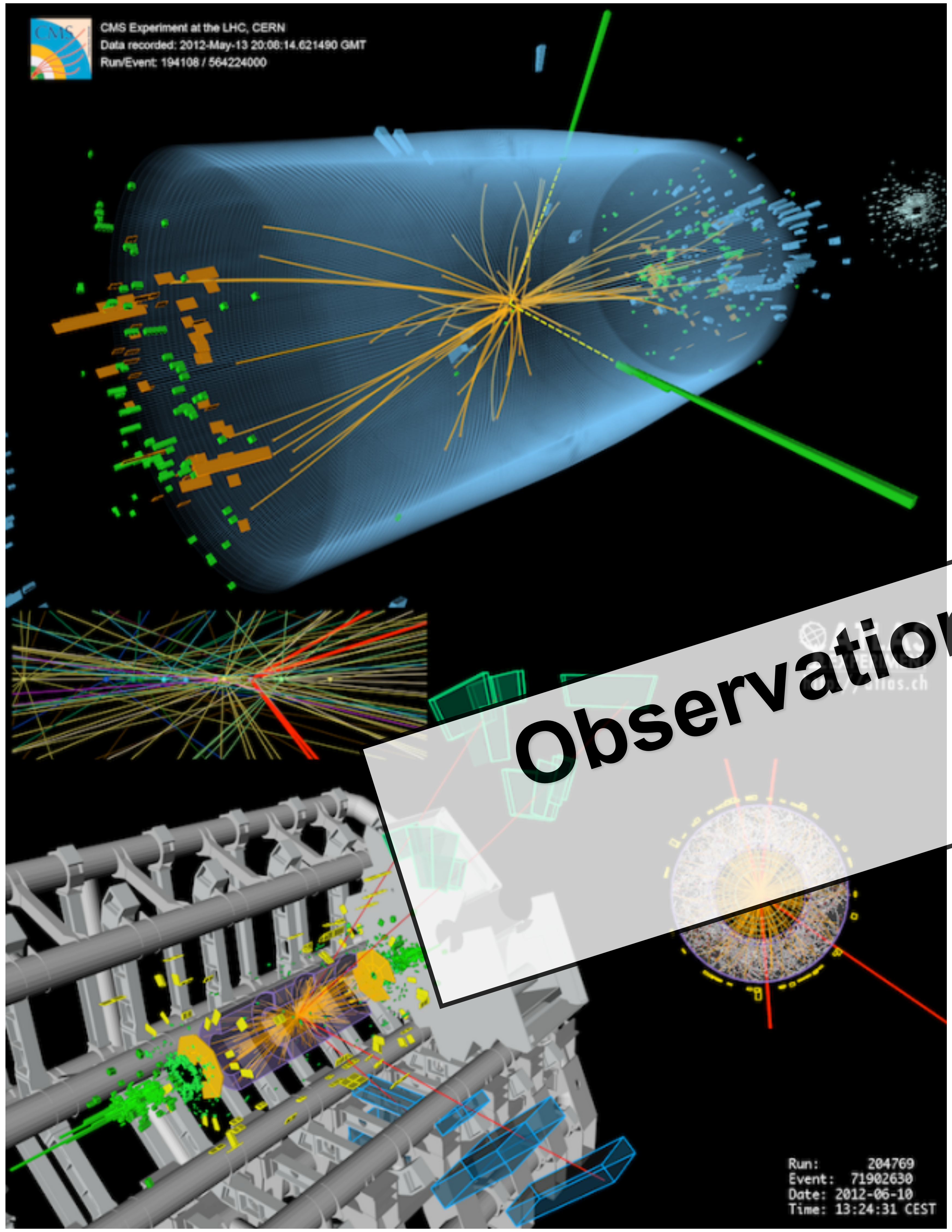

Observation of a new boson near 125 GeV

[Phys. Lett. B 716 (2012) 1]

[Phys. Lett. B 716 (2012) 30]

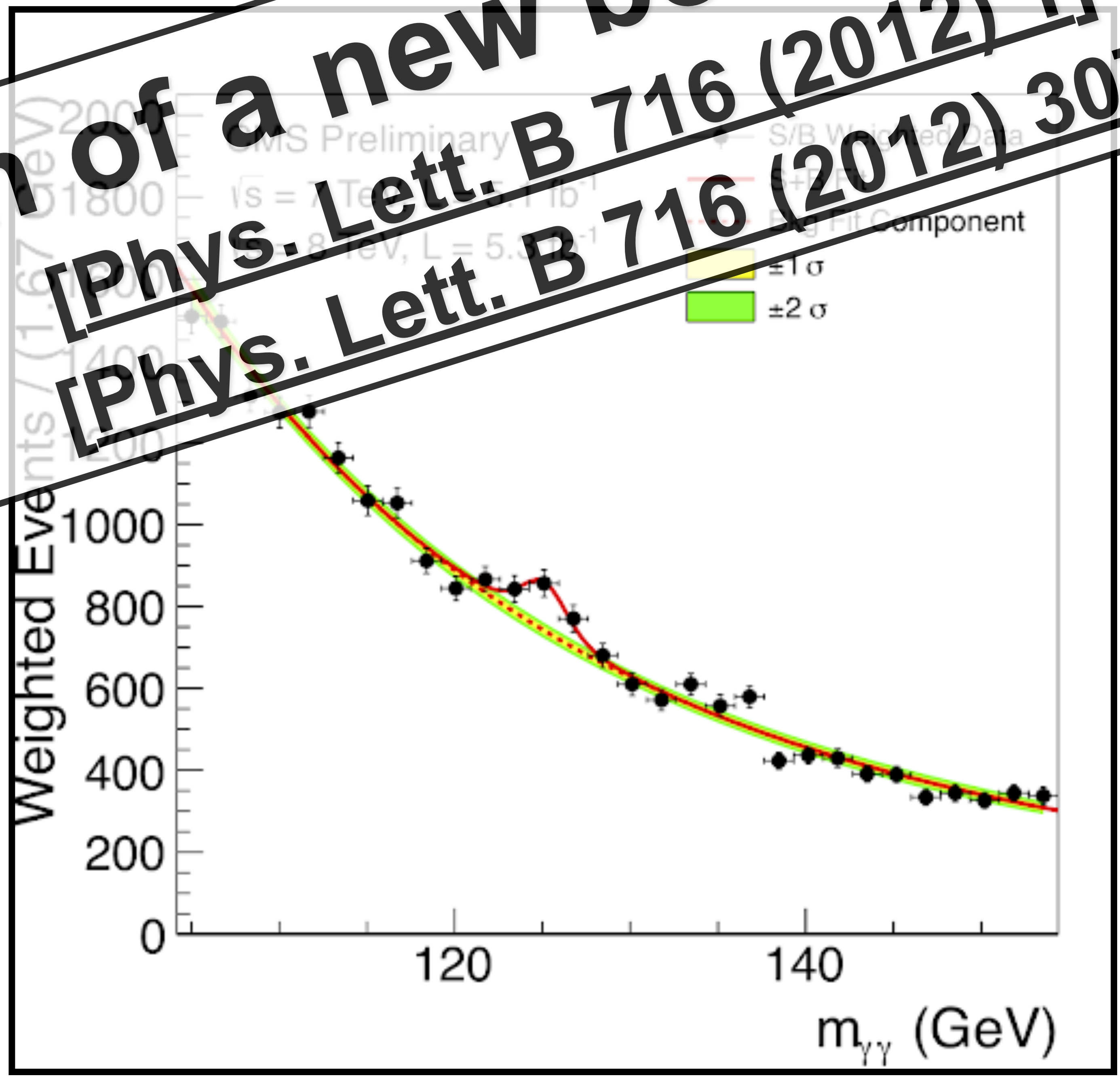

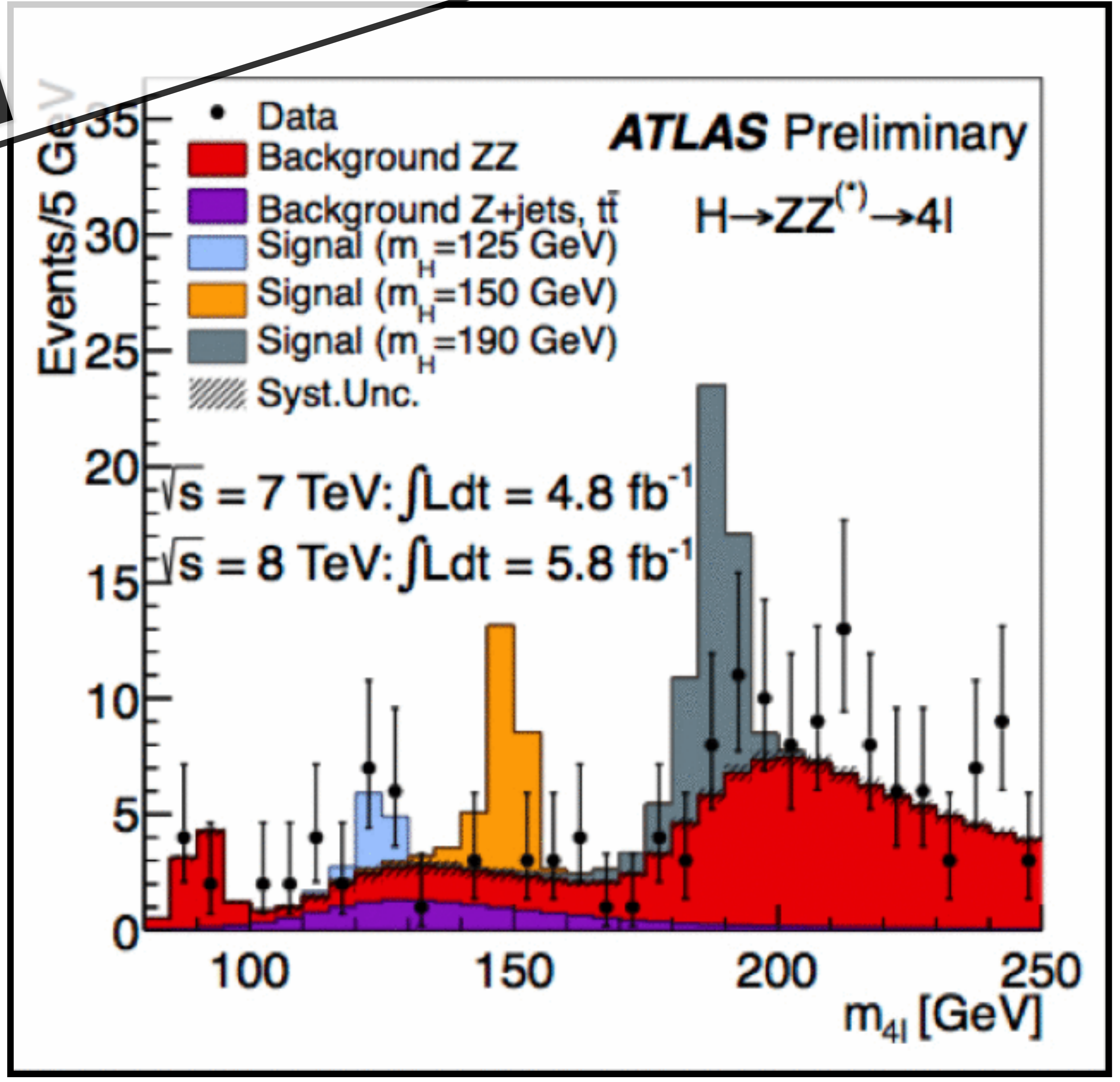

Higgs boson physics in 2020 with CMS

*Since the Higgs discovery, CMS performed **measurements** of its properties and interactions with SM particles*

Higgs boson properties

- Mass (m_H), spin-parity J^{CP}, constraints on width (Γ_H)
- Most precise measurement of m_H = 125.38 ± 0.14 GeV

- ***Higgs interactions*** with ***bosons*** (W, Z) and ***3rd generation of fermions*** (t, b, and τ)
- Found to be consistent with SM expectation

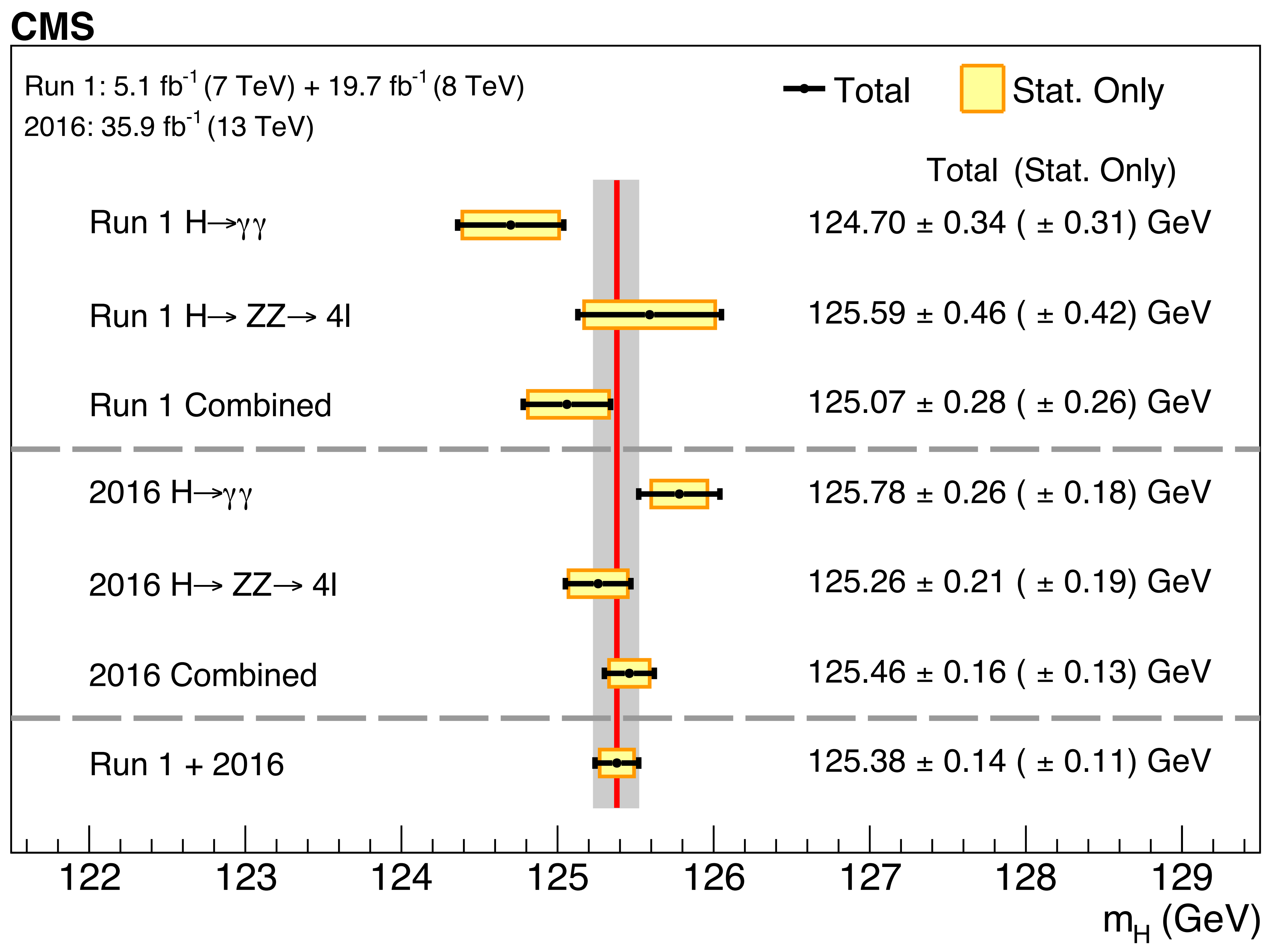

Phys. Lett. B 805 135425

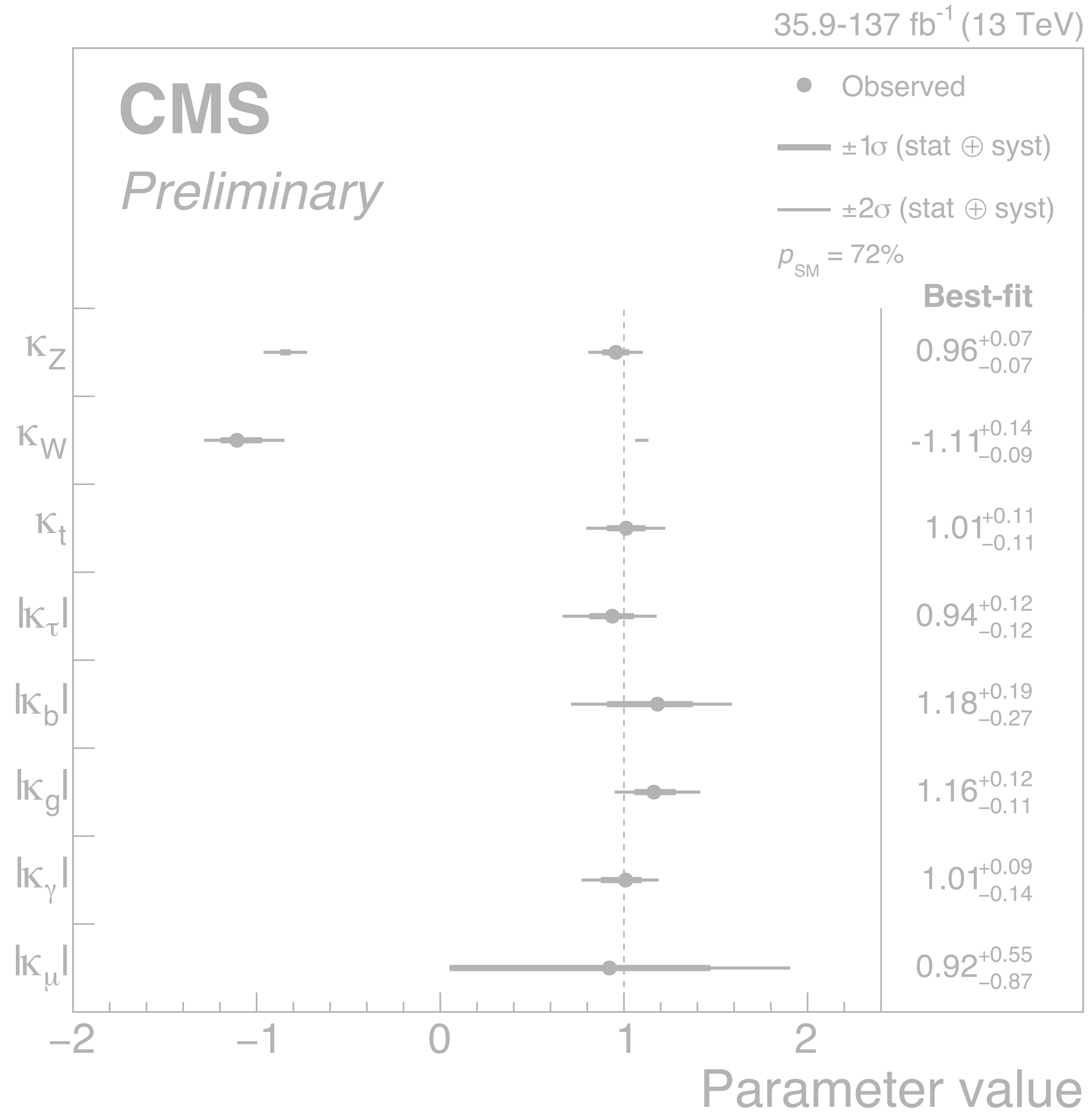

CMS-PAS-HIG-19-005

Higgs boson physics in 2020 with CMS

*Since the Higgs discovery, CMS performed **measurements** of its properties and interactions with SM particles*

Higgs boson properties

- Mass (m_H), spin-parity J^{CP}, constraints on width (Γ_H)
- Most precise measurement of m_H = 125.38 ± 0.14 GeV

- ***Higgs interactions*** with ***bosons*** (W, Z) and ***3rd generation of fermions*** (t, b, and τ)
- Found to be consistent with SM expectation

Phys. Lett. B 805 135425

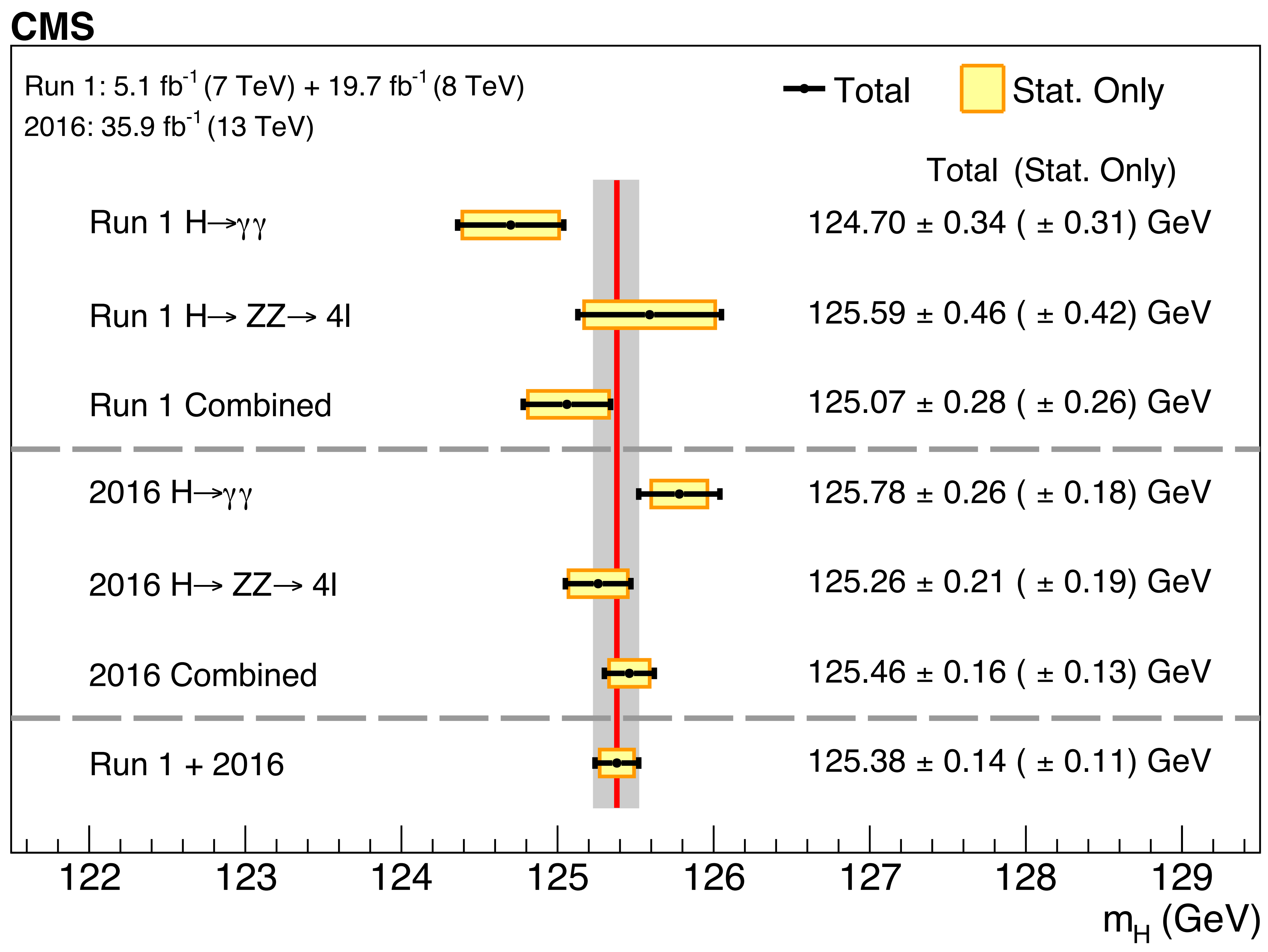

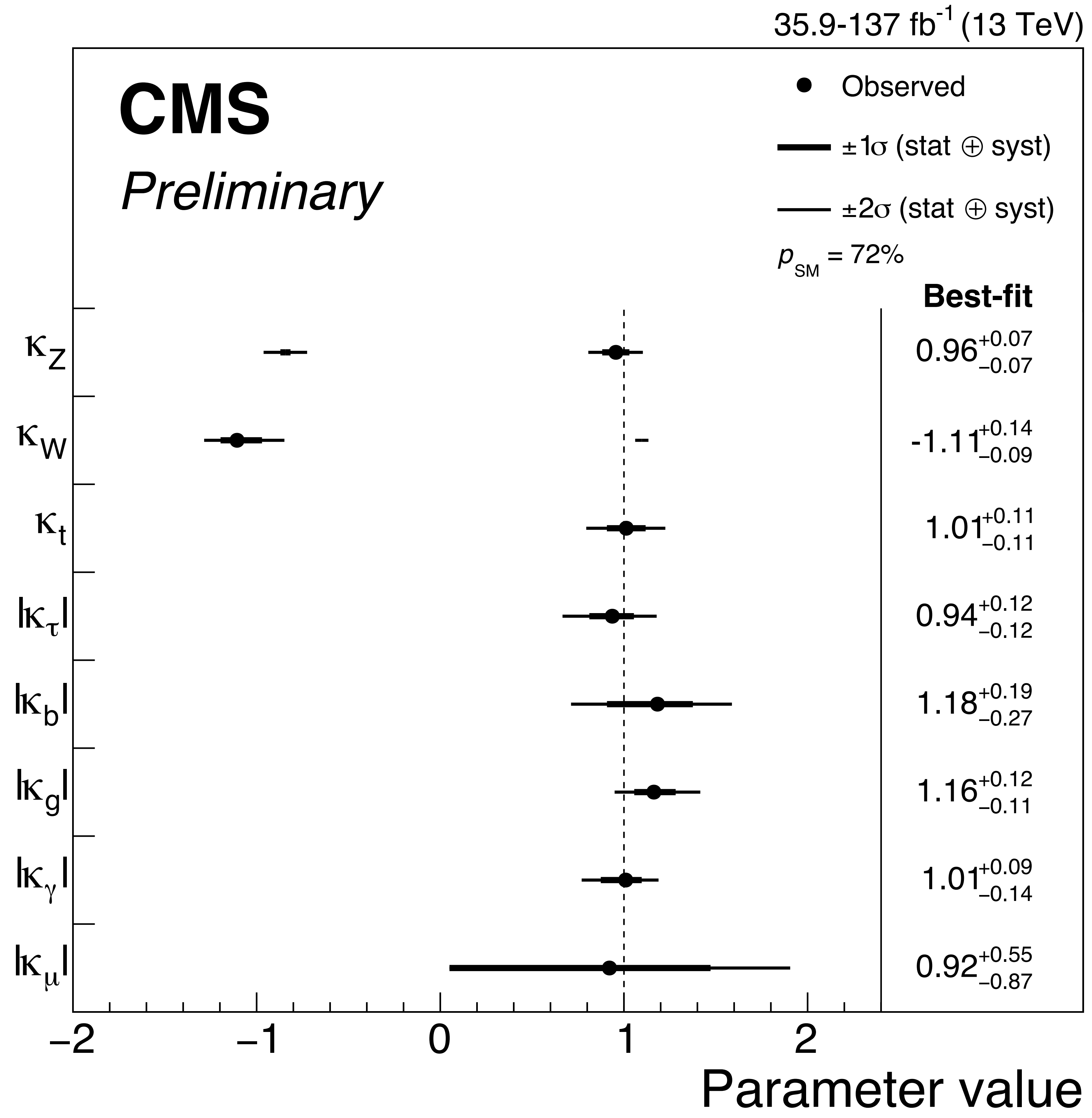

CMS-PAS-HIG-19-005

Next frontier → second fermion generation

- Probe the ***Yukawa interactions*** between the Higgs boson and ***2nd generation fermions***

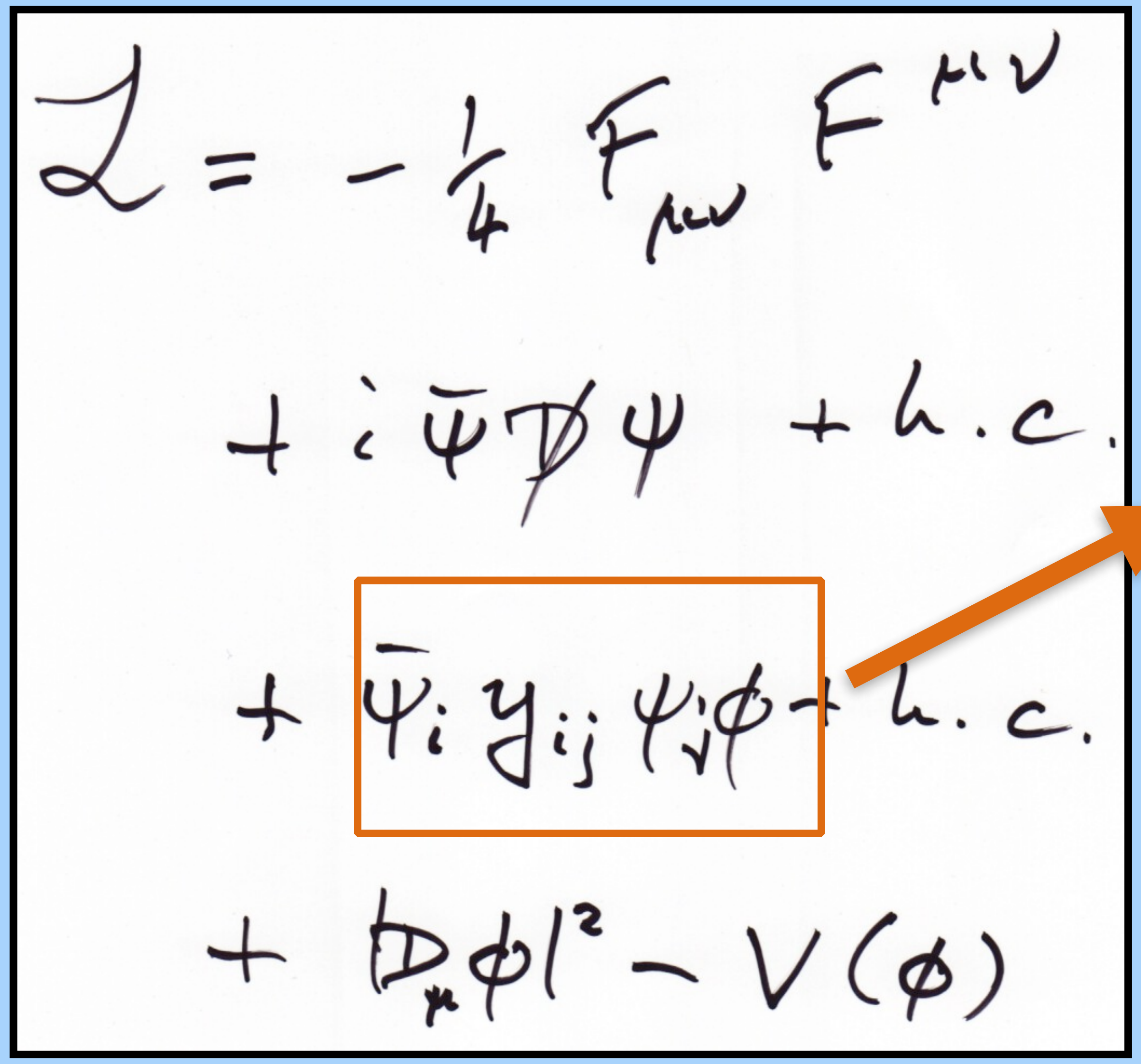

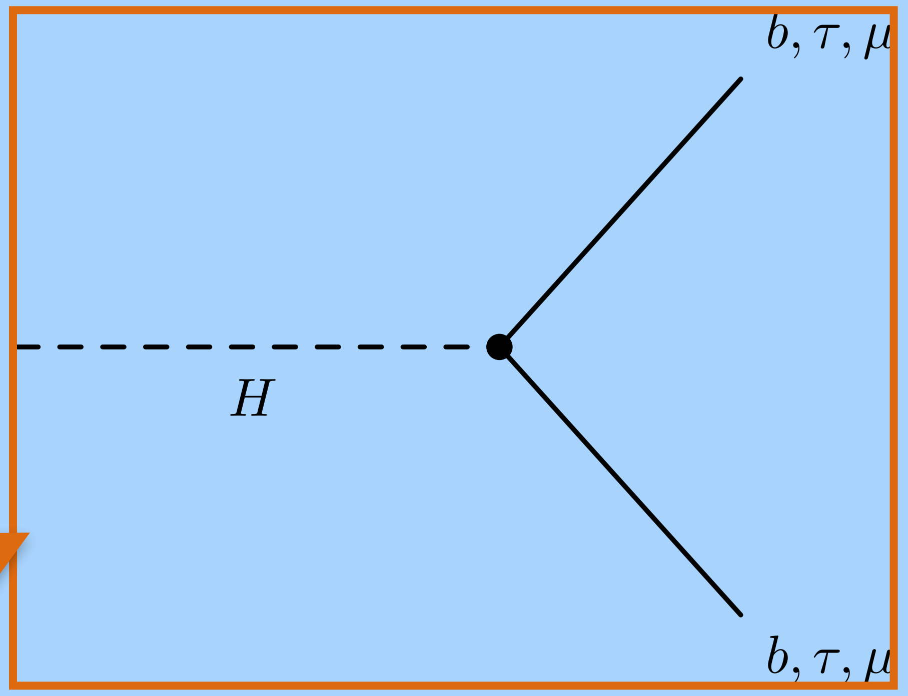

$$L_{\text{Yuk}} = (1 + \frac{H}{v}) m_f \bar{f}_L f_R$$

- ***Small expected branching ratio*** since Higgs couplings to fermions is proportional → $\Gamma \propto \frac{m_f^2}{v^2}$
- ***Small expected S/B*** ratio in LHC collisions
- ***H→cc*** offers the largest rate but very challenging at LHC due to large background contamination

H→μμ is probably the only accessible 2nd generation interaction at the LHC

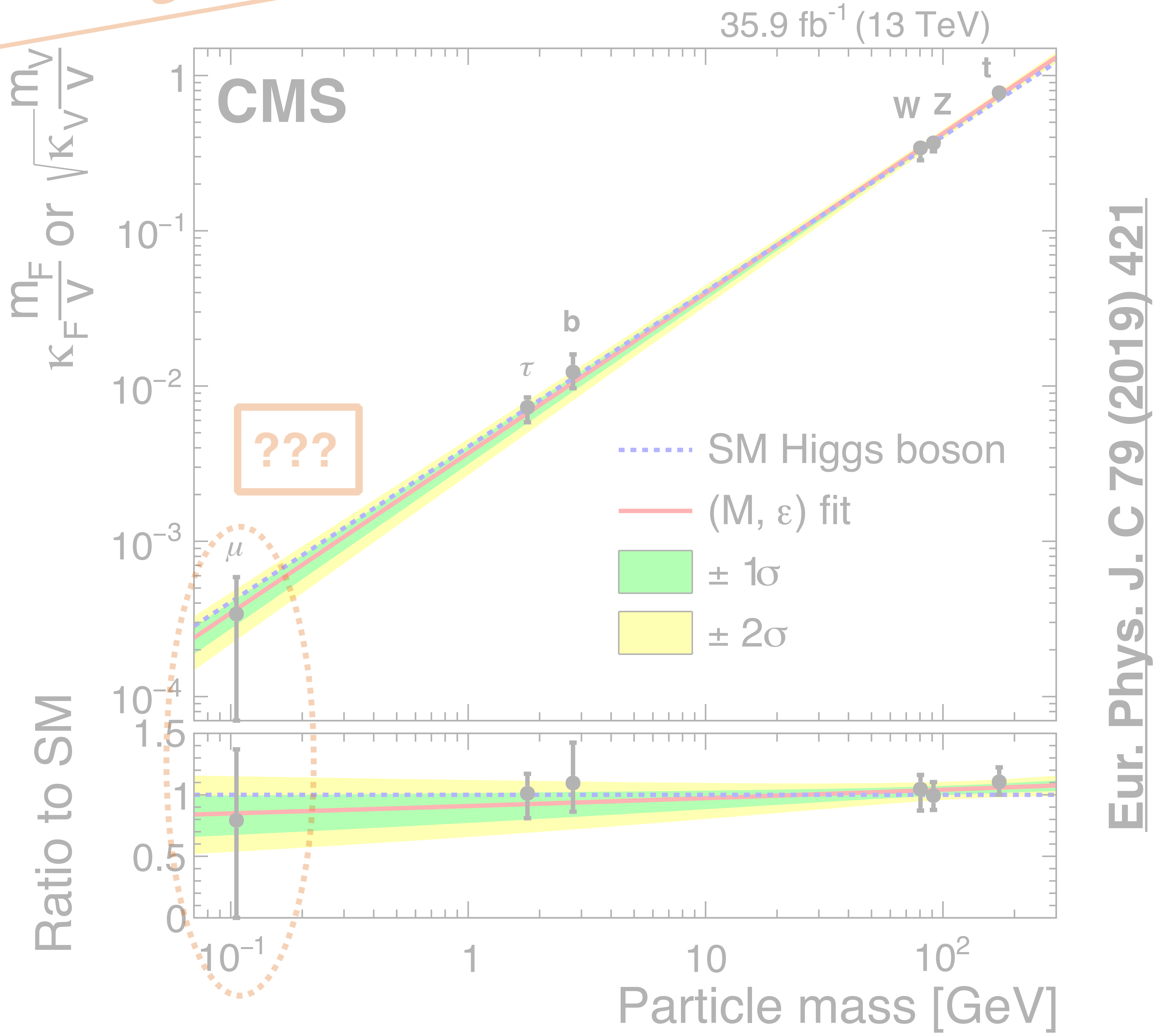

Next frontier → second fermion generation

- Probe the ***Yukawa interactions*** between the Higgs boson and ***2nd generation fermions***

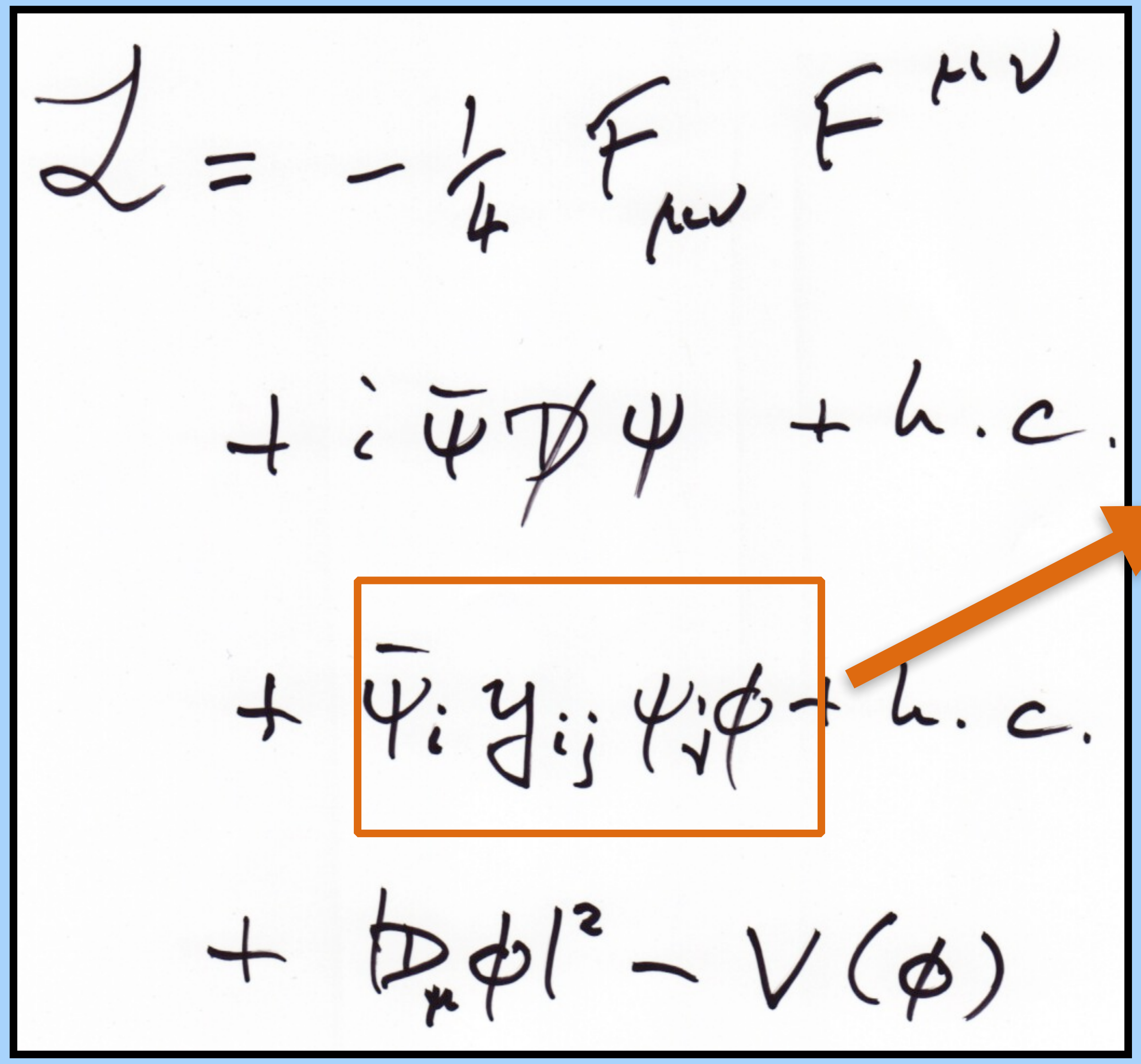

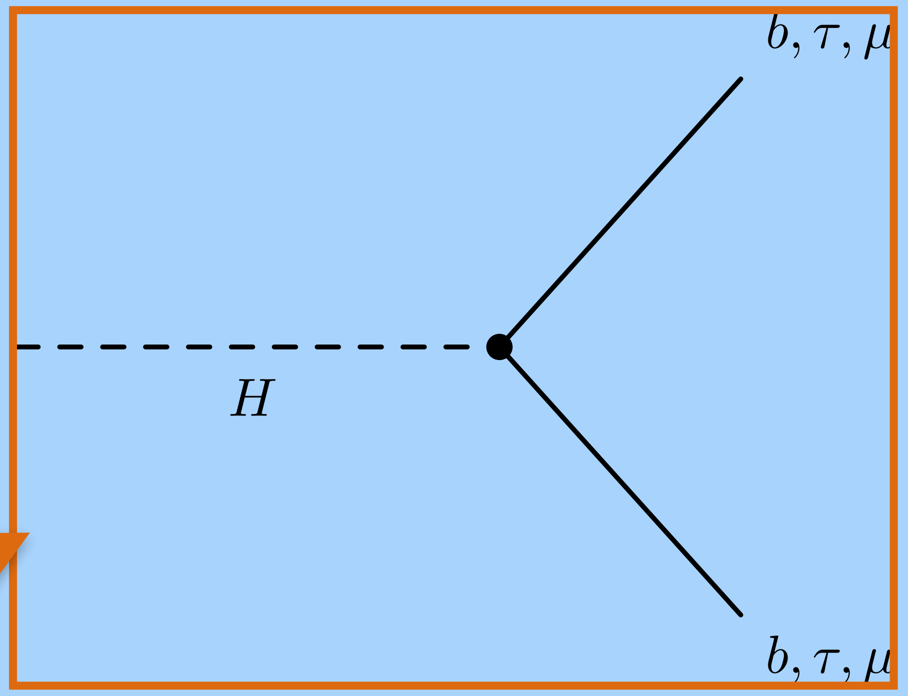

$$L_{\text{Yuk}} = (1 + \frac{H}{v}) m_f \bar{f}_L f_R$$

- ***Small expected branching ratio*** since Higgs couplings to fermions is proportional → $\Gamma \propto \frac{m_f^2}{v^2}$
- ***Small expected S/B*** ratio in LHC collisions
- ***H→cc*** offers the largest rate but very challenging at LHC due to large background contamination

H→μμ is probably the only accessible 2nd generation interaction at the LHC

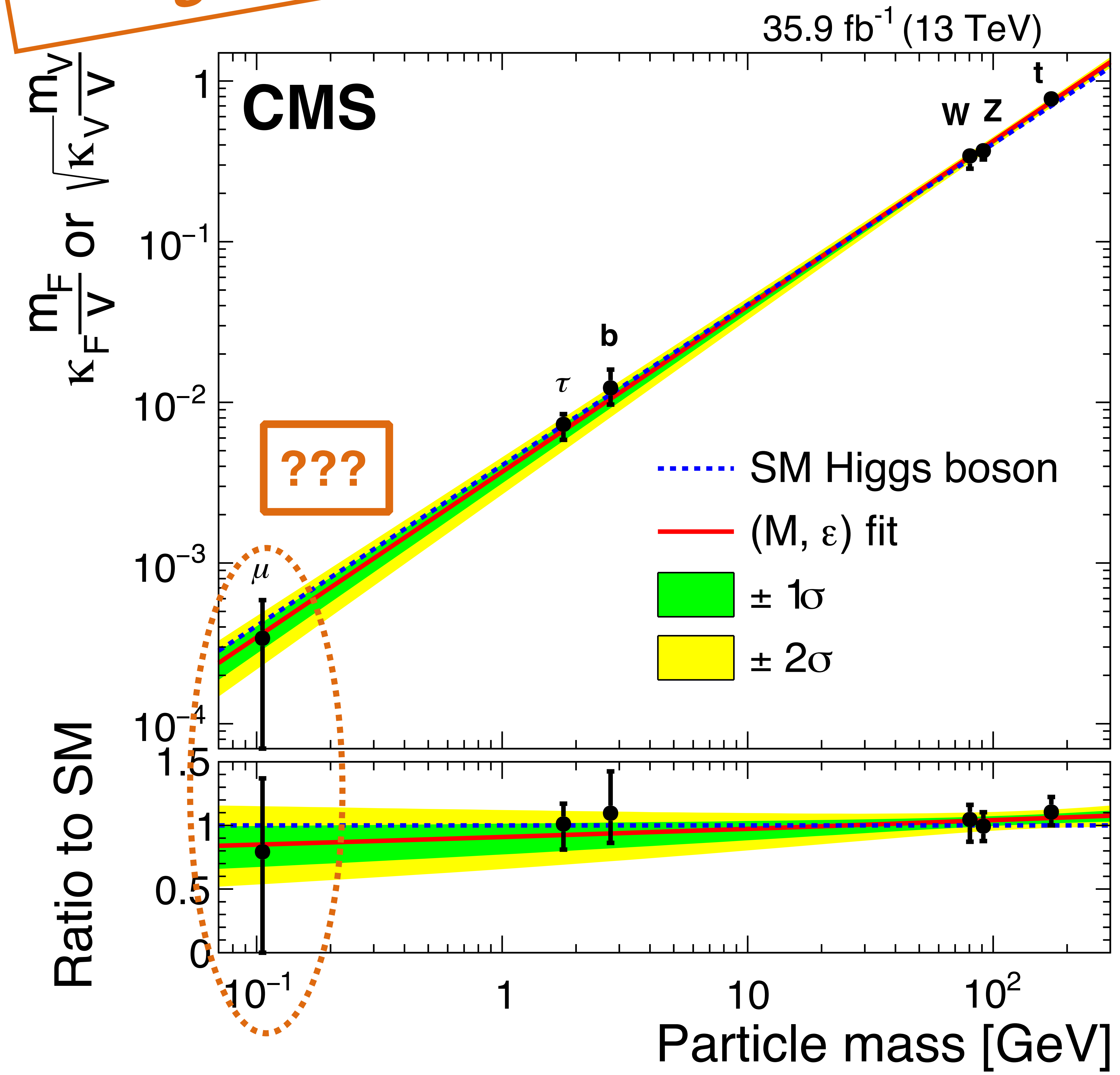

Eur. Phys. J. C 79 (2019) 421

The CMS detector

Transverse slice of the CMS detector

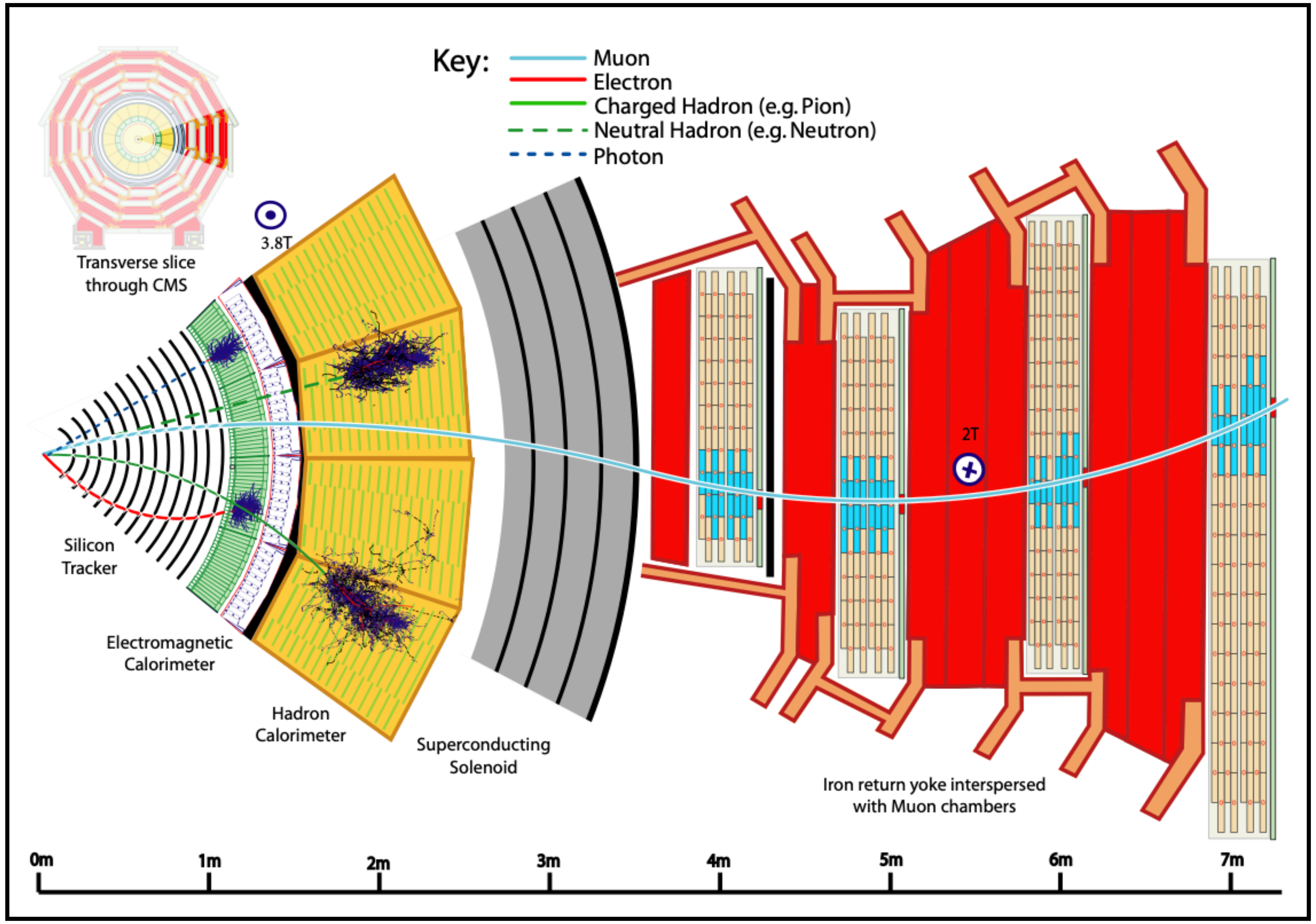

- CMS was designed to efficiently trigger, reconstruct, and identify muons produced in pp collisions
- The muon p_T is precisely measured thanks to the high ***magnetic field (4T)***, and excellent tracking performances from ***inner tracker*** and ***muon chambers***

The CMS detector

Transverse slice of the CMS detector

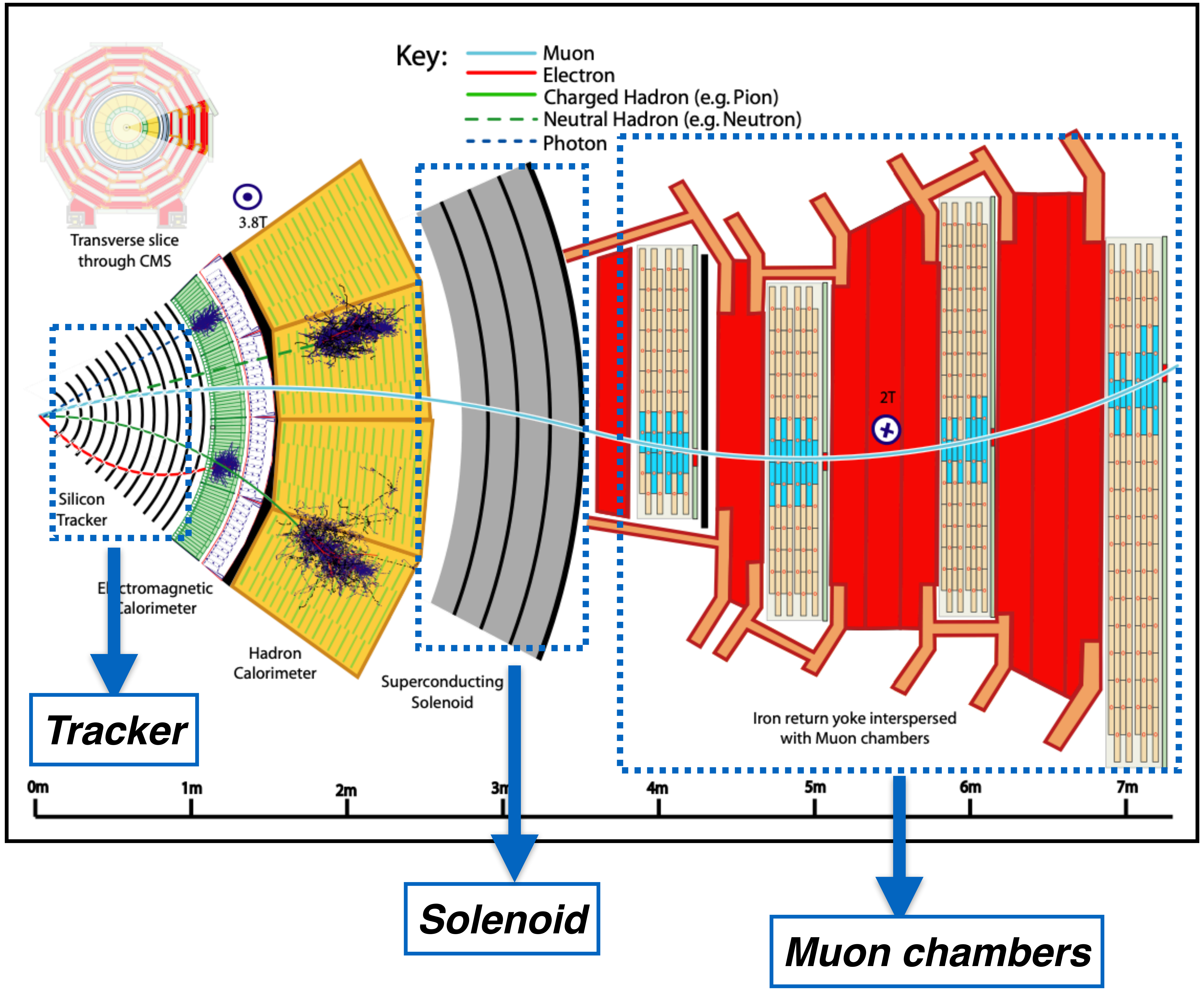

- CMS was designed to efficiently trigger, reconstruct, and identify muons produced in pp collisions
- The muon p_T is precisely measured thanks to the high ***magnetic field (4T)***, and excellent tracking performances from ***inner tracker*** and ***muon chambers***

The CMS detector

Transverse slice of the CMS detector

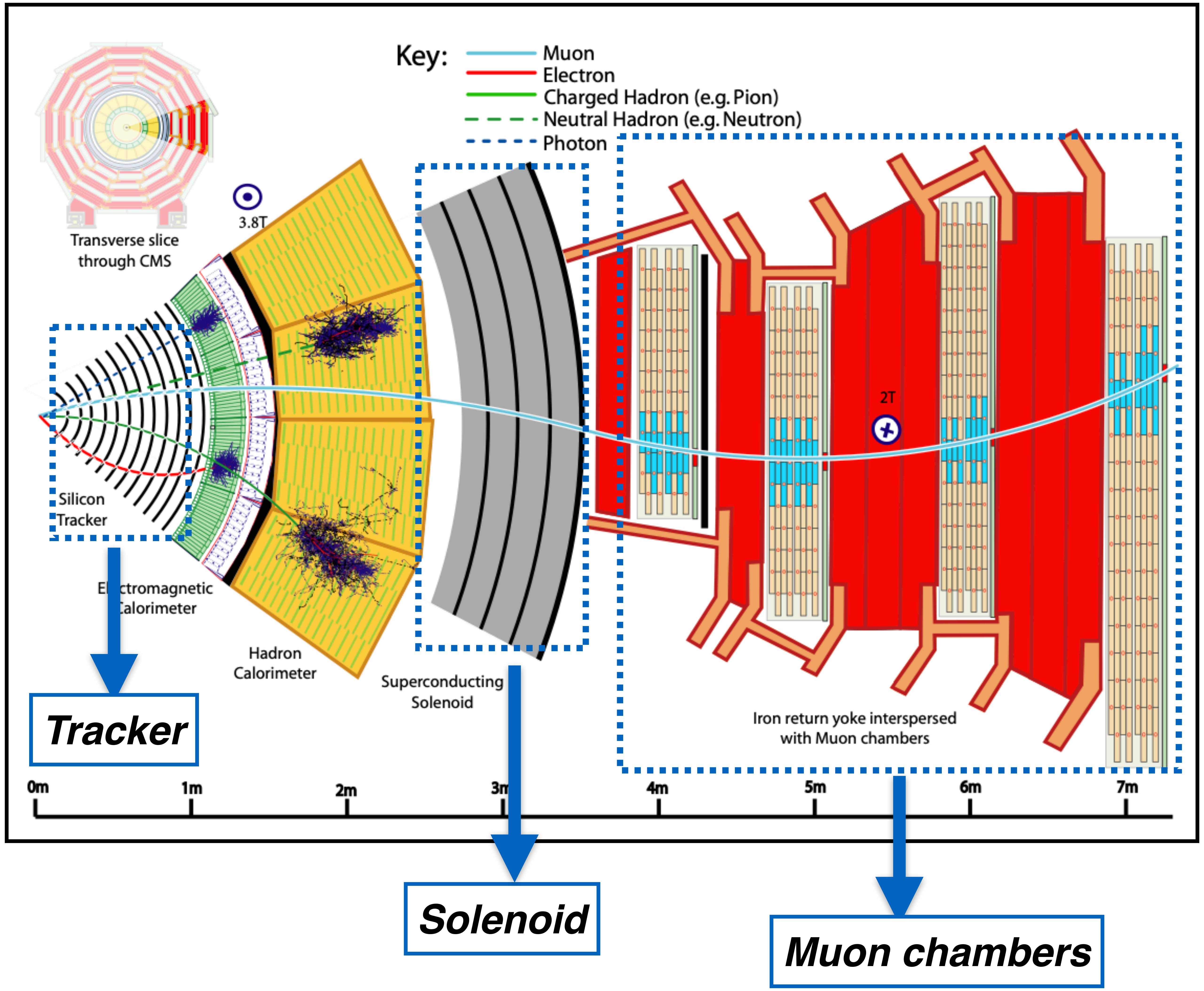

- CMS was designed to efficiently trigger, reconstruct, and identify muons produced in pp collisions
- The muon p_T is precisely measured thanks to the high ***magnetic field (4T)***, and excellent tracking performances from ***inner tracker*** and ***muon chambers***

muon p_T resolution in $Z \to \mu\mu$

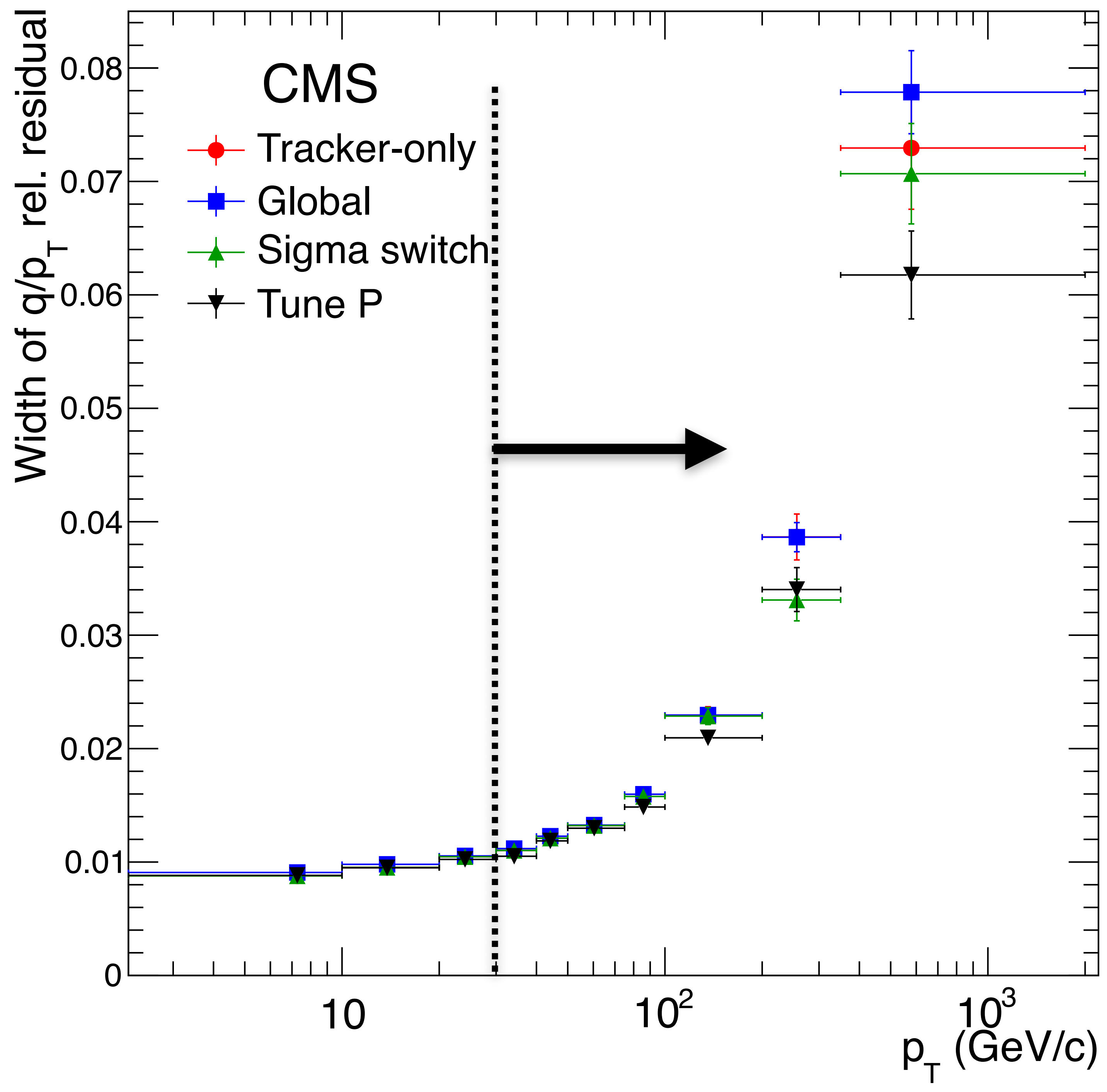

Hunting H → μμ decays

- **Basic characteristics of H→μμ analysis:**
  - The kinematics of the Higgs is fully accessible in H→μμ decays
  - Look for a ***narrow mass peak*** at the Higgs mass (m_H ~ 125 GeV)

However, it is challenging to observe this peak @125 GeV

Why ????

Small expected signal rate

- Inclusive Higgs production cross section at 13 TeV is **50 pb**
- BR(H→μμ) is about **2.1 x 10^{-4}**
- ***Cross section x decay ~ 0.01 pb***

Given the Run2 integrated luminosity of 137 fb^{-1} ***we expect to produce ~ 1500 H→μμ events***

Inclusively small S/B

- Main bkg. from DY production
- **Effective cross section** in the H→μμ region of about ***15 pb***

We expect order of a million background events in H→μμ ***preselected sample***

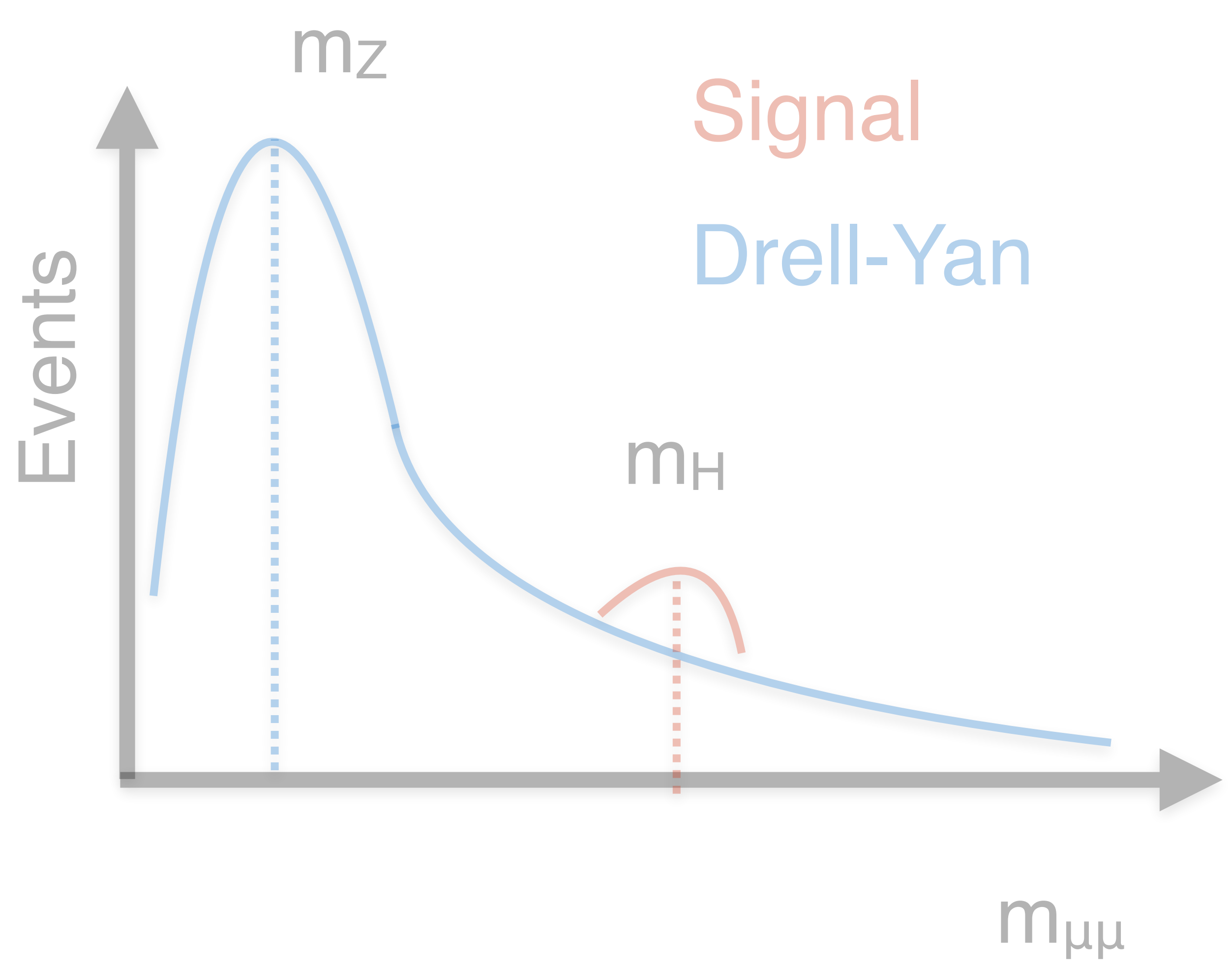

H→μμ is a bump hunt

Hunting H → μμ decays

- **Basic characteristics of H→μμ analysis:**
  - The kinematics of the Higgs is fully accessible in H→μμ decays
  - Look for a ***narrow mass peak*** at the Higgs mass (m_H ~ 125 GeV)

→ ***However, it is challenging to observe this peak @125 GeV***

Why ????

Small expected signal rate

- Inclusive Higgs production cross section at 13 TeV is **50 pb**
- BR(H→μμ) is about **2.1 x 10^{-4}**
- ***Cross section x decay ~ 0.01 pb***

↓

Given the Run2 integrated luminosity of 137 fb^{-1}
we expect to produce ~ 1500 H→μμ events

Inclusively small S/B

- Main bkg. from DY production
- **Effective cross section** in the H→μμ region of about ***15 pb***

↓

We expect order of a million background events in H→μμ ***preselected sample***

→

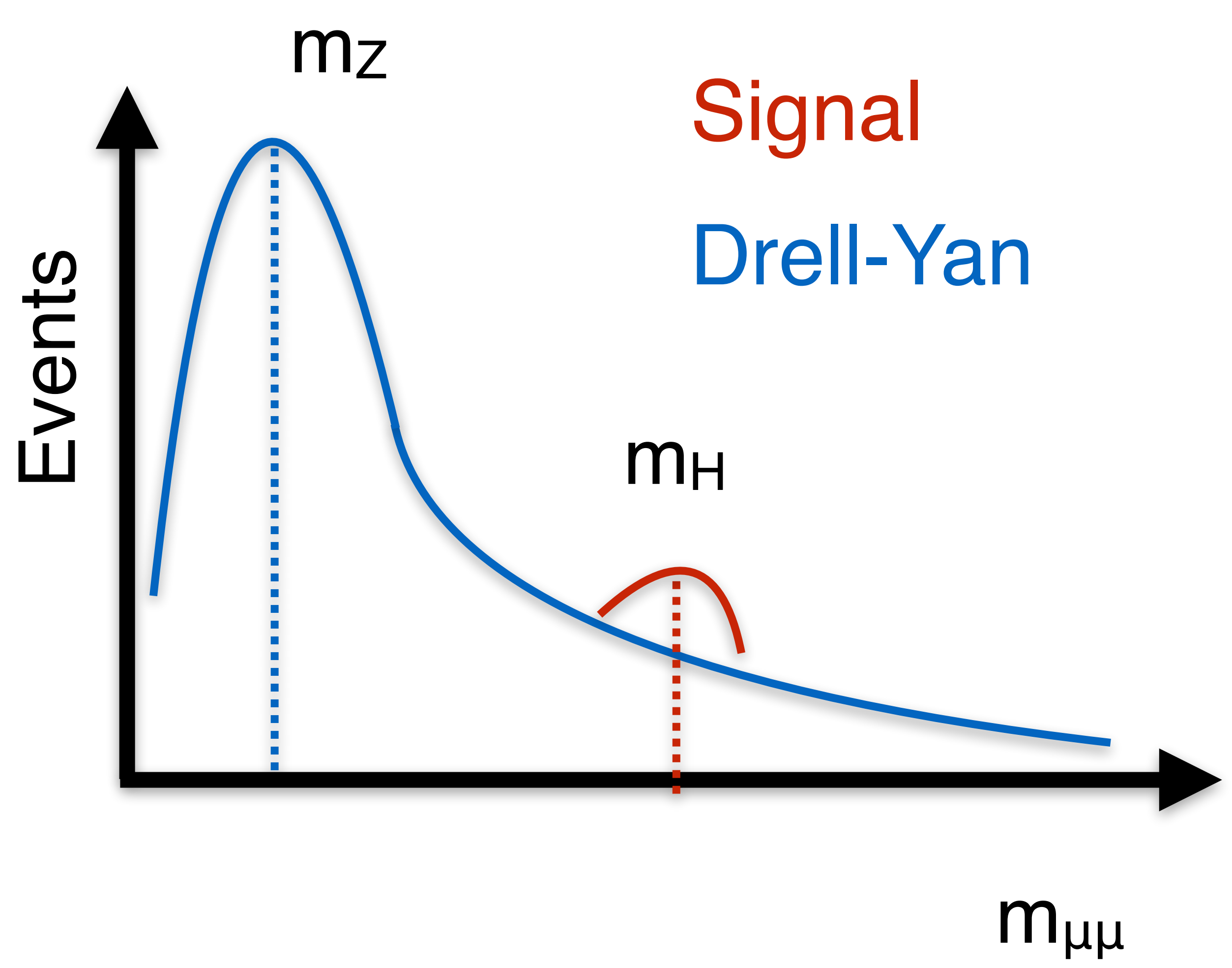

H→μμ is a bump hunt

Higgs boson production modes

In order to ***maximise the sensitivity***, the ***H→μμ search combines exclusive analyses targeting*** the ***main Higgs boson production modes*** at the LHC

Gluon fusion mode (ggH)

- ***87%*** of the H cross section
- ***Low purity*** due to large DY

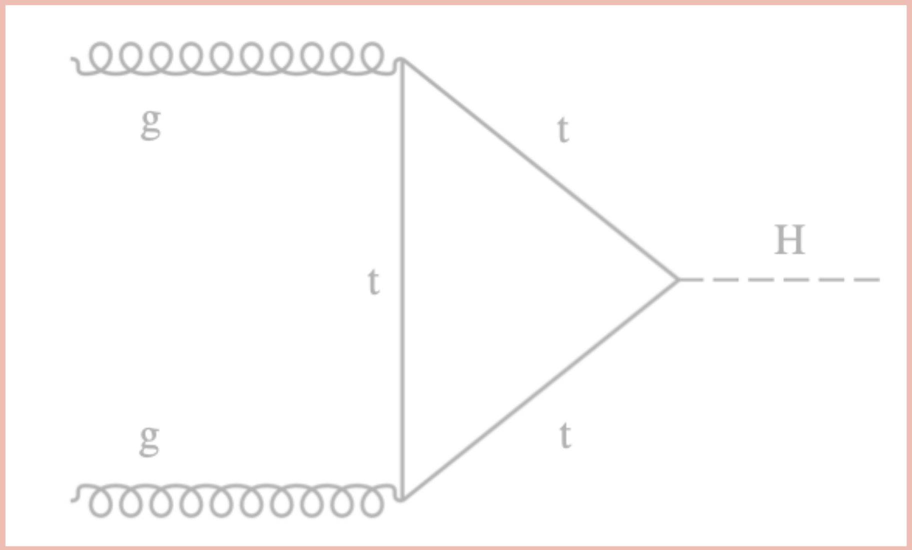

VBF mode

- ***7%*** of the H cross section
- ***Good signal purity*** thanks to ***VBF-jets*** → large m_{jj} and $\Delta\eta_{jj}$

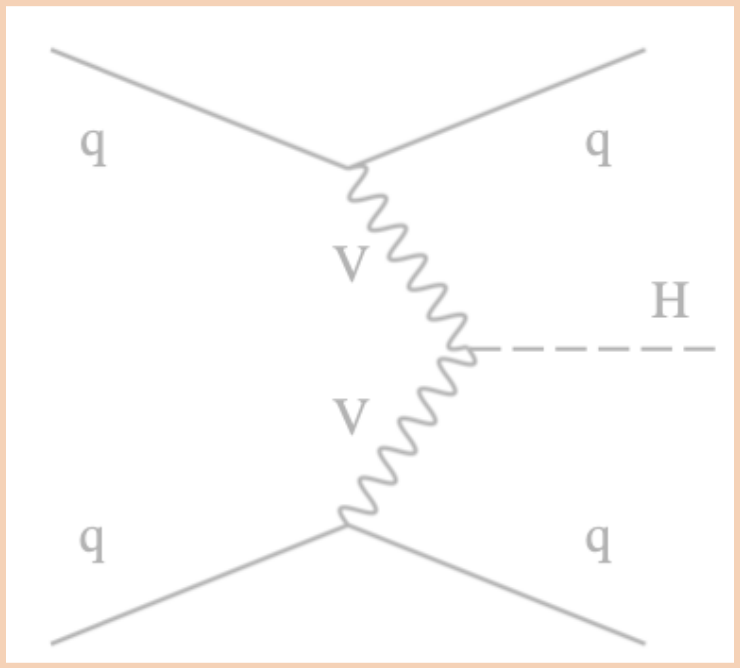

VH mode

- ***4%*** of the H cross section
- ***Leptonic decays*** of W or Z bosons offer topologies with ***high purity***

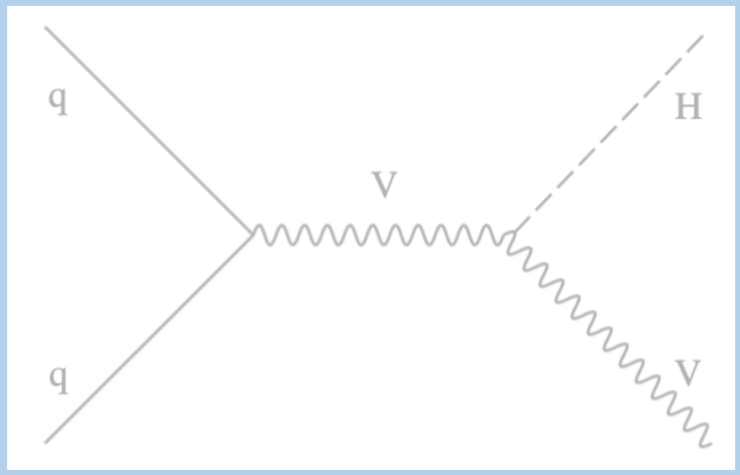

ttH mode

- ***1%*** of the H cross section
- Additional jets, ***b-jets***, and ***leptons*** from ***top decays*** offer topologies with ***high signal purity***

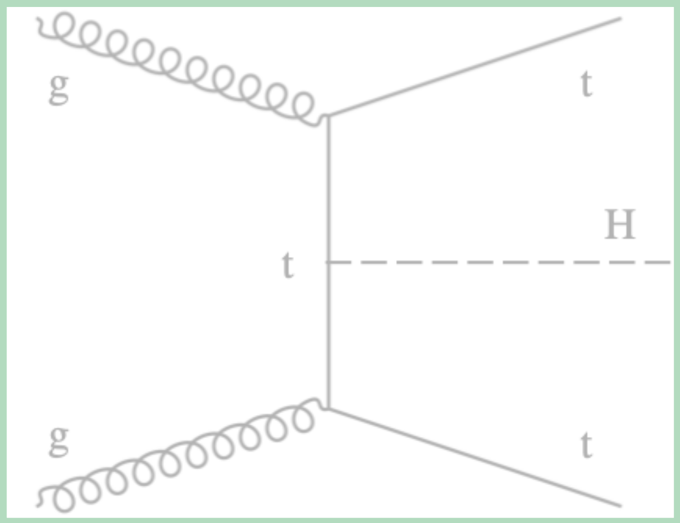

Purity S/(S+B)

**** Rule of thumb: richer final state topology → better purity*

Cross Section (pb)

Higgs boson production modes

In order to ***maximise the sensitivity***, the ***H→μμ search combines exclusive analyses targeting*** the ***main Higgs boson production modes*** at the LHC

Gluon fusion mode (ggH)

- ***87%*** of the H cross section
- ***Low purity*** due to large DY

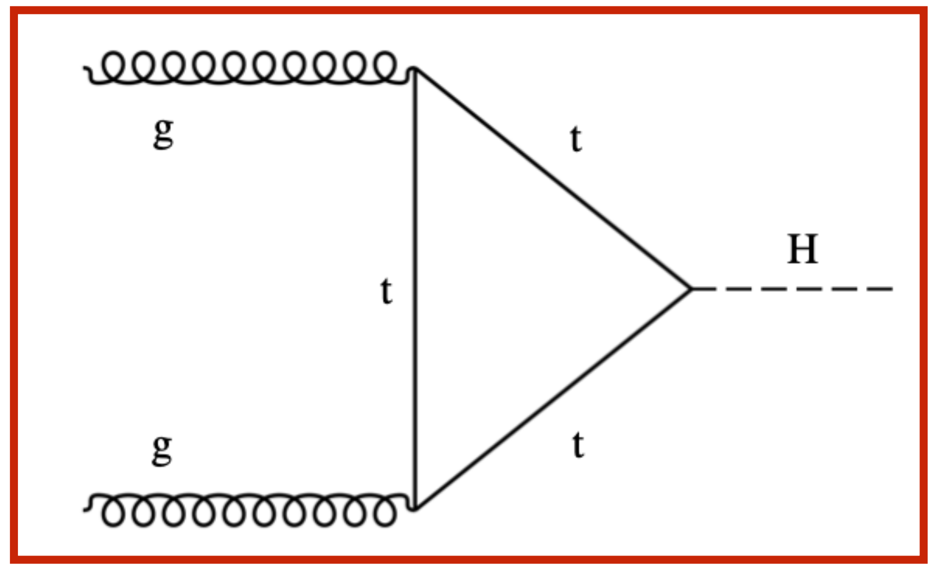

VBF mode

- *7%* of the H cross section
- ***Good signal purity*** thanks to ***VBF-jets*** → large m_{jj} and $\Delta\eta_{jj}$

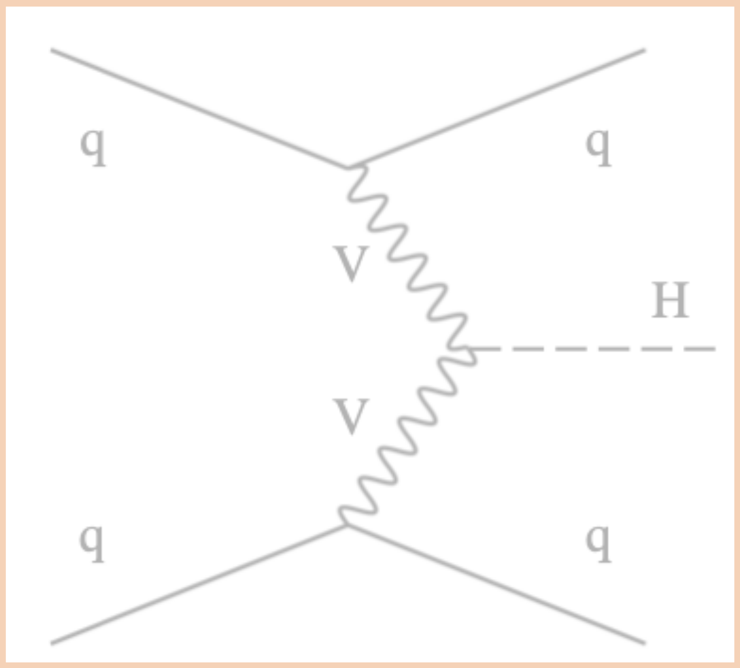

VH mode

- ***4%*** of the H cross section
- ***Leptonic decays*** of W or Z bosons offer topologies with ***high purity***

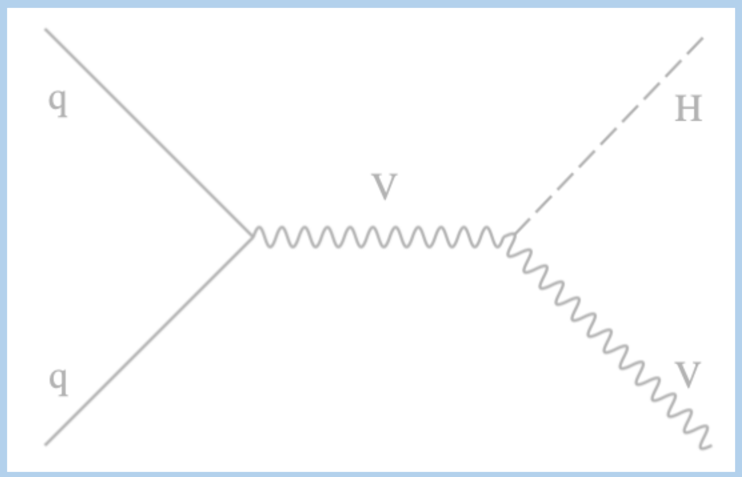

ttH mode

- ***1%*** of the H cross section
- Additional jets, ***b-jets***, and ***leptons*** from ***top decays*** offer topologies with ***high signal purity***

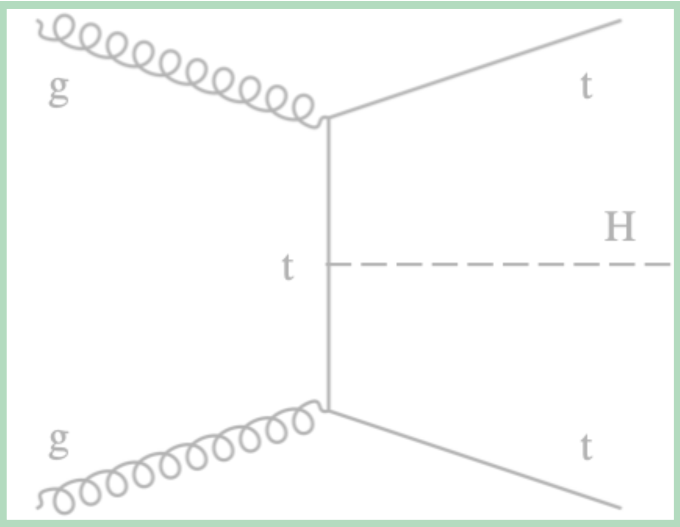

**** Rule of thumb: richer final state topology → better purity*

Purity S/(S+B)

Cross Section (pb)

Higgs boson production modes

In order to ***maximise the sensitivity***, the ***H→μμ search combines exclusive analyses targeting*** the ***main Higgs boson production modes*** at the LHC

Gluon fusion mode (ggH)

- ***87%*** of the H cross section
- ***Low purity*** due to large DY

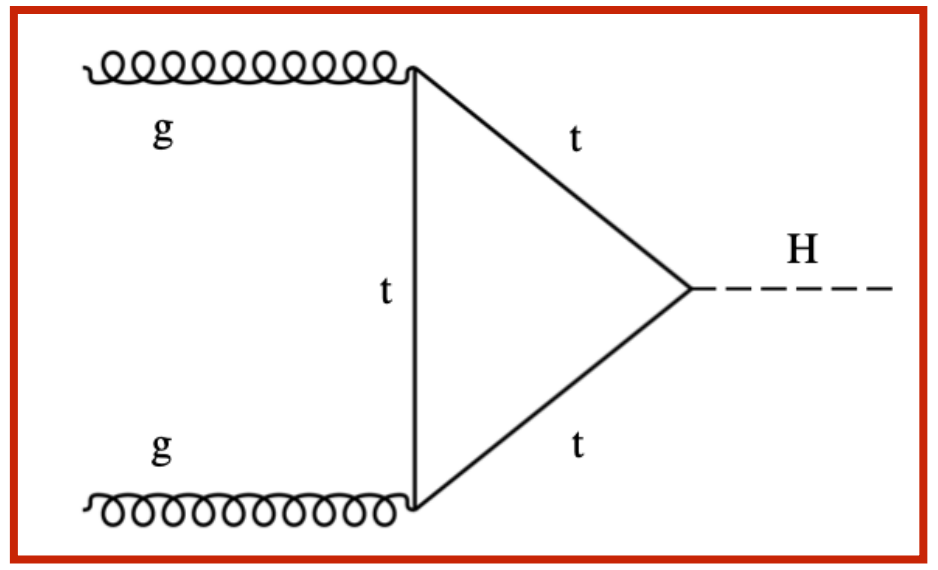

VBF mode

- ***7%*** of the H cross section
- ***Good signal purity*** thanks to ***VBF-jets*** → large m_{jj} and $\Delta\eta_{jj}$

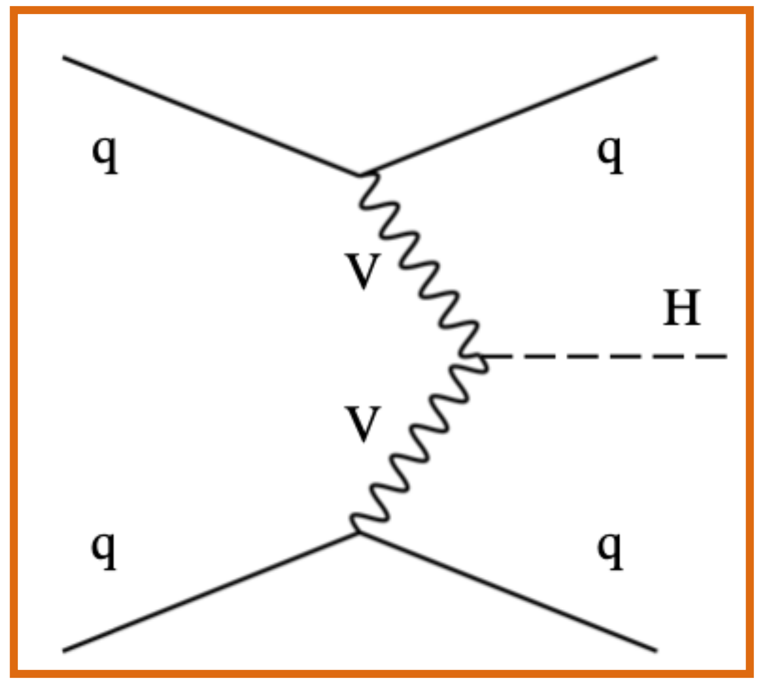

VH mode

- ***4%*** of the H cross section
- ***Leptonic decays*** of W or Z bosons offer topologies with ***high purity***

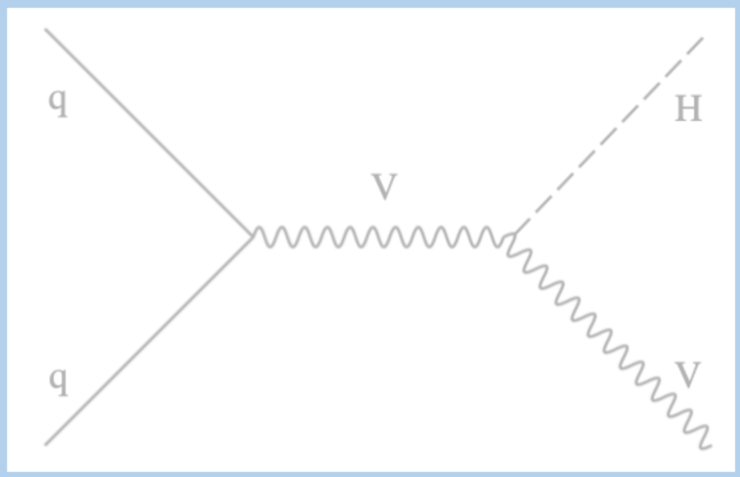

ttH mode

- ***1%*** of the H cross section
- Additional jets, ***b-jets***, and ***leptons*** from ***top decays*** offer topologies with ***high signal purity***

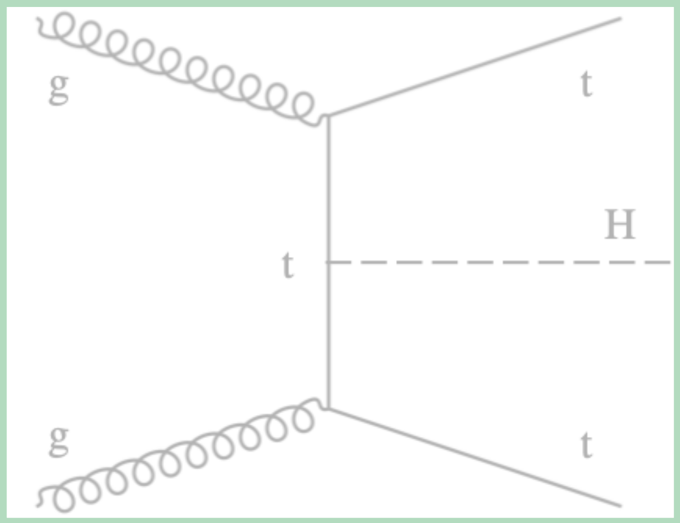

**** Rule of thumb: richer final state topology → better purity*

Purity S/(S+B)

Cross Section (pb)

Higgs boson production modes

In order to ***maximise the sensitivity***, the ***H→μμ search combines exclusive analyses targeting*** the ***main Higgs boson production modes*** at the LHC

Gluon fusion mode (ggH)

- ***87%*** of the H cross section
- ***Low purity*** due to large DY

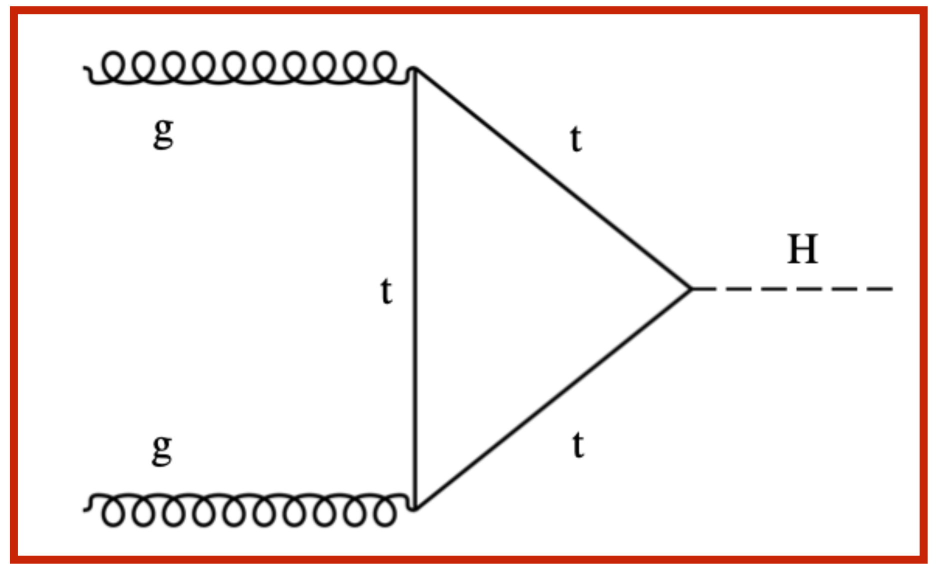

VBF mode

- ***7%*** of the H cross section
- ***Good signal purity*** thanks to ***VBF-jets*** → large m_{jj} and $\Delta\eta_{jj}$

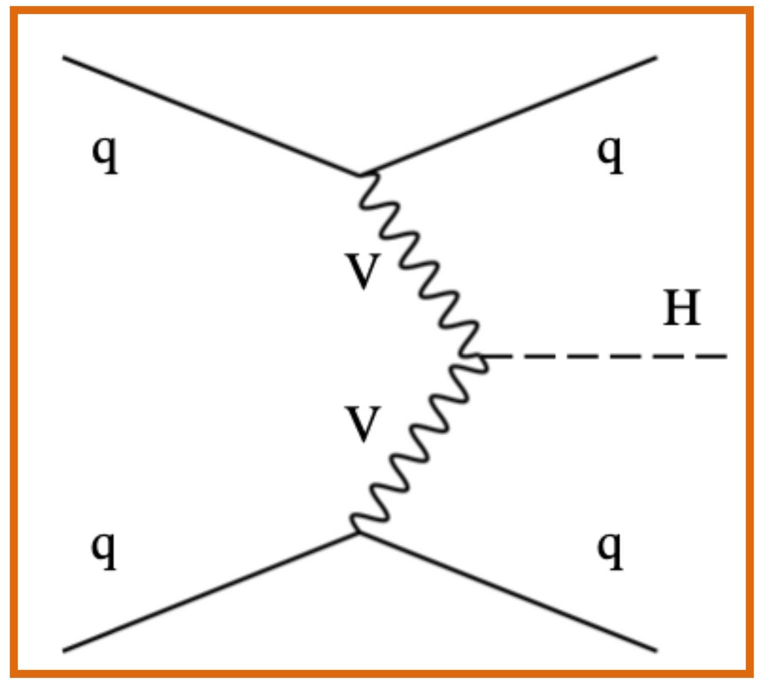

VH mode

- ***4%*** of the H cross section
- ***Leptonic decays*** of W or Z bosons offer topologies with ***high purity***

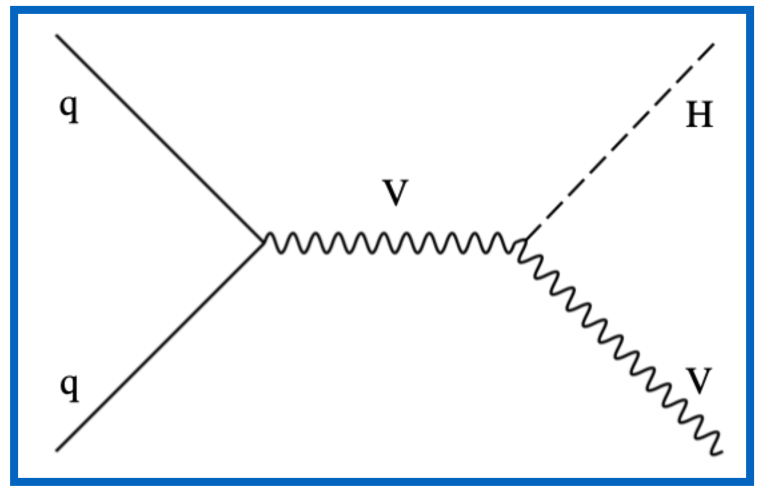

ttH mode

- ***1%*** of the H cross section
- Additional jets, ***b-jets***, and ***leptons*** from ***top decays*** offer topologies with ***high signal purity***

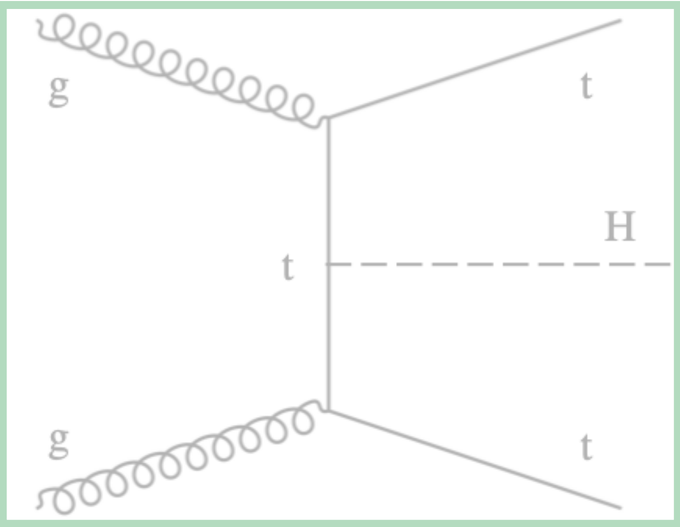

**** Rule of thumb: richer final state topology → better purity*

Purity S/(S+B)

Cross Section (pb)

Higgs boson production modes

In order to ***maximise the sensitivity***, the ***H→μμ search combines exclusive analyses targeting*** the ***main Higgs boson production modes*** at the LHC

Gluon fusion mode (ggH)

- ***87%*** of the H cross section
- ***Low purity*** due to large DY

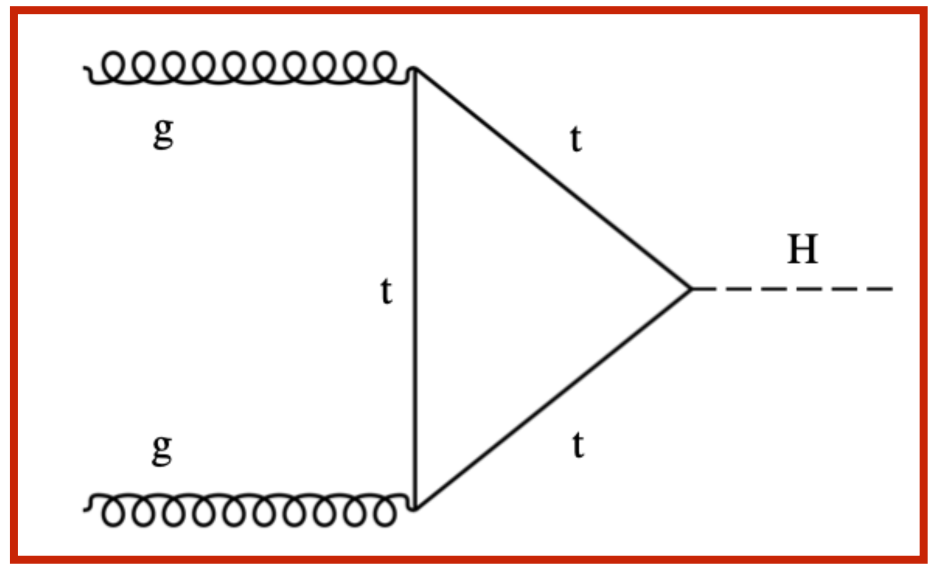

VBF mode

- ***7%*** of the H cross section
- ***Good signal purity*** thanks to ***VBF-jets*** → large m_{jj} and $\Delta\eta_{jj}$

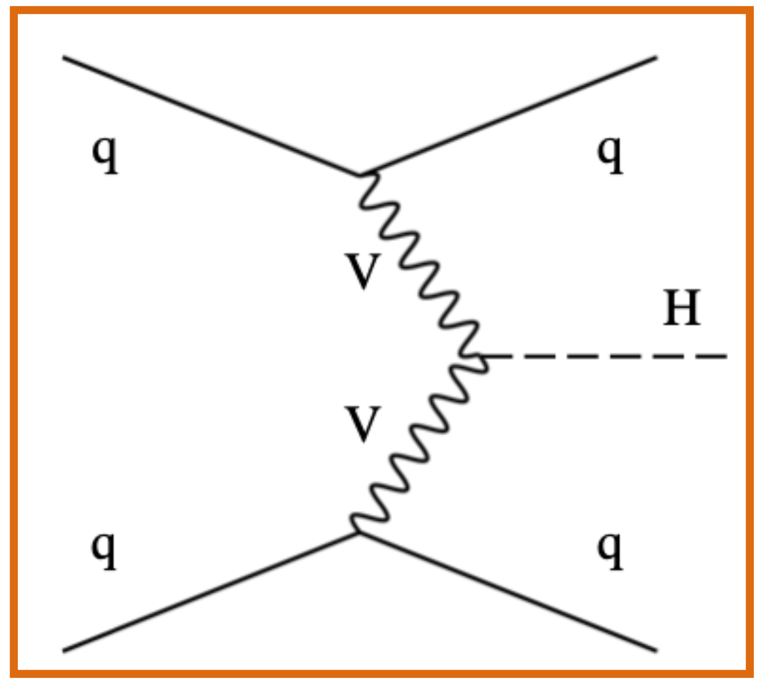

VH mode

- ***4%*** of the H cross section
- ***Leptonic decays*** of W or Z bosons offer topologies with ***high purity***

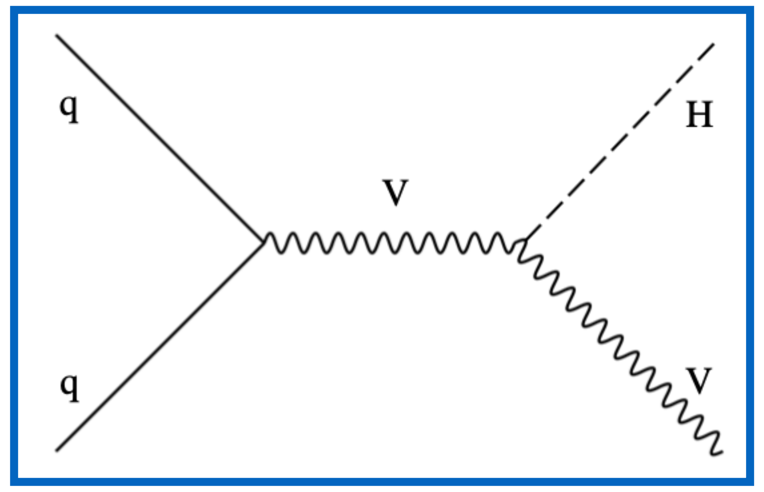

ttH mode

- ***1%*** of the H cross section
- Additional jets, ***b-jets***, and ***leptons*** from ***top decays*** offer topologies with ***high signal purity***

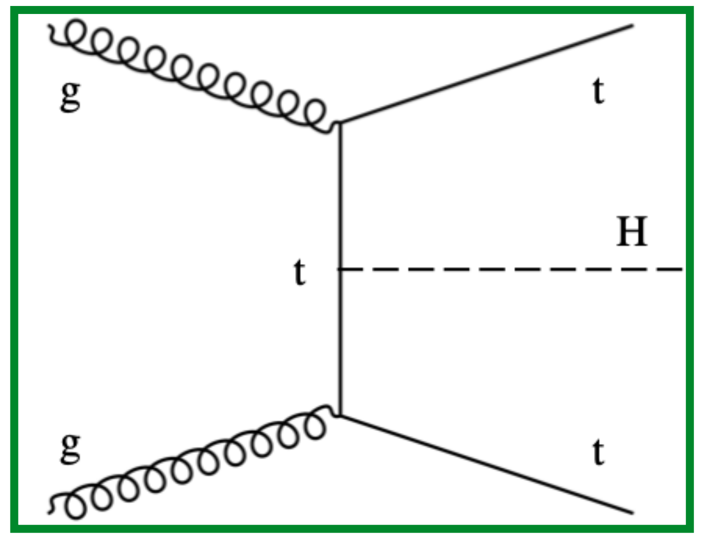

**** Rule of thumb: richer final state topology → better purity*

Purity S/(S+B)

Cross Section (pb)

H→μμ candidate selection

Baseline selection

- Events are collected via ***single-muon triggers***
- Require ***two opposite-sign muons*** with $p_T > 20$ GeV, $|\eta| < 2.4$
- One muon with $p_T > 26$ (29) GeV in 2016, 2018 (2017) data
  - Ensure consistency with online trigger thresholds
  - Trigger efficiency is ~93% per muon
- Muons required to be ***identified*** and ***isolated*** → ~95% efficiency

Signal events characterised by ***sharp peak*** at ***125 GeV***
$m_{\mu\mu}$ resolution plays a ***crucial role*** in the ***final sensitivity***

- **Recovery of final state photon radiation** → 3% gain in $m_{\mu\mu}$ resolution
- ***Improvements in mass resolution ~5%*** by ***constraining*** the muon ***tracks*** to ***pass*** from the ***position of the interaction point*** (in jargon called beam spot)

Higgs signal peak in MC

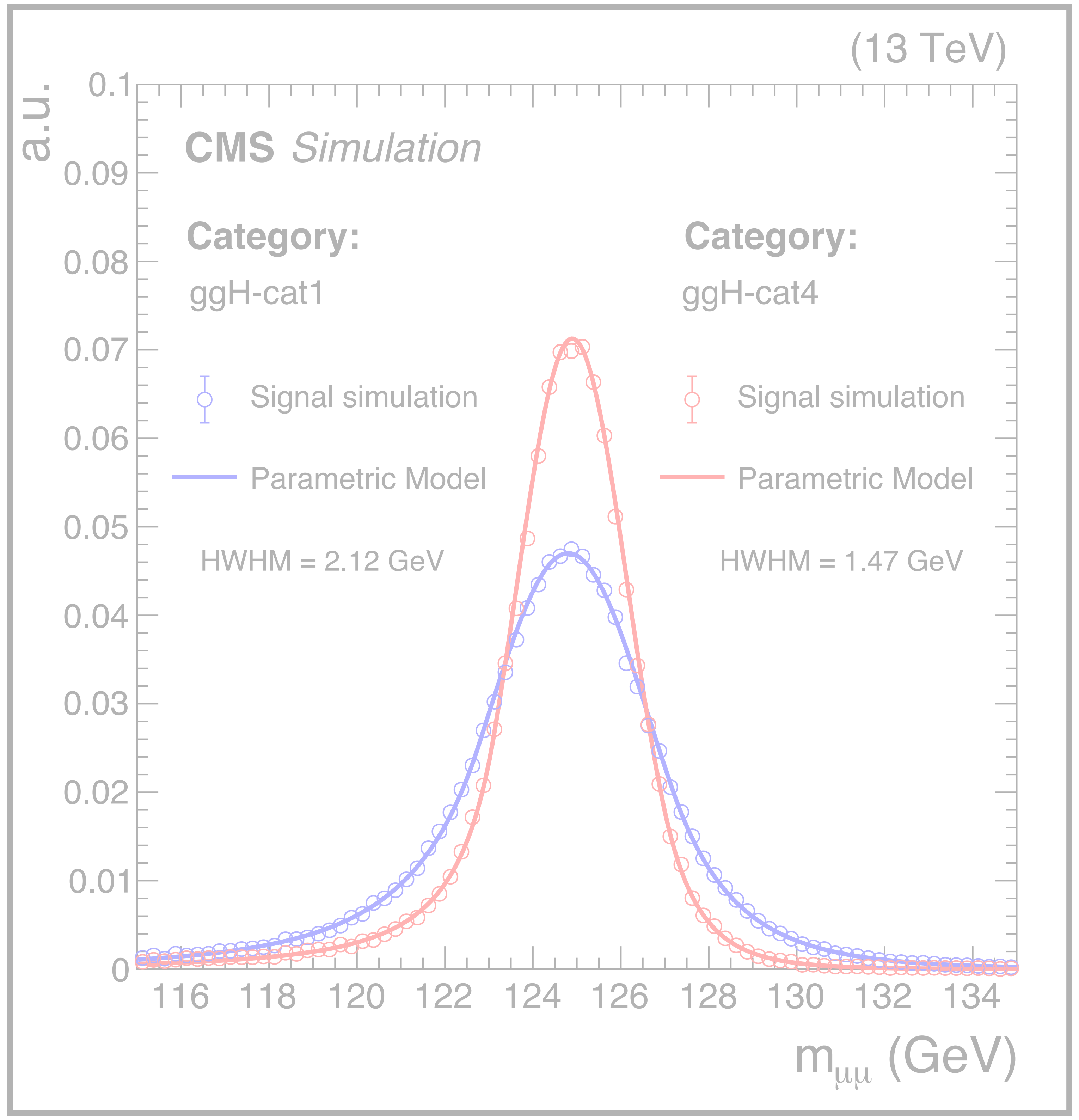

$m_{\mu\mu}$ resolution roughly ranges from 1-2%, depending on muon η and p_T

H→μμ candidate selection

Baseline selection

- Events are collected via ***single-muon triggers***
- Require ***two opposite-sign muons*** with $p_T > 20$ GeV, $|\eta| < 2.4$
- One muon with $p_T > 26$ (29) GeV in 2016, 2018 (2017) data
  - Ensure consistency with online trigger thresholds
  - Trigger efficiency is ~93% per muon
- Muons required to be ***identified*** and ***isolated*** → ~95% efficiency

Signal events characterised by ***sharp peak*** at ***125 GeV***
$m_{\mu\mu}$ resolution plays a ***crucial role*** in the ***final sensitivity***

- **Recovery of final state photon radiation** → 3% gain in $m_{\mu\mu}$ resolution
- ***Improvements in mass resolution ~5%*** by ***constraining*** the muon ***tracks*** to ***pass*** from the ***position of the interaction point*** (in jargon called beam spot)

Higgs signal peak in MC

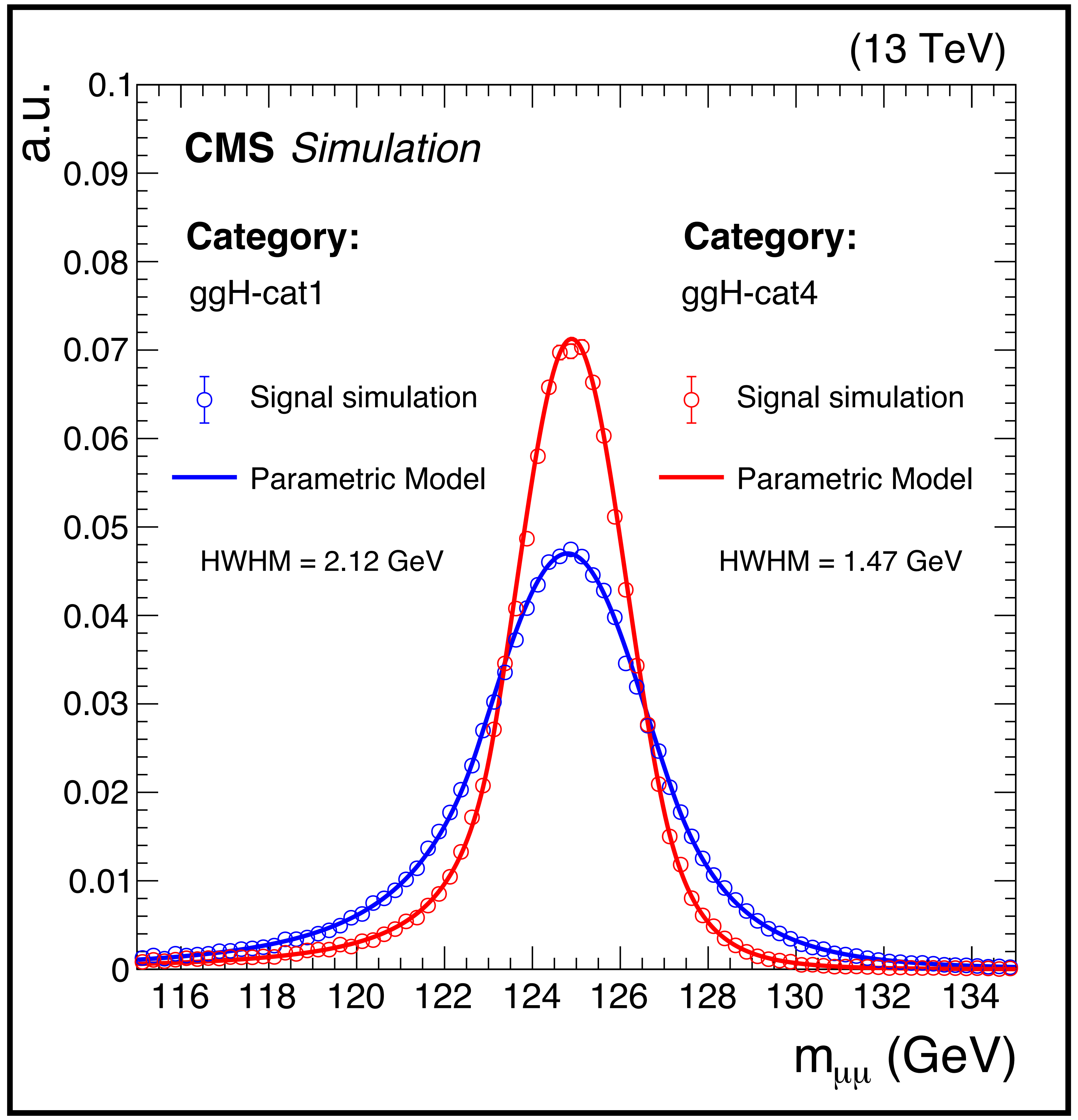

$m_{\mu\mu}$ resolution ($\sigma/m_{\mu\mu}$) ranges from 1-2%, depending on muon η and p_T

H→μμ production categories

From the ***baseline selection,*** events divided in ***6 exclusive production categories***

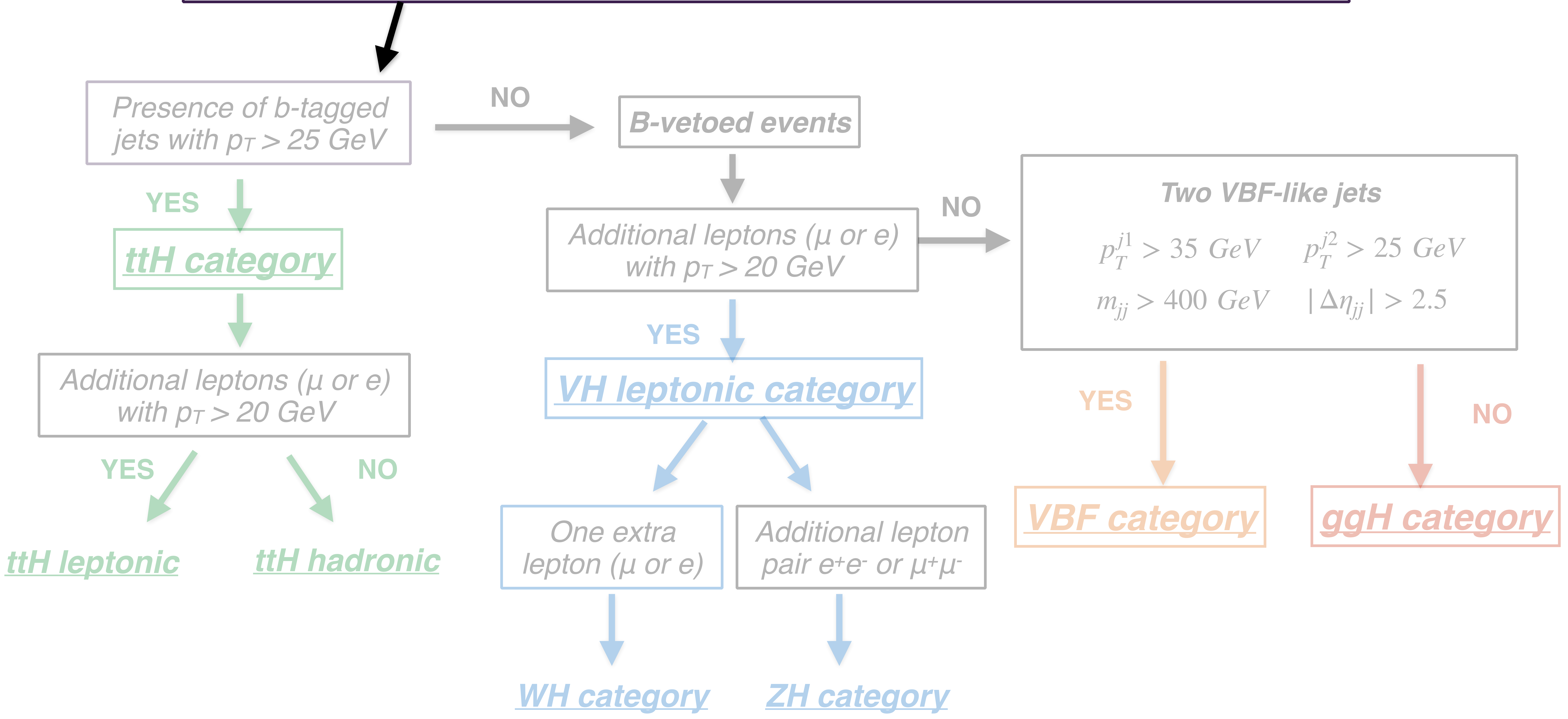

H→μμ production categories

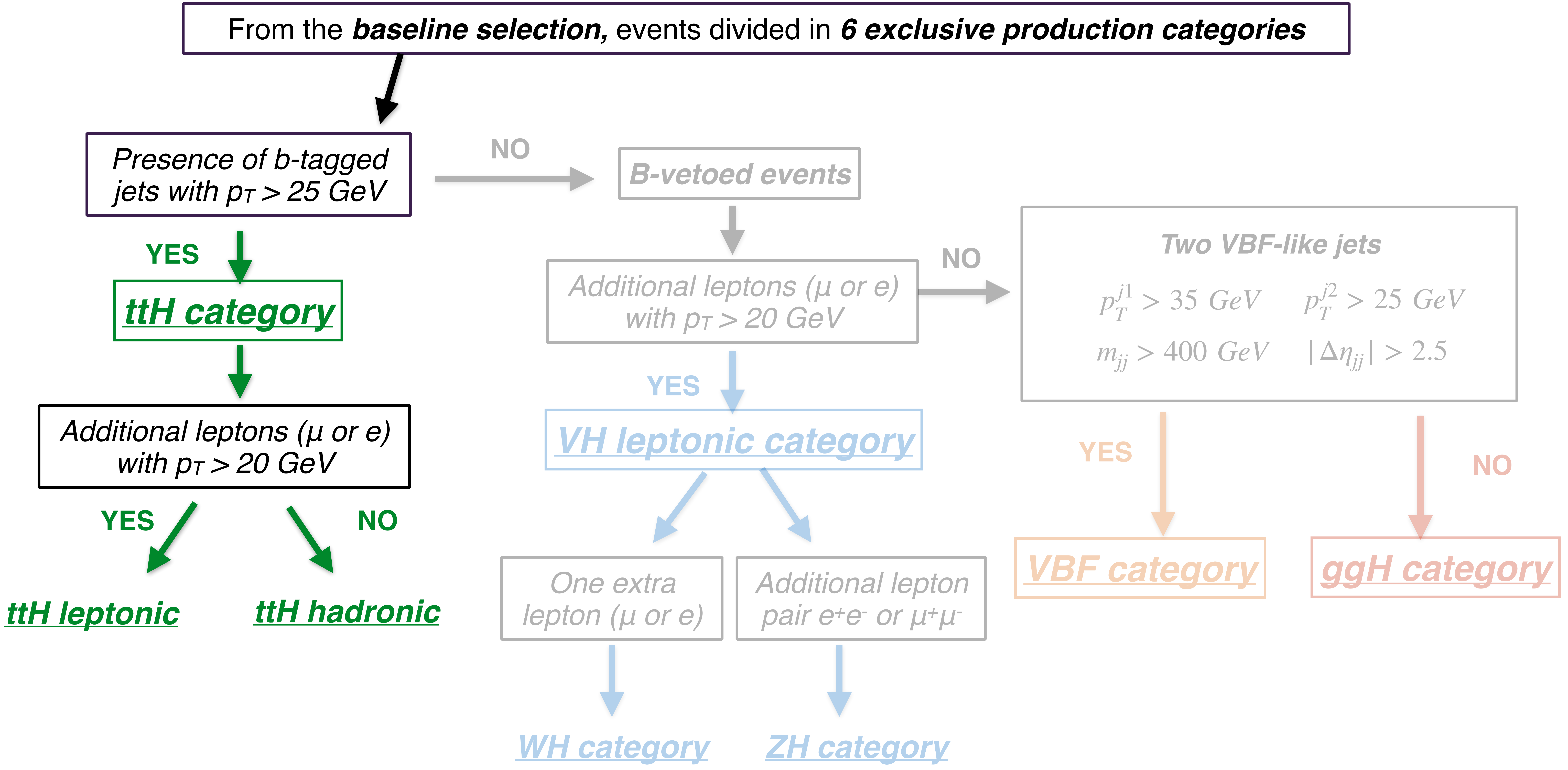

H→μμ production categories

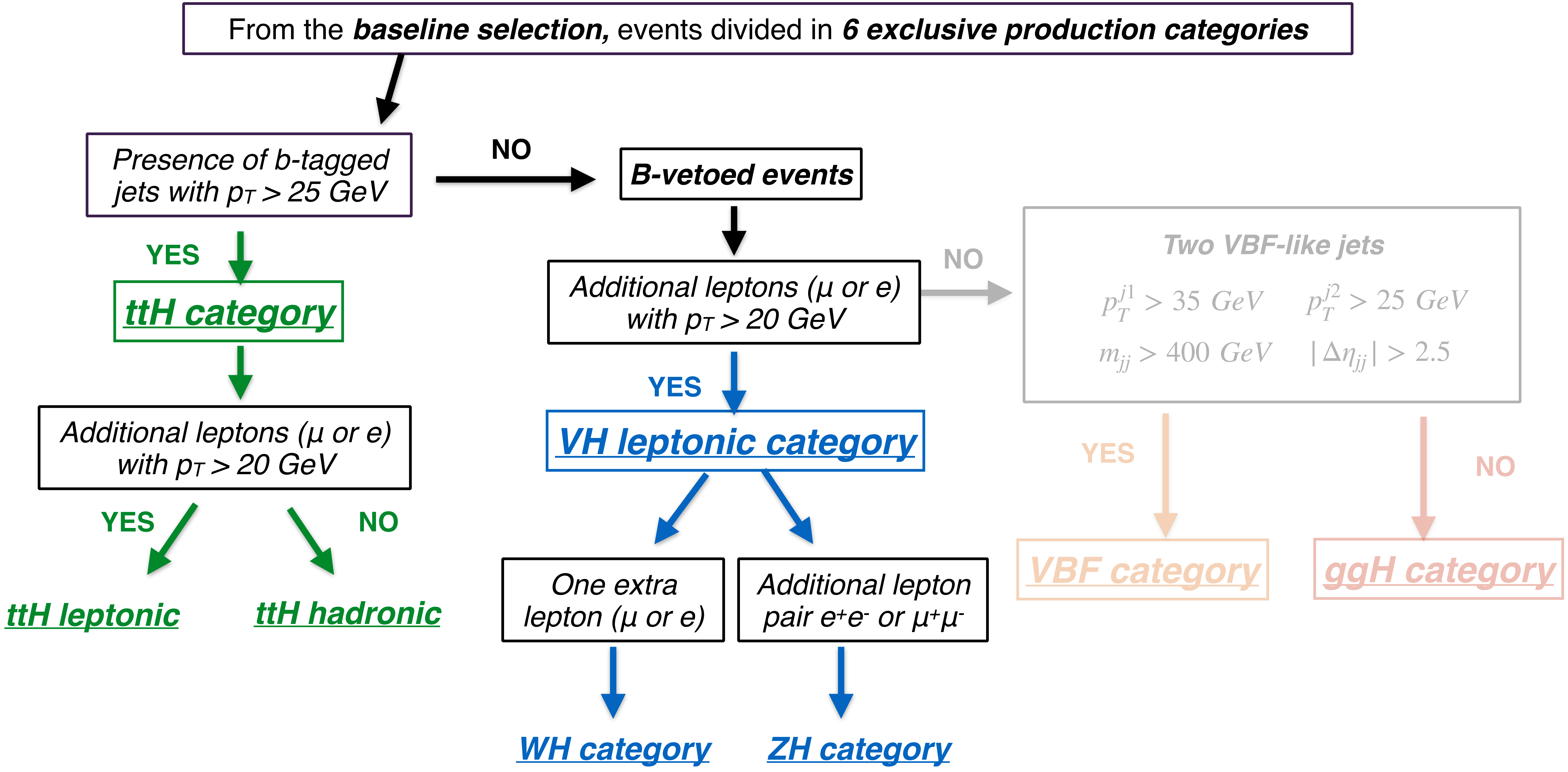

H→μμ production categories

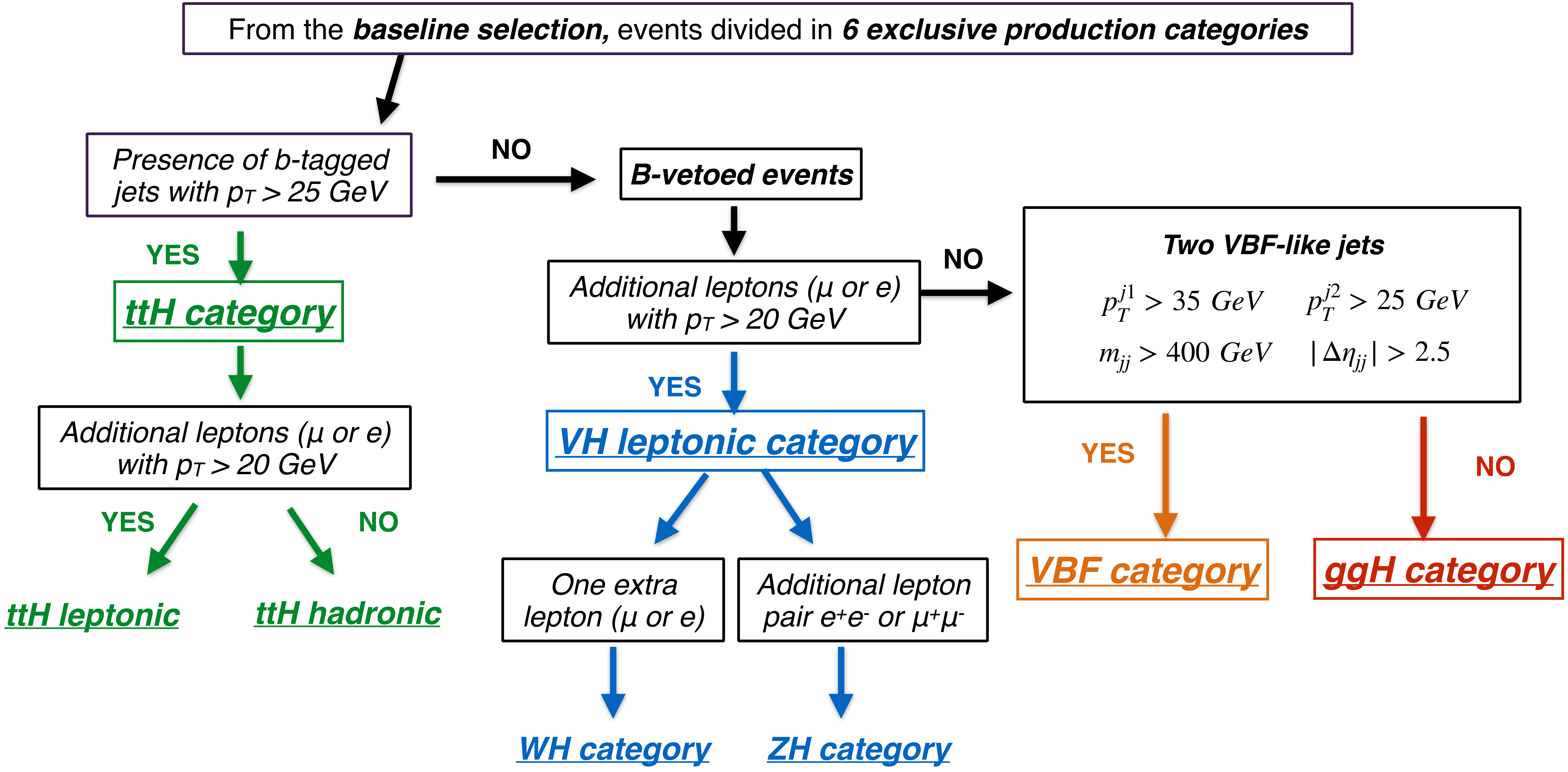

H→μμ production categories

Fraction of H→ μμ expected signal events with m(μμ) in the 110-150 GeV range

ggH category

VBF category

VH leptonic category

ttH category

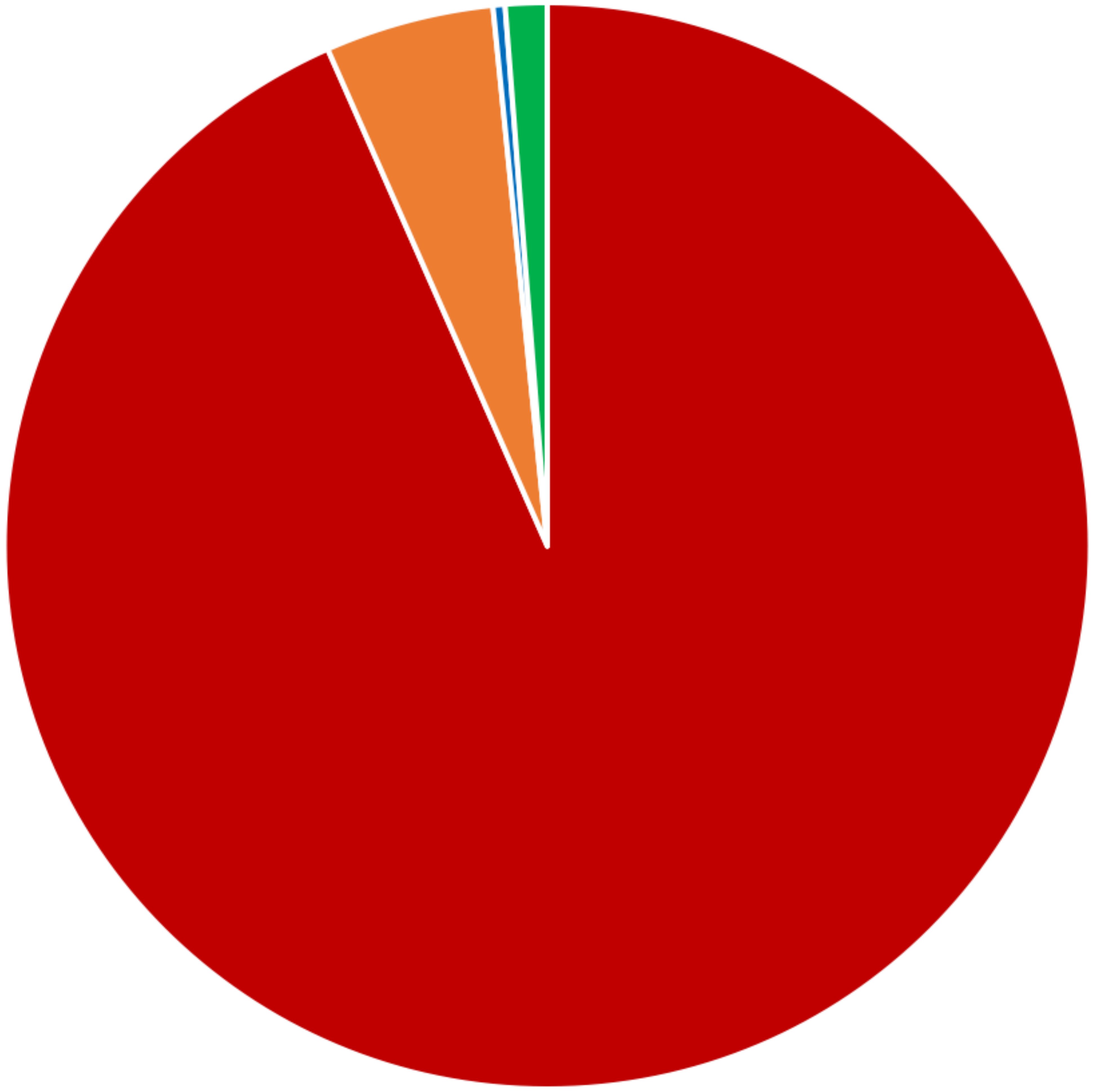

93.4% in ggH

5% in VBF

0.4% in VH

1.2% in ttH

H→μμ search in a nutshell

*The **divide-n-fit** is a common **strategy** used in **bump hunts** to **increase** the **sensitivity***

MVA training

- ***Train*** a MVA classifier to separate signal from SM backgrounds
- Exploit full ***kinematics*** of the event apart from the $\mathbf{m_{\mu\mu}}$
- Input features ***uncorrelated with*** $\boldsymbol{m_{\mu\mu}}$
- ***Signal*** events ***weighted by*** $\boldsymbol{1/(\sigma_m/m)}$ in the training to assign to ***high resolution*** events a ***higher score***

Event categories

- ***Divide*** events into exclusive categories based on the classifier output by ***maximising*** the ***significance***
- ***Purity increases*** as a function of the MVA output

Signal extraction

- ***Signal extracted*** by ***fitting*** $\boldsymbol{m_{\mu\mu}}$ distributions in each subcategories
- Signal and background modelled via ***parametric functions***
- ***Data-driven background prediction***

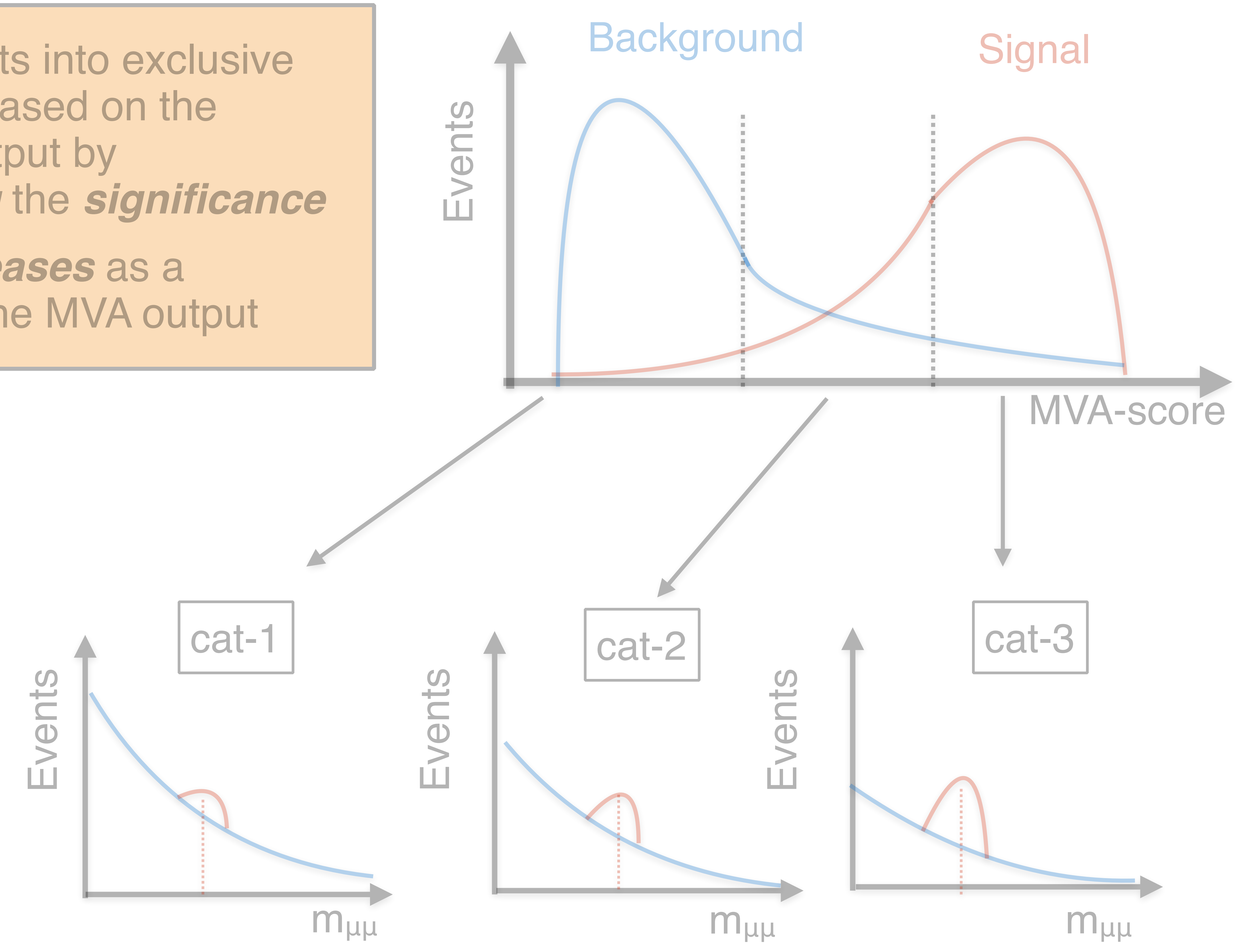

H→μμ search in a nutshell

*The **divide-n-fit** is a common **strategy** used in **bump hunts** to **increase** the **sensitivity***

MVA training

- ***Train*** a MVA classifier to separate signal from SM backgrounds
- Exploit full ***kinematics*** of the event apart from the **$m_{\mu\mu}$**
- Input features ***uncorrelated with $m_{\mu\mu}$***
- ***Signal*** events ***weighted by $1/(\sigma_m/m)$*** in the training to assign to ***high resolution*** events a ***higher score***

Event categories

- ***Divide*** events into exclusive categories based on the classifier output by ***maximising*** the ***significance***
- ***Purity increases*** as a function of the MVA output

Signal extraction

- ***Signal extracted*** by ***fitting $m_{\mu\mu}$*** distributions in each subcategories
- Signal and background modelled via ***parametric functions***
- ***Data-driven background prediction***

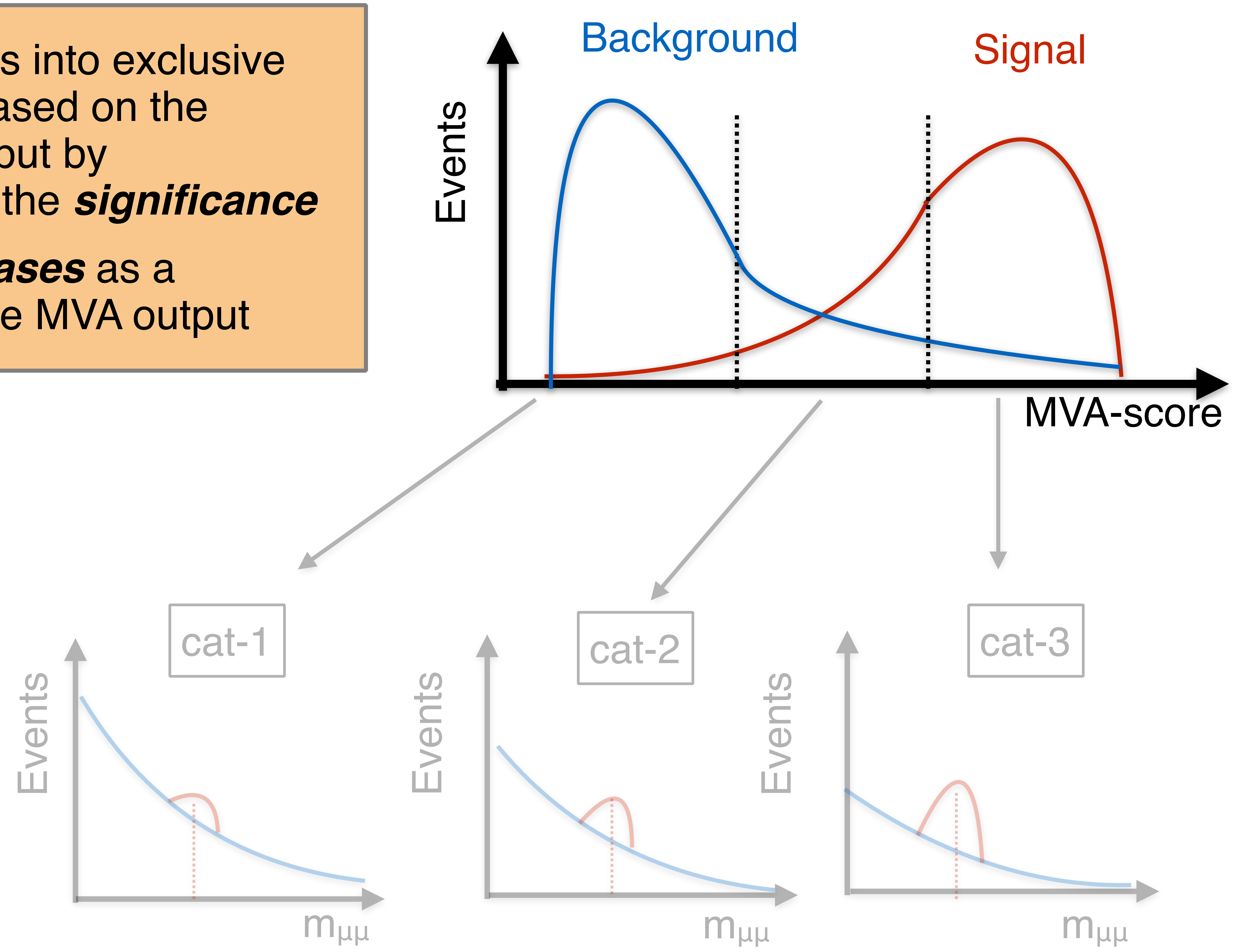

H→μμ search in a nutshell

*The **divide-n-fit** is a common **strategy** used in **bump hunts** to **increase** the **sensitivity***

MVA training

- ***Train*** a MVA classifier to separate signal from SM backgrounds
- Exploit full ***kinematics*** of the event apart from the $\mathbf{m_{\mu\mu}}$
- Input features ***uncorrelated with*** $\boldsymbol{m_{\mu\mu}}$
- ***Signal*** events ***weighted by*** $\boldsymbol{1/(\sigma_m/m)}$ in the training to assign to ***high resolution*** events a ***higher score***

Event categories

- ***Divide*** events into exclusive categories based on the classifier output by ***maximising*** the ***significance***
- ***Purity increases*** as a function of the MVA output

Signal extraction

- ***Signal extracted*** by ***fitting*** $\boldsymbol{m_{\mu\mu}}$ distributions in each subcategories
- Signal and background modelled via ***parametric functions***
- ***Data-driven background prediction***

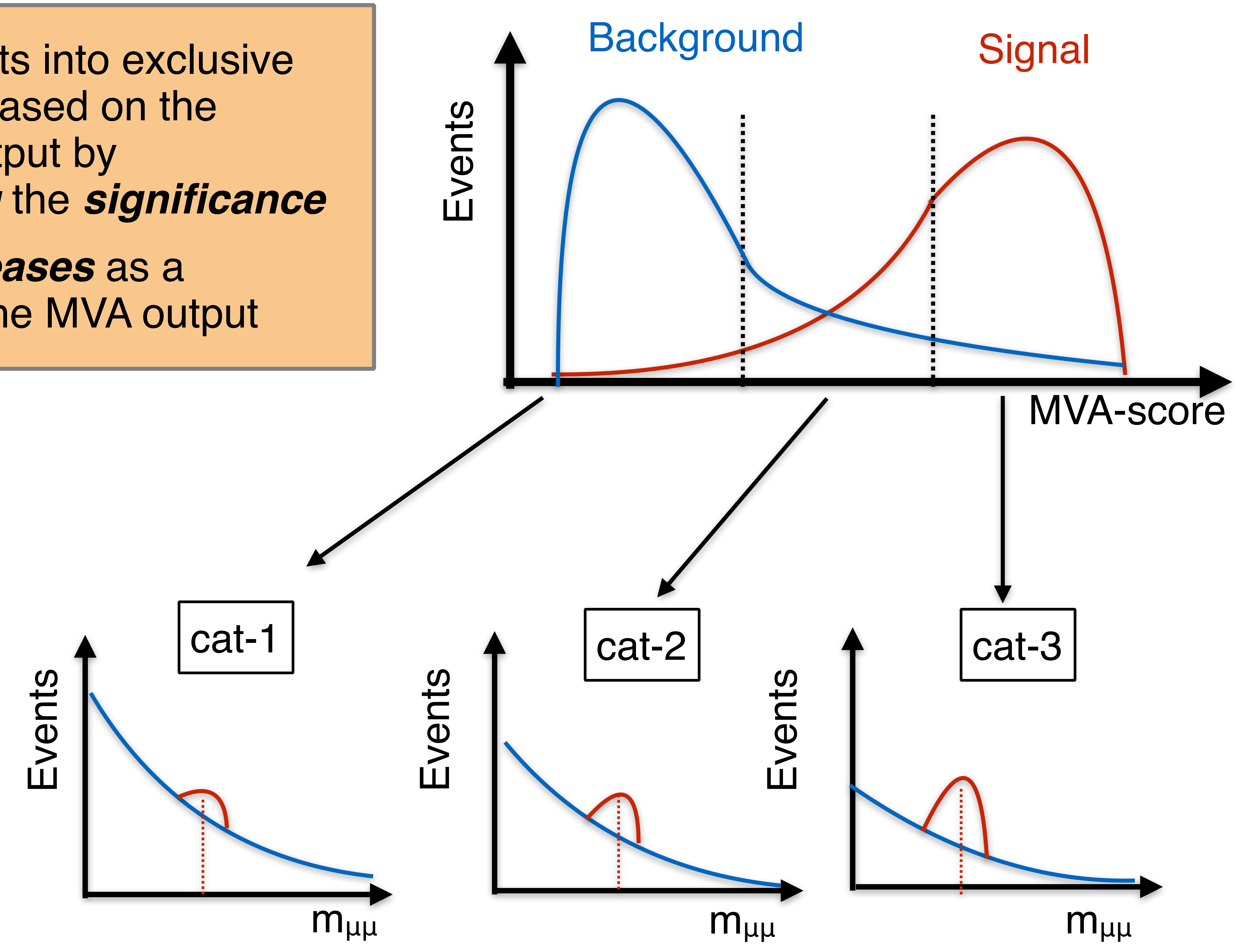

ttH-leptonic event candidate

How does a ttH-leptonic event look like?

ttH-leptonic event candidate

How does a ttH-leptonic event look like?

Higgs candidate

Dimuon pair with $m_{\mu\mu}$ in [110,150] GeV

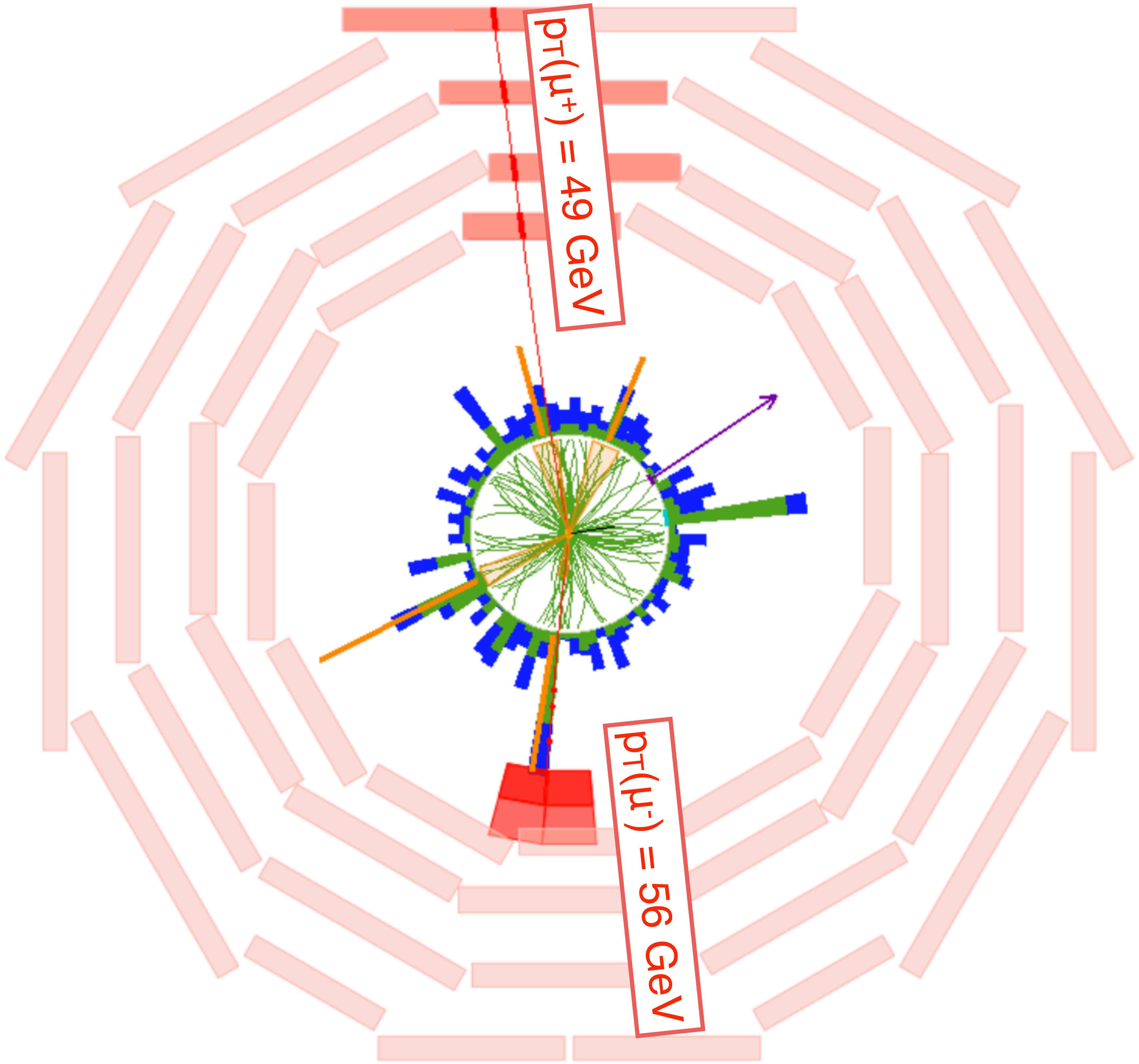

ttH-leptonic event candidate

How does a ttH-leptonic event look like?

Higgs candidate

Dimuon pair with $m_{\mu\mu}$ in [110,150] GeV

↓

At least one b-tagged jet in the event with p_T > 25 GeV

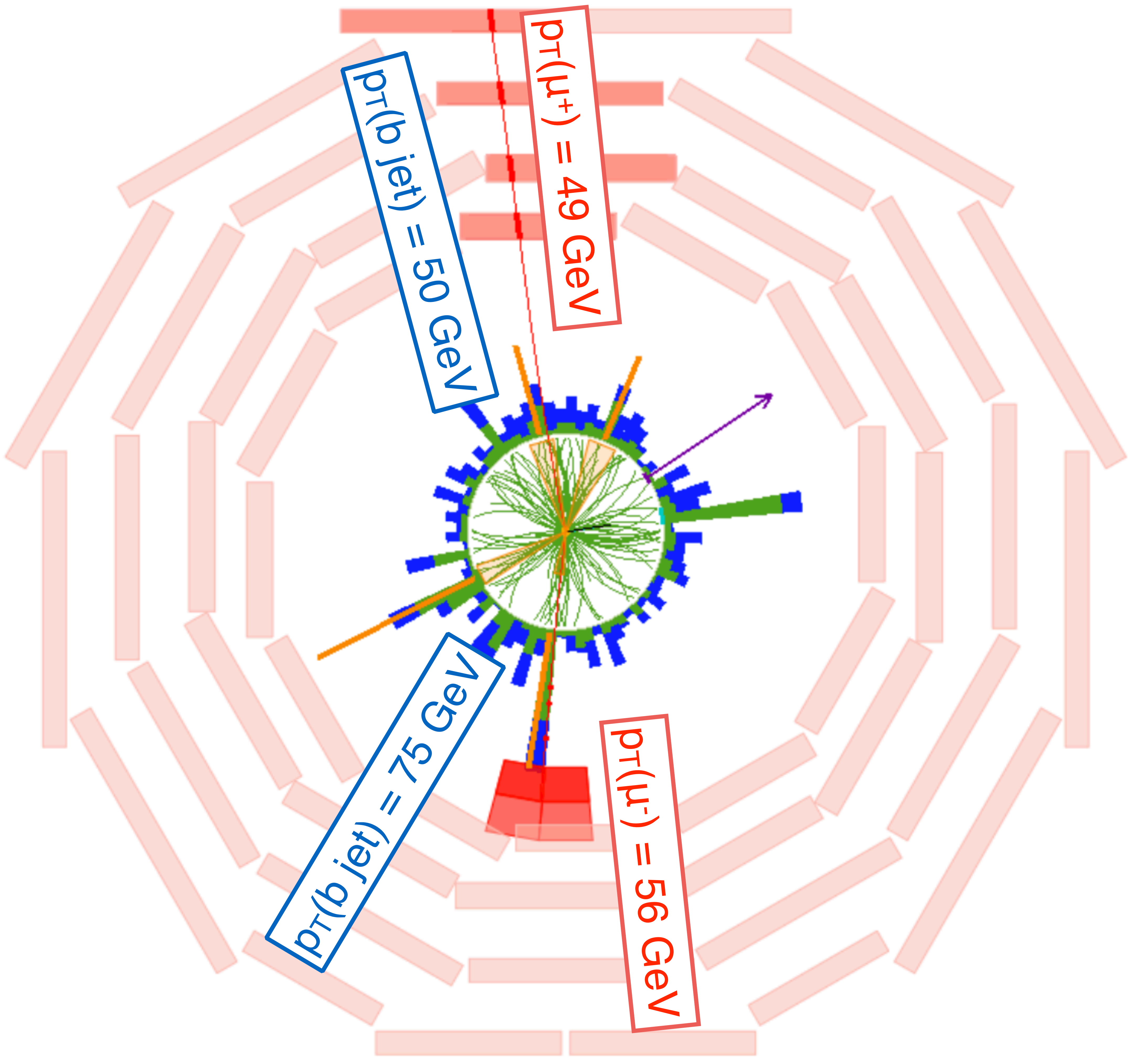

ttH-leptonic event candidate

How does a ttH-leptonic event look like?

Higgs candidate

Dimuon pair with $m_{\mu\mu}$ in [110,150] GeV

↓

At least one b-tagged jet in the event with $p_T > 25$ GeV

↓

One *or* ***two additional leptons*** with $p_T > 20$ GeV

↓

Significant ***missing transverse momentum***

ttH leptonic

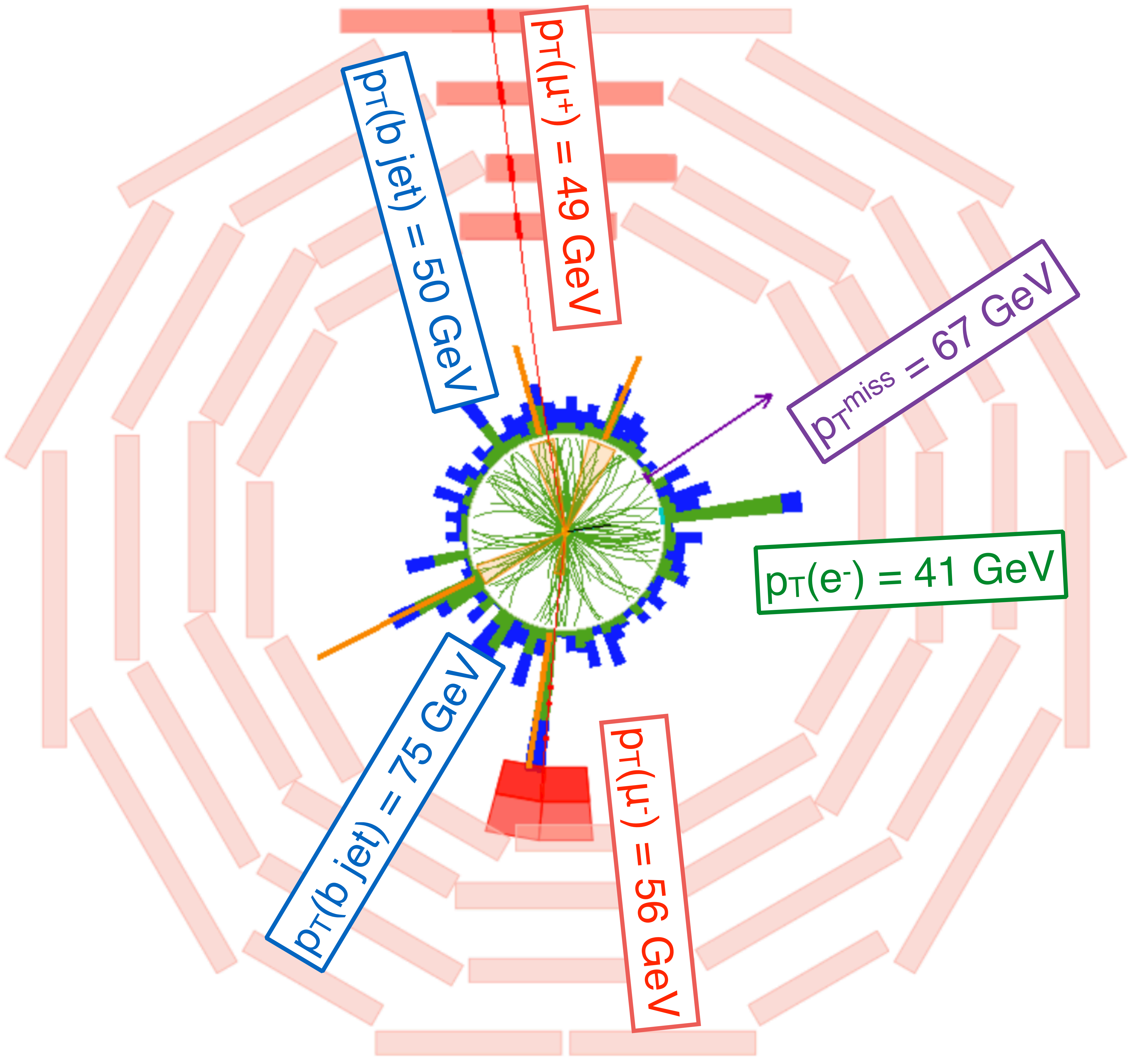

ttH-hadronic event candidate

How does a ttH-hadronic event look like?

Higgs candidate

Dimuon pair with $m_{\mu\mu}$ in [110,150] GeV

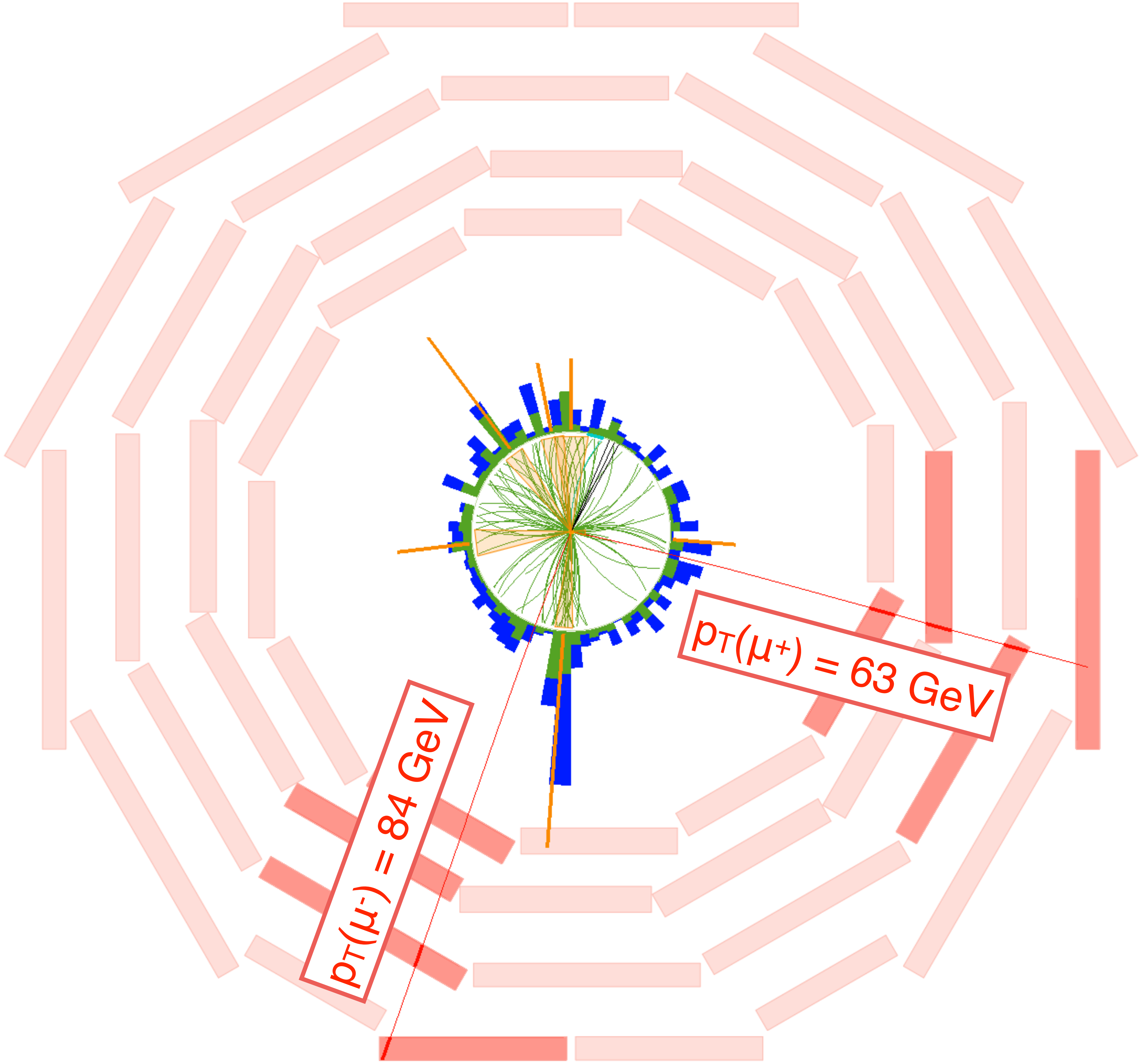

ttH-hadronic event candidate

How does a ttH-hadronic event look like?

Higgs candidate
Dimuon pair with $m_{\mu\mu}$ in [110,150] GeV

↓

At least one b-tagged jet in the event with $p_T > 25$ GeV

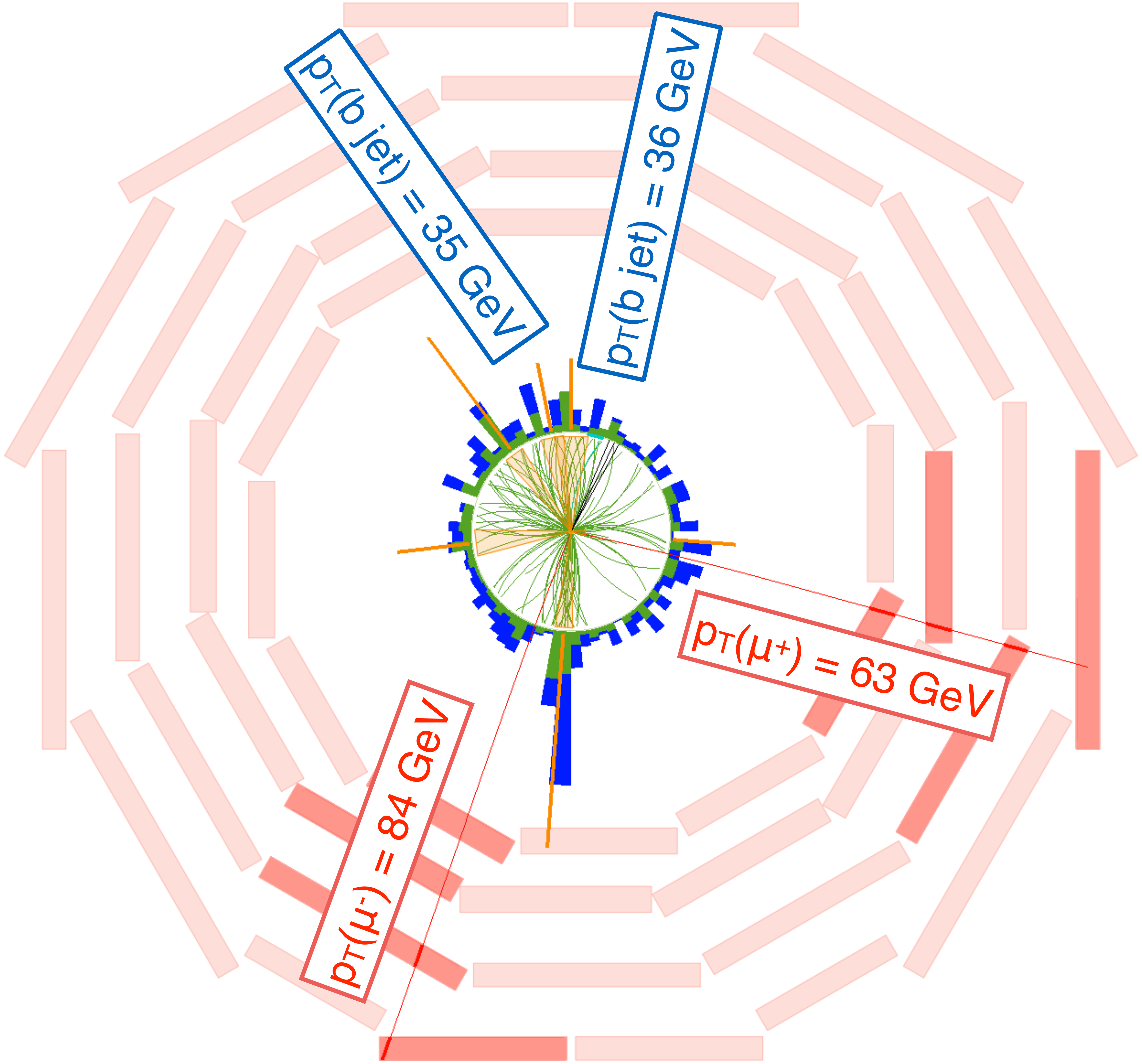

ttH-hadronic event candidate

How does a ttH-hadronic event look like?

Higgs candidate
Dimuon pair with $m_{\mu\mu}$ in [110,150] GeV

↓

At least one b-tagged jet in the event with $p_T > 25$ GeV

↓

No additional leptons with $p_T > 20$ GeV

↓

Hadronic activity

- At least 3-jets with $p_T > 25$ GeV
- Leading jet $p_T > 50$ GeV
- At least one jet triplet with $100 < m_{jjj} < 300$ GeV

ttH hadronic

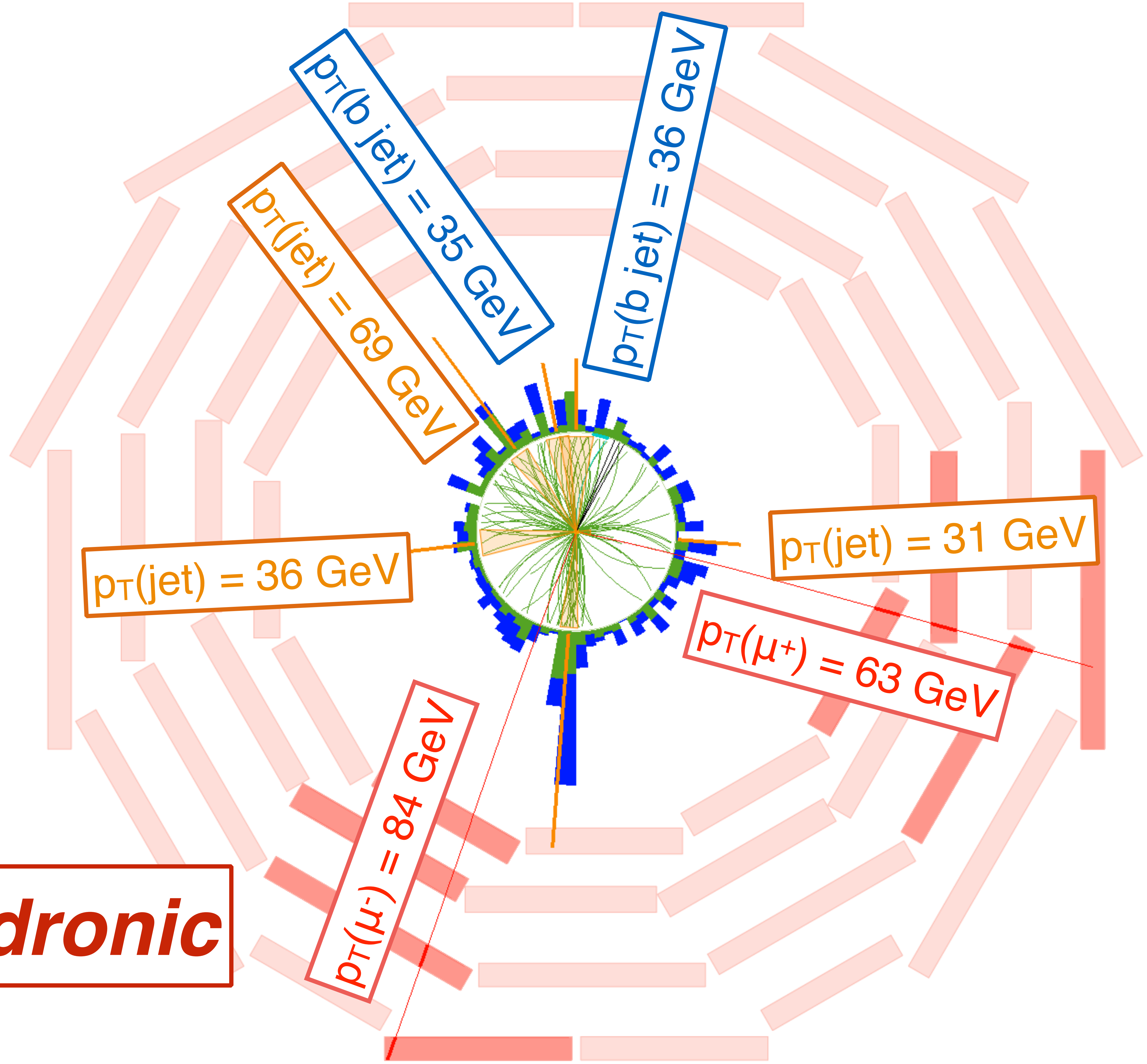

ttH event categories

- ***Divide-n-fit*** strategy employed in the signal extraction

ttH hadronic BDT

- **Higgs candidate:** p_T, rapidity, decay angles (ϕ_{cs}, $\cos(\theta)_{CS}$)
- N_{jets}, H_T, H_T^{miss}, and E_T^{miss}
- p_T and η of the ***three leading jets***
- **Top candidate:** RHTT, top p_T, p_T balance ($\mu\mu$,top) ..
- **RHTT** is a BDT trained to identify top quarks decaying to three resolved jets

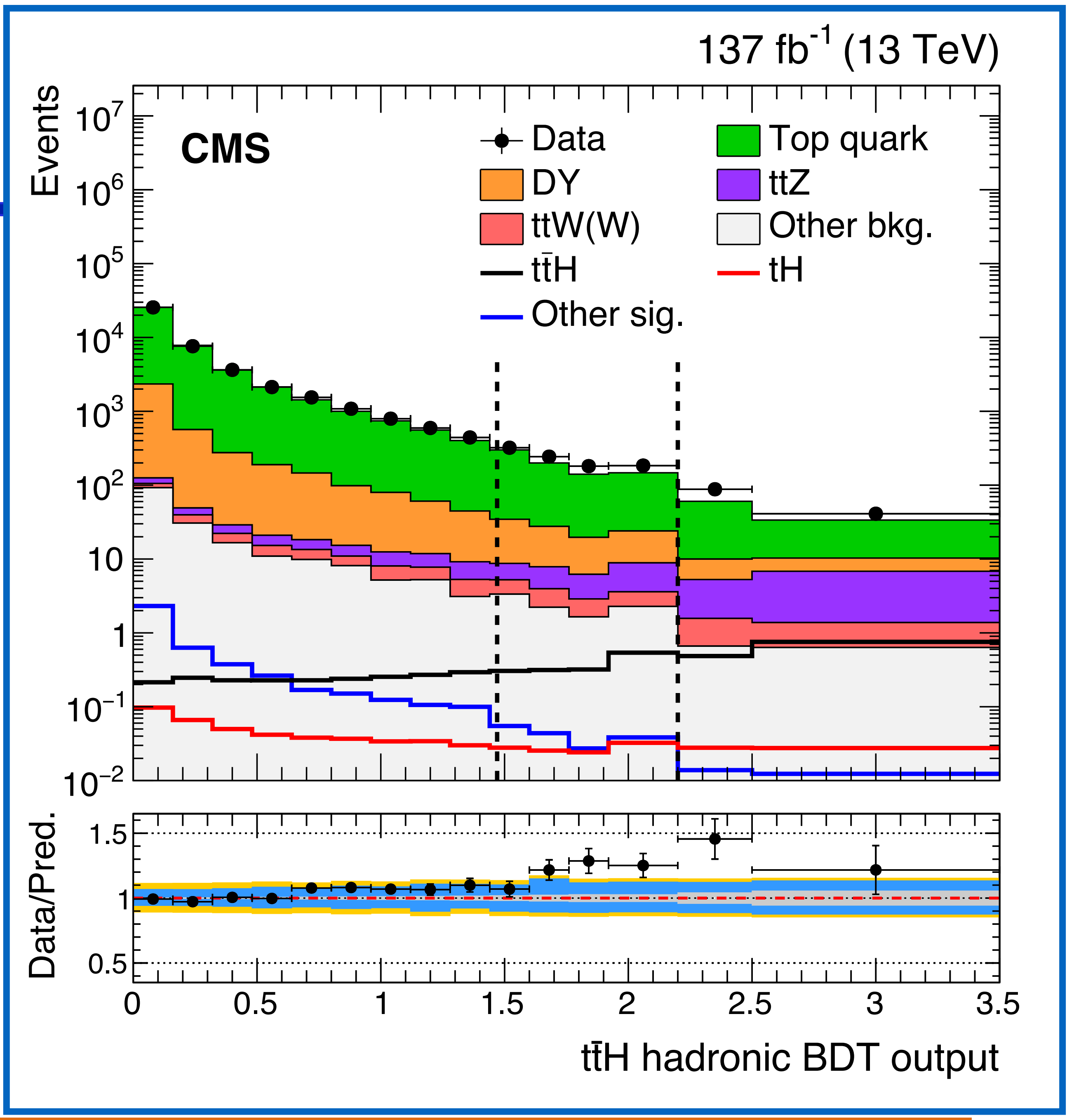

ttH leptonic BDT

- **Higgs candidate:** p_T, rapidity, decay angles (ϕ_{cs}, $\cos(\theta)_{CS}$)
- N_{jets}, H_T, H_T^{miss}, and E_T^{miss}
- Highest p_T ***additional lepton*** (ℓ_T): p_T and flavour
- $\Delta\phi(\mu\mu, \ell_T)$, $m(\ell_T$,b-tagged jet), $m_T(E_T^{miss},\ell_T)$
- Other variables ….

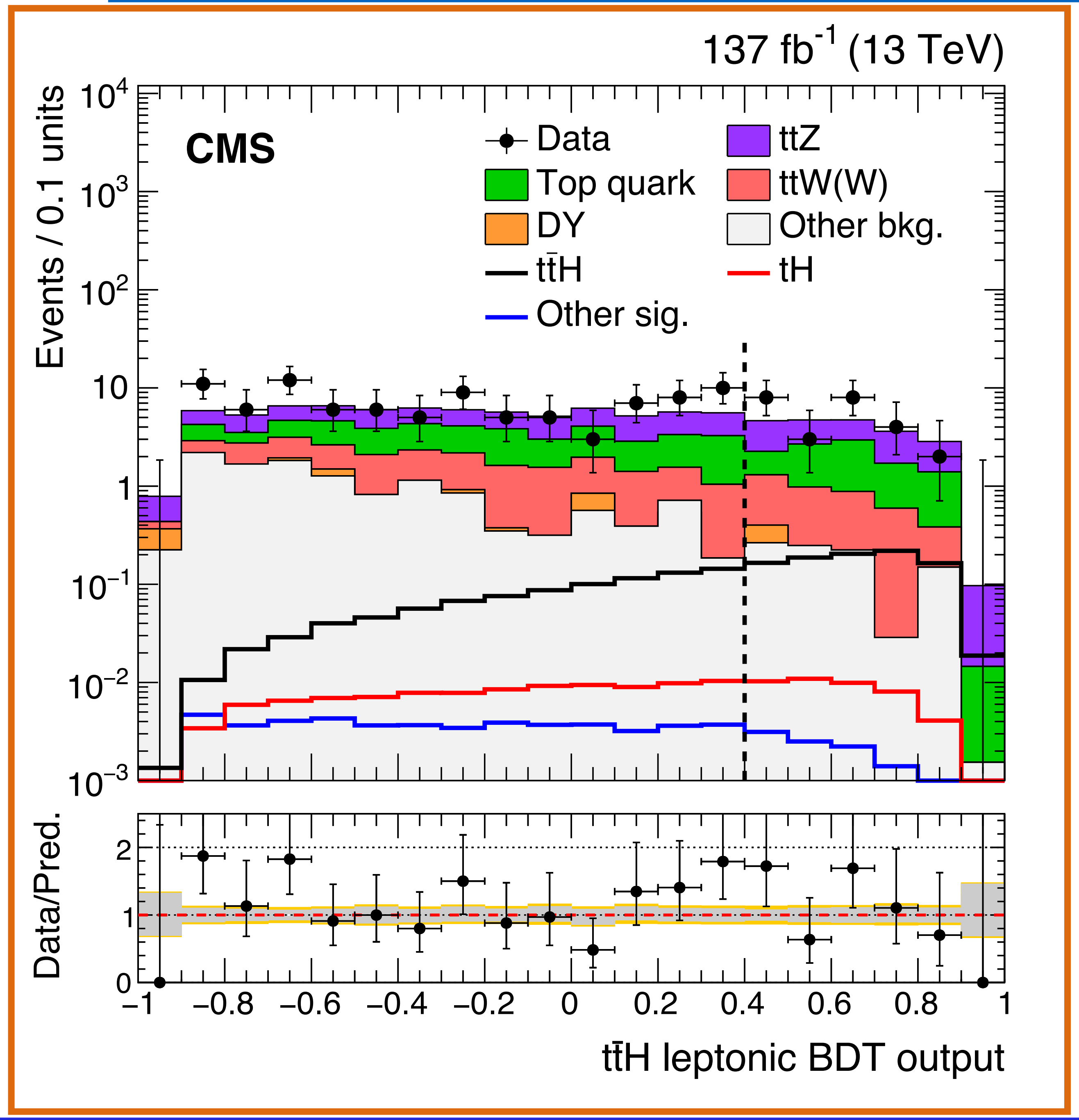

ttH event categories

- ***Divide-n-fit*** strategy employed in the signal extraction

ttH hadronic BDT

- **Higgs candidate:** p_T, rapidity, decay angles (ϕ_{cs}, $\cos(\theta)_{CS}$)
- N_{jets}, H_T, H_T^{miss}, and E_T^{miss}
- p_T and η of the ***three leading jets***
- **Top candidate:** RHTT, top p_T, p_T balance ($\mu\mu$,top) ..
- **RHTT** is a BDT trained to identify top quarks decaying to three resolved jets

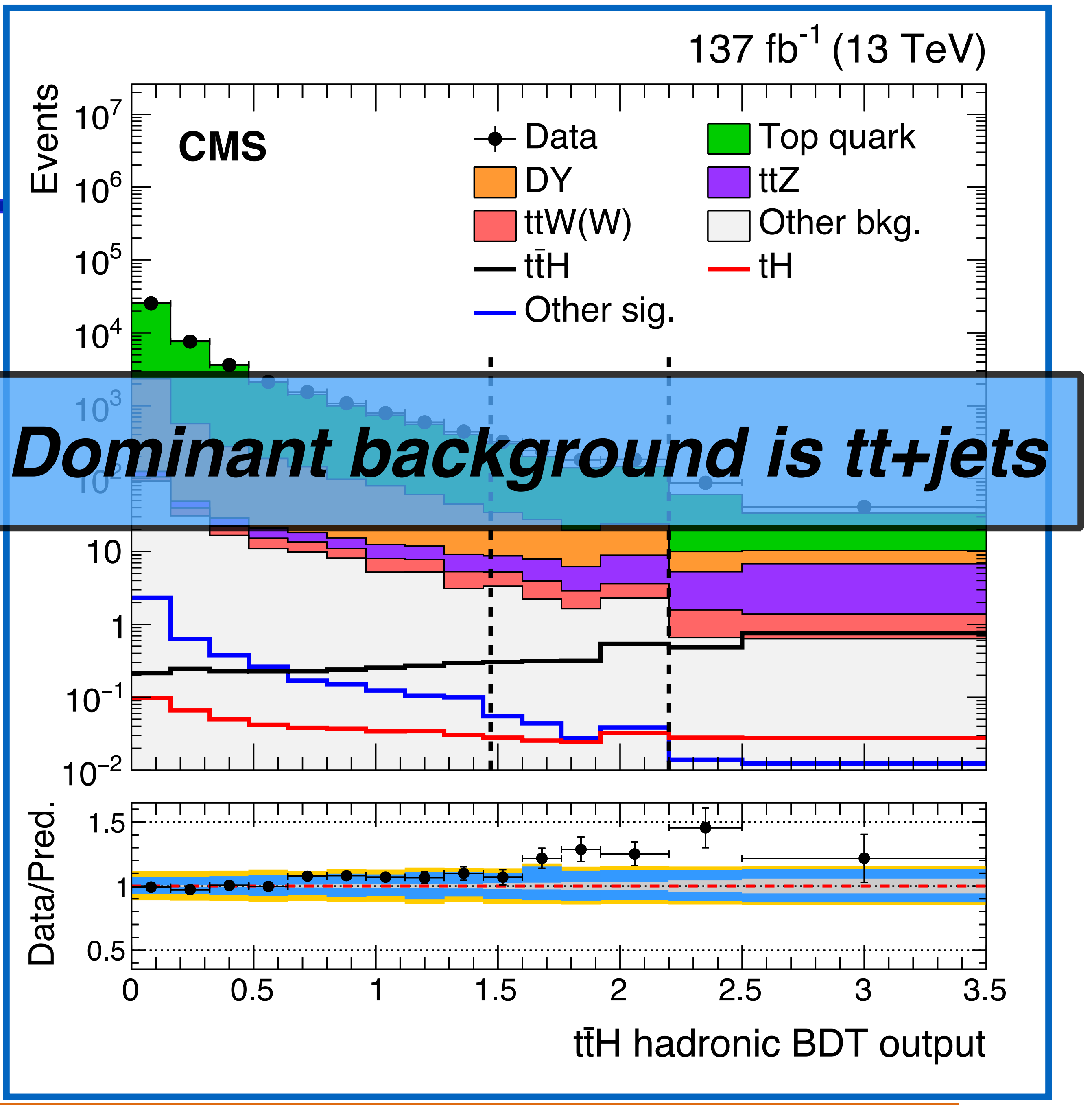

Dominant background is tt+jets

ttH leptonic BDT

- **Higgs candidate:** p_T, rapidity, decay angles (ϕ_{cs}, $\cos(\theta)_{CS}$)
- N_{jets}, H_T, H_T^{miss}, and E_T^{miss}
- Highest p_T ***additional lepton*** (ℓ_T): p_T and flavour
- $\Delta\phi(\mu\mu, \ell_T)$, $m(\ell_T$,b-tagged jet), $m_T(E_T^{miss}, \ell_T)$
- Other variables ….

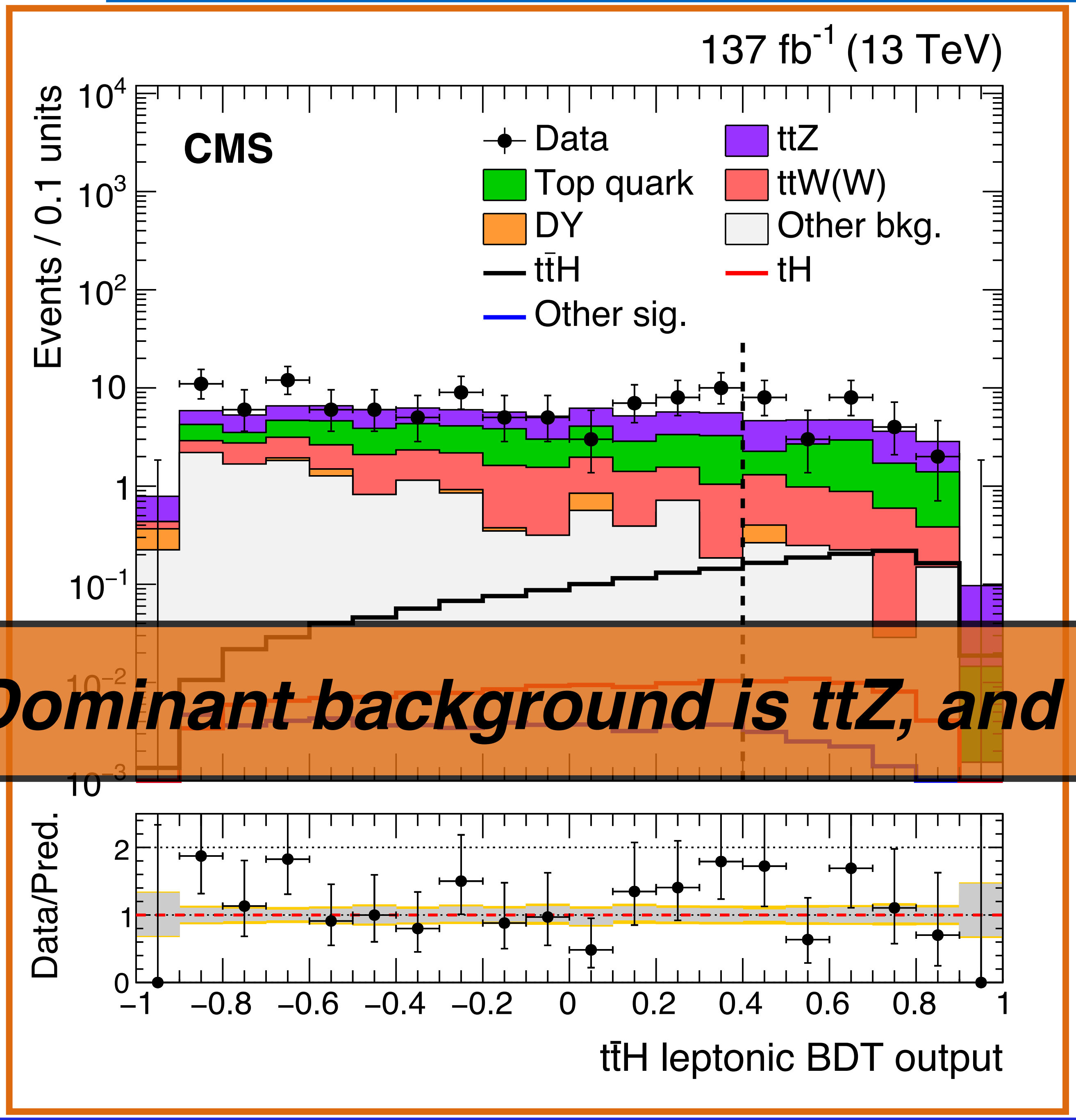

Dominant background is ttZ, and tt+jets

ttH category results

- ***Divide-n-fit*** strategy → ***three*** subcategories in ***ttH-hadronic*** and ***two*** subcategories in ***ttH-leptonic***
- ***Signal*** → $m_{\mu\mu}$ distributions parametrised via Double Crystal-Ball function
- ***Background*** → $m_{\mu\mu}$ distributions modelled via ***empirical functions*** chosen to provide a ***negligible bias*** in the S+B fit

Highest purity ttH categories

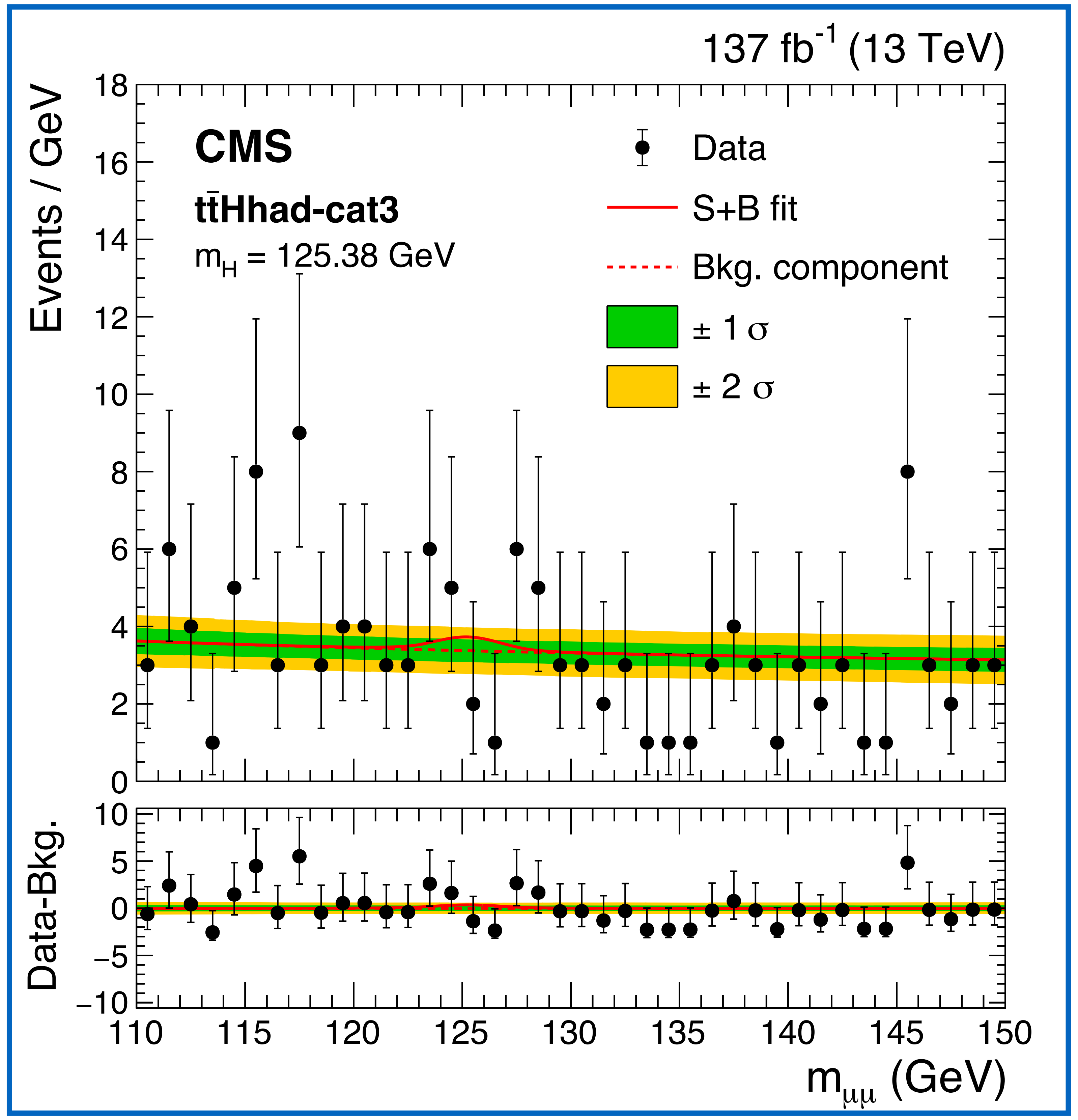

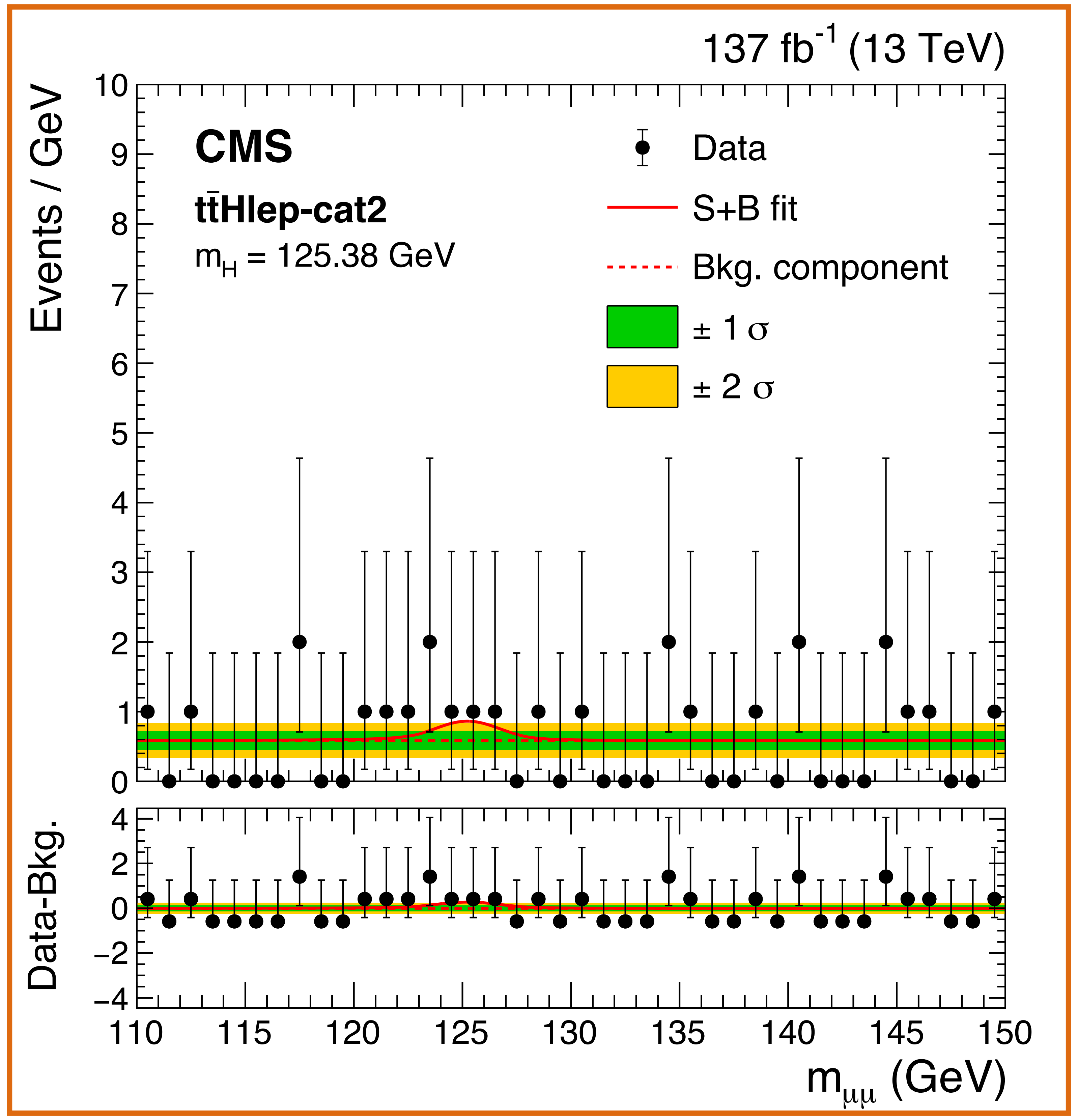

ttH category results

- ***Expected*** significance of 0.5σ
- ***Observed*** significance of 1.2σ
- **Signal strength** $\mu = 2.32^{+2.27}_{-1.95}$

WH event candidate

How does a WH-leptonic event look like?

WH event candidate

How does a WH-leptonic event look like?

Higgs candidate
Dimuon pair with $m_{\mu\mu}$ in [110,150] GeV

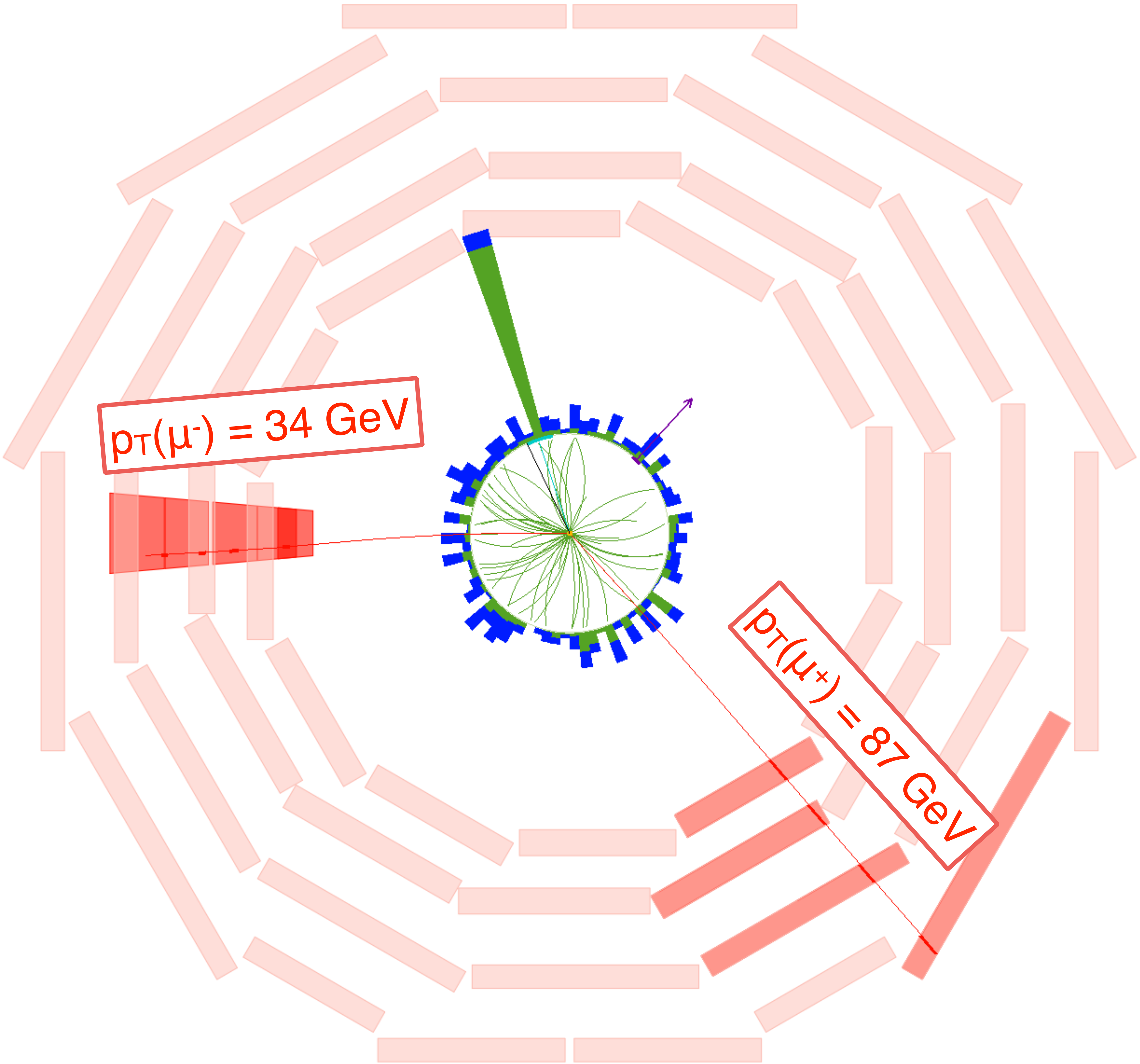

WH event candidate

How does a WH-leptonic event look like?

Higgs candidate
Dimuon pair with $m_{\mu\mu}$ in [110,150] GeV

↓

No b-tagged jets in the event

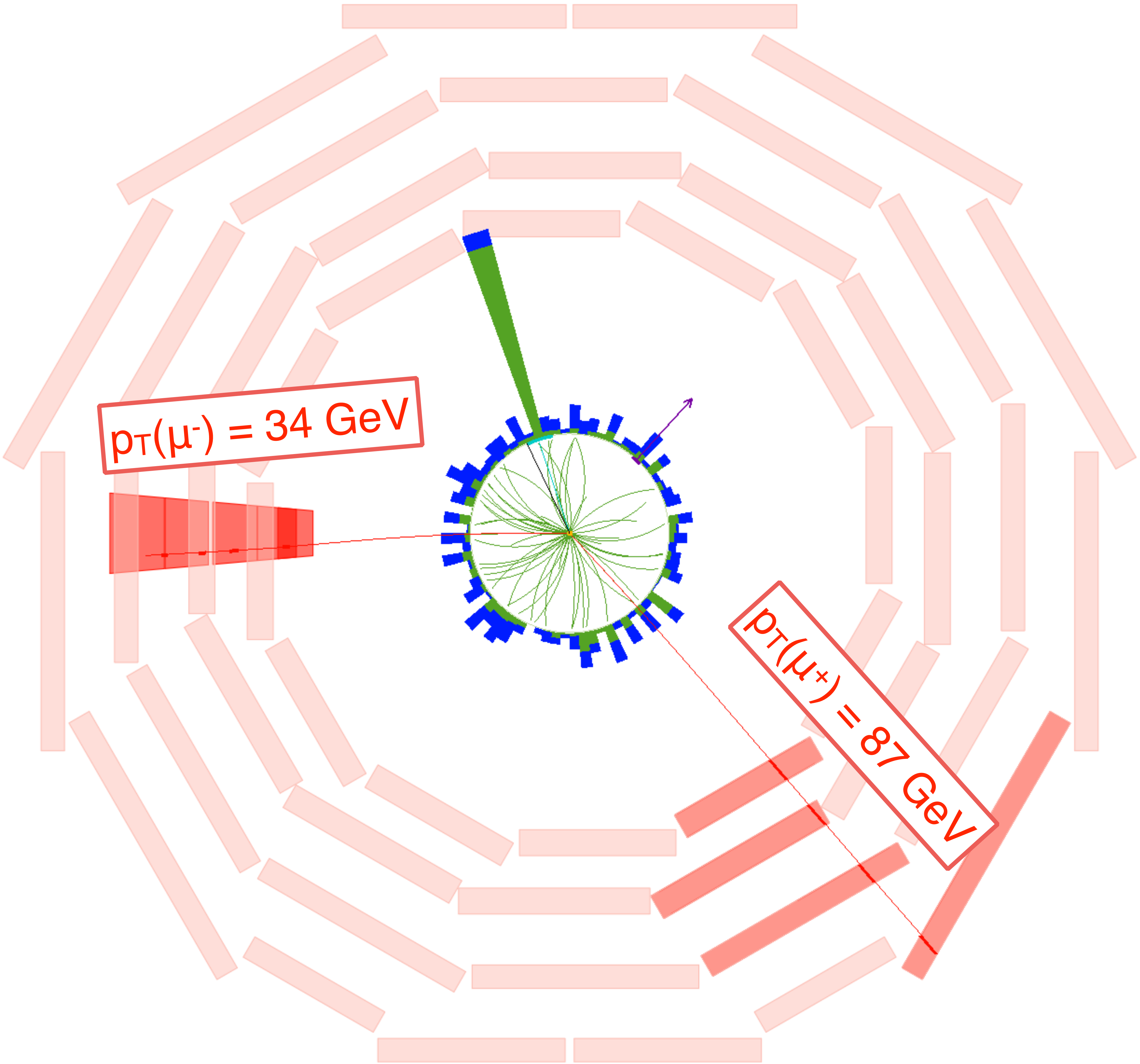

WH event candidate

How does a WH-leptonic event look like?

Higgs candidate
Dimuon pair with $m_{\mu\mu}$ in [110,150] GeV

↓

No b-tagged jets in the event

↓

One additional lepton
with $p_T > 20$ GeV

↓

Significant ***missing transverse momentum***

WH leptonic

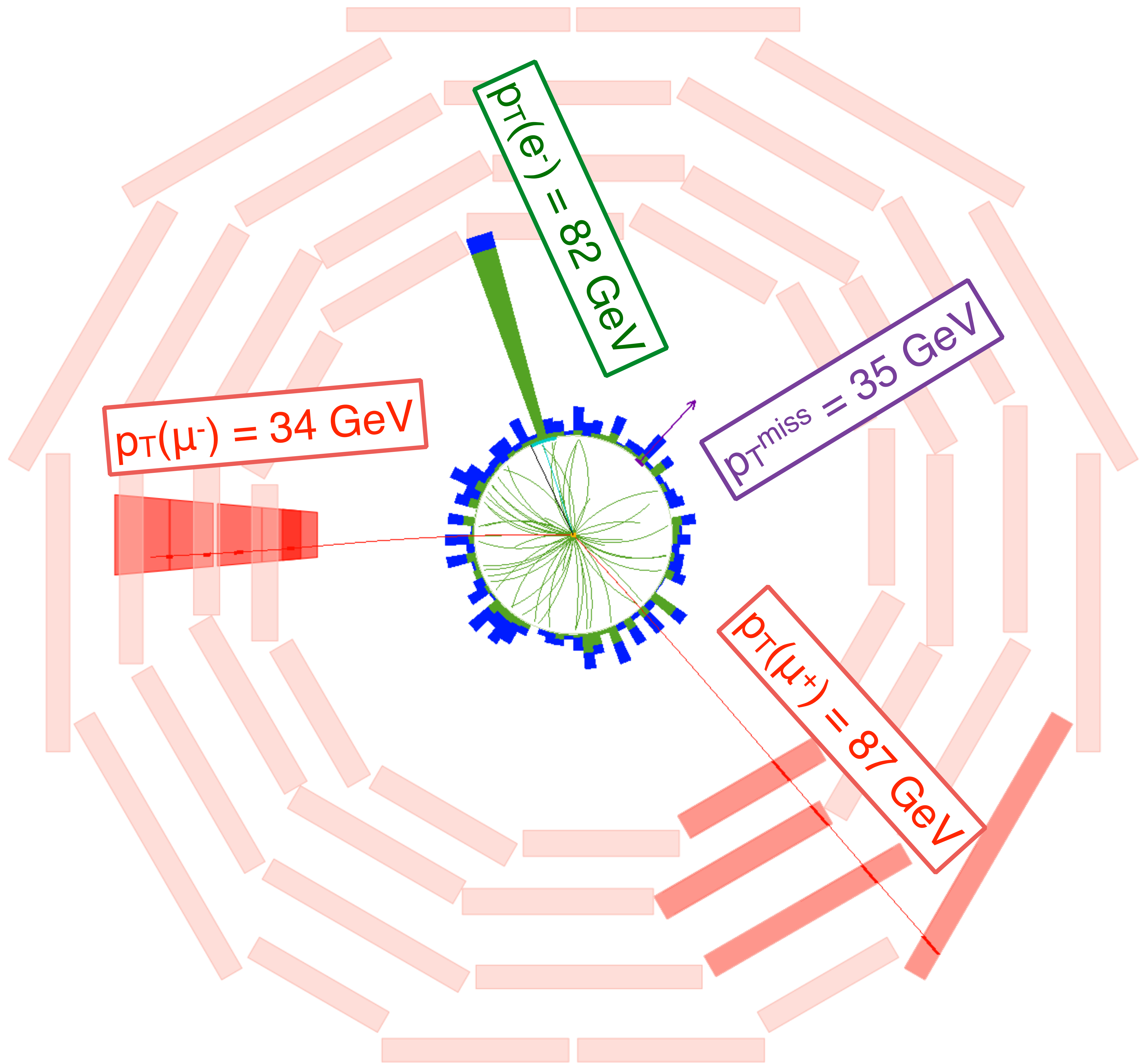

ZH event candidate

How does a ZH leptonic event look like?

ZH event candidate

How does a ZH leptonic event look like?

Higgs candidate

Dimuon pair with $m_{\mu\mu}$ in [110,150] GeV

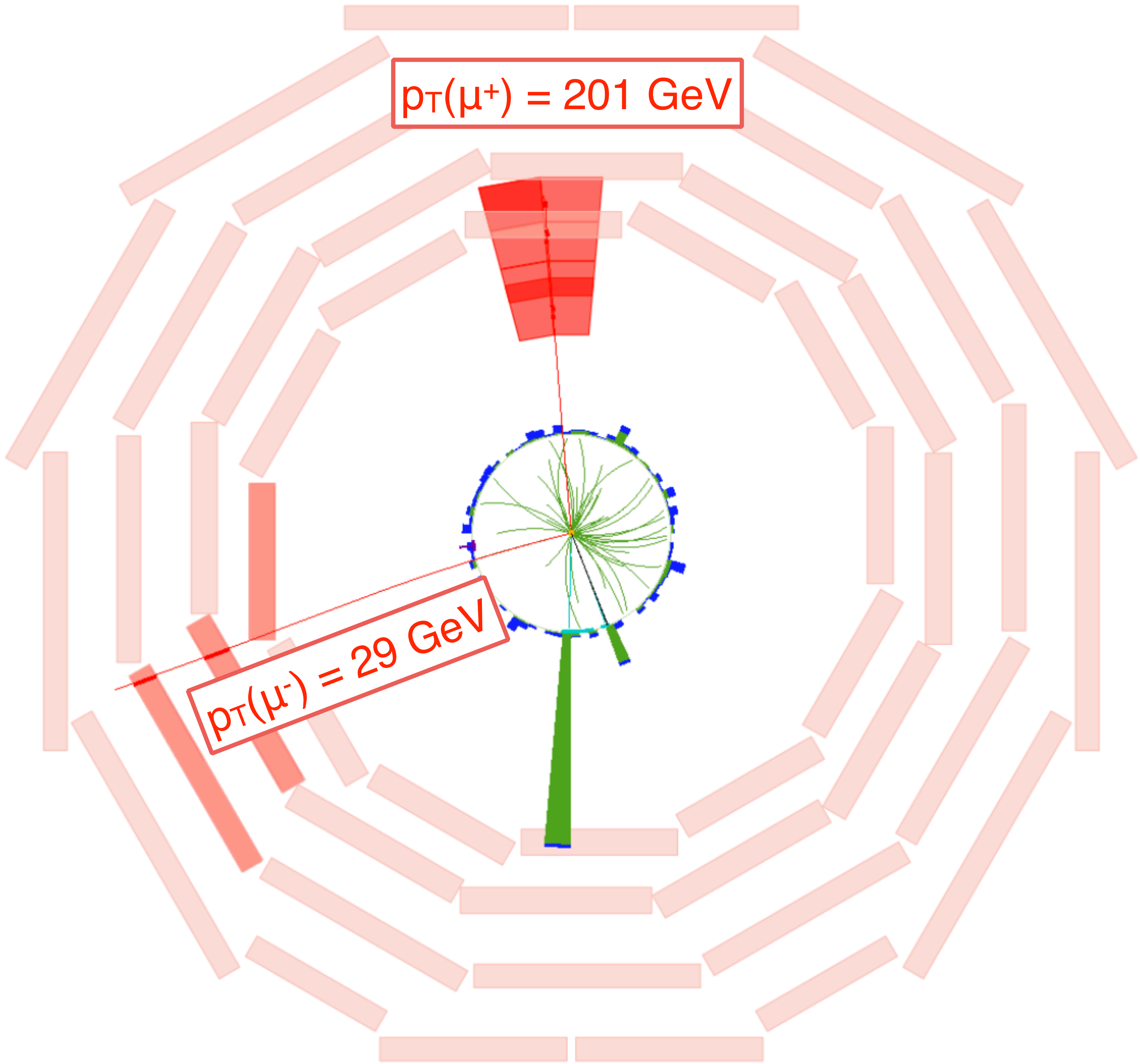

ZH event candidate

How does a ZH leptonic event look like?

Higgs candidate

Dimuon pair with $m_{\mu\mu}$ in [110,150] GeV

↓

No b-tagged jets in the event with $p_T > 25$ GeV

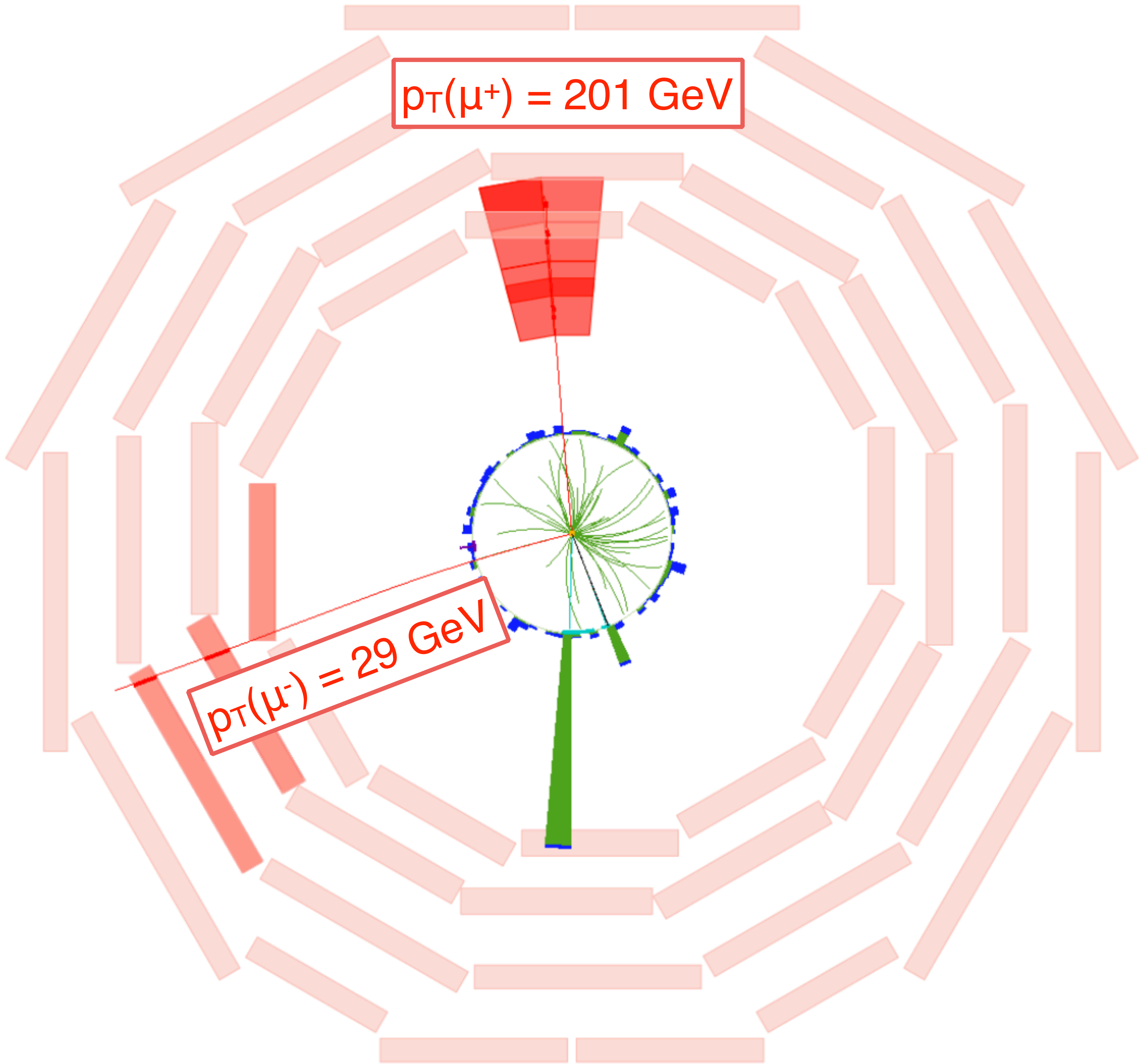

ZH event candidate

How does a ZH leptonic event look like?

Higgs candidate

Dimuon pair with $m_{\mu\mu}$ in [110,150] GeV

↓

No b-tagged jets in the event with $p_T > 25$ GeV

↓

Additional e^+e^- or $\mu^+\mu^-$ pair

$81 < m_{\mu\mu} < 101$ GeV

$71 < m_{ee} < 111$ GeV

ZH leptonic

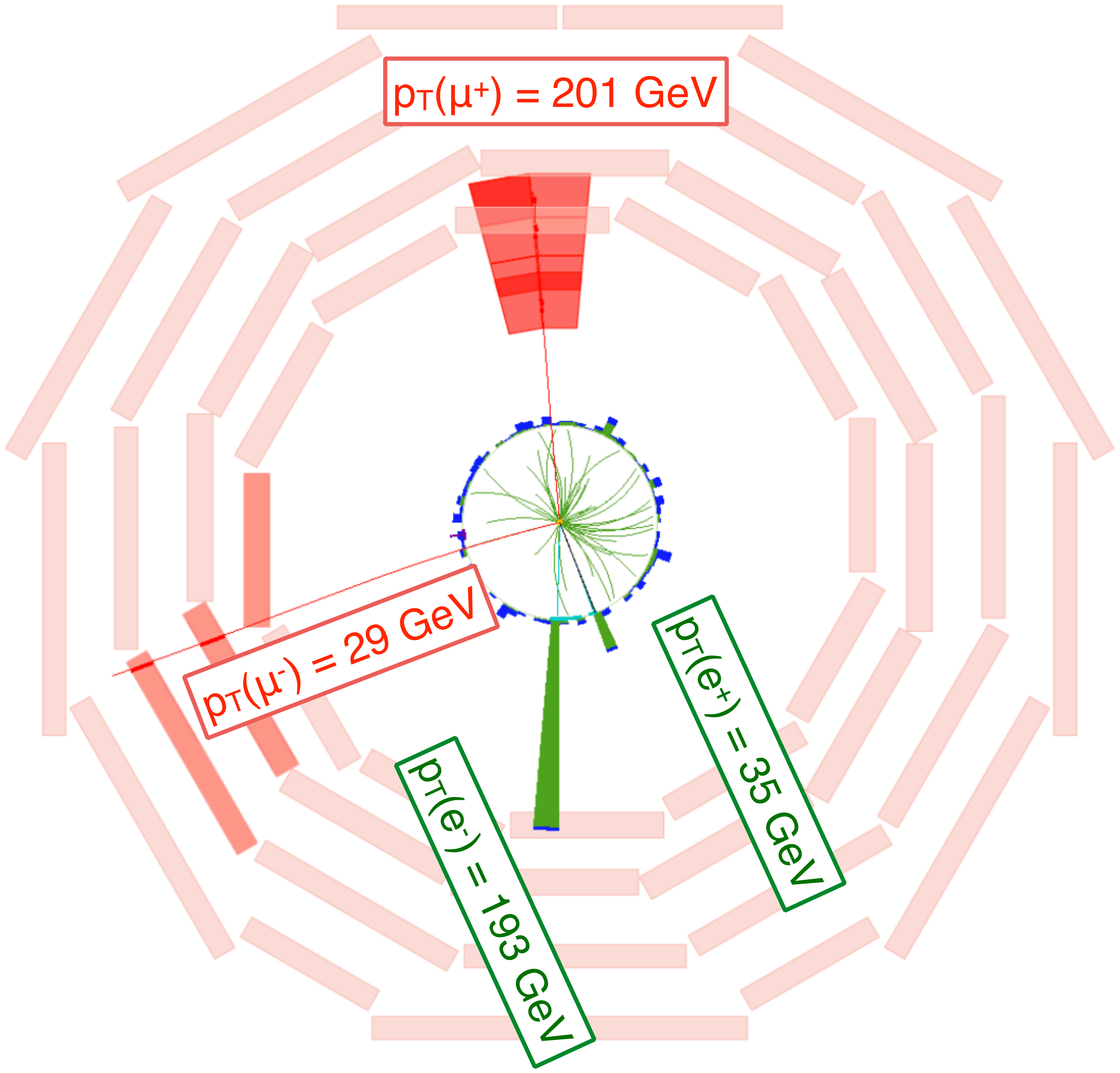

VH event categories

- ***Divide-n-fit*** strategy employed in the signal extraction

WH leptonic BDT

- **Higgs candidate:** p_T, rapidity, decay angles (ϕ_{cs}, $\cos(\theta)_{CS}$)
- H_T^{miss} and E_T^{miss}
- ***Additional lepton*** in the event (ℓ_W): p_T and flavour
- $\Delta\phi(\mu\mu,\ell_W)$, $\Delta\eta(\mu\mu,\ell_W)$,, $\Delta\phi(\ell_W,H_T^{miss})$, etc …
- $m_T(\ell_W,H_T^{miss})$

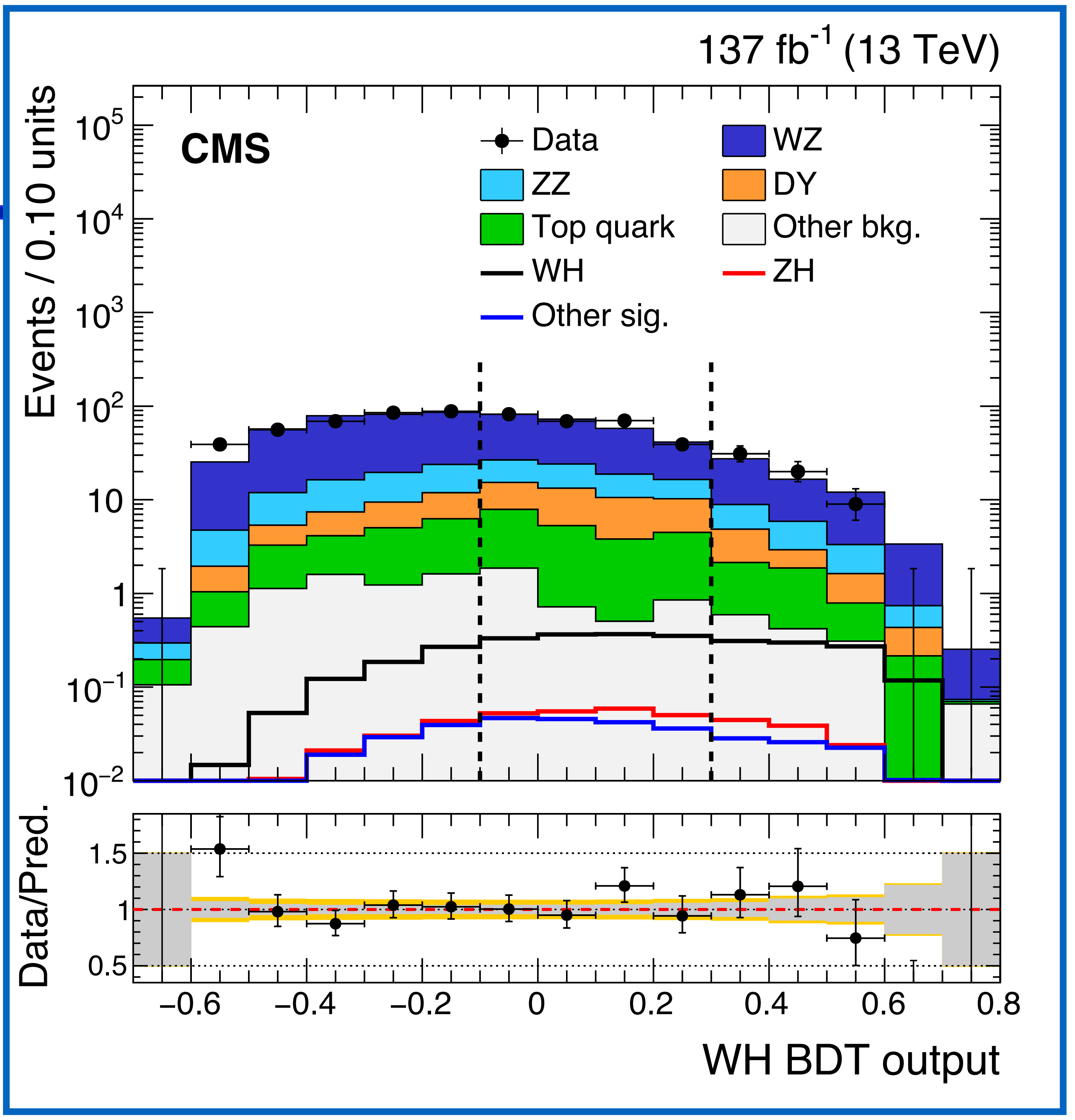

ZH leptonic BDT

- **Higgs candidate:** p_T, rapidity, decay angles (ϕ_{cs}, $\cos(\theta)_{CS}$)
- η of muons from the Higgs candidate
- **Z boson candidate:** p_T, rapidity, invariant mass, flavour
- $\Delta\phi$($\mu\mu$ from H), ΔR($\ell\ell$ from Z), $\Delta\phi$($\mu\mu$ from H, $\ell\ell$ from Z)

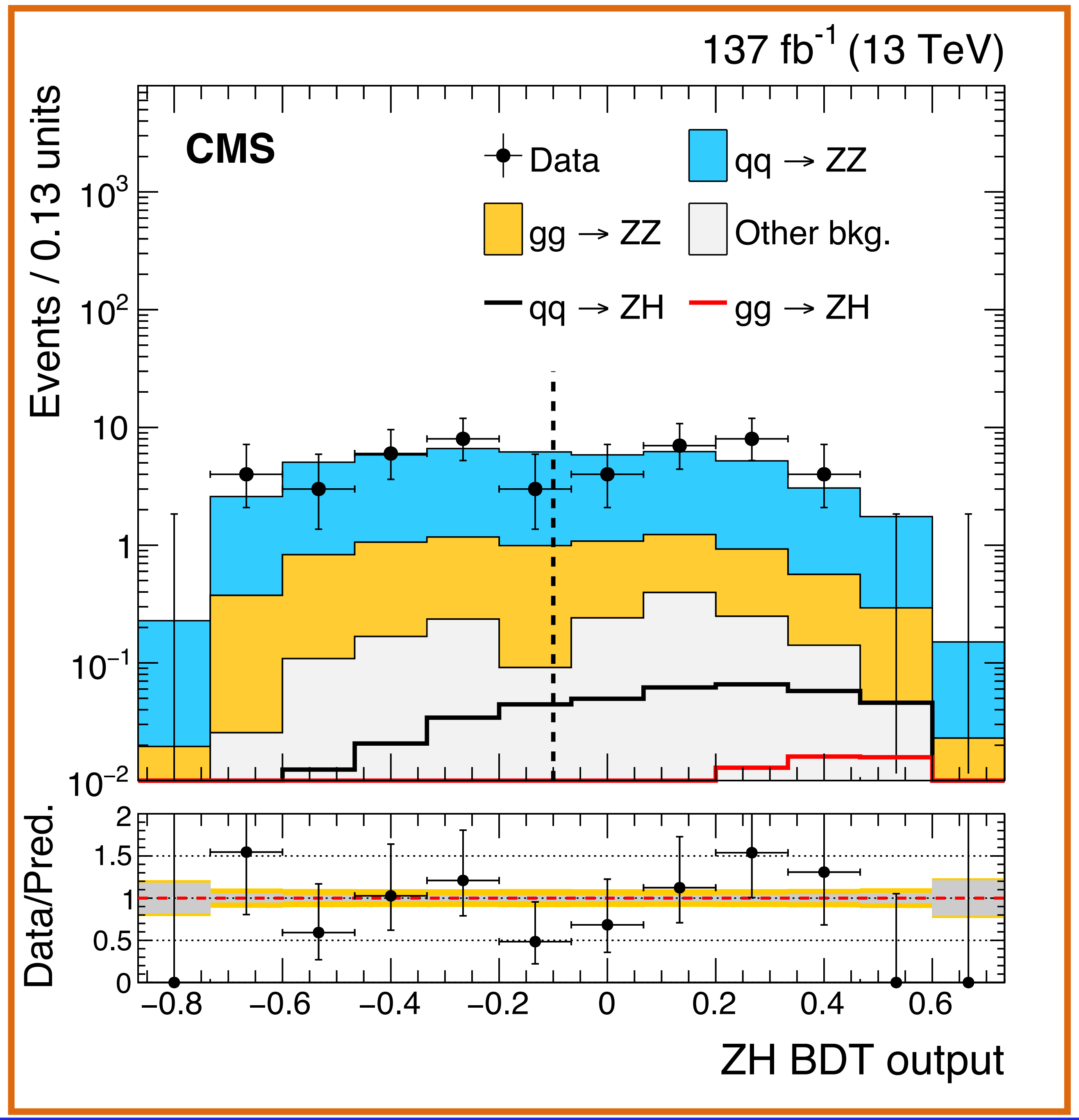

VH event categories

- ***Divide-n-fit*** strategy employed in the signal extraction

WH leptonic BDT

- **Higgs candidate:** p_T, rapidity, decay angles (ϕ_{CS}, $\cos(\theta)_{CS}$)
- H_T^{miss} and E_T^{miss}
- ***Additional lepton*** in the event (ℓ_W): p_T and flavour
- $\Delta\phi(\mu\mu,\ell_W)$, $\Delta\eta(\mu\mu,\ell_W)$,, $\Delta\phi(\ell_W,H_T^{miss})$, etc …
- $m_T(\ell_W,H_T^{miss})$

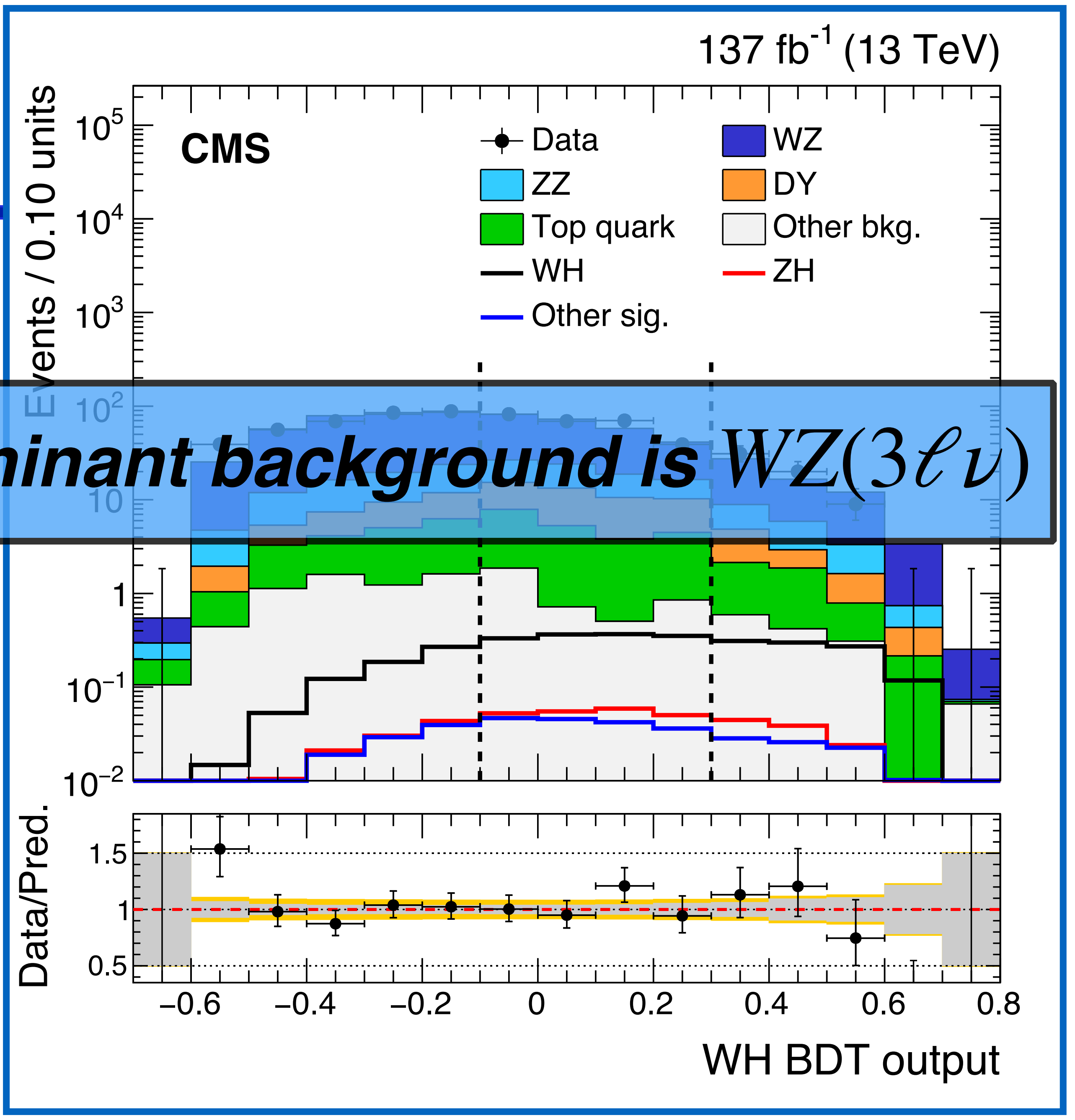

Dominant background is $WZ(3\ell\nu)$

ZH leptonic BDT

- **Higgs candidate:** p_T, rapidity, decay angles (ϕ_{CS}, $\cos(\theta)_{CS}$)
- η of muons from the Higgs candidate
- **Z boson candidate:** p_T, rapidity, invariant mass, flavour
- $\Delta\phi$($\mu\mu$ from H), ΔR($\ell\ell$ from Z), $\Delta\phi$($\mu\mu$ from H, $\ell\ell$ from Z)

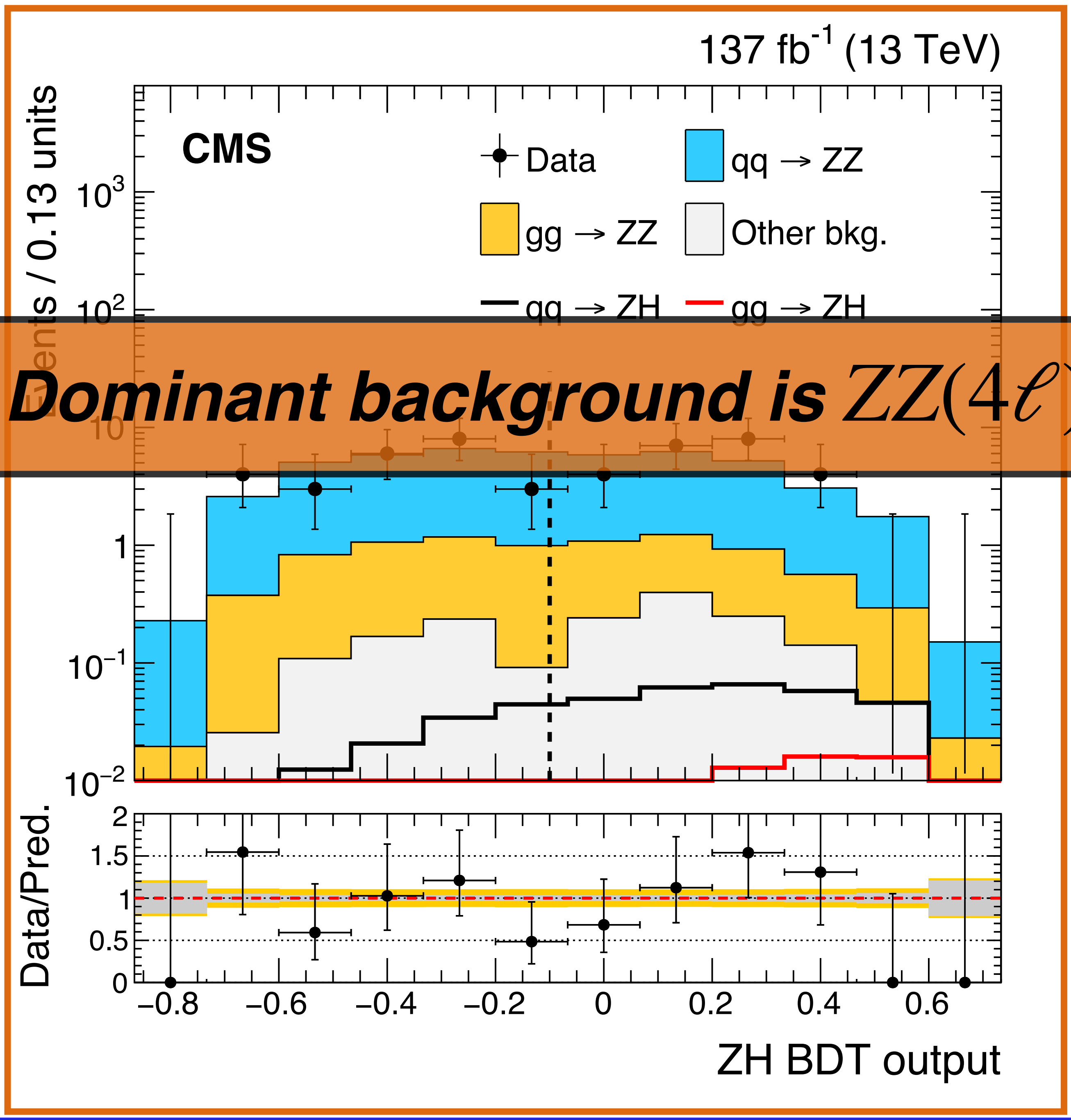

Dominant background is $ZZ(4\ell)$

VH category results

- ***Divide-n-fit*** strategy → ***three*** subcategories in ***WH-leptonic*** and ***two*** subcategories in ***ZH-leptonic***
- ***Signal*** → $m_{\mu\mu}$ distributions parametrised via Double Crystal-Ball function
- ***Background*** → $m_{\mu\mu}$ distributions modelled via ***empirical functions*** chosen to provide a ***negligible bias*** in the S+B fit

Highest purity categories

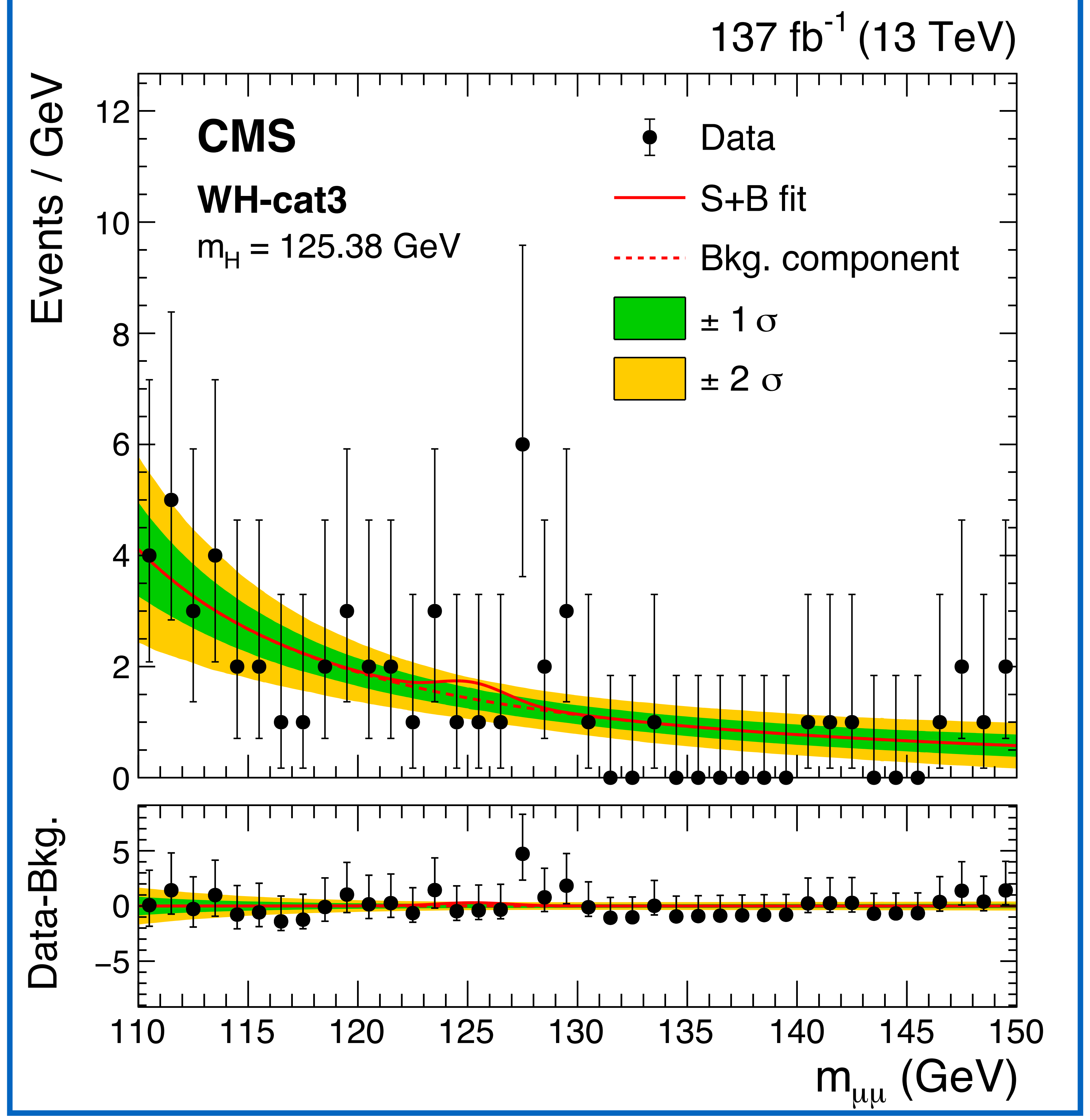

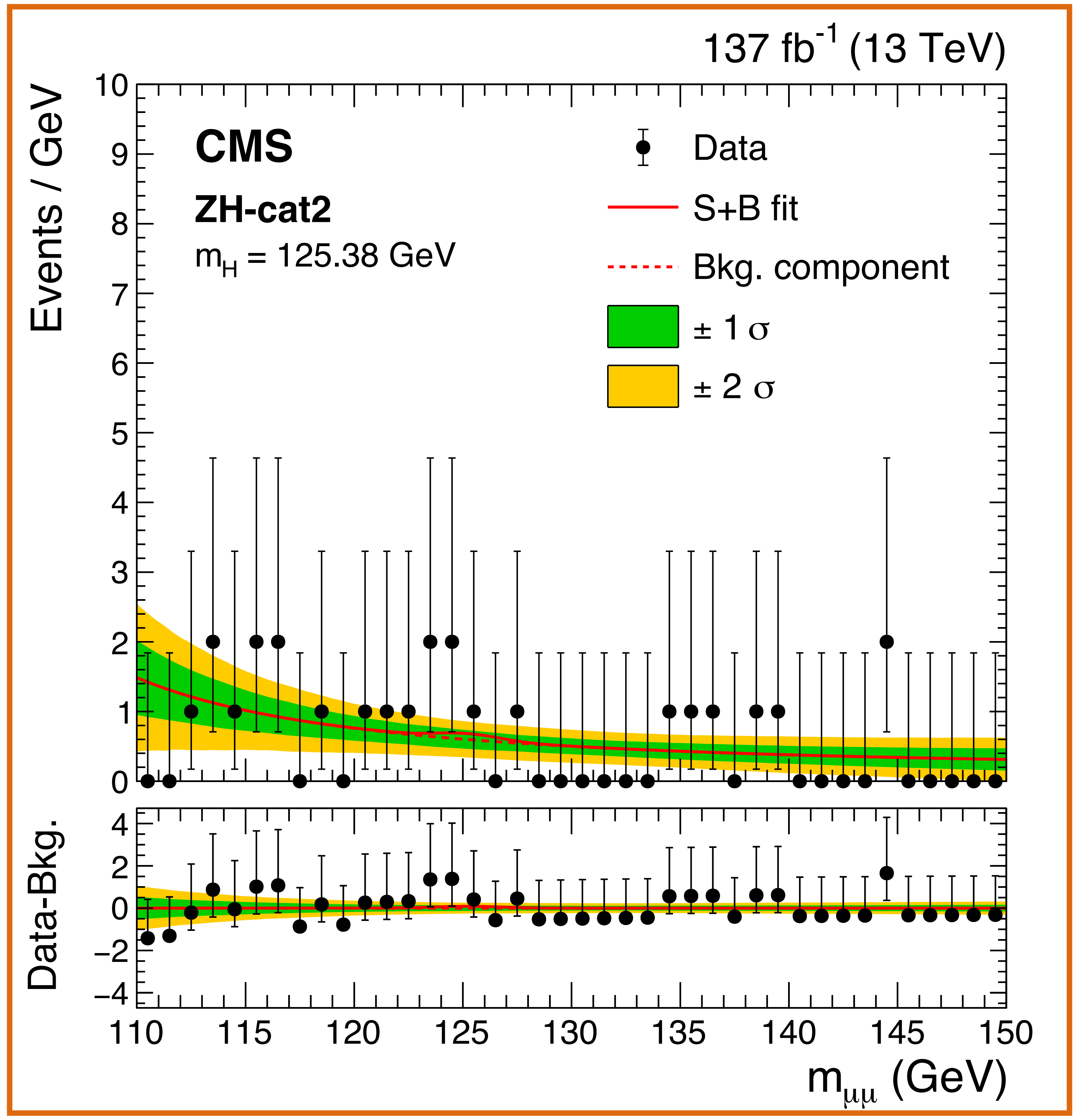

VH category results

- ***Expected*** significance of 0.4σ
- ***Observed*** significance of 2.0σ
- **Signal strength** $\mu = 5.48^{+3.10}_{-2.83}$

ggH event candidate

How does a ggH event look like?

ggH event candidate

How does a ggH event look like?

Higgs candidate

Dimuon pair with $m_{\mu\mu}$ in [110,150] GeV

↓

No b-tagged jets in the event with $p_T > 25$ GeV

↓

No additional leptons (e, μ) in the event with $p_T > 20$ GeV

↓

VBF veto

In events with two or more jets $p_T > 25$ GeV

$m_{jj} < 400$ GeV or $|\Delta\eta_{jj}| < 2.5$ or $p_T(j_1) < 35$ GeV

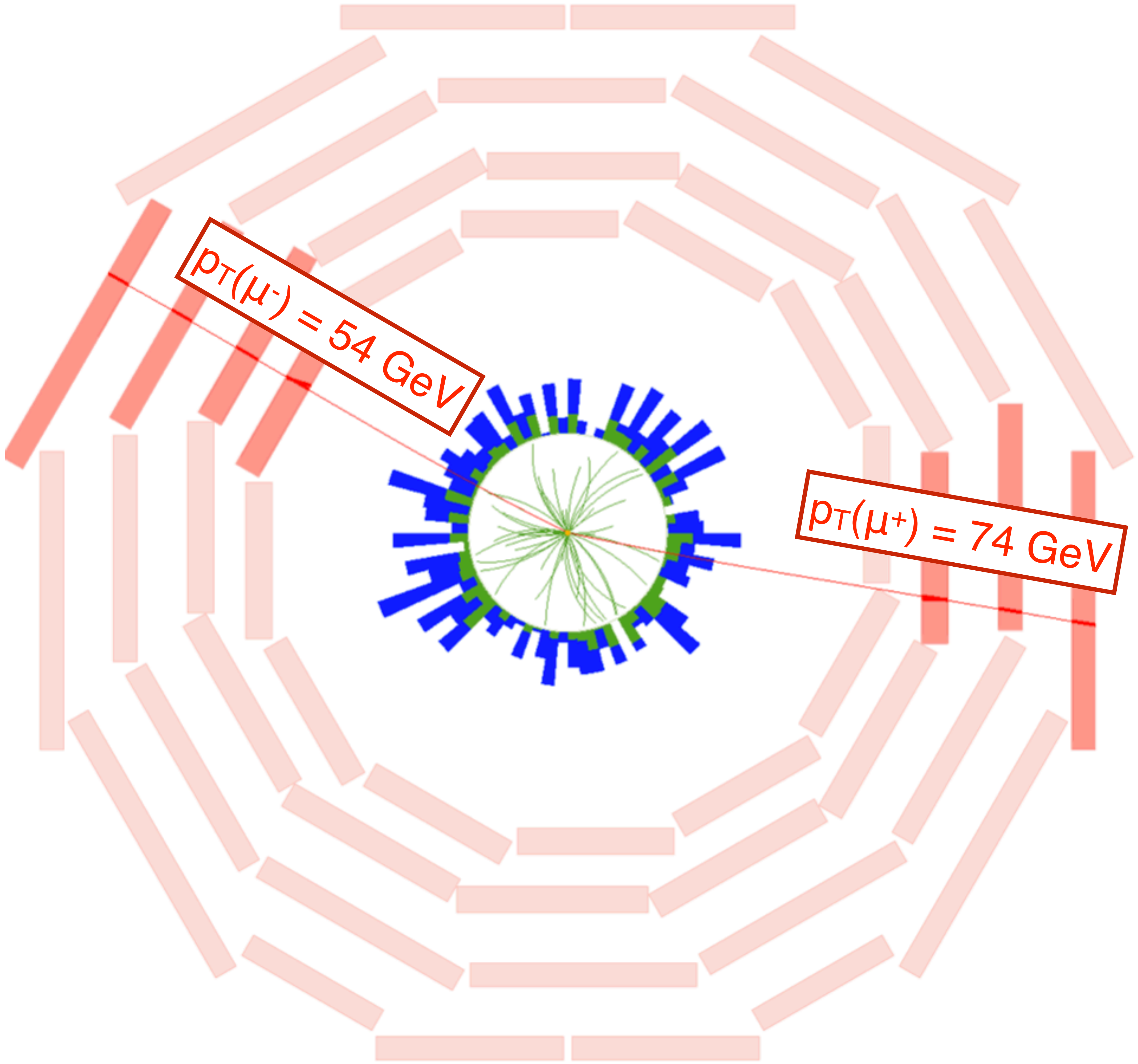

ggH event categories

- ***Divide-n-fit*** strategy employed in the signal extraction
- ***BDT classifier*** trained to separate at best signal from background events

ggH BDT

- **Higgs candidate:** p_T, rapidity, decay angles (ϕ_{CS}, $\cos(\theta)_{CS}$)
- η and $p_T/m_{\mu\mu}$ of the muons from Higgs candidate
- N_{jets}, p_T and η of the leading jet
- ***Events with one jet***: $\Delta\eta(\mu\mu,j)$ and $\Delta\phi(\mu\mu,j)$
- ***Events with ≥ 2 jets***: m_{jj}, $\Delta\eta_{jj}$, $\Delta\phi_{jj}$, Zeppenfeld, min-$\Delta\eta(\mu\mu,j)$, min-$\Delta\phi(\mu\mu,j)$

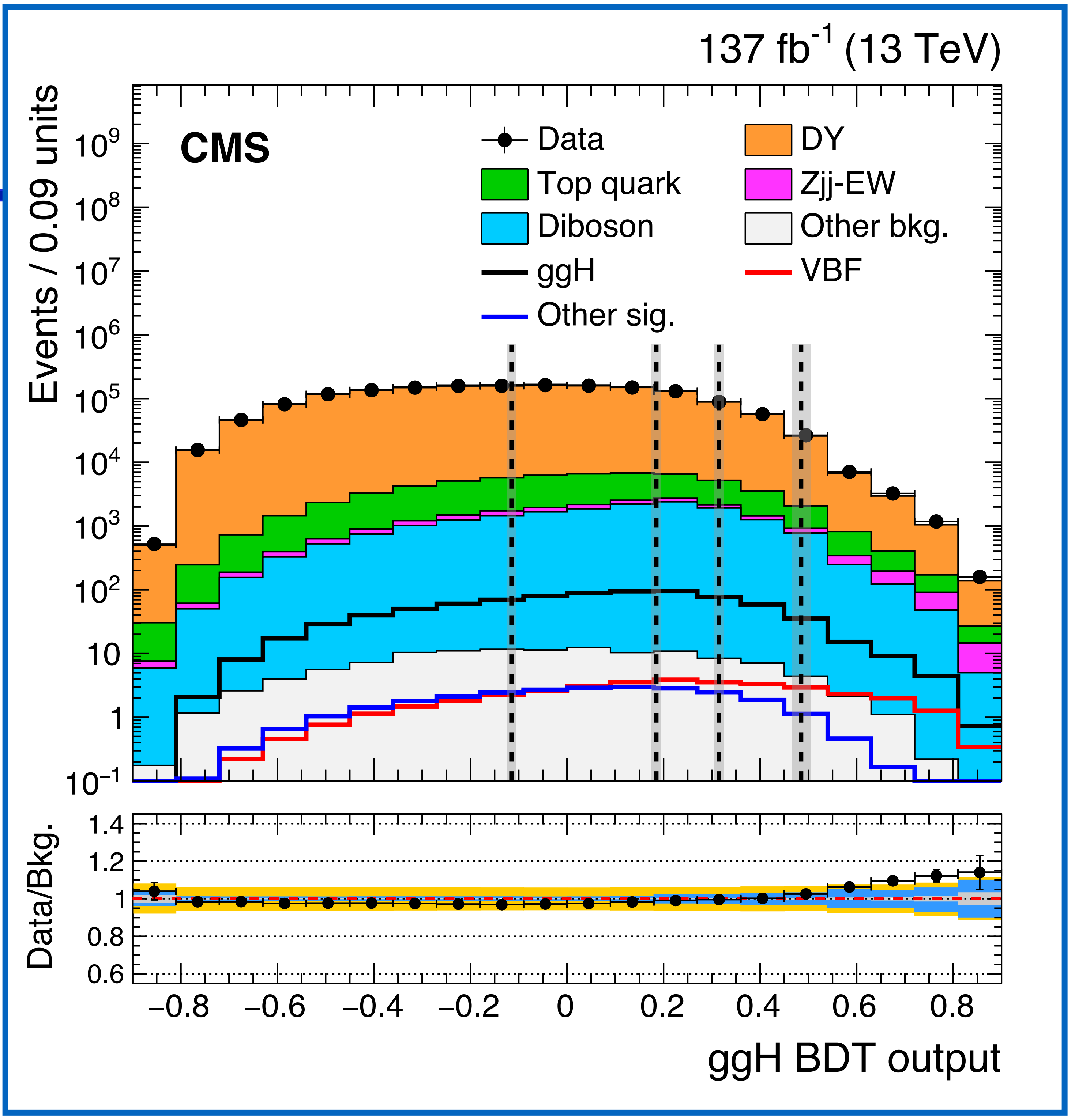

$m_{\mu\mu}$ resolution

- Signal events weighted by $1/(\sigma_m/m)$ during training
- Events with **high $m_{\mu\mu}$ resolution** promoted to **high score**

Event category	HWHM (GeV)
ggH-cat1	2.12
ggH-cat2	1.75
ggH-cat3	1.60
ggH-cat4	1.47
ggH-cat5	1.50

ggH event categories

- ***Divide-n-fit*** strategy employed in the signal extraction
- ***BDT classifier*** trained to separate at best signal from background events

ggH BDT

- **Higgs candidate:** p_T, rapidity, decay angles (ϕ_{cs}, $\cos(\theta)_{CS}$)
- η and $p_T/m_{\mu\mu}$ of the muons from Higgs candidate
- N_{jets}, p_T and η of the leading jet
- ***Events with one jet***: $\Delta\eta(\mu\mu,j)$ and $\Delta\phi(\mu\mu,j)$
- ***Events with ≥ 2 jets***: m_{jj}, $\Delta\eta_{jj}$, $\Delta\phi_{jj}$, Zeppenfeld, min-$\Delta\eta(\mu\mu,j)$, min-$\Delta\phi(\mu\mu,j)$

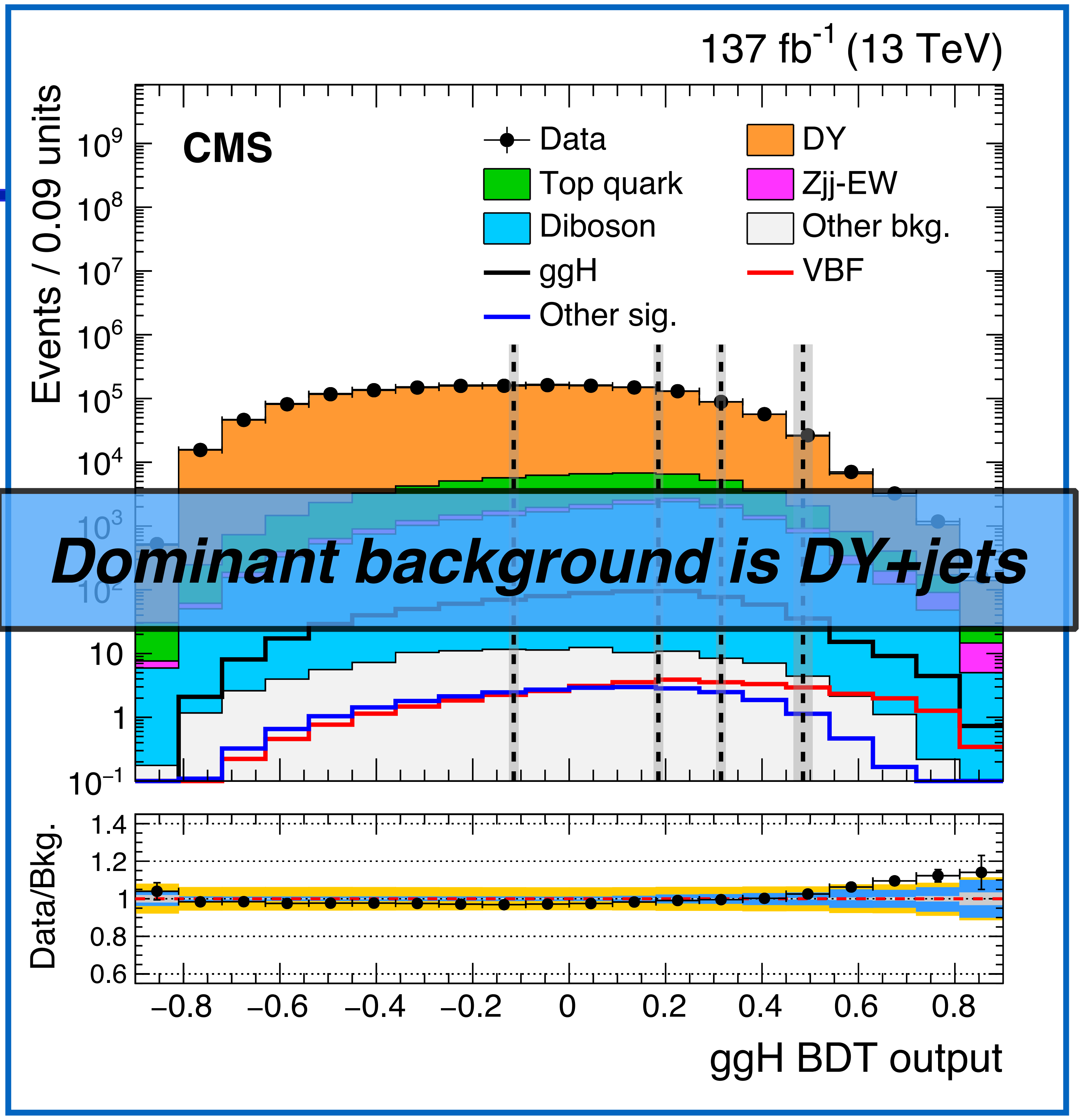

$m_{\mu\mu}$ resolution

- Signal events weighted by $1/(\sigma_m/m)$ during training
- Events with **high $m_{\mu\mu}$ resolution** promoted to **high score**

Event category	HWHM (GeV)
ggH-cat1	2.12
ggH-cat2	1.75
ggH-cat3	1.60
ggH-cat4	1.47
ggH-cat5	1.50

ggH category: background estimate

- The *“**classical approach**”* is to fit the $m_{\mu\mu}$ distribution in each subcategory independently
- The fit in one subcategory is not influenced by background parameters in other subcategories

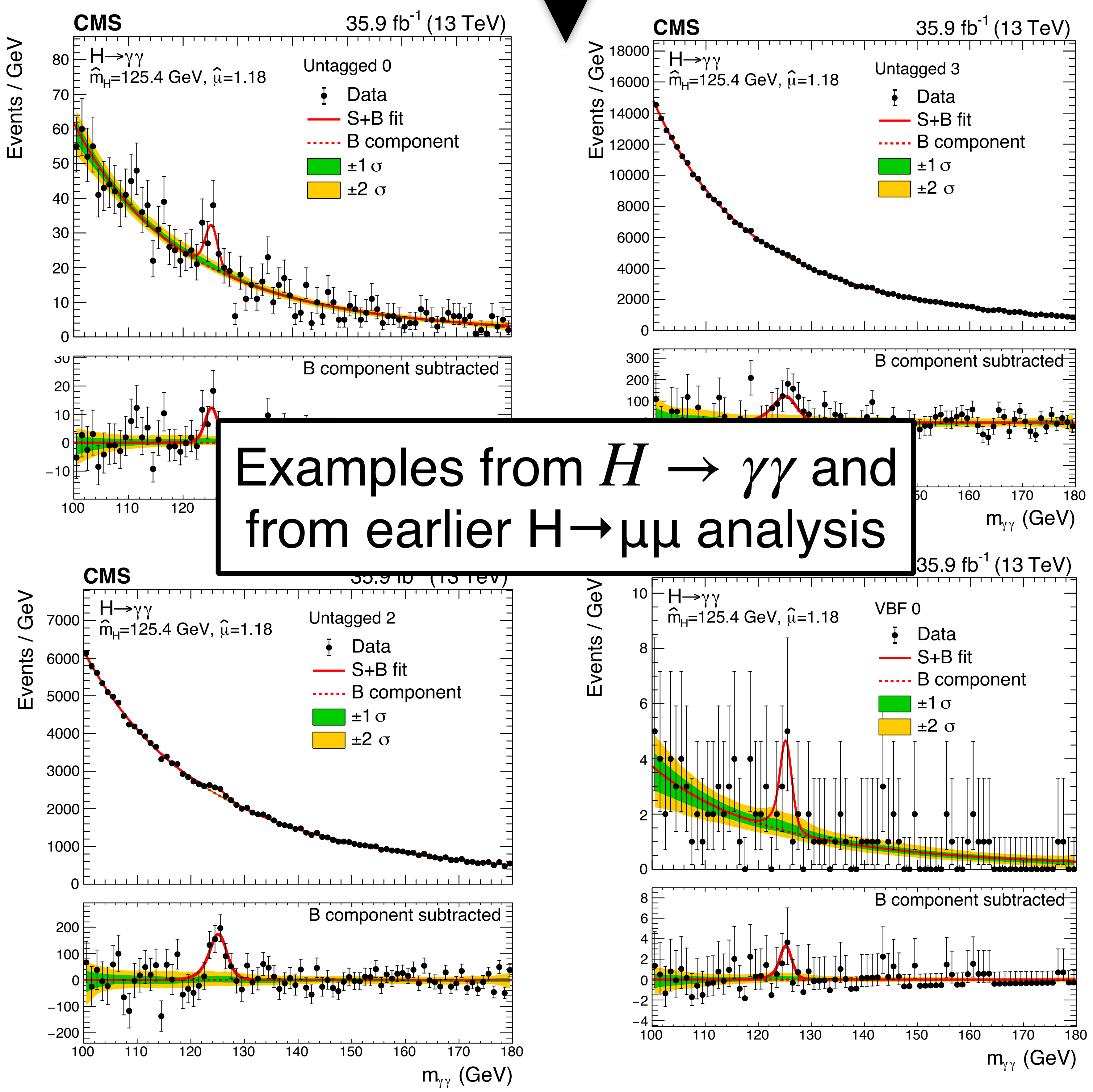

Examples from $H \rightarrow \gamma\gamma$ and from earlier H→μμ analysis

Background composition

- Background composition in the ***ggH subcategories*** well known from simulation
- Background shape ***similar*** across subcategories driven by the tail of the Z-boson peak in DY+jets events
- ***Minor variations*** across subcategories are due to difference in muon kinematics and mass resolution

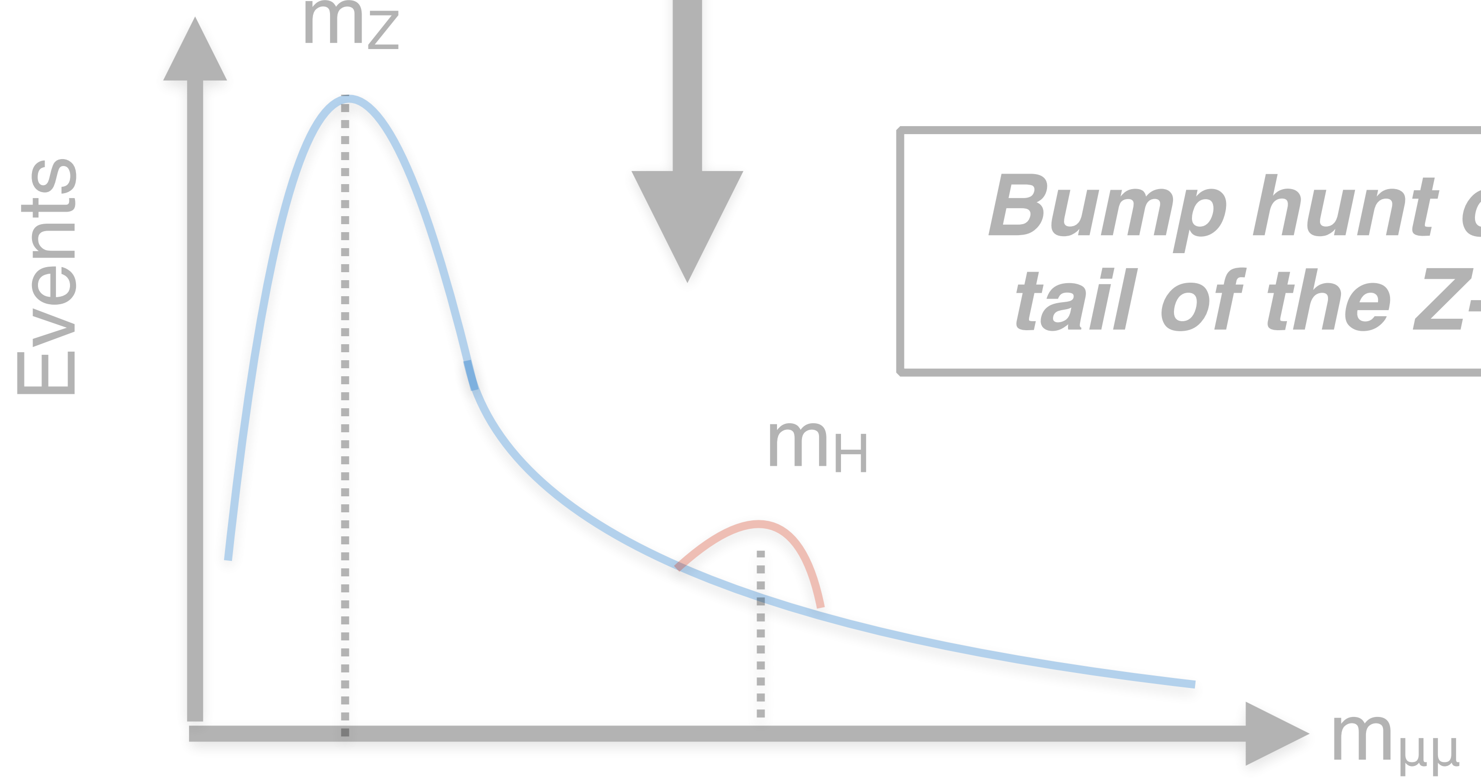

Bump hunt on the tail of the Z-peak

ggH category: background estimate

- The ***“classical approach”*** is to fit the $m_{\mu\mu}$ distribution in each subcategory independently
- The fit in one subcategory is not influenced by background parameters in other subcategories

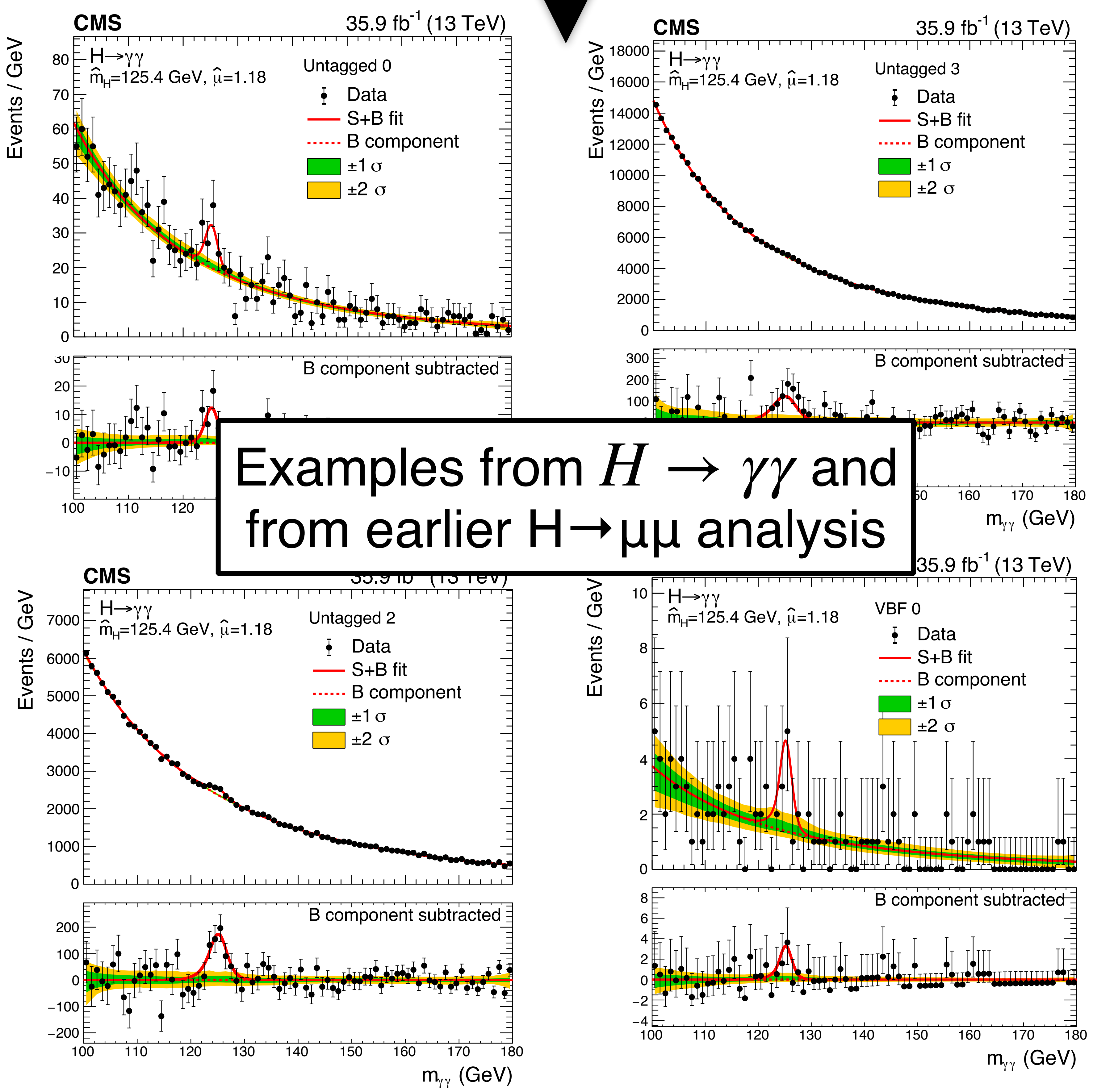

Examples from $H \to \gamma\gamma$ and from earlier H→μμ analysis

Background composition

- Background composition in the ***ggH subcategories*** well known from simulation
- Background shape ***similar*** across subcategories driven by the tail of the Z-boson peak in DY+jets events
- ***Minor variations*** across subcategories are due to difference in muon kinematics and mass resolution

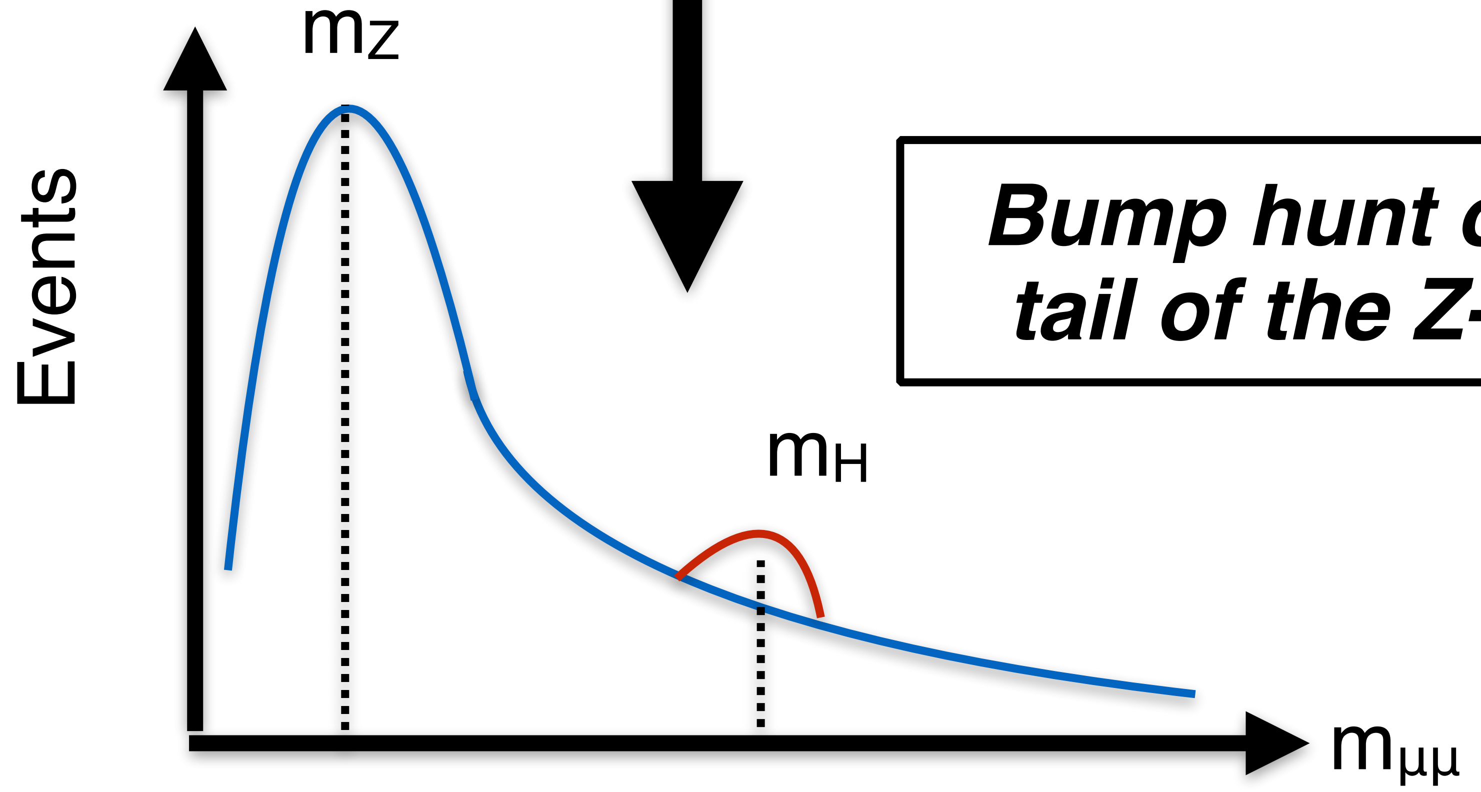

Bump hunt on the tail of the Z-peak

ggH: background estimate

Given the similarities in the background $m_{\mu\mu}$ shape across ggH subcategories

Background model in a subcategory = ***Core function*** X ***Per-category shape modifier*** X ***Background yield***

Core function

- ***Common shape*** across categories
- ***Parameters*** are ***constrained*** by data in ***all categories***
- ***Discrete likelihood profile*** of functions (inspired by theory or empirical) able to ***model*** the ***DY spectrum***

Per-category shape modifier

- ***2nd or 3rd*** order Chebyshev ***polynomial***
- ***Parameters*** are ***uncorrelated*** across categories
- ***Account*** for ***shape variations*** across categories

Background yield

- ***Per-category*** total ***background rate***

ggH: background estimate

Given the similarities in the background $m_{\mu\mu}$ shape across ggH subcategories

Background model in a subcategory = ***Core function*** X ***Per-category shape modifier*** X ***Background yield***

Core function

- ***Common shape*** across categories
- ***Parameters*** are ***constrained*** by data in ***all categories***
- ***Discrete likelihood profile*** of functions (inspired by theory or empirical) able to ***model*** the ***DY spectrum***

Per-category shape modifier

- ***2nd or 3rd*** order Chebyshev ***polynomial***
- ***Parameters*** are ***uncorrelated*** across categories
- ***Account*** for ***shape variations*** across categories

Background yield

- ***Per-category*** total ***background rate***

ggH: background estimate

Given the similarities in the background $m_{\mu\mu}$ shape across ggH subcategories

Background model in a subcategory = ***Core function*** X ***Per-category shape modifier*** X ***Background yield***

Core function

- ***Common shape*** across categories
- ***Parameters*** are ***constrained*** by data in ***all categories***
- ***Discrete likelihood profile*** of functions (inspired by theory or empirical) able to ***model*** the ***DY spectrum***

Per-category shape modifier

- ***2nd or 3rd*** order Chebyshev ***polynomial***
- ***Parameters*** are ***uncorrelated*** across categories
- ***Account*** for ***shape variations*** across categories

Background yield

- ***Per-category*** total ***background rate***

ggH: background estimate

Given the similarities in the background $m_{\mu\mu}$ shape across ggH subcategories

This background model allows to use fewer parameters to the describe the background w.r.t classical approach

It allows for a 10% improvement in the sensitivity while keeping a negligible bias in the signal extraction

Background model in a subcategory = ***Core function*** × ***…aifier*** × ***…ground yield***

- ***…hape*** across cat… …data ***…ategories***
- ***Discrete likelihood profile*** of functions (inspired by theory or empirical) able to ***model*** the ***DY spectrum***

- ***…polynomial***
- ***Parameters*** are ***uncorrelated*** across categories
- ***Account*** for ***shape variations*** across categories

- ***Per-category*** total ***background rate***

ggH category results

- ***Divide-n-fit*** strategy → **five** subcategories
- ***Signal*** → $m_{\mu\mu}$ distributions parametrised via Double Crystal-Ball function
- ***Background*** → $m_{\mu\mu}$ mass distributions modelled via the method described before

Highest purity ggH categories

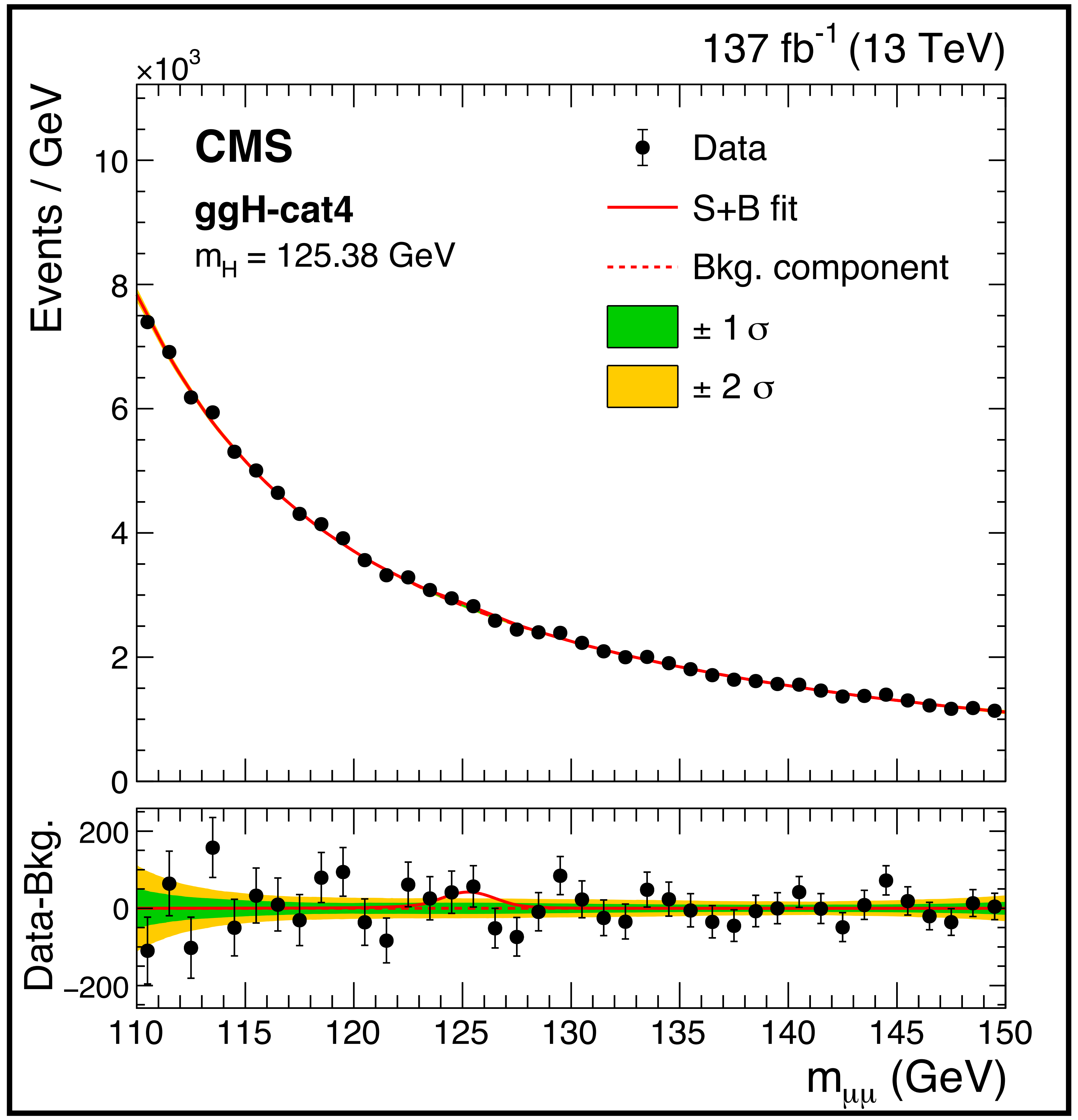

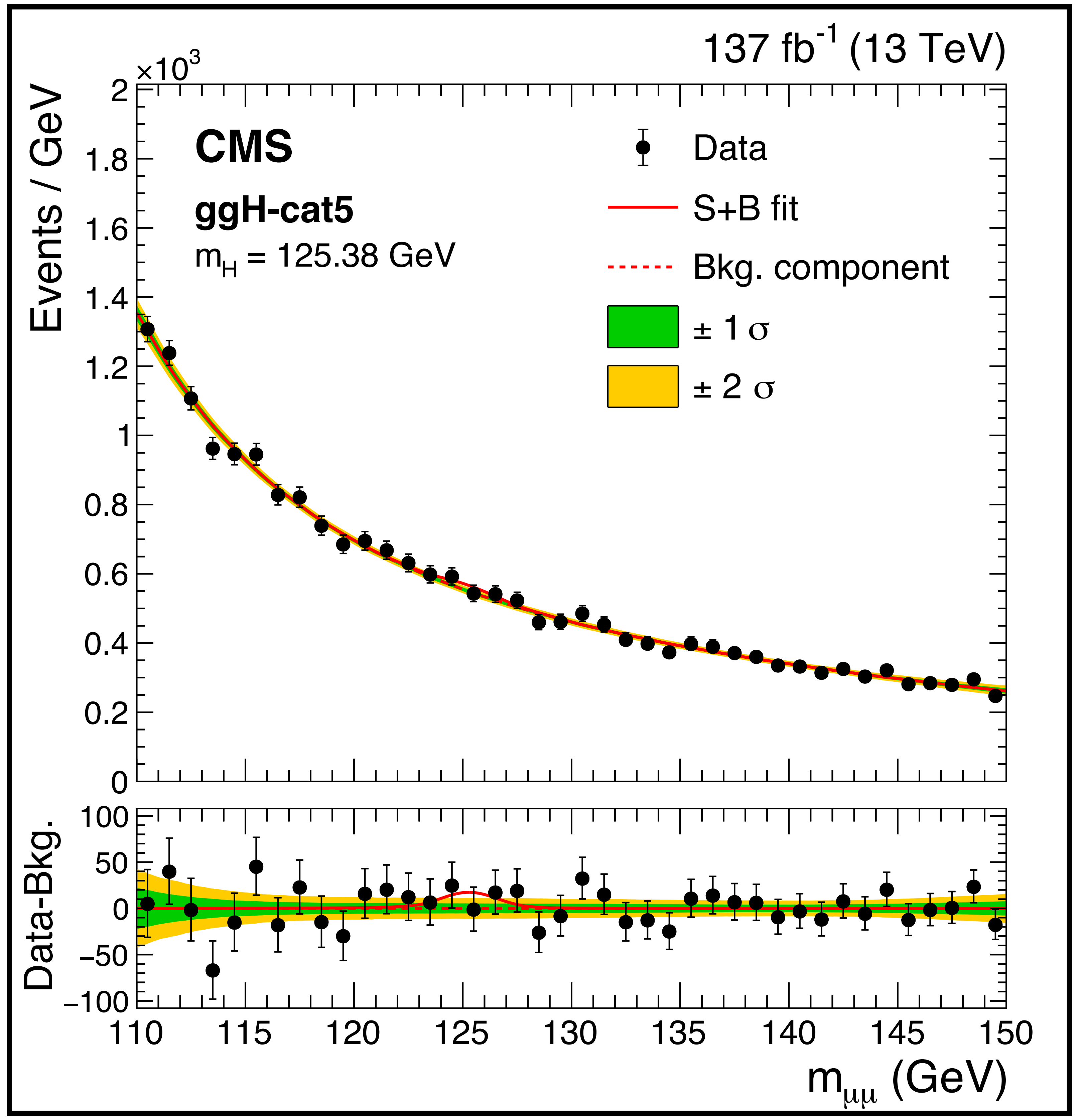

ggH category results

- ***Expected*** significance of 1.6σ
- ***Observed*** significance of 1.0σ
- **Signal strength** $\mu = 0.63^{+0.65}_{-0.64}$

VBF event candidate

How does a VBF event look like?

VBF event candidate

How does a VBF event look like?

Higgs candidate

Dimuon pair with $m_{\mu\mu}$ in [110,150] GeV

No b-tagged jets in the event with $p_T > 25$ GeV

Lepton veto: no additional e or μ with $p_T > 20$ GeV

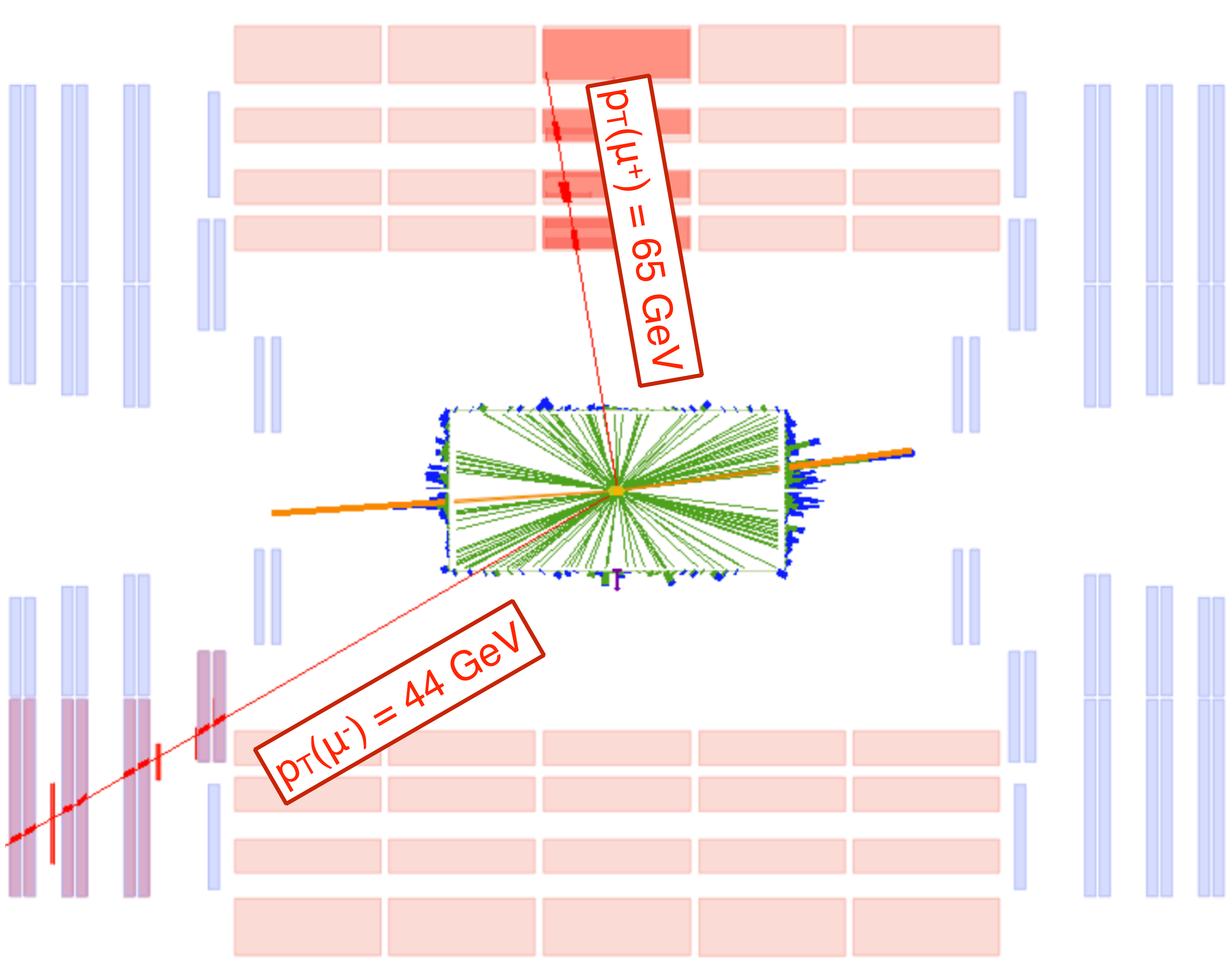

VBF event candidate

How does a VBF event look like?

Higgs candidate
Dimuon pair with $m_{\mu\mu}$ in [110,150] GeV

↓

No b-tagged jets in the event with $p_T > 25$ GeV

↓

Lepton veto: no additional e or μ with $p_T > 20$ GeV

↓

VBF selection

- At least two jets with $p_T > 25$ GeV
- Leading jet $p_T > 35$ GeV
- $m_{jj} > 400$ GeV
- $|\Delta\eta_{jj}| > 2.5$

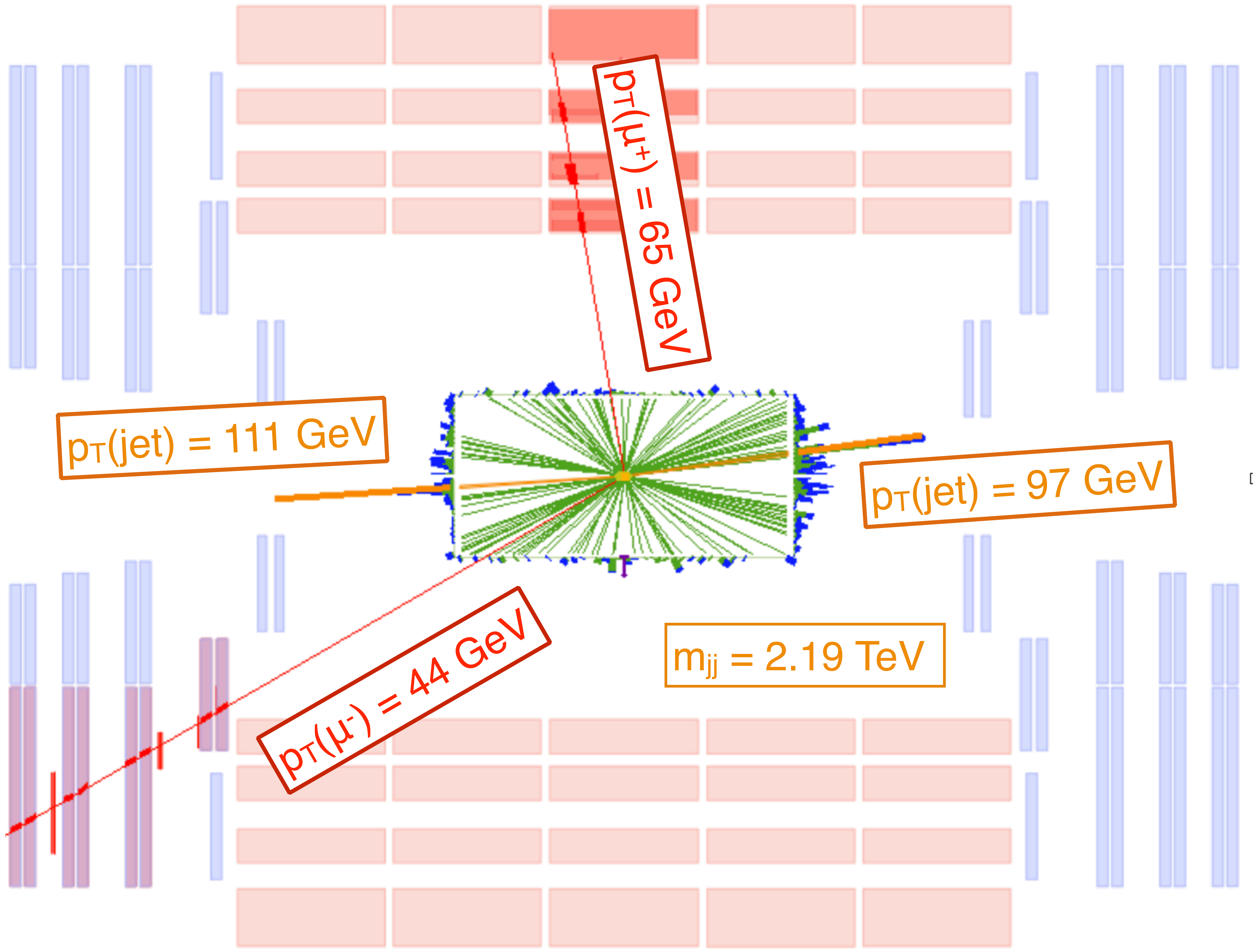

VBF analysis strategy

- ***Pros of divide-n-fit strategy** → fully data-driven background estimate*
  - Useful when the background cannot be reliably modelled via simulation
  - Useful when an alternative analysis based on MC predictions is systematically limited

- ***Cons of divide-n-fit strategy*** → add categories at high signal purity does not improve the performance
  - *At high signal purity, the small number of observed events in sideband may limit the sensitivity*

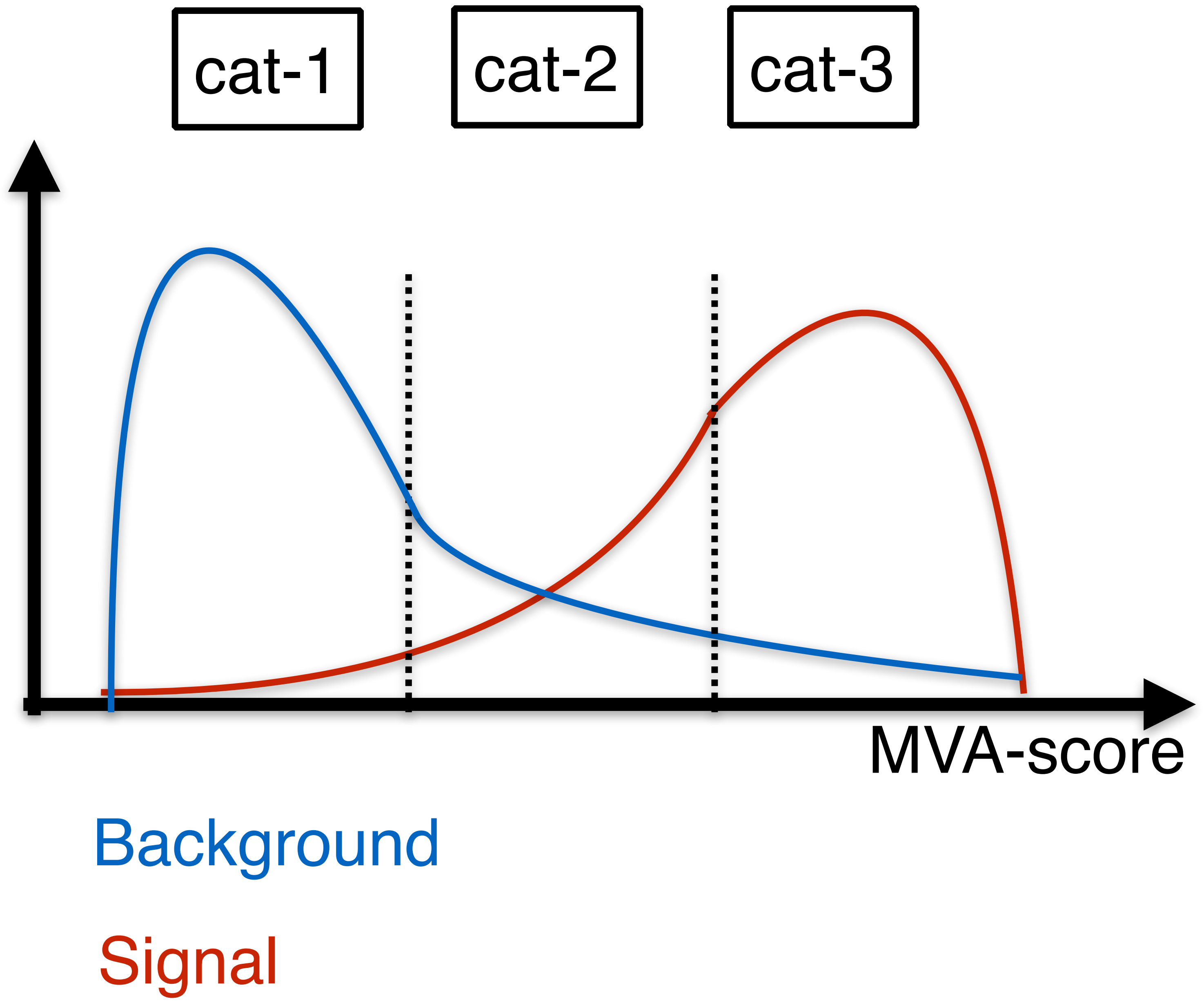

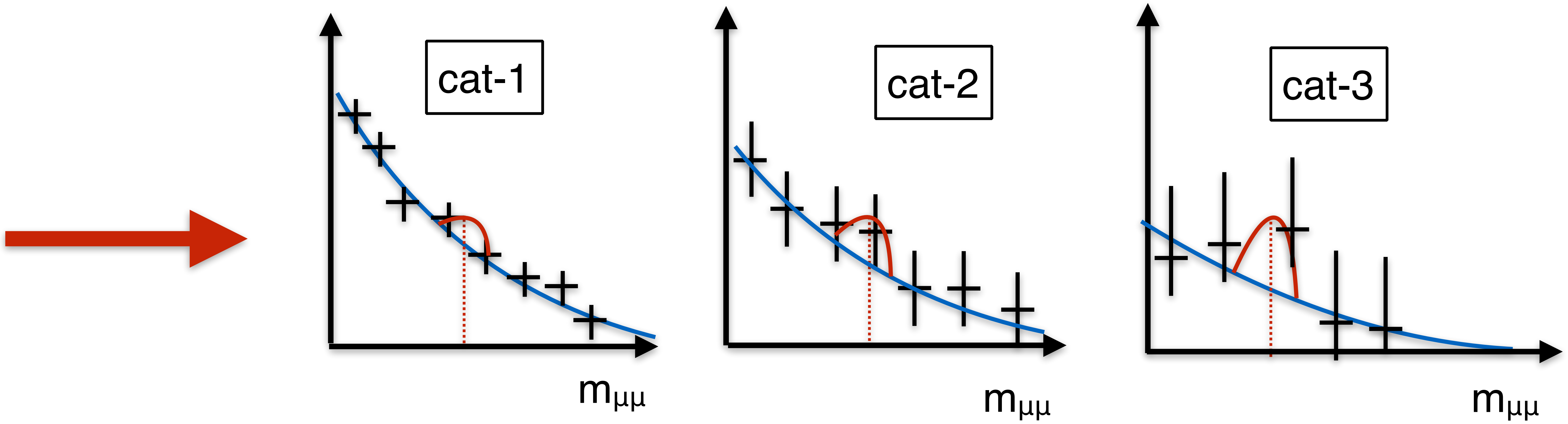

Moving from low to high MVA score, progressively smaller constraint power from the observed data in the mass sidebands

VBF analysis strategy

- In the VBF analysis, it is possible to reach ***30-40% purity at high m_{jj}, $\Delta\eta_{jj}$***
  - In this regime, ***few events*** in the ***mass sidebands*** (SB) to ***constrain*** the ***bkg***. with a ***parametric fit***
  - This translates in a ***30-50% uncertainty*** on the ***predicted background yield under the Higgs peak***

Different approach simulation based

- ***Include $m_{\mu\mu}$*** in the MVA classifier
- Extract the signal via a ***fit to the MVA output***
- ***Background*** estimation ***from simulation***

** Analysis strategy inspired from the one used in the H(bb) observation reported in PRL 121 (2018) 121801

Motivations

- DY and Zjj-EW simulations can well reproduce the observation in data as demonstrated in EPJC 78 (2018) 589
- ***Simulation*** provides a ***background prediction*** with ***better precision***, including systematics, than a parametric fit
- ***About 20% improvement*** in expected significance ***w.r.t. divide-n-fit strategy***

VBF analysis strategy

- In the VBF analysis, it is possible to reach ***30-40% purity at high m_{jj}, $\Delta\eta_{jj}$***
  - In this regime, ***few events*** in the ***mass sidebands*** (SB) to ***constrain*** the ***bkg***. with a ***parametric fit***
  - This translates in a ***30-50% uncertainty*** on the ***predicted background yield under the Higgs peak***

Different approach simulation based

- ***Include $m_{\mu\mu}$*** in the MVA classifier
- Extract the signal via a ***fit to the MVA output***
- ***Background*** estimation ***from simulation***

** Analysis strategy inspired from the one used in the H(bb) observation reported in **PRL 121 (2018) 121801**

Motivations

- DY and Zjj-EW simulations can well reproduce the observation in data as demonstrated in **EPJC 78 (2018) 589**
- ***Simulation*** provides a ***background prediction*** with ***better precision***, including systematics, than a parametric fit
- ***About 20% improvement*** in expected significance ***w.r.t. divide-n-fit strategy***

VBF analysis strategy

- In the VBF analysis, it is possible to reach ***30-40% purity at high m_{jj}, $\Delta\eta_{jj}$***
  - In this regime, ***few events*** in the ***mass sidebands*** (SB) to ***constrain*** the ***bkg***. with a ***parametric fit***
  - This translates in a ***30-50% uncertainty*** on the ***predicted background yield under the Higgs peak***

Different approach simulation based

- ***Include $m_{\mu\mu}$*** in the MVA classifier
- Extract the signal via a ***fit to the MVA output***
- ***Background*** estimation ***from simulation***

** Analysis strategy inspired from the one used in the H(bb) observation reported in **PRL 121 (2018) 121801**

Motivations

- DY and Zjj-EW simulations can well reproduce the observation in data as demonstrated in **EPJC 78 (2018) 589**
- ***Simulation*** provides a ***background prediction*** with ***better precision***, including systematics, than a parametric fit
- ***About 20% improvement*** in expected significance ***w.r.t. divide-n-fit strategy***

VBF DNN classifier

- ***DNN classifier*** → trained to maximise the separation between VBF Higgs and background events
  - **Higgs candidate: $m_{\mu\mu}$,** p_T, rapidity, and decay angles (ϕ_{CS} , cos θ_{CS})
  - **VBF jets:** $p_T(j_1)$, $p_T(j_2)$, $\eta(j_1)$, $\eta(j_2)$, $\phi(j_1)$, $\phi(j_2)$, $\Delta\eta_{jj}$, m_{jj}, $\Delta\phi_{jj}$, Zeppenfeld, p_T balance ($\mu\mu$,jj)
  - **Additional activity:** soft track-jets reconstructed from tracks associated to PV with $p_T > 5$ GeV

Binned template fit

- Fit performed ***simultaneously across data-taking periods*** and in ***signal*** and ***sideband regions***
- **VBF-SR:** $115 < m_{\mu\mu} < 135$ GeV
- **VBF-SB:** $110 < m_{\mu\mu} < 115$ GeV or $135 < m_{\mu\mu} < 150$ GeV
- ***Mass-decorrelated DNN*** used in the VBF-SB → defined by fixing $m_{\mu\mu}$ to be 125 GeV

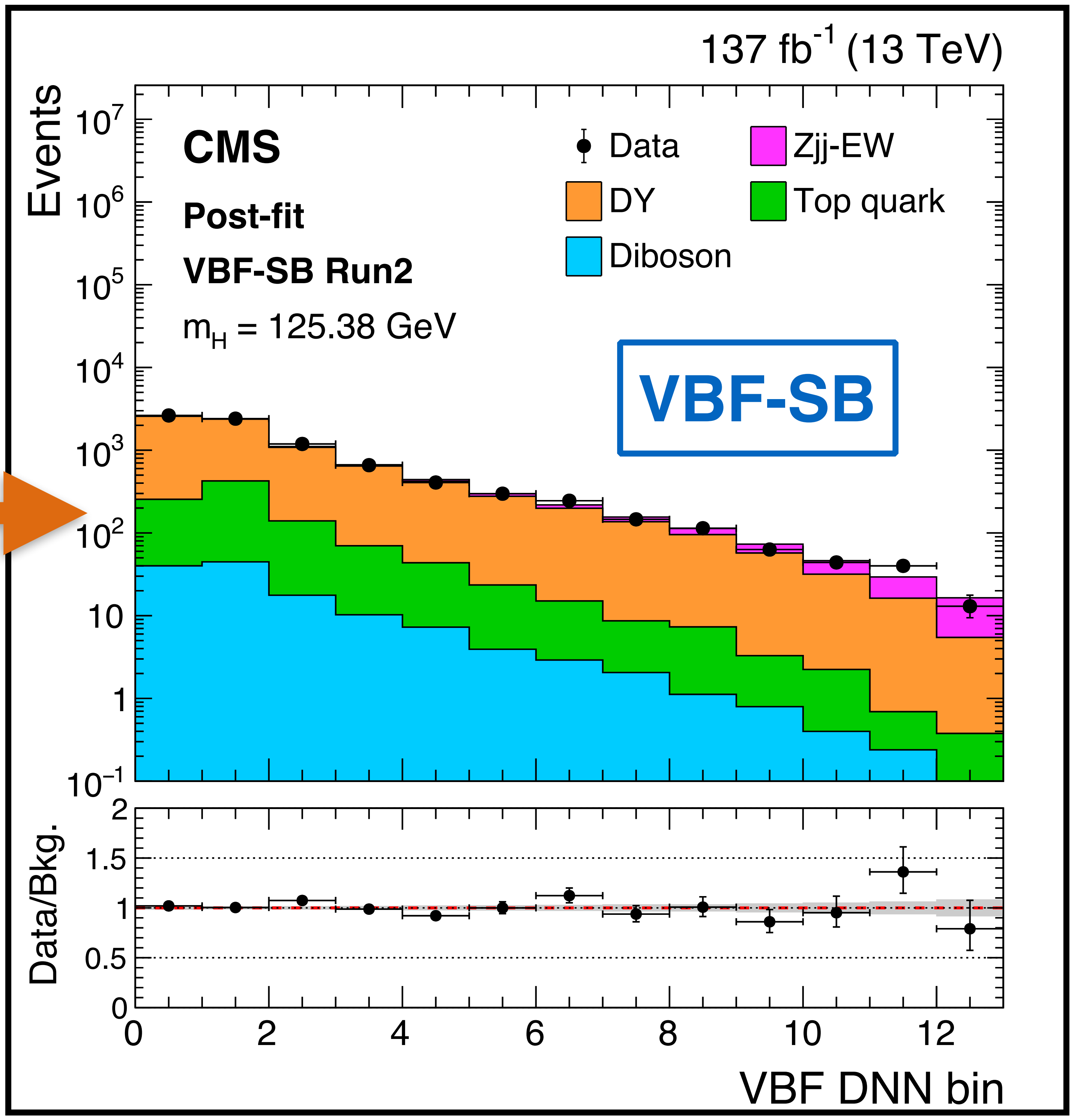

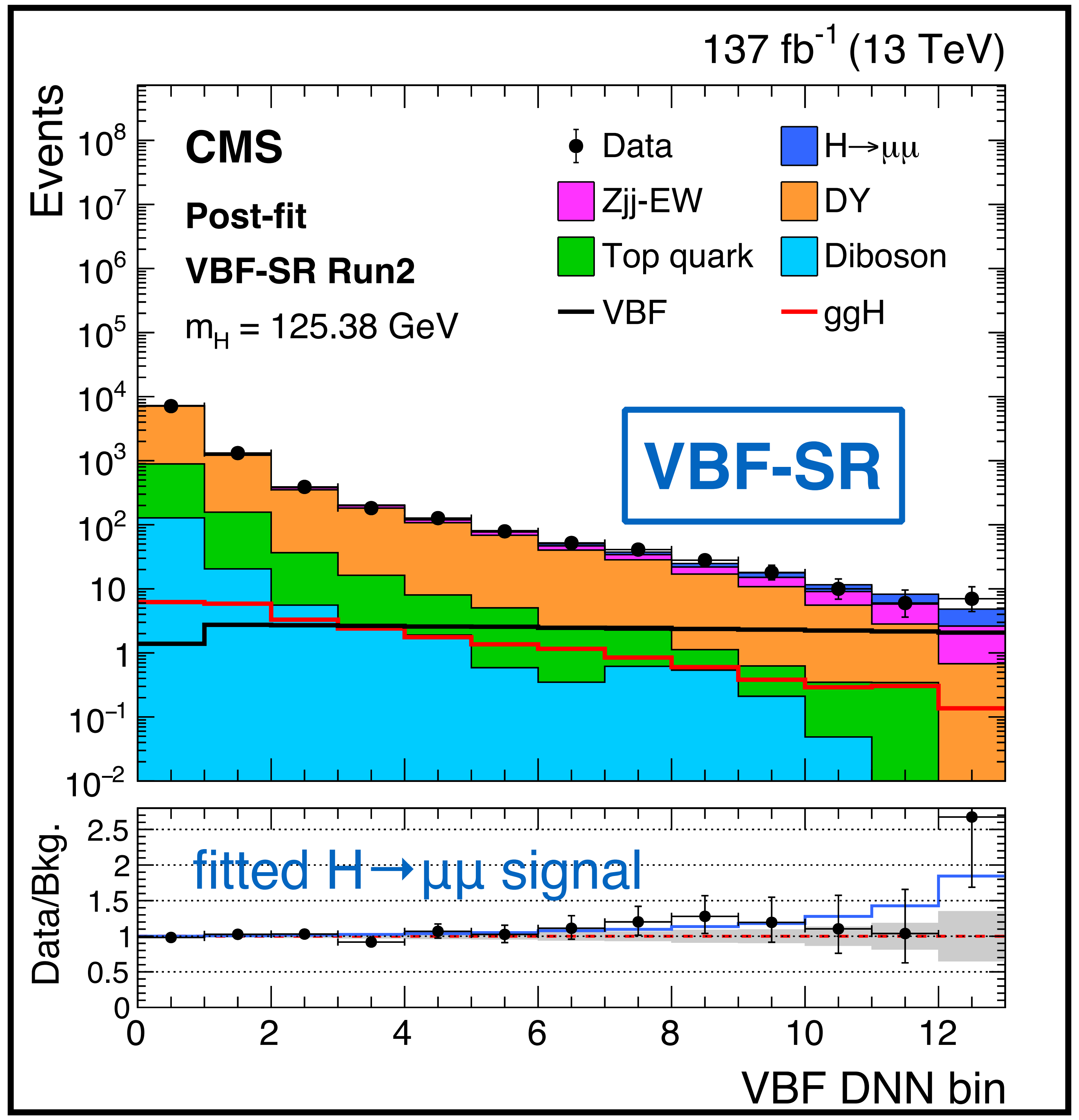

VBF DNN: systematic uncertainties

- DNN classifier trained to maximise the separation between VBF signal and background events
- In the ***DNN high-score region*** → ***statistical uncertainty*** in the most sensitive bins ranges in ***40-70%***
- ***Systematic uncertainties*** on the ***background prediction*** are ***<< statistical uncertainty***

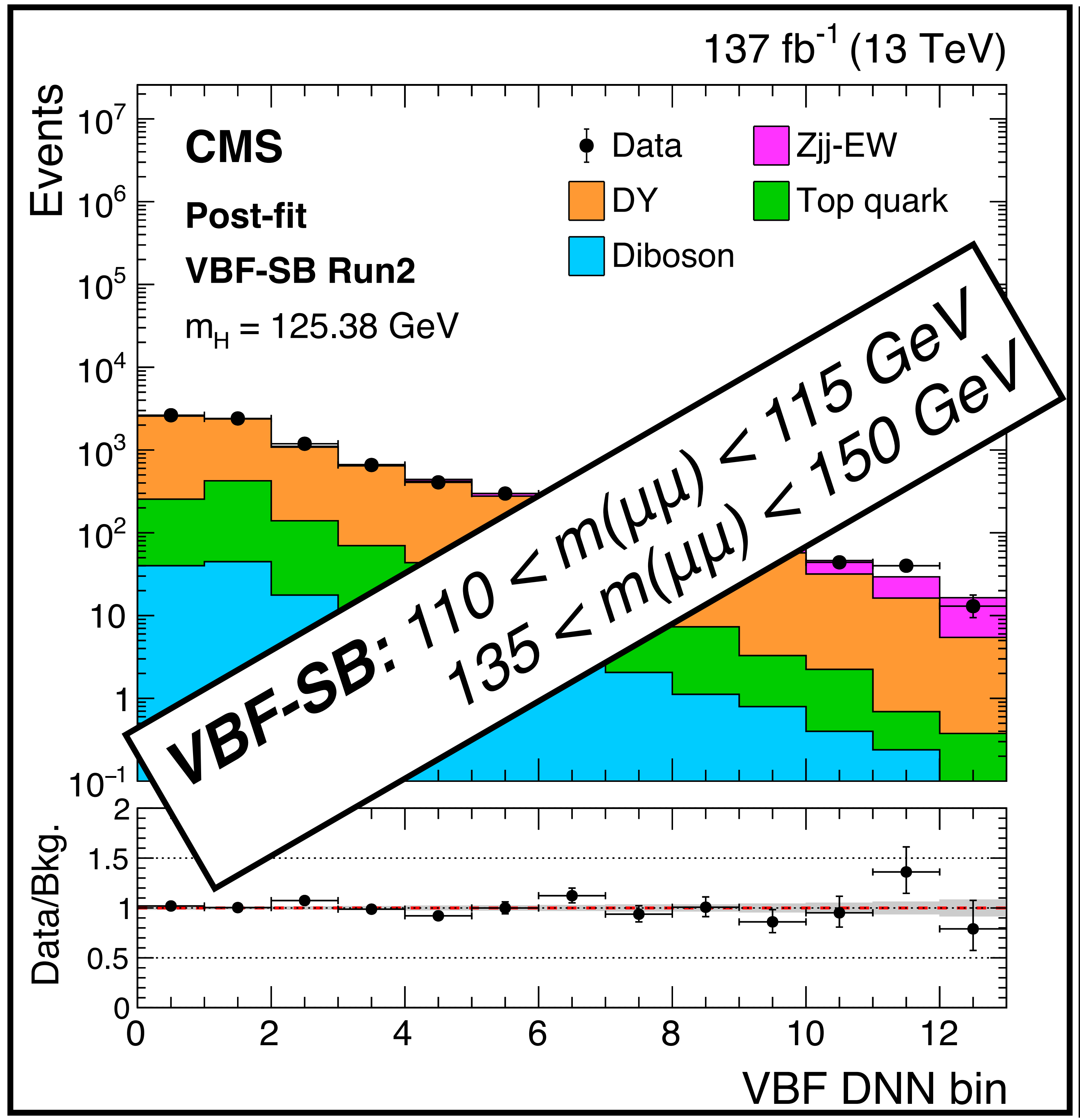

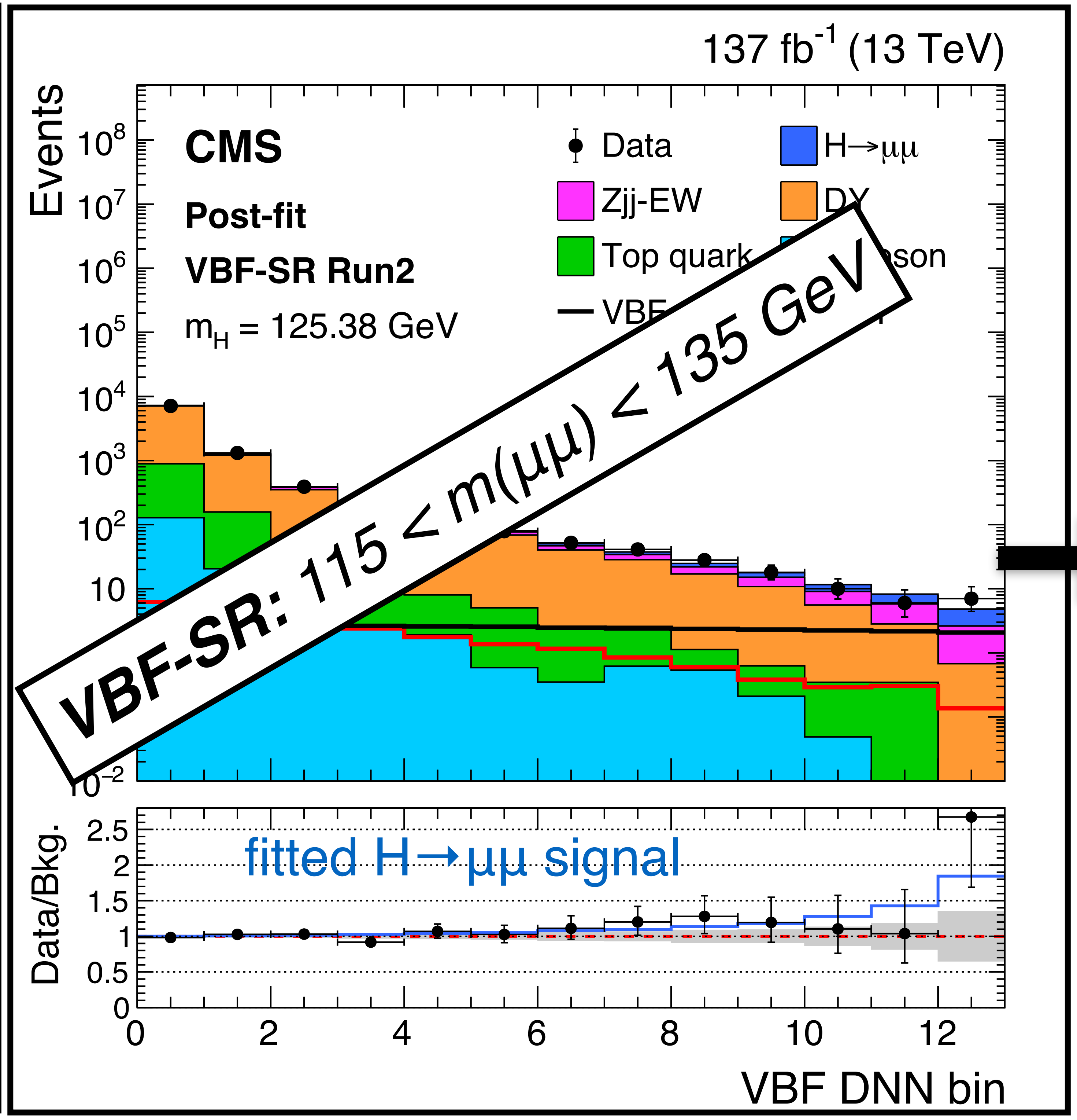

Impact of systematic uncertainties is ~5%

Leading systematic uncertainties

- ***Parton shower*** modelling of VBF-H and Zjj-EW (Pythia vs Herwig)
- ***Jet energy scale*** and ***resolution***
- ***DY*** events from ***one*** or ***more pileup jets***
- ***Statistical*** precision of ***simulation***
- ***Theory uncertainties***: missing higher order corrections, etc ..

VBF analysis results

- ***Signal extraction:*** simultaneous fit performed across data-taking periods, VBF-SB and VBF-SR regions

Result in VBF-SR

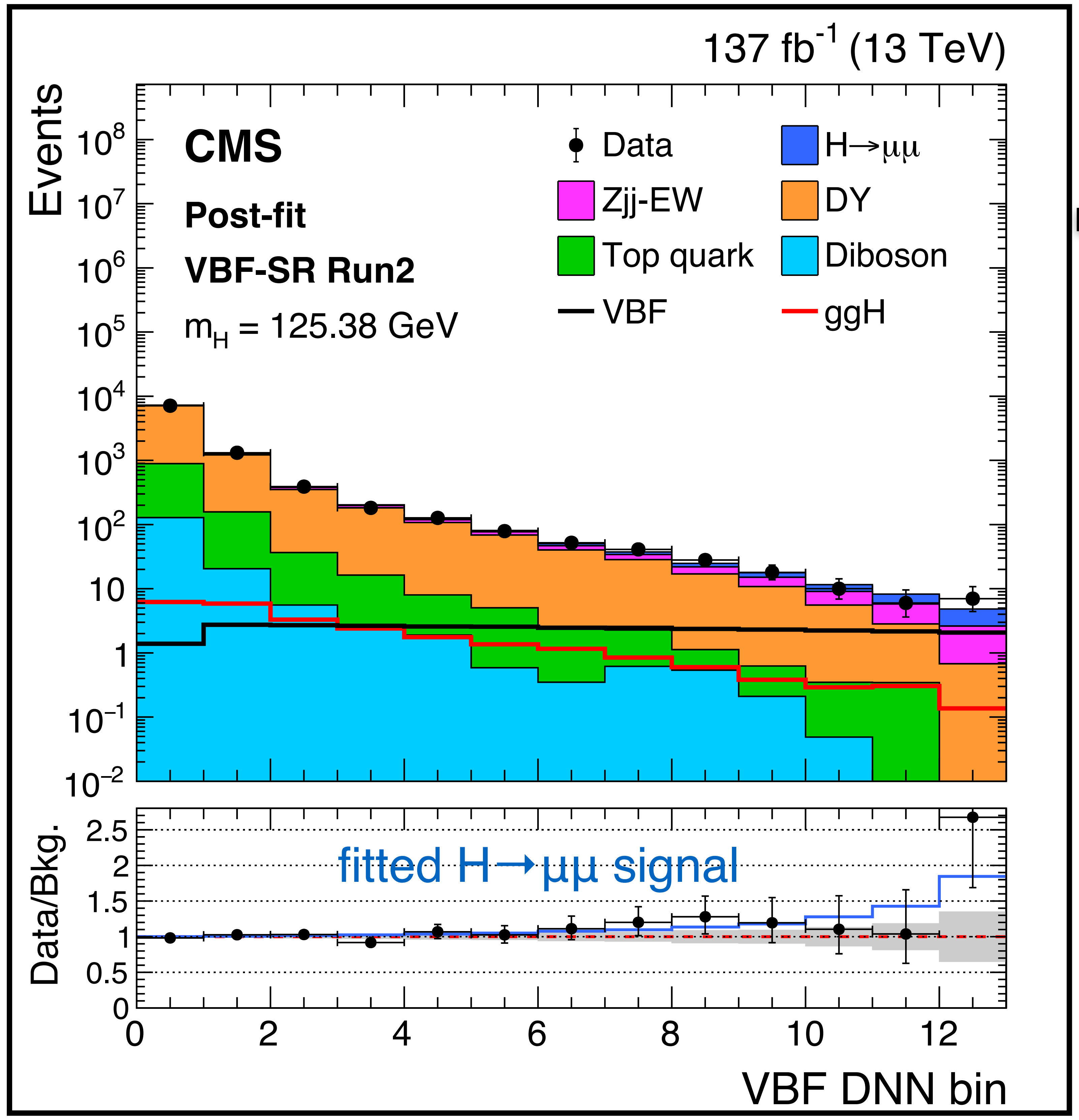

A mass distribution for VBF-SR obtained via a decorrelation procedure equivalent to the one used in the DNN for the VBF-SB. Events are S/(S+B) weighted

for illustration only

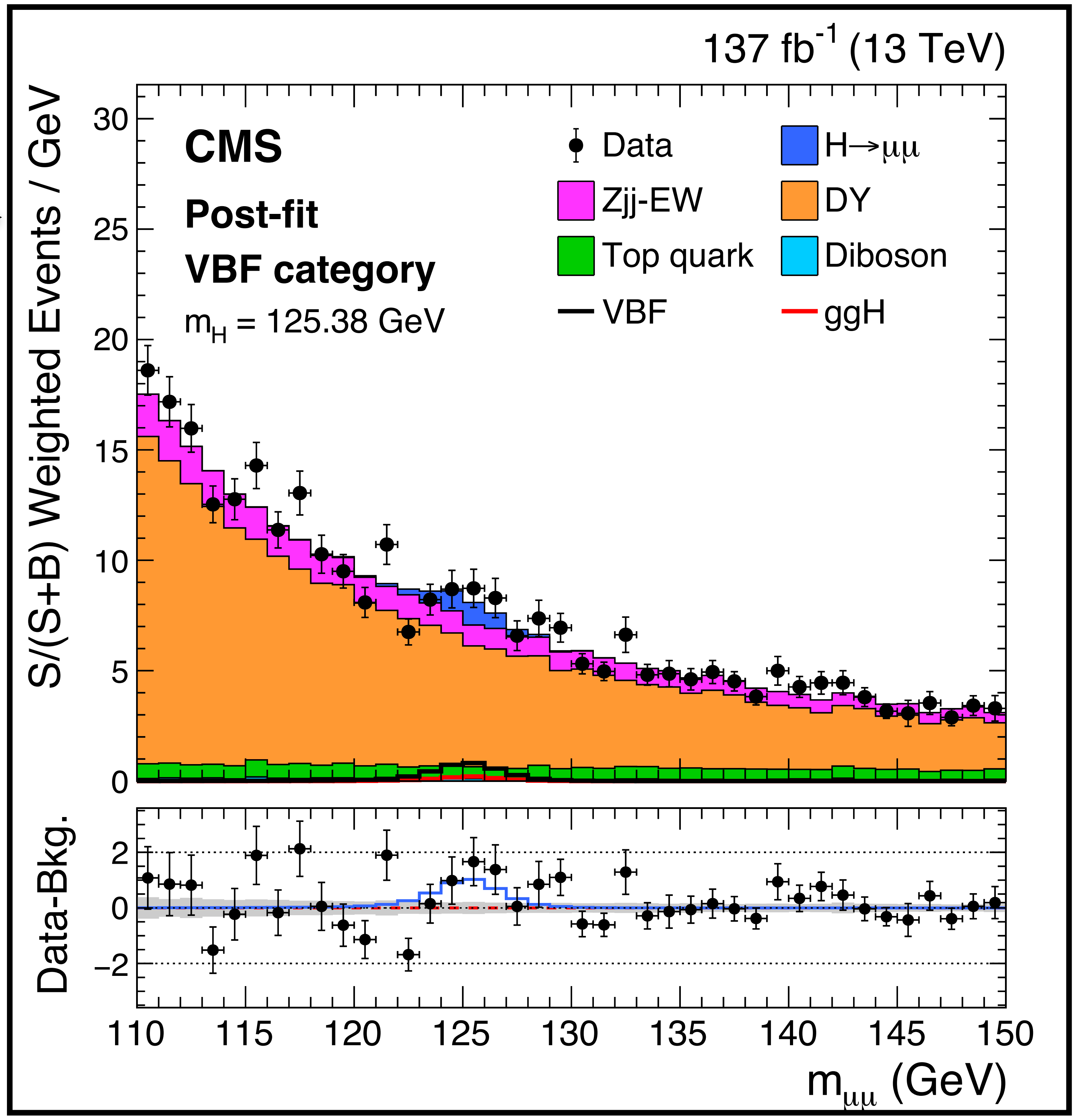

VBF category results

- ***Expected*** significance of 1.8σ
- ***Observed*** significance of 2.4σ
- ***Signal strength*** $\mu = 1.36^{+0.69}_{-0.61}$

Summary of event categories

- ***H→μμ analysis*** divided in ***exclusive production categories*** targeting ***ggH***, ***VBF***, ***VH***, and ***ttH*** modes
- Each of them is further ***divided into subcategories*** optimising the significance for H→μμ decays

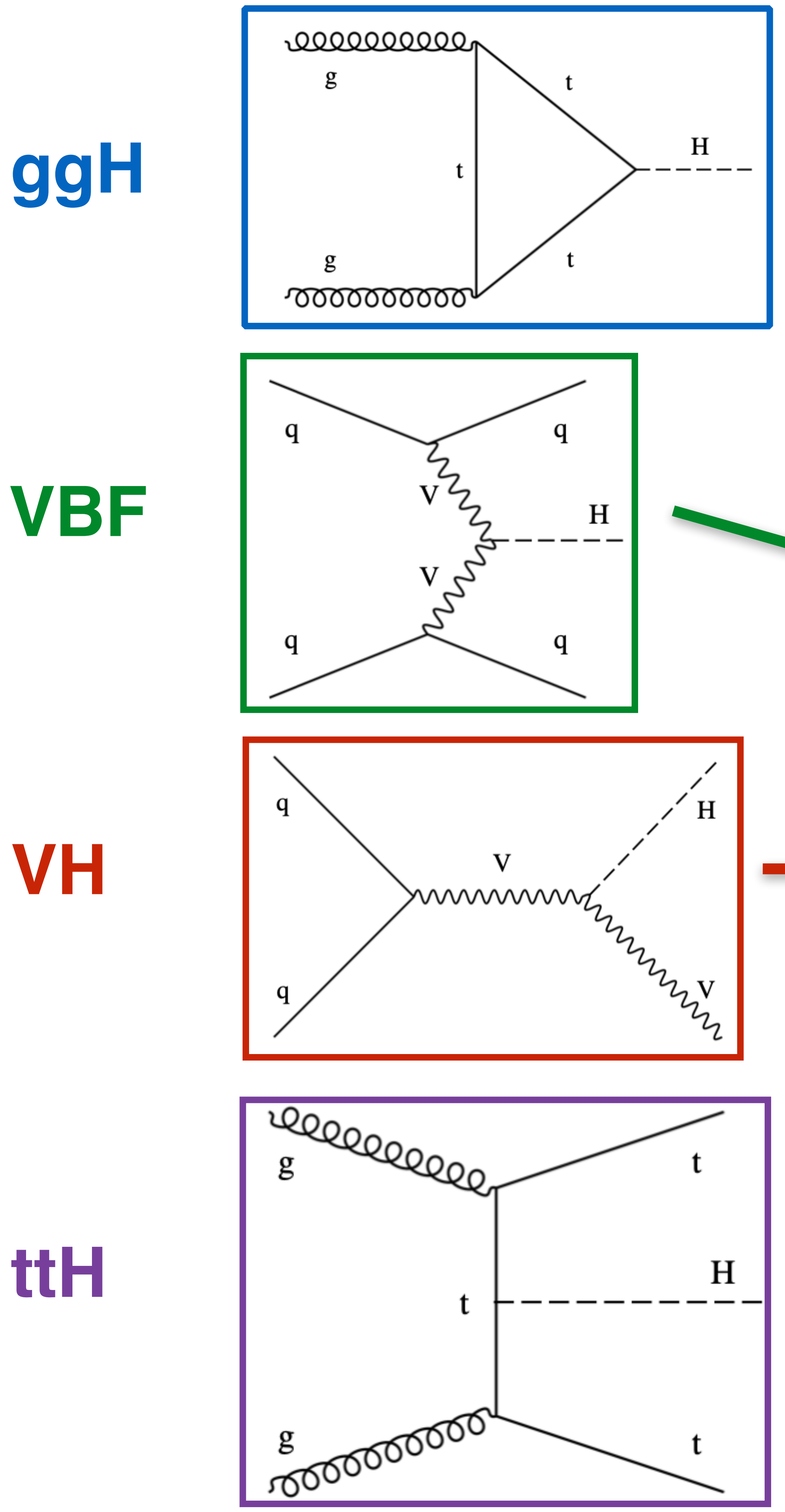

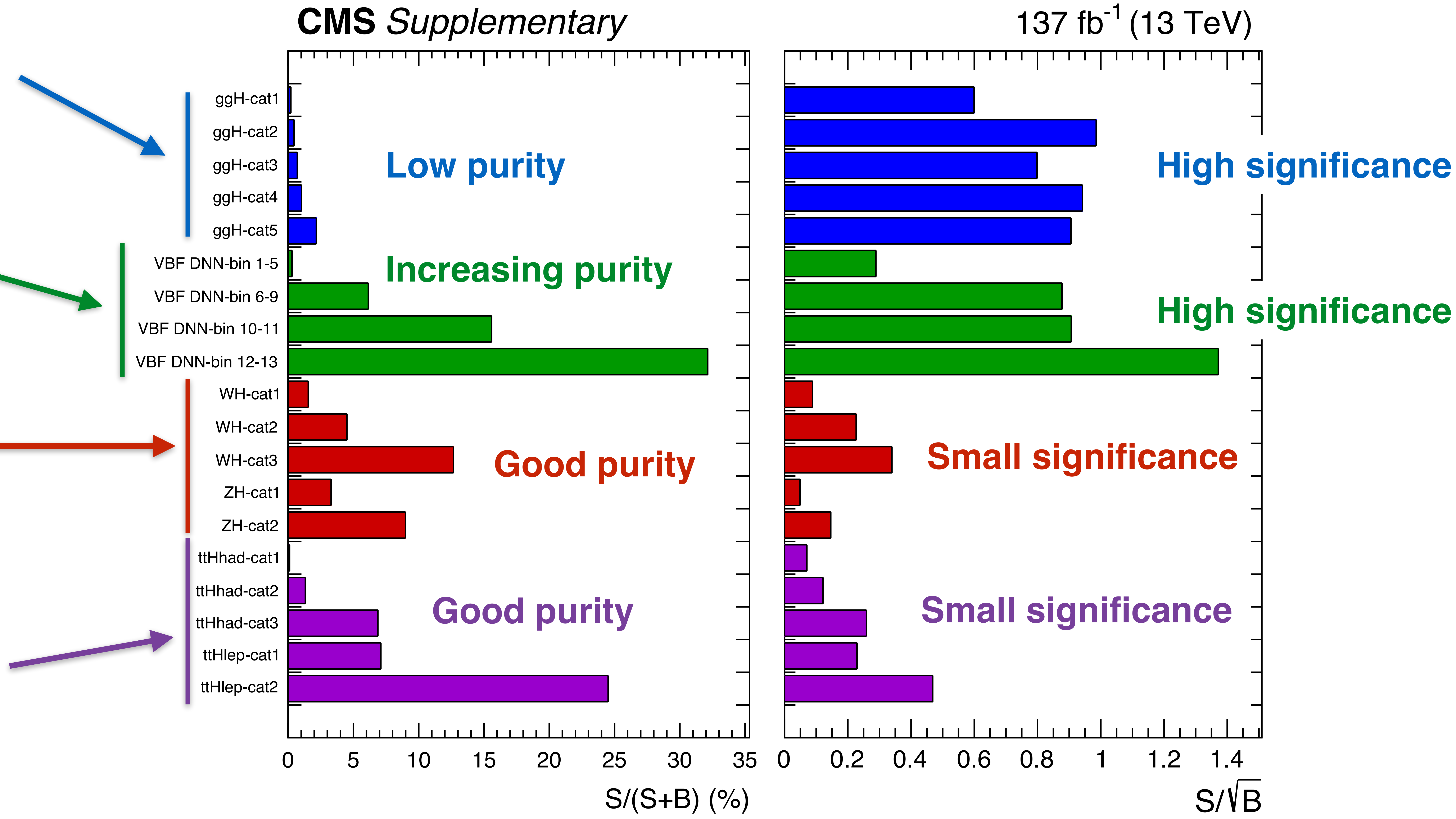

Local p-values vs Higgs mass

- ***Combined fit*** performed ***across all event categories*** (ggH, VBF, VH, and ttH)
- Systematic uncertainties are typically correlated across data-taking periods and categories

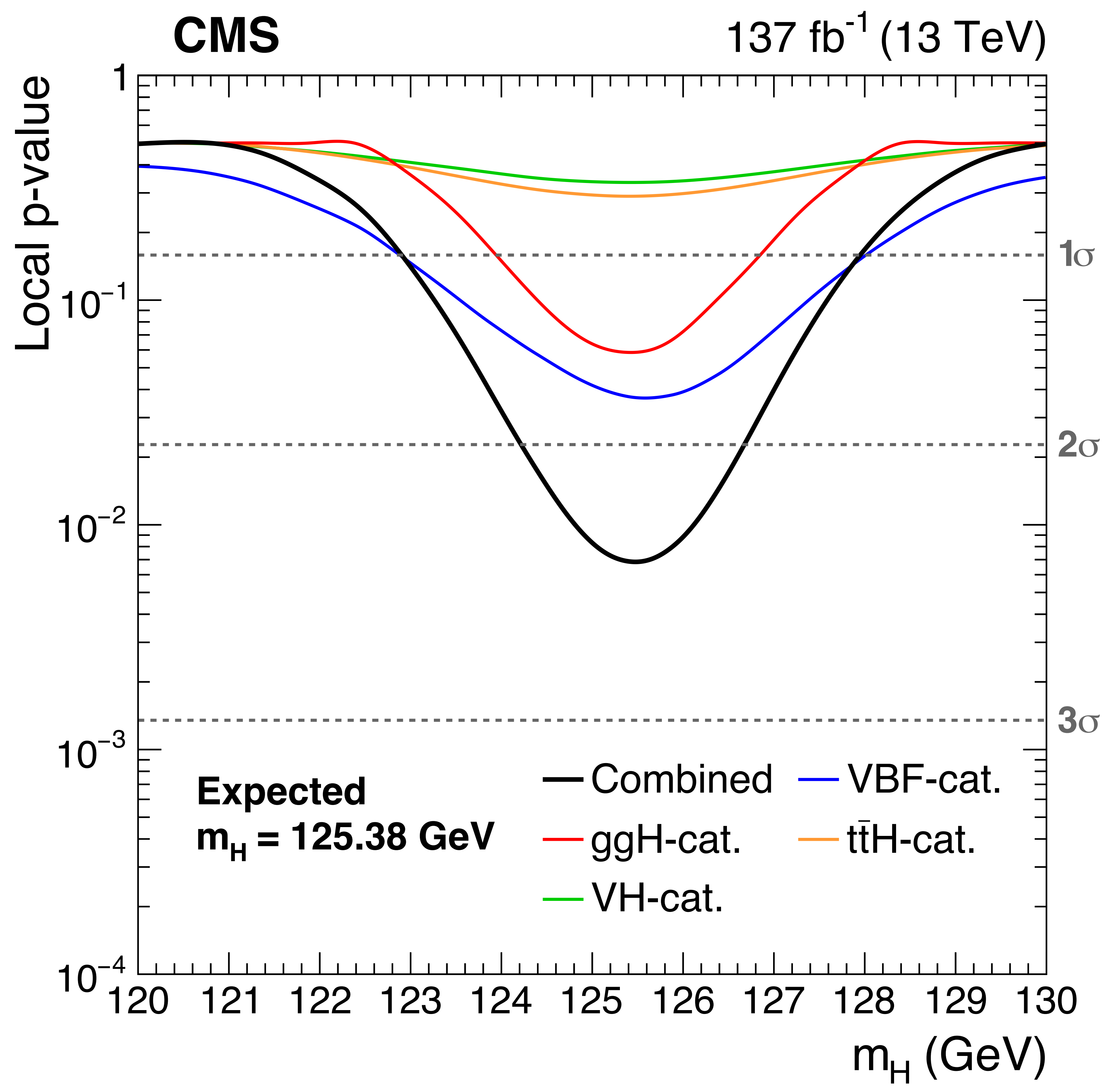

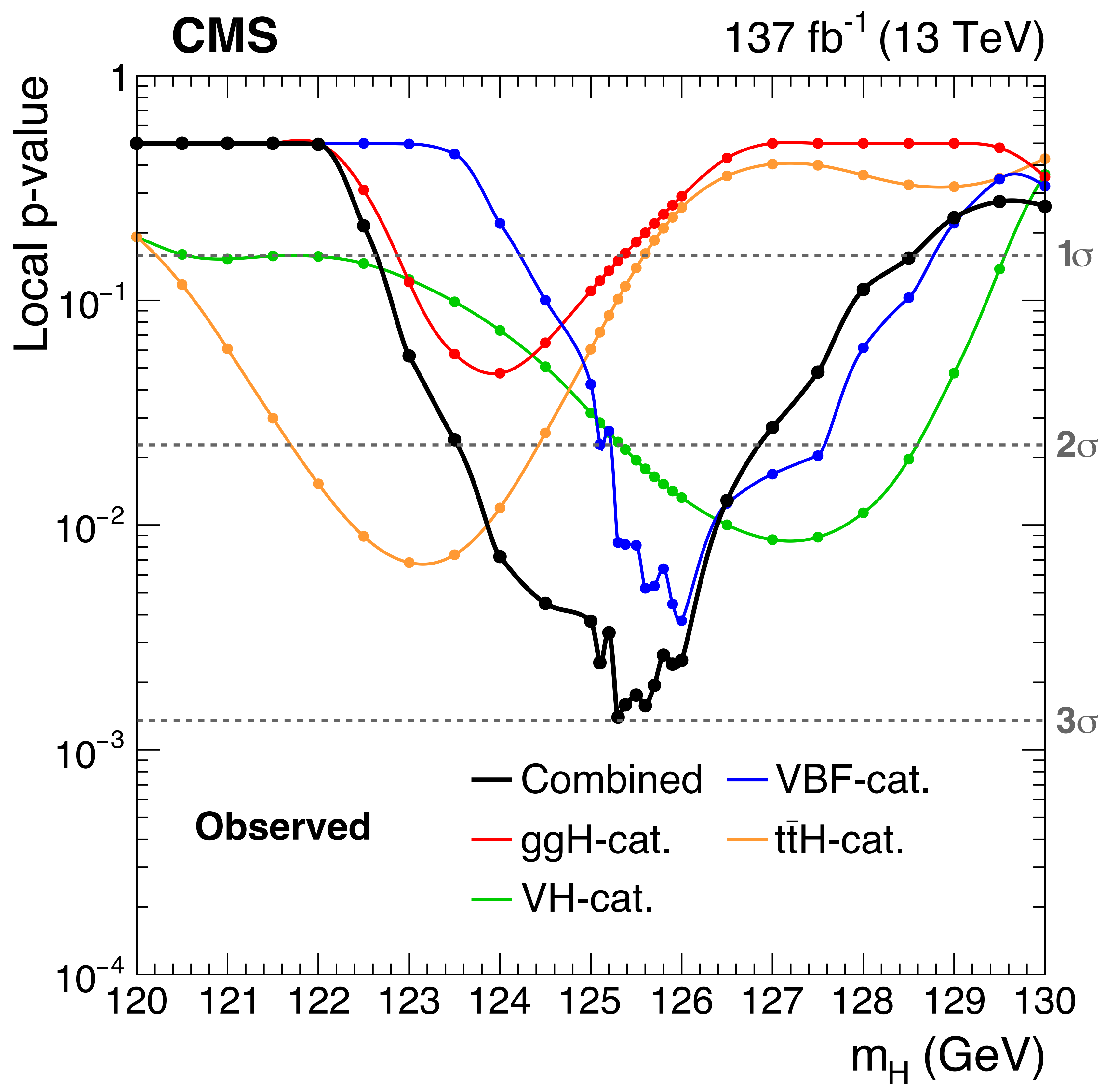

Expected significance for m_H = 125.38 GeV is **2.5σ**

Observed significance for m_H = 125.38 GeV is **3.0σ**

Local p-values vs Higgs mass

- ***Combined fit*** performed ***across all event categories*** (ggH, VBF, VH, and ttH)
- Systematic uncertainties are typically correlated across data-taking periods and categories

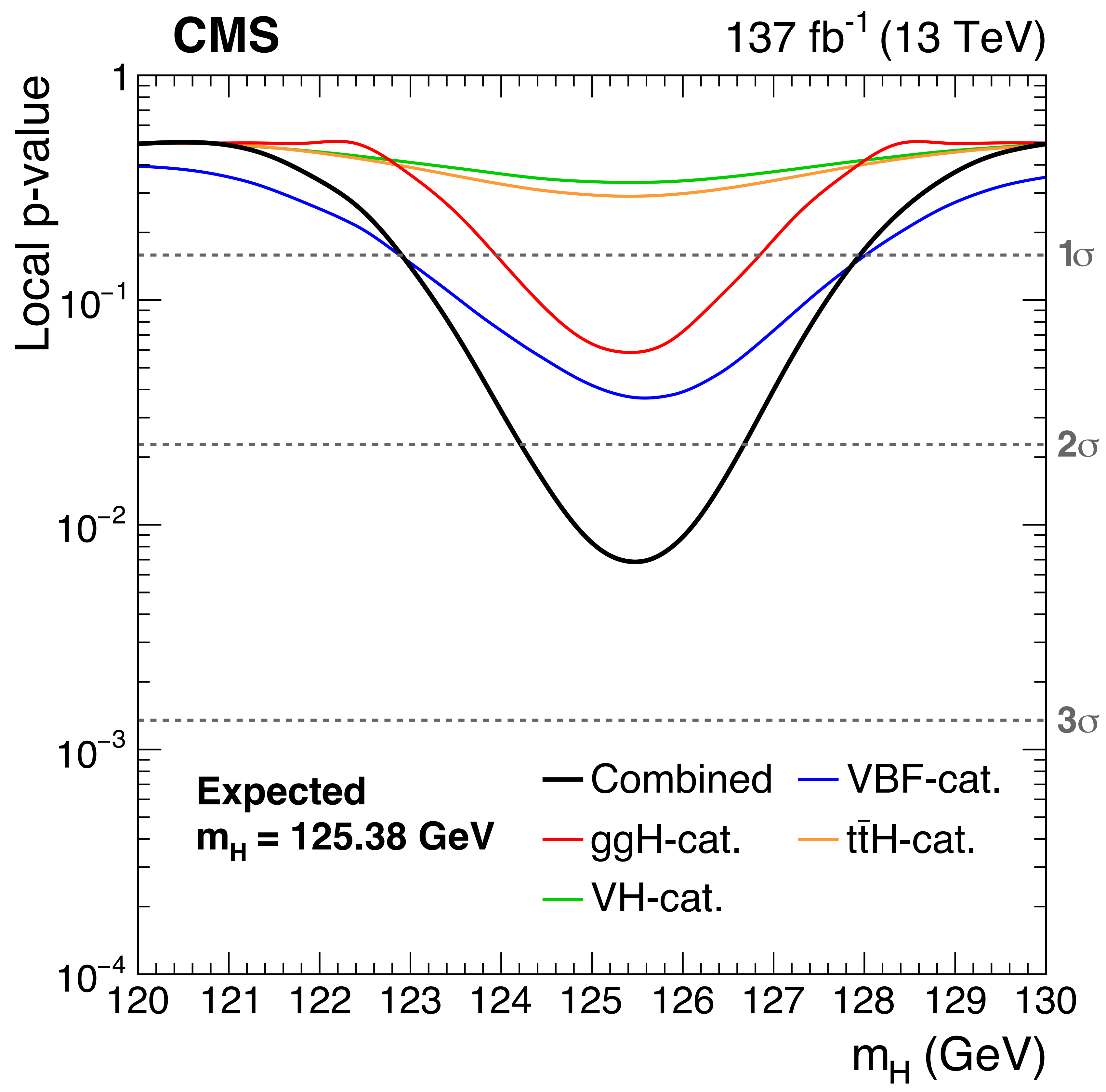

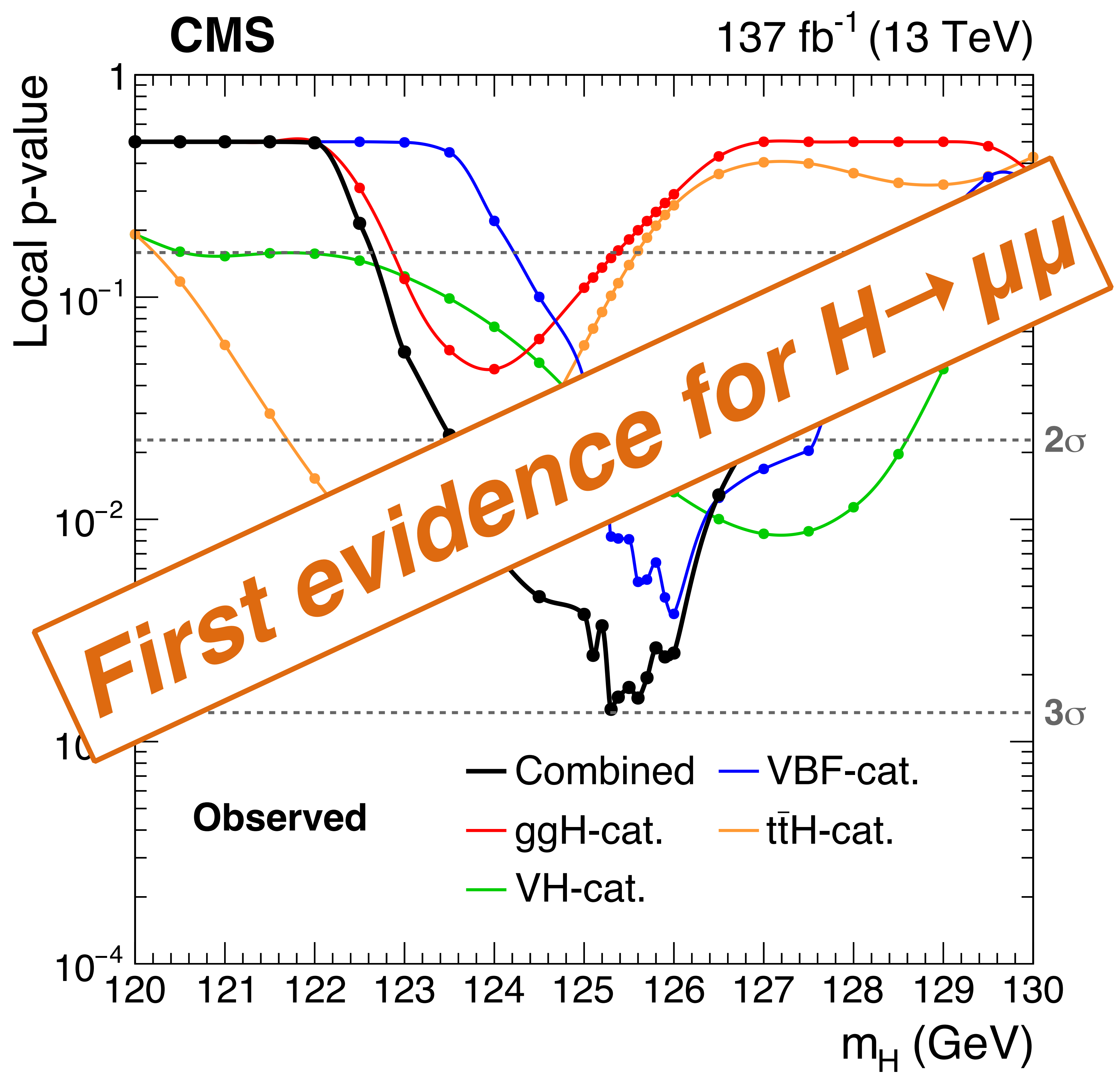

Expected significance for m_H = 125.38 GeV is **2.5σ**

Observed significance for m_H = 125.38 GeV is **3.0σ**

H → μμ fitted signal

Signal strength for m_H = 125.38 GeV
in the ***four production categories***

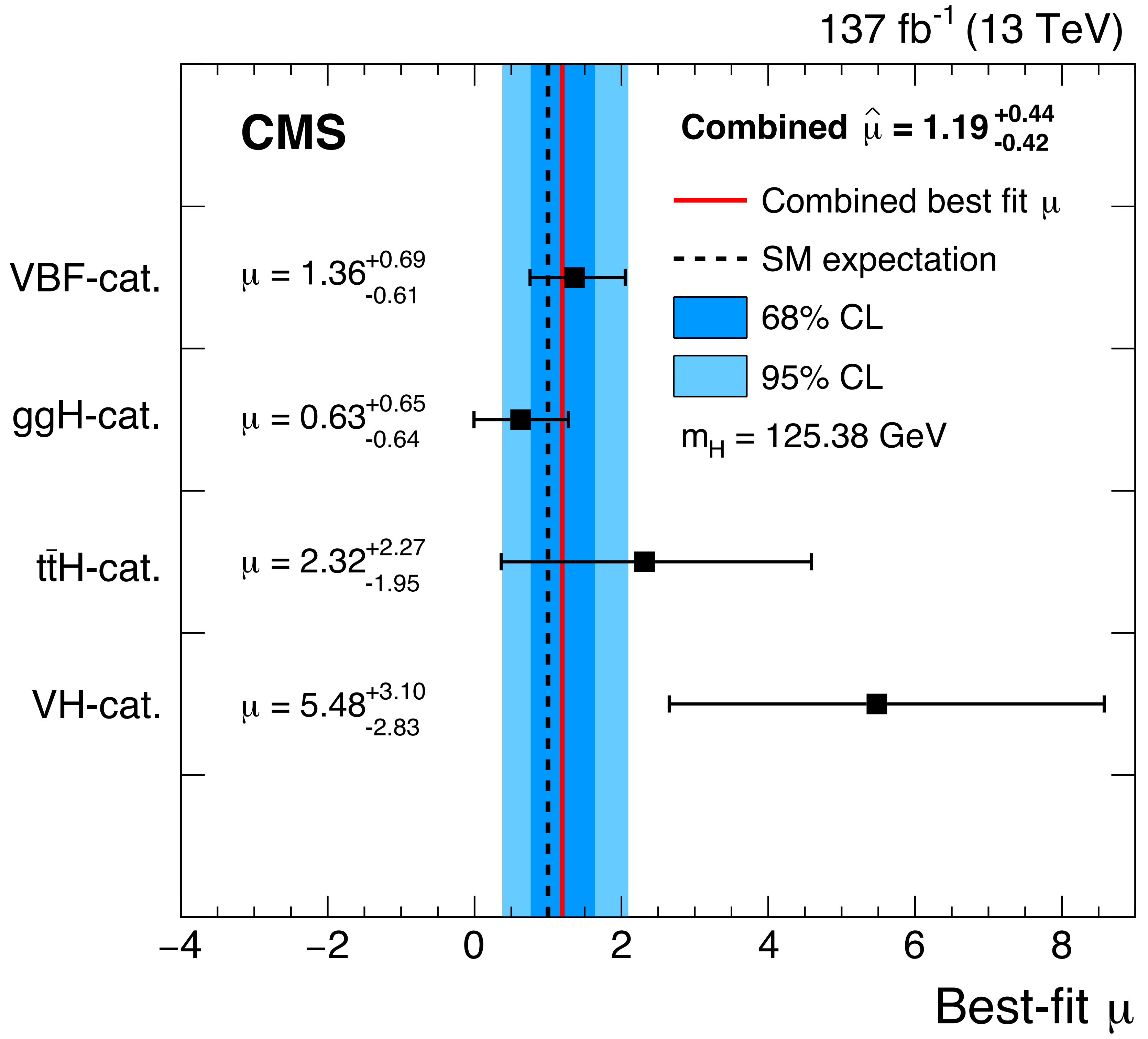

- **Best fit** $\mu = 1.19^{+0.44}_{-0.42}$
- Results compatible with SM expectations
- ***Uncertainty dominated by statistics***

Combining $m_{\mu\mu}$ spectrums from different categories weighting then by the expected S/(S+B)

for illustration only

H → μμ fitted signal

Signal strength for m_H = 125.38 GeV
in the ***four production categories***

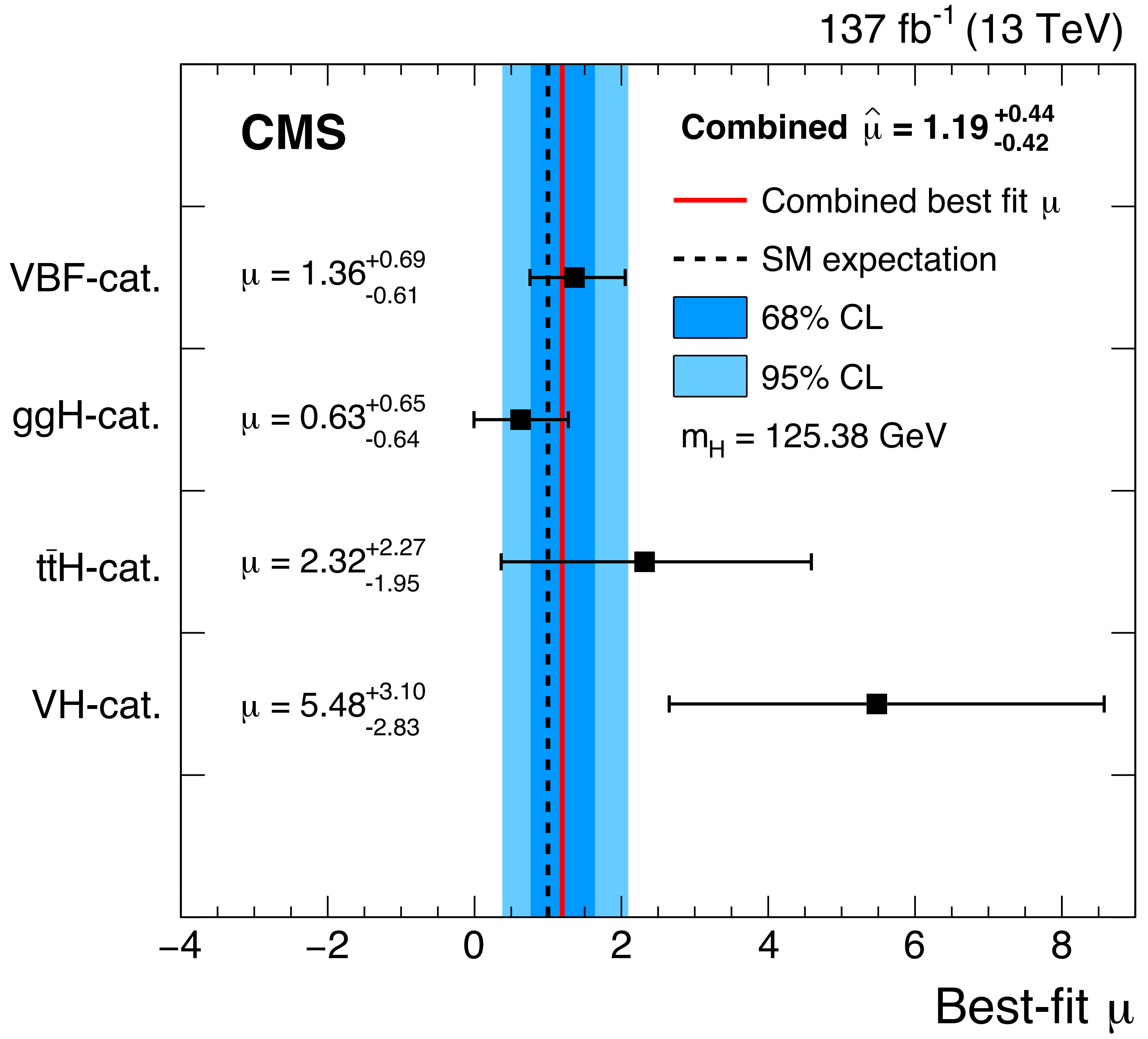

- **Best fit** $\mu = 1.19^{+0.44}_{-0.42}$
- Results compatible with SM expectations
- ***Uncertainty dominated by statistics***

Combining $m_{\mu\mu}$ spectrums from different categories weighting then by the expected S/(S+B)

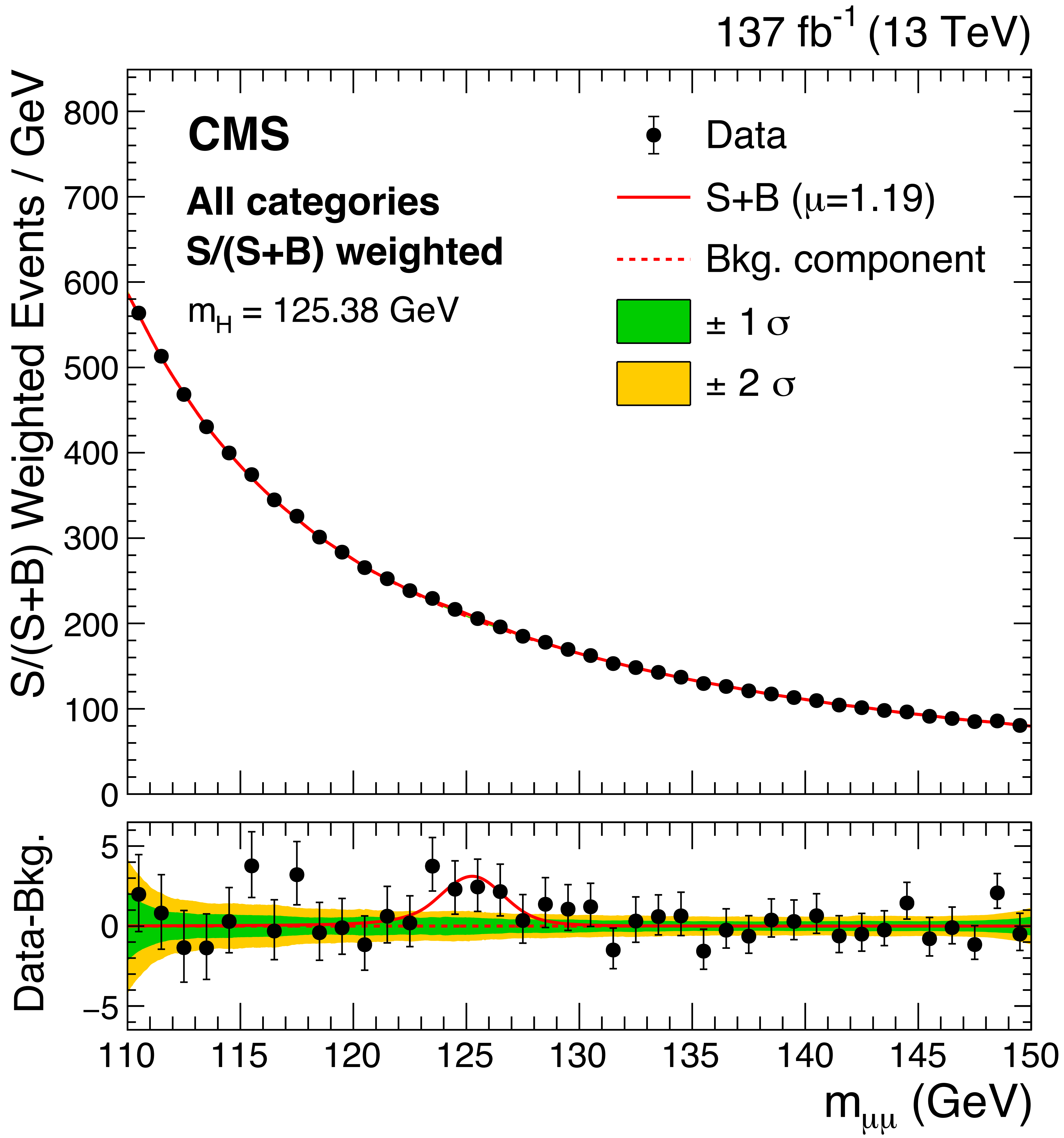

for illustration only

Higgs boson couplings to muons

- The ***H→μμ coupling strength*** is obtained from a combination with measurements from ***other Higgs channels***
- ***This H→μμ result*** is ***combined*** with the ***analyses reported*** in ***CMS-PAS-HIG-19-005***
- The ***resolved k-framework*** model is adopted to extract ***estimates*** for the ***Higgs boson couplings*** to ***SM particles***

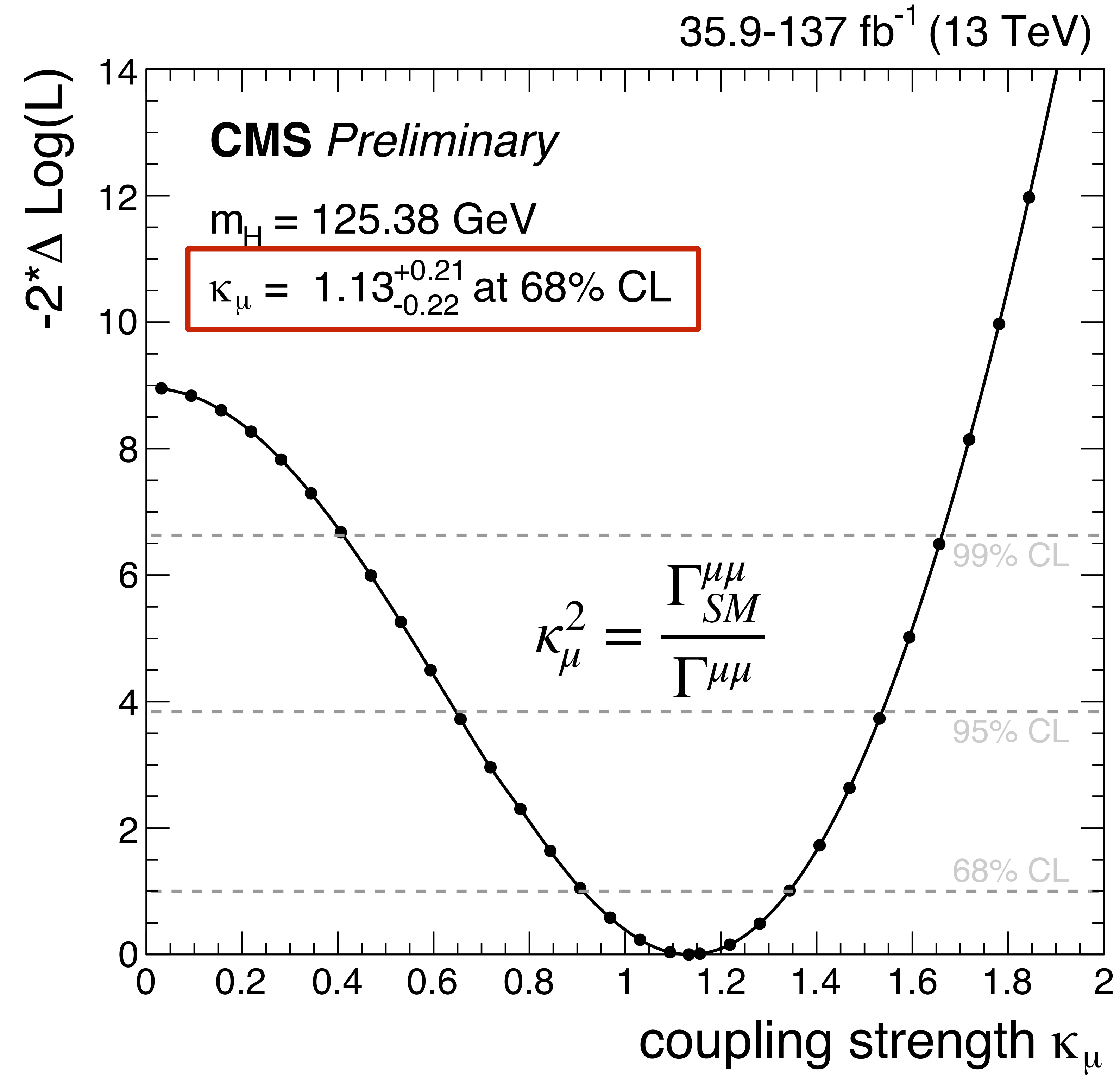

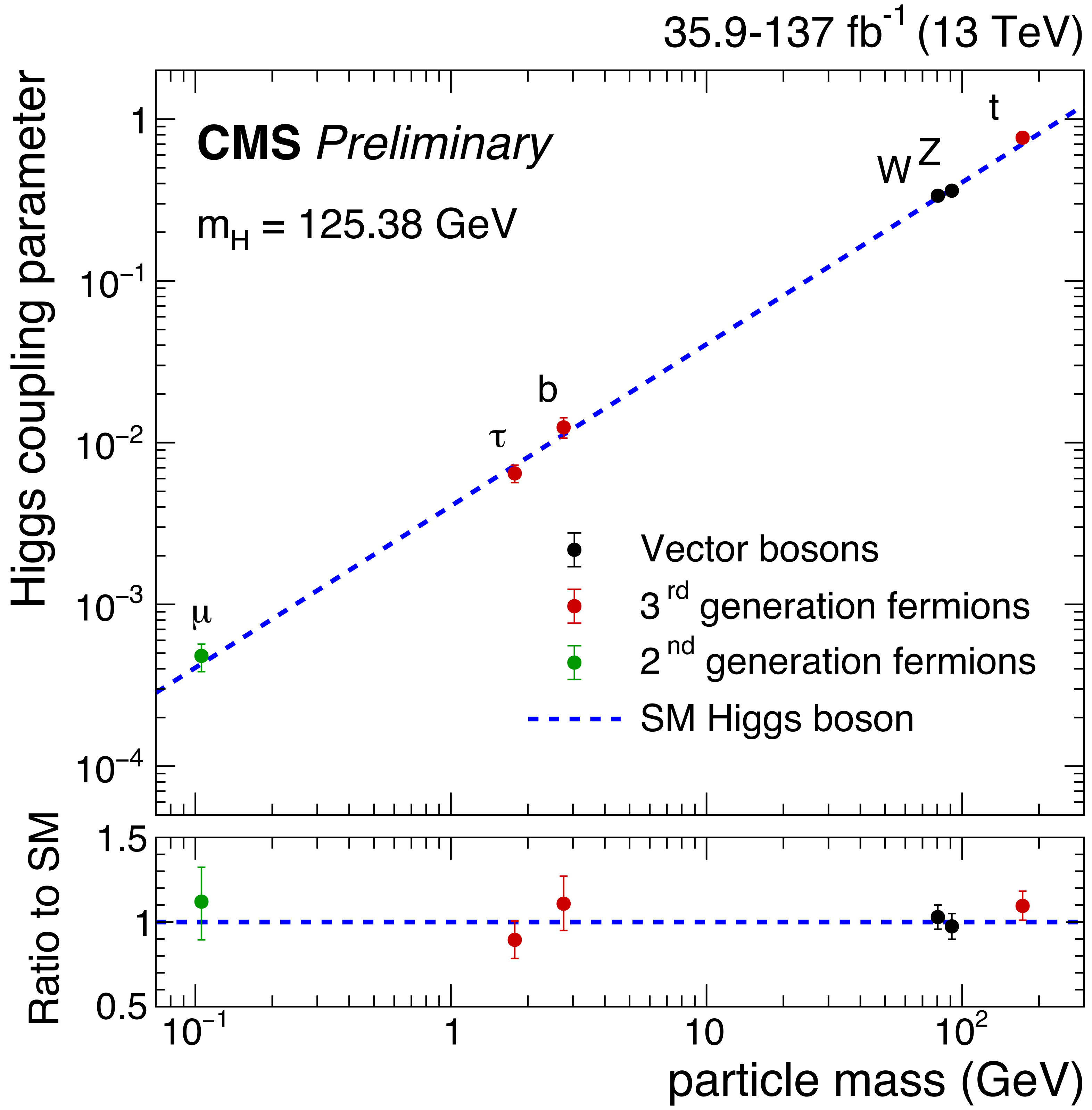

Observed H→μμ coupling strength compatible with SM with ***~20% uncertainty***

Coupling vs mass → ***remarkable success of the SM***

$H \rightarrow \mu\mu$ analysis: ATLAS vs CMS

*** **Disclaimer:** an apple-to-apple comparison between ***ATLAS*** and ***CMS*** results is not straightforward, ***can be only based*** on information provided in the corresponding ***papers*** submitted to PLB and JHEP, respectively

*** **Disclaimer:** ATLAS results interpreted for m_H = 125.09 GeV, CMS ones for m_H = 125.38 GeV

ATLAS vs CMS: results

Similarities

- Both experiments rely on ***single-muon triggers*** with similar overall efficiency
- ***Comparable acceptance*** of the baseline dimuon selection
- Both experiments developed ***dedicated analyses*** for ttH, VH, VBF, and ggH production modes
- ***ttH, VH, VBF,*** and ***ggH*** MVAs exploit similar input features to maximise the S to B separation
- Similar choice for ***signal event generation***: NNLOPS prediction used as target for ggH, POWHEG NLO for other processes (VBF, VH, ttH)

Differences

- **mass resolution:** CMS has a substantially better resolution on muon p_T
- In CMS all ***MVAs*** are ***sensitive*** to both ***event kinematic*** and ***$m_{\mu\mu}$ resolution***, while ATLAS does not embed the resolution information
- The p_T threshold for ***additional leptons*** in ttH and VH are lower in ATLAS than in CMS
- ***VBF analysis:*** ATLAS uses a divide-n-fit strategy, while CMS adopted a MC-based analysis
- ***ggH analysis:*** ATLAS trained independent BDTs in each jet-bin, while CMS has a single MVA classifier
- ***ggH analysis:*** ATLAS has 4 categories per MVA, while CMS has just five ggH categories in total

The difference in $m_{\mu\mu}$ resolution is the main reason behind the stronger CMS result

ATLAS vs CMS: results

Similarities

- Both experiments rely on ***single-muon triggers*** with similar overall efficiency
- ***Comparable acceptance*** of the baseline dimuon selection
- Both experiments developed ***dedicated analyses*** for ttH, VH, VBF, and ggH production modes
- ***ttH, VH, VBF,*** and ***ggH*** MVAs exploit similar input features to maximise the S to B separation
- Similar choice for ***signal event generation***: NNLOPS prediction used as target for ggH, POWHEG NLO for other processes (VBF, VH, ttH)

Differences

- **mass resolution:** CMS has a substantially better resolution on muon p_T
- In CMS all ***MVAs*** are ***sensitive*** to both ***event kinematic*** and ***$m_{\mu\mu}$ resolution***, while ATLAS does not embed the resolution information
- The p_T threshold for ***additional leptons*** in ttH and VH are lower in ATLAS than in CMS
- ***VBF analysis:*** ATLAS uses a divide-n-fit strategy, while CMS adopted a MC-based analysis
- ***ggH analysis:*** ATLAS trained independent BDTs in each jet-bin, while CMS has a single MVA classifier
- ***ggH analysis:*** ATLAS has 4 categories per MVA, while CMS has just five ggH categories in total

The difference in $m_{\mu\mu}$ resolution is the main reason behind the stronger CMS result

ATLAS vs CMS: results

Similarities

- Both experiments rely on ***single-muon triggers*** with similar overall efficiency
- ***Comparable acceptance*** of the baseline dimuon selection
- Both experiments developed ***dedicated analyses*** for ttH, VH, VBF, and ggH production modes
- ***ttH, VH, VBF,*** and ***ggH*** MVAs exploit similar input features to maximise the S to B separation
- Similar choice for ***signal event generation***: NNLOPS prediction used as target for ggH, POWHEG NLO for other processes (VBF, VH, ttH)

Differences

- **mass resolution:** CMS has a substantially better resolution on muon p_T
- In CMS all ***MVAs*** are ***sensitive*** to both ***event kinematic*** and ***$m_{\mu\mu}$ resolution***, while ATLAS does not embed the resolution information
- The p_T threshold for ***additional leptons*** in ttH and VH are lower in ATLAS than in CMS
- ***VBF analysis:*** ATLAS uses a divide-n-fit strategy, while CMS adopted a MC-based analysis
- ***ggH analysis:*** ATLAS trained independent BDTs in each jet-bin, while CMS has a single MVA classifier
- ***ggH analysis:*** ATLAS has 4 categories per MVA, while CMS has just five ggH categories in total

The difference in $m_{\mu\mu}$ resolution is the main reason behind the stronger CMS result

ATLAS vs CMS: mass resolution

ATLAS categories

Category	Data	S_{SM}	S	B	$S/\sqrt{B}$	S/B [%]	σ [GeV]
VBF Very High	15	2.81 ± 0.27	3.3 ± 1.7	14.5 ± 2.1	0.86	22.6	3.0
VBF High	39	3.46 ± 0.36	4.0 ± 2.1	32.5 ± 2.9	0.71	12.4	3.0
VBF Medium	112	4.8 ± 0.5	5.6 ± 2.8	85 ± 4	0.61	6.6	2.9
VBF Low	284	7.5 ± 0.9	9 ± 4	273 ± 8	0.53	3.2	3.0
2-jet Very High	1030	17.6 ± 3.3	21 ± 10	1024 ± 22	0.63	2.0	3.1
2-jet High	5433	50 ± 8	58 ± 30	5440 ± 50	0.77	1.0	2.9
2-jet Medium	18 311	79 ± 15	90 ± 50	18 320 ± 90	0.66	0.5	2.9
2-jet Low	36 409	63 ± 17	70 ± 40	36 340 ± 140	0.37	0.2	2.9
1-jet Very High	1097	16.5 ± 2.4	19 ± 10	1071 ± 22	0.59	1.8	2.9
1-jet High	6413	46 ± 7	54 ± 28	6320 ± 50	0.69	0.9	2.8
1-jet Medium	24 576	90 ± 11	100 ± 50	24 290 ± 100	0.67	0.4	2.7
1-jet Low	73 459	125 ± 17	150 ± 70	73 480 ± 190	0.53	0.2	2.8
0-jet Very High	15 986	59 ± 11	70 ± 40	16 090 ± 90	0.55	0.4	2.6
0-jet High	46 523	99 ± 13	120 ± 60	46 190 ± 150	0.54	0.3	2.6
0-jet [illegible]	[illegible]	[illegible]	[illegible]	[illegible]	[illegible]	[illegible]	2.7
0-jet [illegible]	[illegible]	[illegible]	[illegible]	[illegible]	[illegible]	[illegible]	2.7
VH4 [illegible]	[illegible]	[illegible]	[illegible]	[illegible]	[illegible]	[illegible]	2.9
VH3 [illegible]	[illegible]	[illegible]	[illegible]	[illegible]	[illegible]	[illegible]	3.1
VH3 [illegible]	[illegible]	[illegible]	[illegible]	[illegible]	[illegible]	[illegible]	3.0
$t\bar{t}H$ [illegible]	[illegible]	[illegible]	[illegible]	[illegible]	[illegible]	[illegible]	3.2

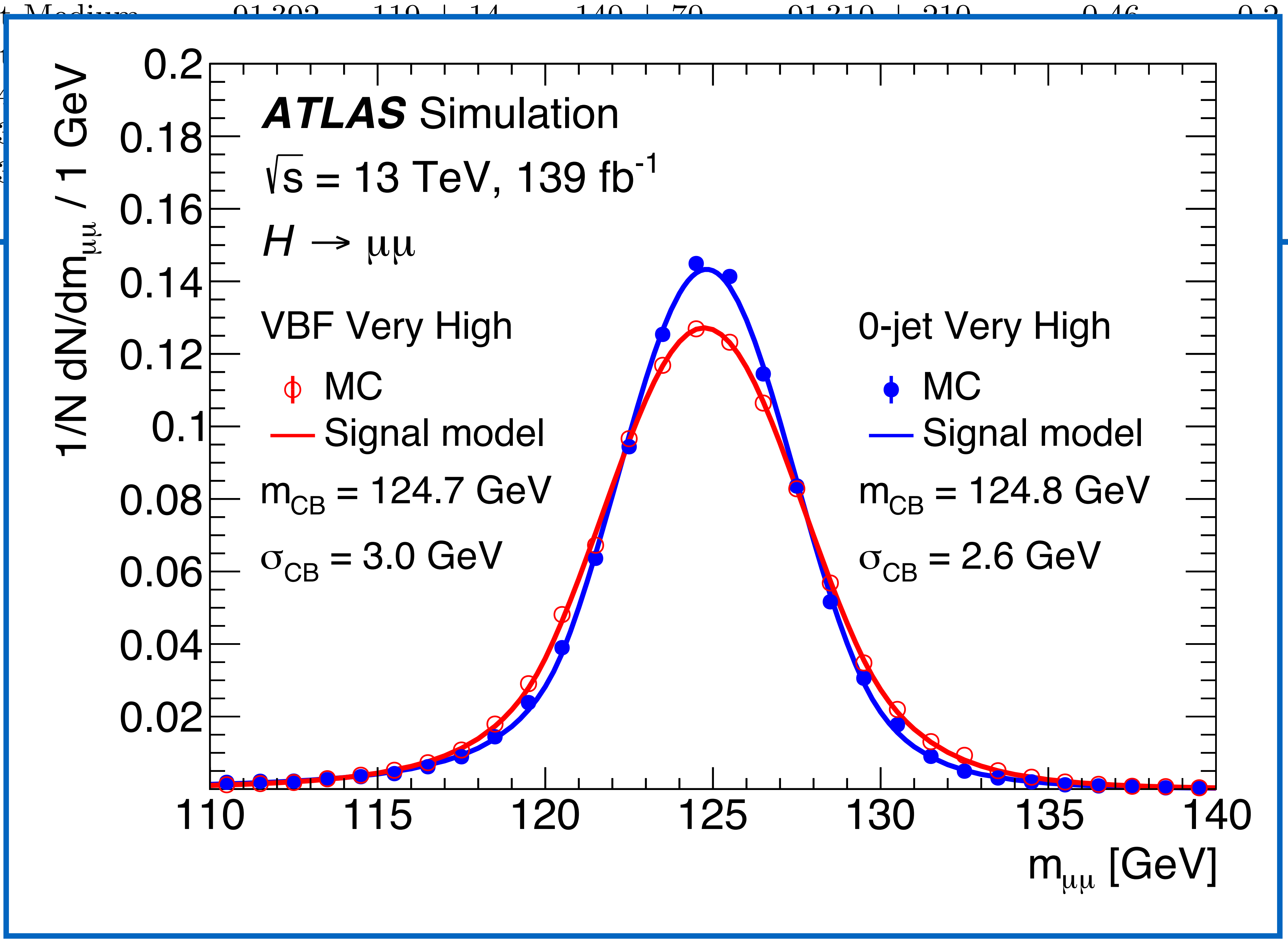

CMS resolution in ggH

Event category	HWHM (GeV)
ggH-cat1	2.12
ggH-cat2	1.75
ggH-cat3	1.60
ggH-cat4	1.47
ggH-cat5	1.50

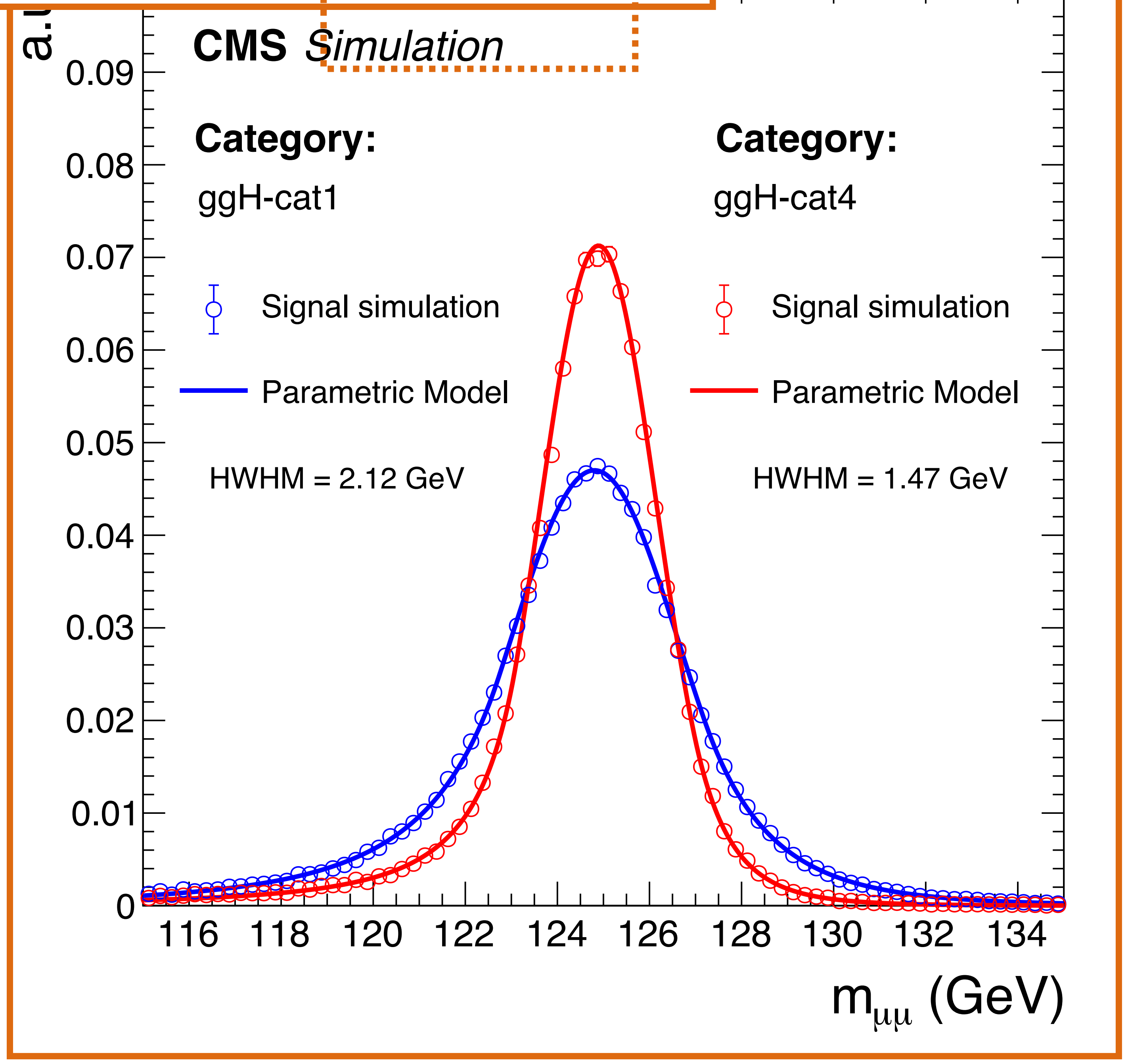

ATLAS vs CMS: results

- Comparison of the final weighted mass distributions from the two experiments

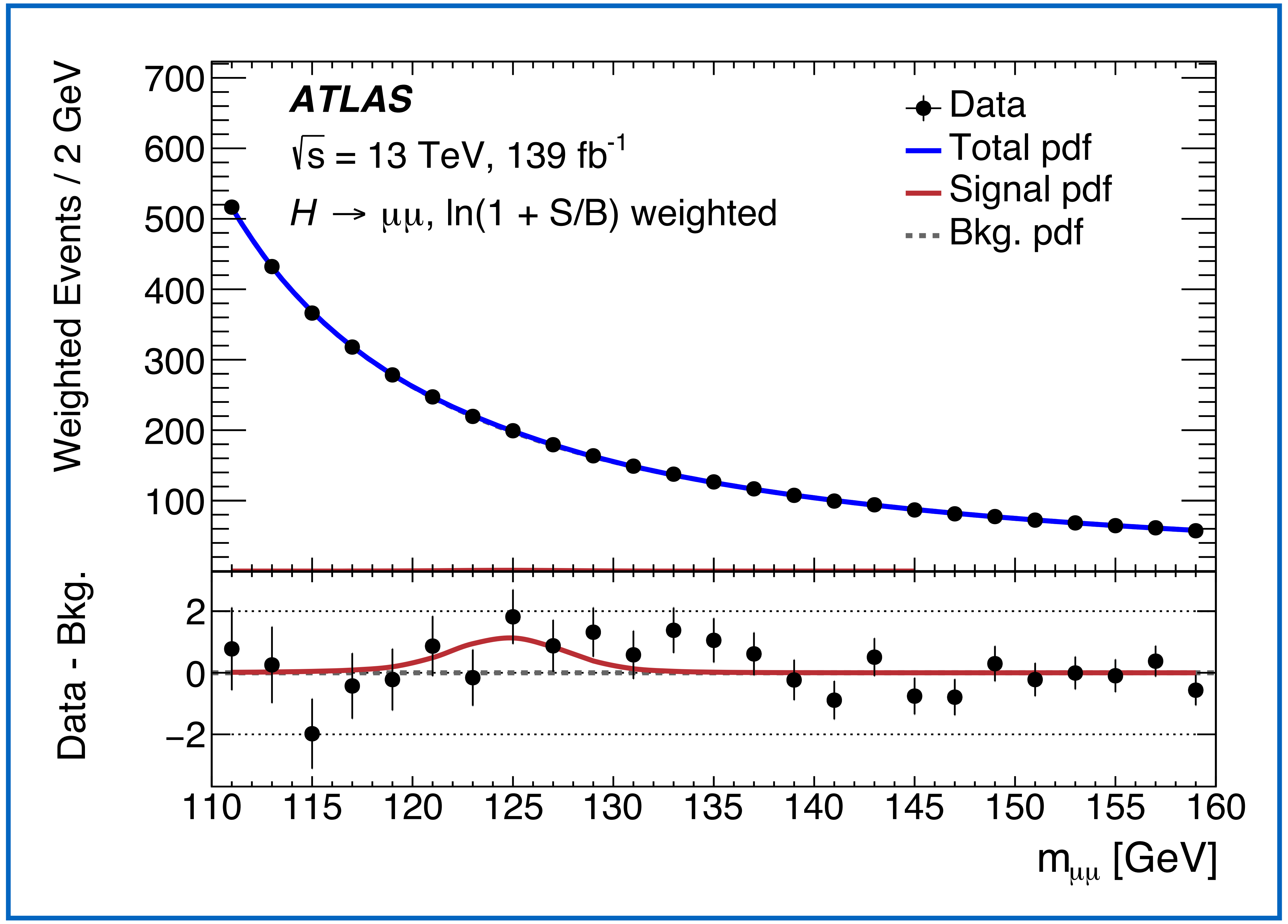

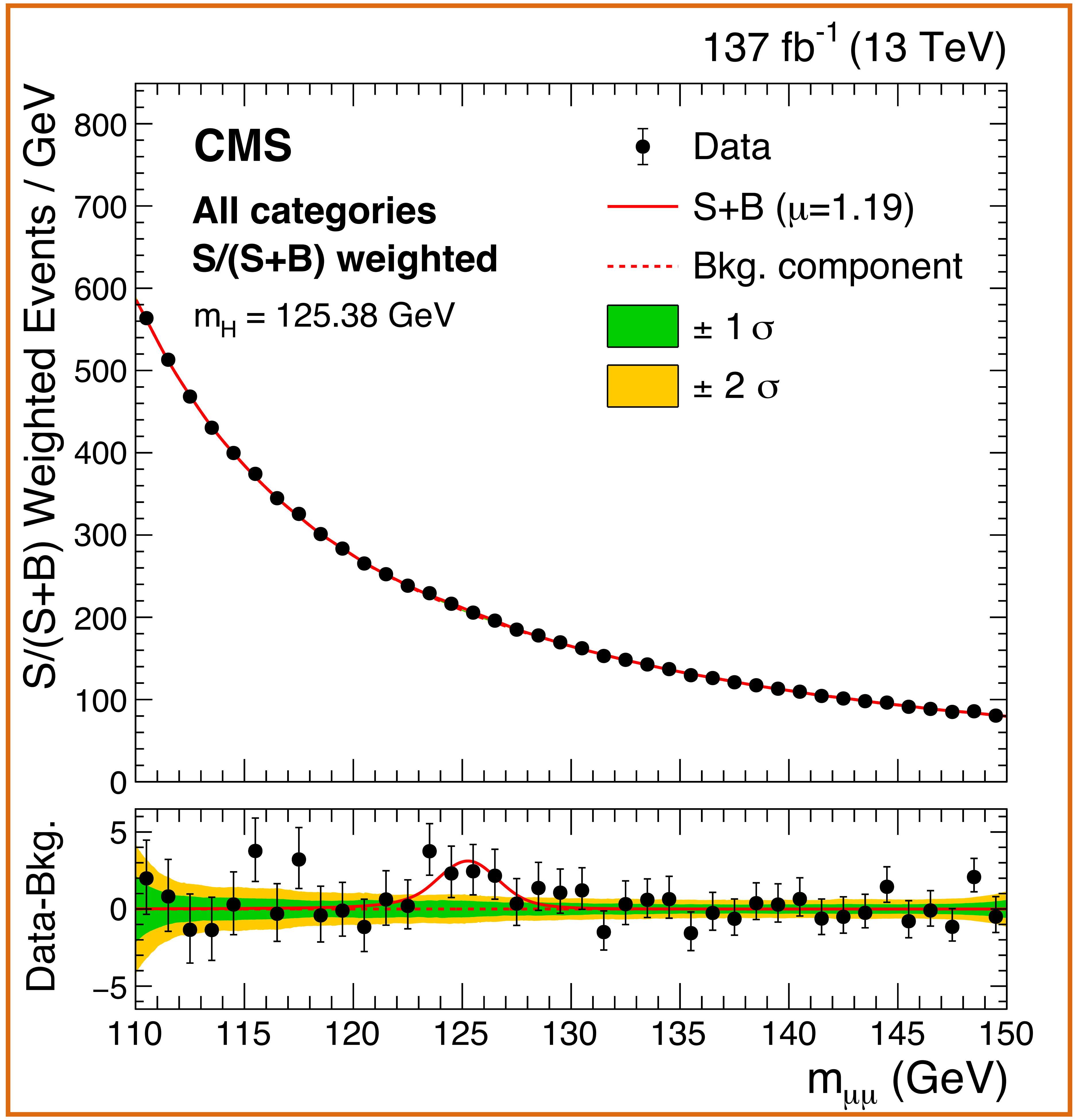

- **ATLAS:** observed (exp) significance 2.0 (1.7) σ
- **CMS:** observed (exp) significance 3.0 (2.5) σ

H→μμ analysis: future prospects

H→μμ analysis in Run3

- The ***LHC Run3*** will begin in February 2022
  - Total integrated luminosity of about **200 fb^{-1}**
  - ***Pileup*** similar to the one of ***2018 data-taking***
  - Center-of-mass energy possibly raised to ***14 TeV***

Small upgrades in the CMS detector performed during LS2

- ***Conservative projections*** for H→μμ reported in ***FTR-18-011***
- Projections from an extrapolation of earlier H→μμ
- ***The result presented before already provides a 40% uncertainty in the BR(H→μμ) estimate***
- ***CMS Run2 result went well beyond previous expectations***

- ***Performance of H→μμ in Run3 expected to be same of Run2***
- Very similar detector, pileup level, trigger setup etc ..
- Analysis ***statistically limited*** so it will ***improve with luminosity***

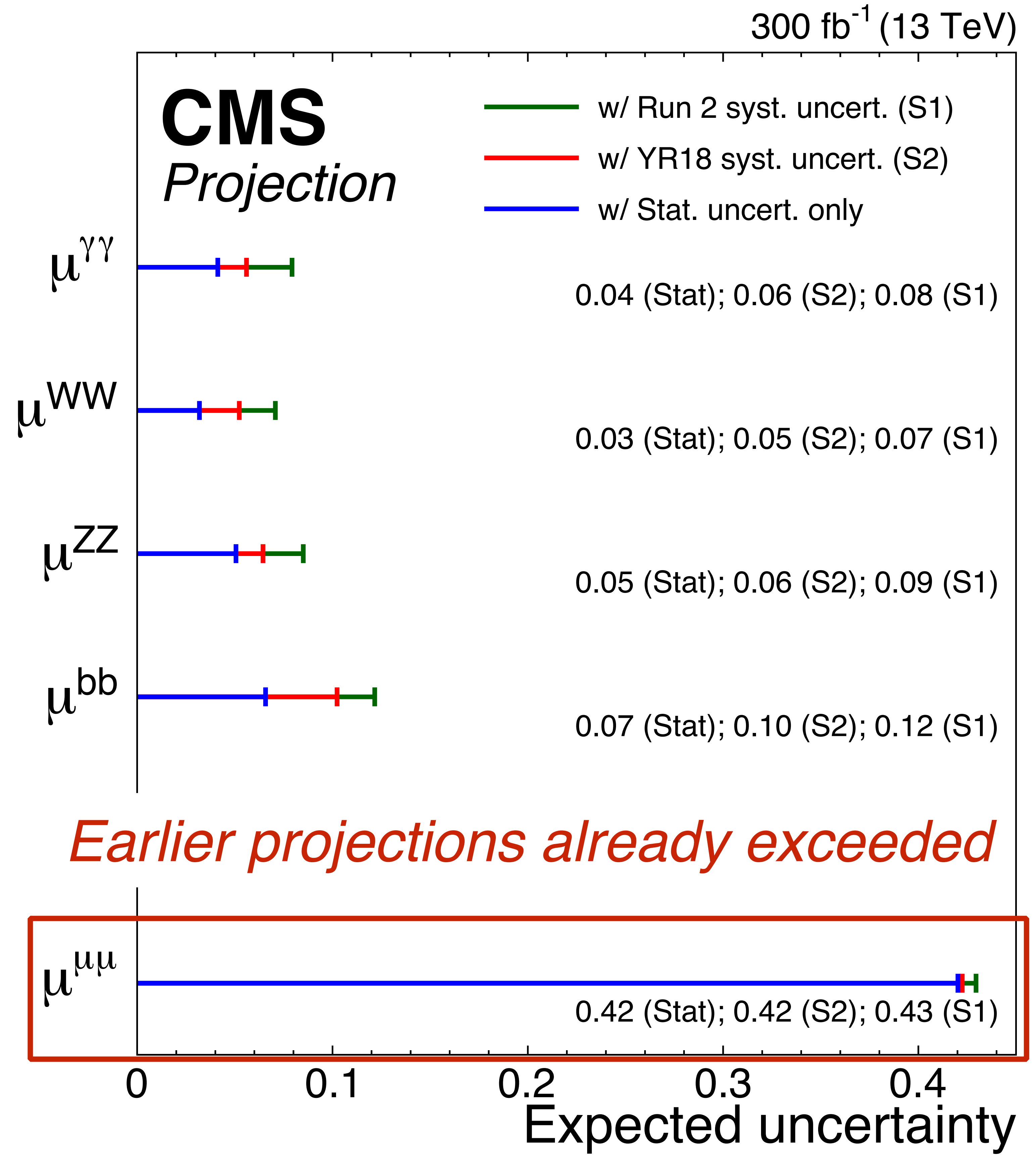

H→μμ analysis in Run3

- The ***LHC Run3*** will begin in February 2022
  - Total integrated luminosity of about **200 fb^{-1}**
  - ***Pileup*** similar to the one of ***2018 data-taking***
  - Center-of-mass energy possibly raised to ***14 TeV***

Sma... ...MS detector ...uring LS2

- ***Conservative projections*** for H→μμ reported in ***FTR***...
- Projections from an extrapolation of earlier H→...
- ***The result presented before already*** ...
  uncertainty in the BR(H→μμ) e...
- ***CMS Run2 result went*** ... ***s expectations***

Assuming no improvements or losses, we expect to reach an expected significance of 4σ with Run2+Run3 dataset

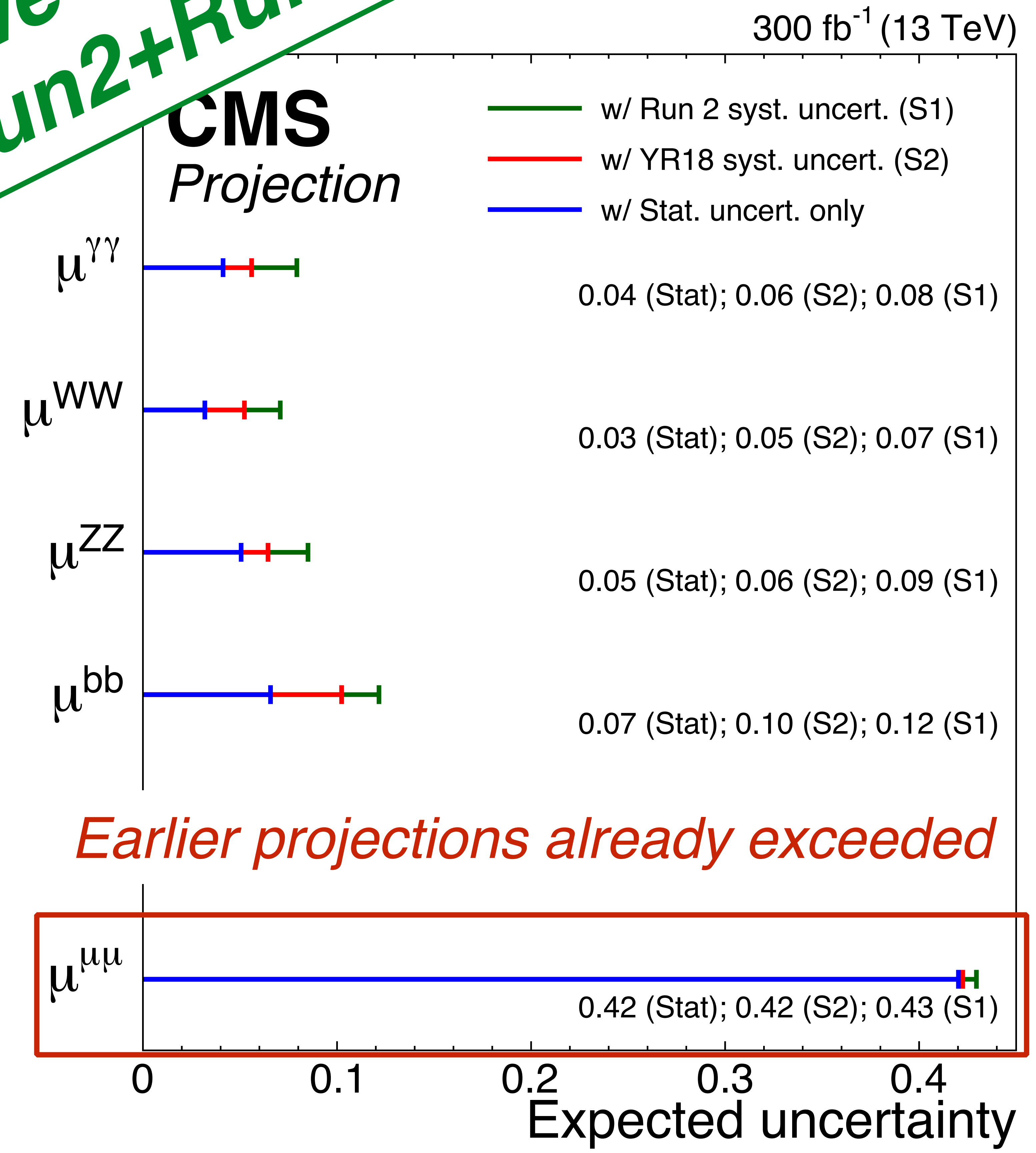

- ***Perfo***... ***→μμ in Run3 expected to be same of Run2***
- Very sin... detector, pileup level, trigger setup etc ..
- Analysis ***statistically limited*** so it will ***improve with luminosity***

H→μμ analysis in HL-LHC

- The HL-LHC will start in 2026 delivering about ***3-4 ab^{-1}*** of pp collision data at ***14 TeV***
  - ***Extreme pileup conditions*** → 200 concurrent interactions every bunch crossing
  - To operate in this environment, ***the detector will upgrade or replace severals subsystems***

Upgraded detector

- ***New tracker*** with coverage up to |η|=4 and L1 track trigger
- ***Upgraded muon system*** with coverage up to |η|=2.8
- ***New high granularity*** endcap ***calorimeter (HGCal)***

Improvements expected in the H→μμ analysis

- Increased acceptance due to muon coverage up to |η|=2.8
- Possibly reconstruct muons with tracker-only up to |η|=4.0
- Substantial improvement in ***muon p_T resolution***
- **VBF category:** improved ***jet-energy-resolution*** for endcap and forward jets
- **VBF category:** improved ***rejection*** of ***pileup jets*** in the ***endcap*** and ***forward region***

H→μμ analysis in HL-LHC

- The HL-LHC will start in 2026 delivering about ***3-4 ab^{-1}*** of pp collision data at ***14 TeV***
  - ***Extreme pileup conditions*** → 200 concurrent interactions every bunch crossing
  - To operate in this environment, ***the detector will upgrade or replace severals subsystems***

Upgraded detector

- ***New tracker*** with coverage up to |η|=4 and L1 track trigger
- ***Upgraded muon system*** with coverage up to |η|=2.8
- ***New high granularity*** endcap ***calorimeter (HGCal)***

Improvements expected in the H→μμ analysis

- Increased acceptance due to muon coverage up to |η|=2.8
- Possibly reconstruct muons with tracker-only up to |η|=4.0
- Substantial improvement in ***muon p_T resolution***
- **VBF category:** improved ***jet-energy-resolution*** for endcap and forward jets
- **VBF category:** improved ***rejection*** of ***pileup jets*** in the ***endcap*** and ***forward region***

H→μμ analysis in HL-LHC

- The HL-LHC will start in 2026 delivering about ***3-4 ab^{-1}*** of pp collision data at ***14 TeV***
  - ***Extreme pileup conditions*** → 200 concurrent interactions every bunch crossing
  - To operate in this environment, ***the detector will upgrade or replace severals subsystems***

Upgraded detector

- ***New tracker*** with coverage up to |η|=4 and L1 track trigger
- ***Upgraded muon system*** with coverage up to |η|=2.8
- ***New high granularity*** endcap ***calorimeter (HGCal)***

Improvements expected in the H→μμ analysis

- Increased acceptance due to muon coverage up to |η|=2.8
- Possibly reconstruct muons with tracker-only up to |η|=4.0
- Substantial improvement in ***muon p_T resolution***
- **VBF category:** improved ***jet-energy-resolution*** for endcap and forward jets
- **VBF category:** improved ***rejection*** of ***pileup jets*** in the ***endcap*** and ***forward region***

H→μμ analysis in HL-LHC

- The HL-LHC will start in 2026 delivering about ***3-4 ab^{-1}*** of pp collision data at ***14 TeV***
  - ***Extreme pileup conditions*** → 200 concurrent interactions every bunch crossing
  - To operate in this environment, ***the detector will upgrade or replace severals subsystems***

Upgraded detector

- ***New tracker*** with coverage up to |η|=4 and L1 track trigger
- ***Upgraded muon system*** with coverage up to |η|=2.8
- ***New high granularity*** endcap ***calorimeter (HGCal)***

Improvements expected in the H→μμ analysis

- Increased acceptance due to muon coverage up to |η|=2.8
- Possibly reconstruct muons with tracker-only up to |η|=4.0
- Substantial improvement in ***muon p_T resolution***
- **VBF category:** improved ***jet-energy-resolution*** for endcap and forward jets
- **VBF category:** improved ***rejection*** of ***pileup jets*** in the ***endcap*** and ***forward region***

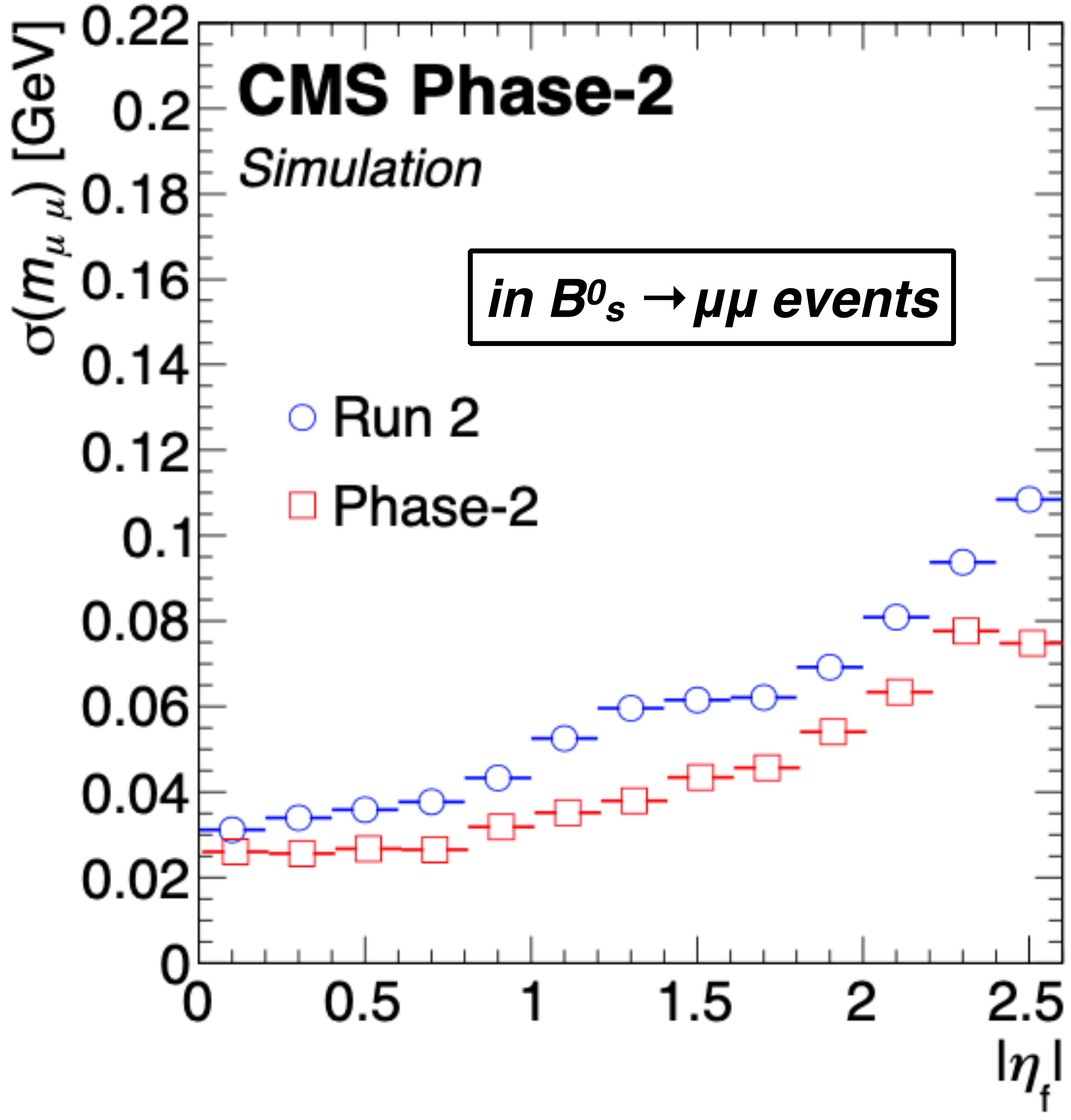

H→μμ analysis in HL-LHC

- The HL-LHC will start in 2026 delivering about ***3-4 ab^{-1}*** of pp collision data at ***14 TeV***
  - ***Extreme pileup conditions*** → 200 concurrent interactions every bunch crossing
  - To operate in this environment, ***the detector will upgrade or replace severals subsystems***

Upgraded detector

- ***New tracker*** with coverage up to |η|=4 and L1 track trigger
- ***Upgraded muon system*** with coverage up to |η|=2.8
- ***New high granularity*** endcap ***calorimeter (HGCal)***

Improvements expected in the H→μμ analysis

- Increased acceptance due to muon coverage up to |η|=2.8
- Possibly reconstruct muons with tracker-only up to |η|=4.0
- Substantial improvement in ***muon p_T resolution***
- **VBF category:** improved ***jet-energy-resolution*** for endcap and forward jets
- **VBF category:** improved ***rejection*** of ***pileup jets*** in the ***endcap*** and ***forward region***

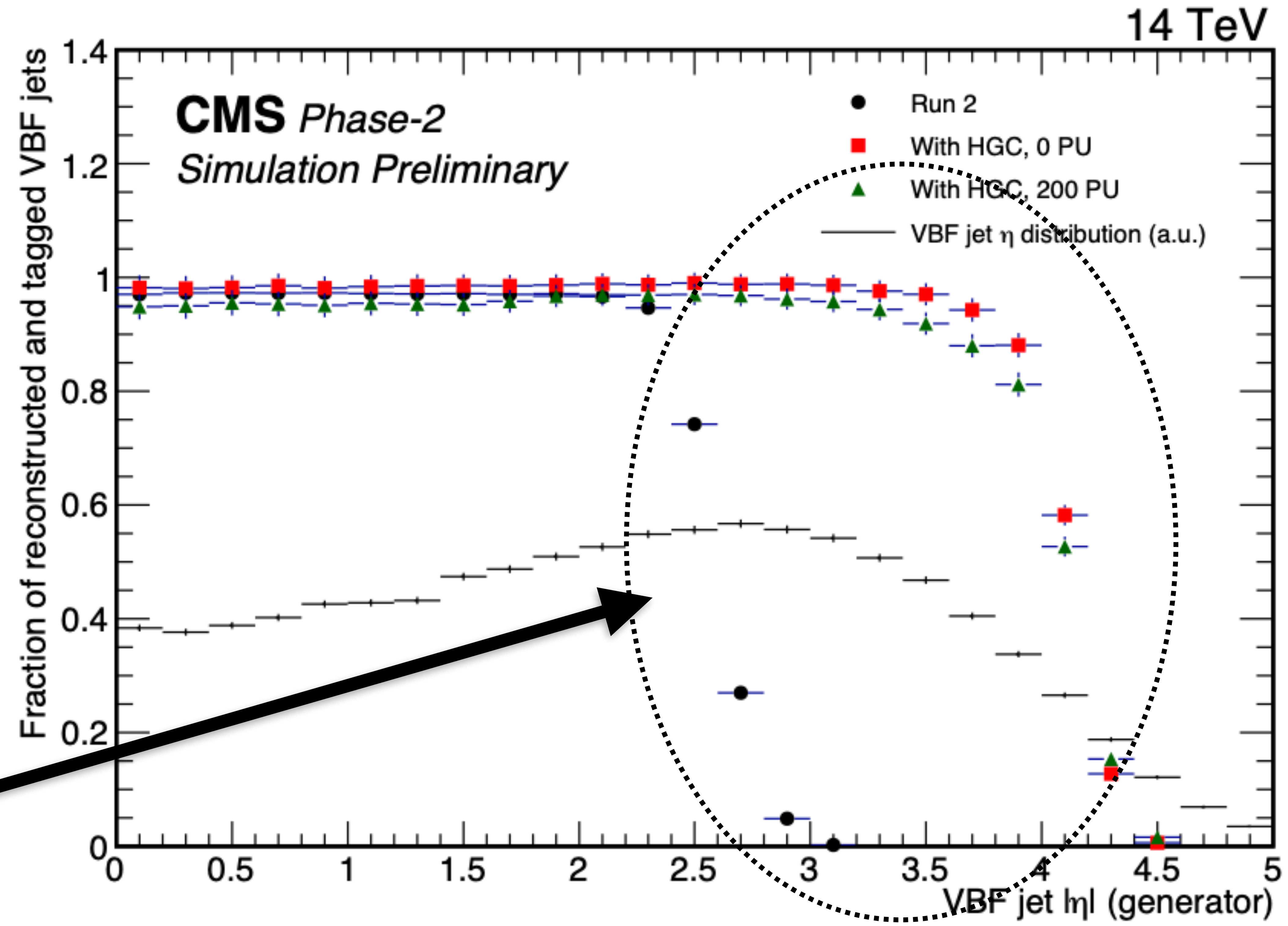

H→μμ analysis in HL-LHC

- The HL-LHC will start in 2026 delivering about ***3-4 ab^{-1}*** of pp collision data at ***14 TeV***
  - ***Extreme pileup conditions*** → 200 concurrent interactions every bunch crossing
  - To operate in this environment, ***the detector will upgrade or replace severals subsystems***

Upgraded detector

- ***New tracker*** with coverage up to |η|=4 and L1 track trigger
- ***Upgraded muon system*** with coverage up to |η|=2.8
- ***New high granularity*** endcap ***calorimeter (HGCal)***

Improvements expected in the H→μμ analysis

- Increased acceptance due to muon coverage up to |η|=2.8
- Possibly reconstruct muons with tracker-only up to |η|=4.0
- Substantial improvement in ***muon p_T resolution***
- **VBF category:** improved ***jet-energy-resolution*** for endcap and forward jets
- **VBF category:** improved ***rejection*** of ***pileup jets*** in the ***endcap*** and ***forward region***

At the HL-LHC, ATLAS+CMS may measure Higgs-to-muon couplings with 4% precision (arXiv 1902.00134)

Conclusions

- H→μμ analysis performed using 137 fb^{-1} of 13 TeV data
- Observed (exp) significance of ***3.0σ (2.5σ)*** at ***m_H = 125.38 GeV***
- ***First evidence for H→μμ decays***
- ***First evidence for Higgs interactions with 2^{nd} generation of fermions***
- Measured signal strength of $\mu = 1.19^{+0.44}_{-0.42}$
- ***The success of the SM continues!***
- Result submitted to JHEP and available in ***arXiv [2009.04363]***

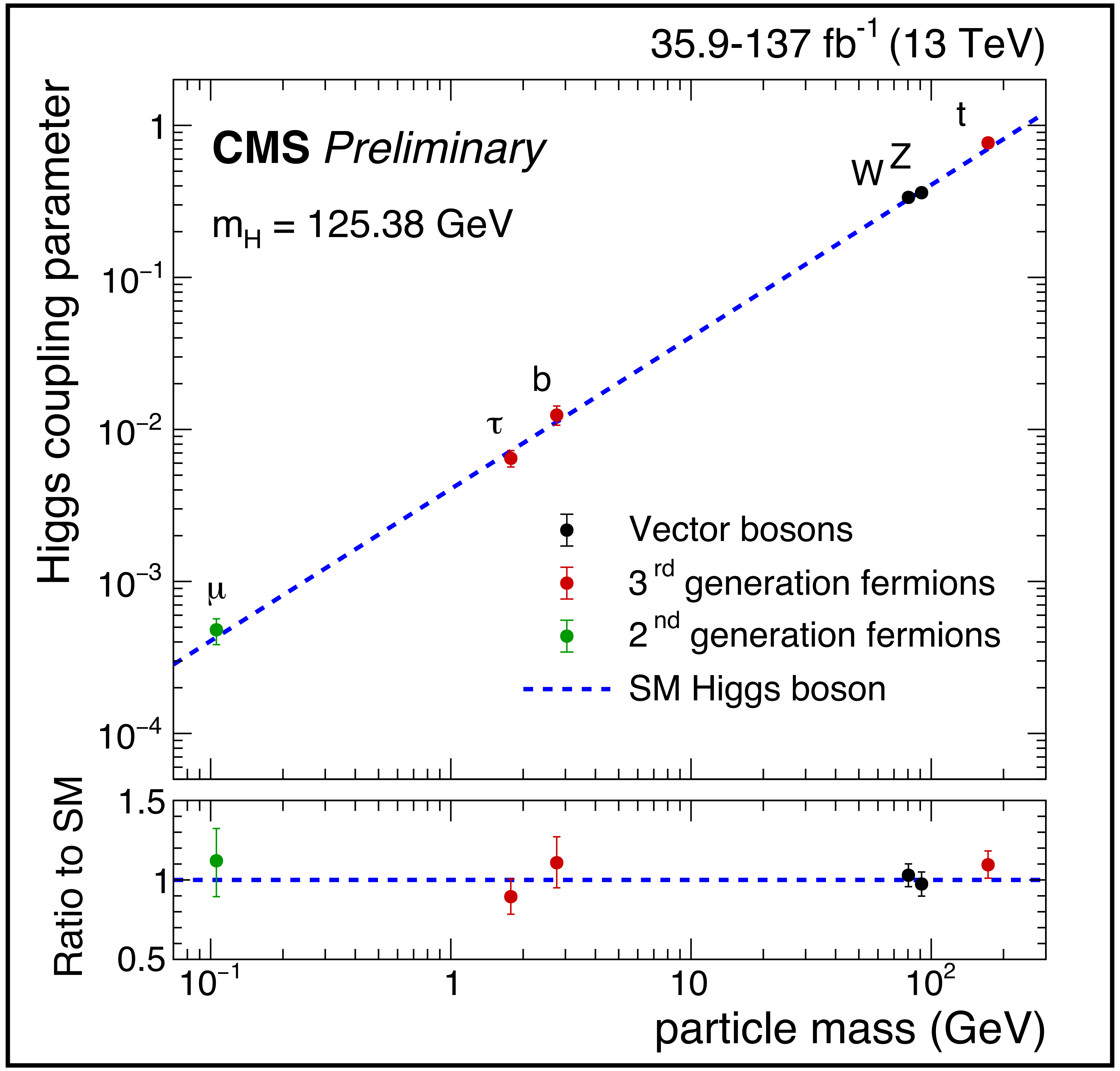

Backup slides

VBF fit breakdown in data-taking periods

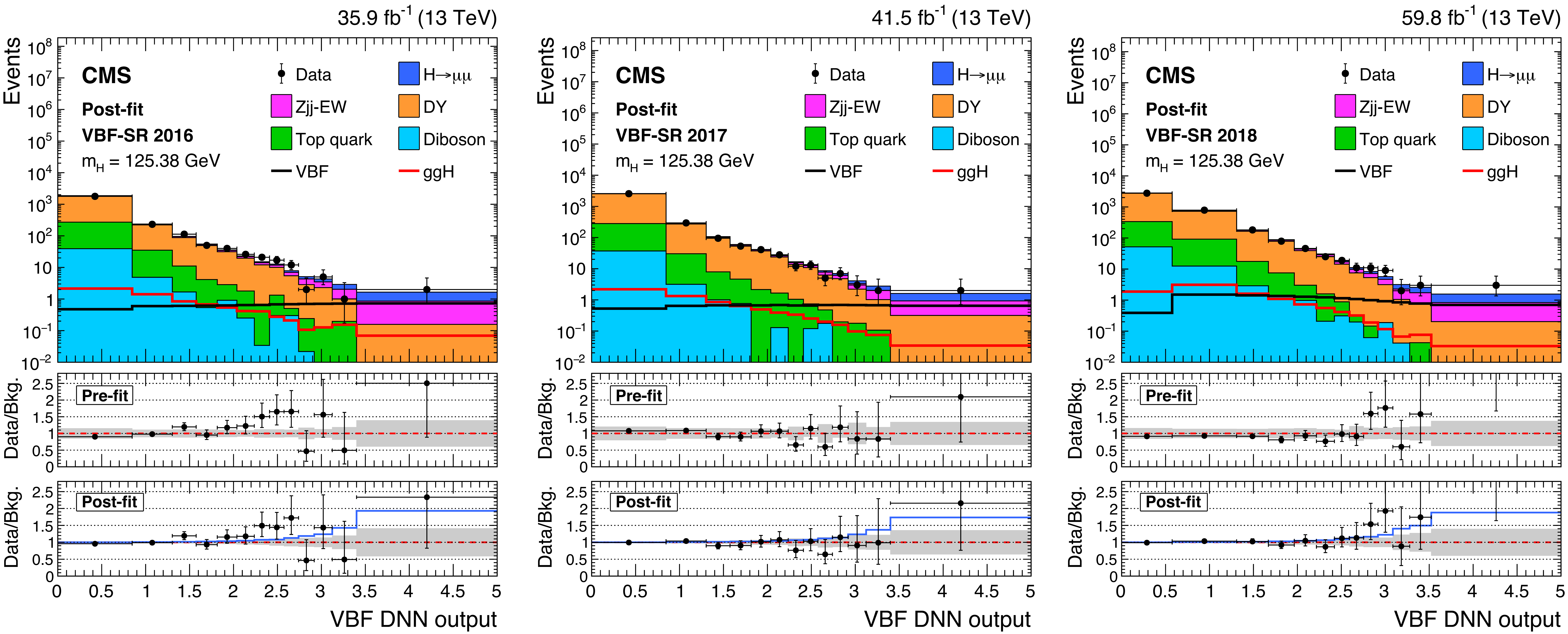

VBF fit breakdown in data-taking periods

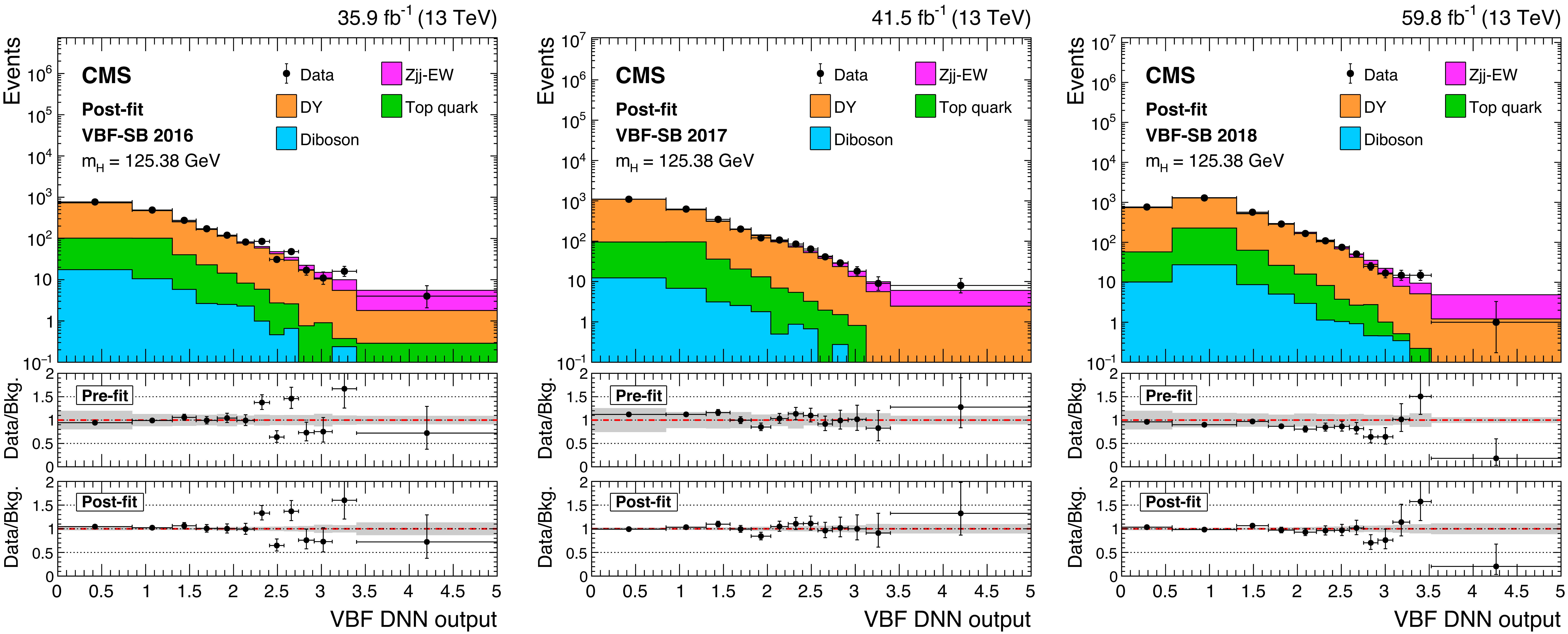

VBF summary tables

Observable	VBF-SB	VBF-SR
Number of loose (medium) b-tagged jets	$\leq$1 (0)	
Number of selected muons	=2	
Number of selected electrons	=0	
Jet multiplicity ($p_T > 25\,\text{GeV}$, $\lvert\eta\rvert < 4.7$)	$\geq$2	
Leading jet p_T	$\geq$35 GeV	
Dijet mass (m_{jj})	$\geq$400 GeV	
Pseudorapidity separation ($\lvert\Delta\eta_{jj}\rvert$)	$\geq$2.5	
Dimuon invariant mass	$110 < m_{\mu\mu} < 115\,\text{GeV}$ or $135 < m_{\mu\mu} < 150\,\text{GeV}$	$115 < m_{\mu\mu} < 135\,\text{GeV}$

DNN bin	Total signal	VBF (%)	ggH (%)	Bkg. $\pm\ \Delta$B	Data	S/(S+B) (%)	S/$\sqrt{B}$
1–3	19.5	30	70	8890 ± 67	8815	0.22	0.21
4–6	11.6	57	43	394 ± 8	388	2.86	0.58
7–9	8.43	73	27	103 ± 4	121	7.56	0.83
10	2.30	85	15	15.1 ± 1.4	18	13.2	0.59
11	2.15	88	12	9.1 ± 1.2	10	19.1	0.71
12	2.10	87	13	5.8 ± 1.1	6	26.6	0.87
13	1.87	94	6	2.6 ± 0.9	7	41.8	1.16

ggH mass distributions

Observable	Selection
Number of loose (medium) b-tagged jets	$\leq$1 (0)
Number of selected muons	=2
Number of selected electrons	=0
VBF selection veto	if $N_{jets} \geq 2$
	$m_{jj} < 400\,\text{GeV}$ or $\lvert\Delta\eta_{jj}\rvert < 2.5$ or $p_T(j_1) < 35\,\text{GeV}$

Background model

- ***Core function*** → discrete envelope of
  - Modified Breit-Wigner function

$$\text{mBW}(m_{\mu\mu}; m_Z, \Gamma_Z, a_1, a_2, a_3) = \frac{e^{a_2 m_{\mu\mu} + a_3 m_{\mu\mu}^2}}{(m_{\mu\mu} - m_Z)^{a_1} + (\Gamma_Z/2)^{a_1}},$$

  - Sum of two exponentials
  - Non parametric shape from spline interpolation of FEWZ prediction times a 3rd Bernstein polynomial
- ***Shape modifier:***
  - 3rd or 2nd order Chebyshev polynomial

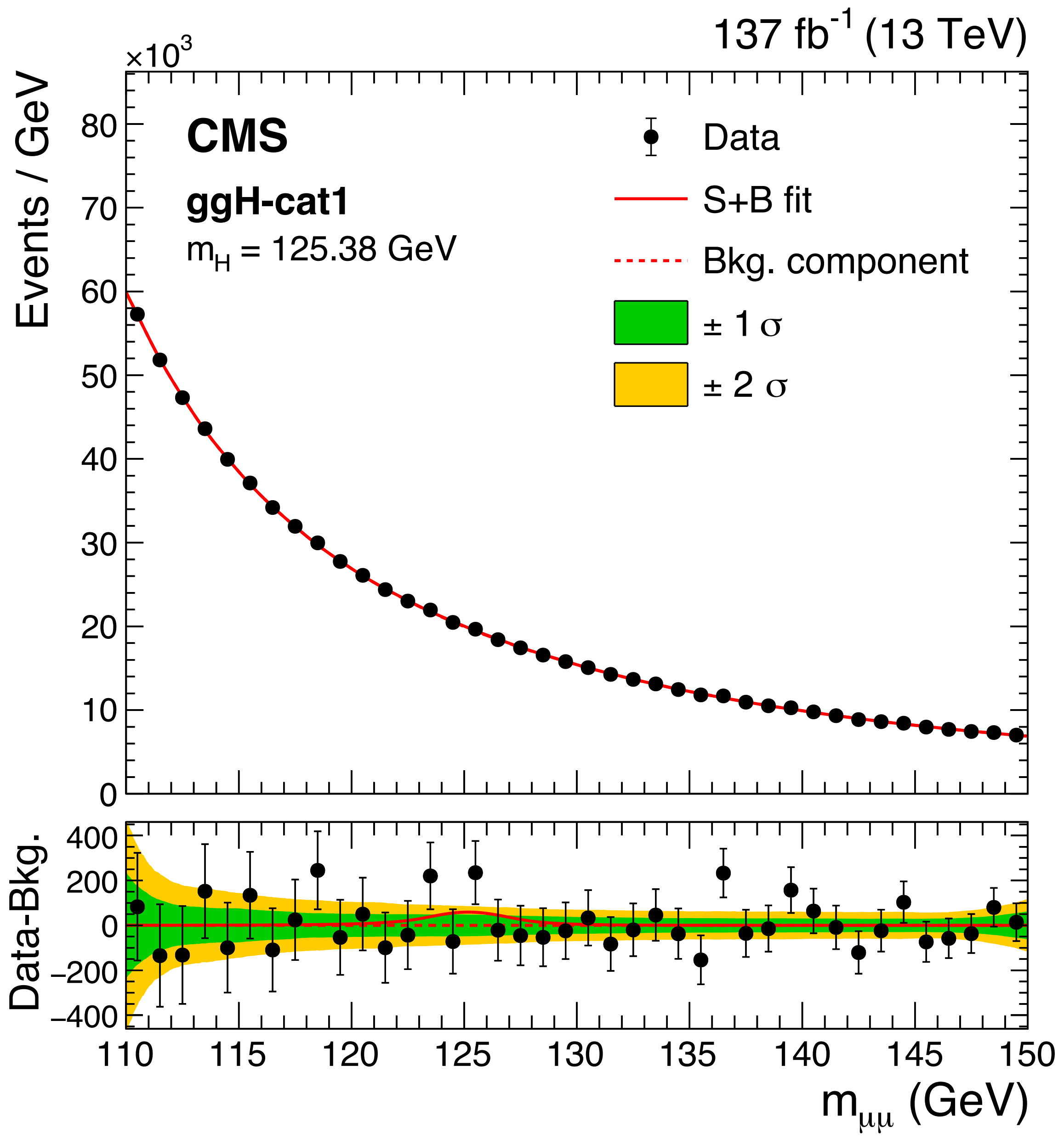

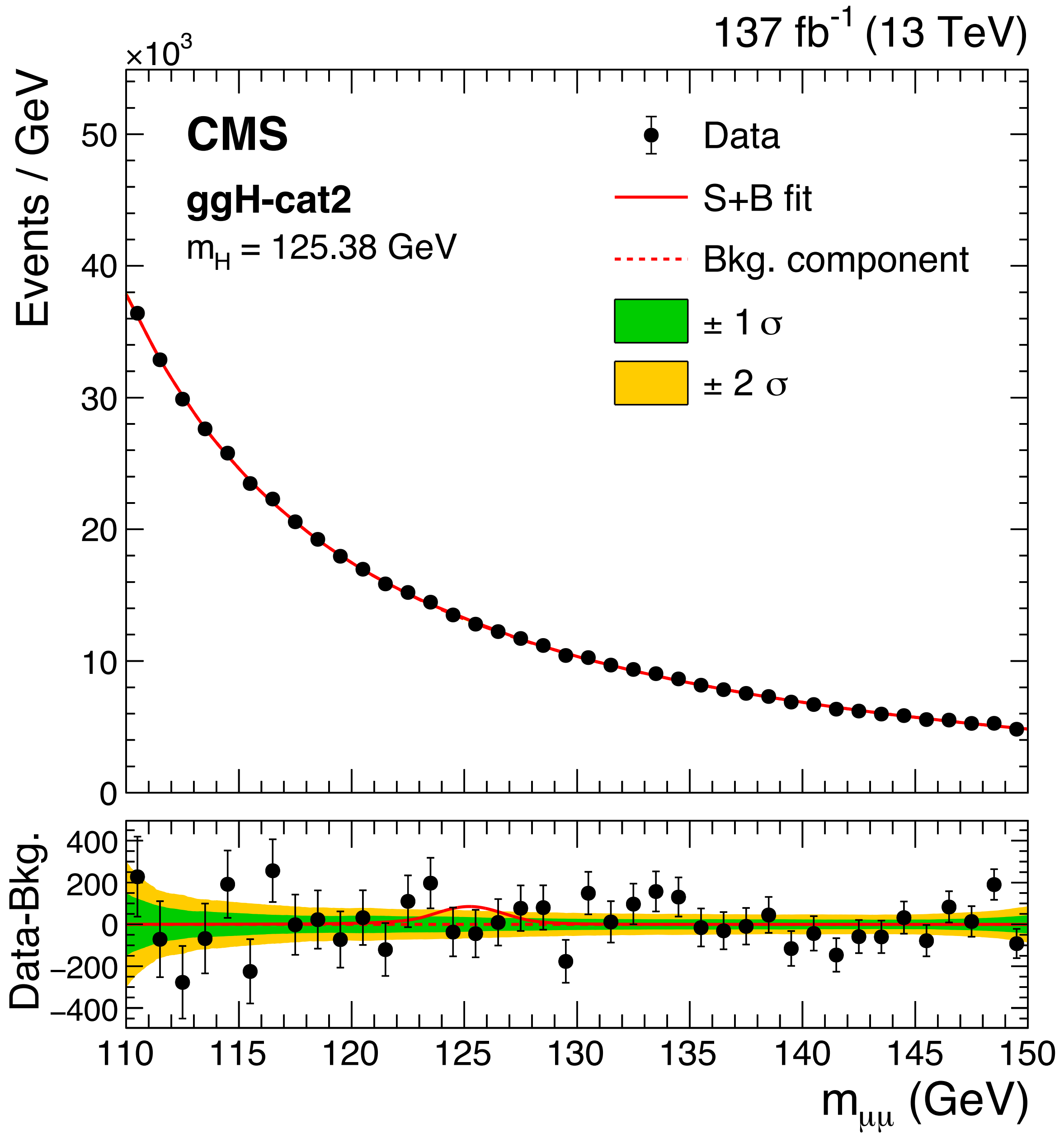

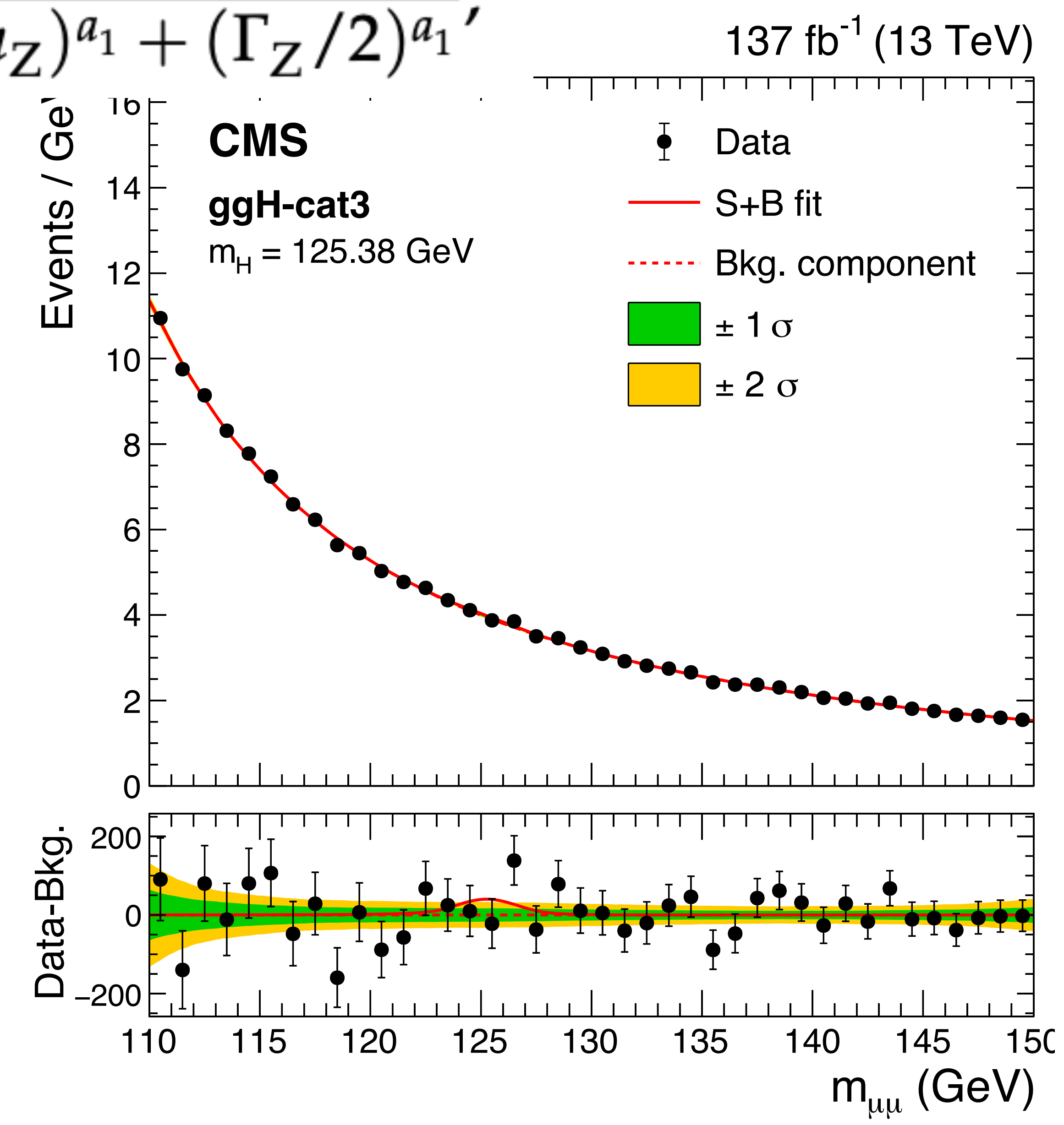

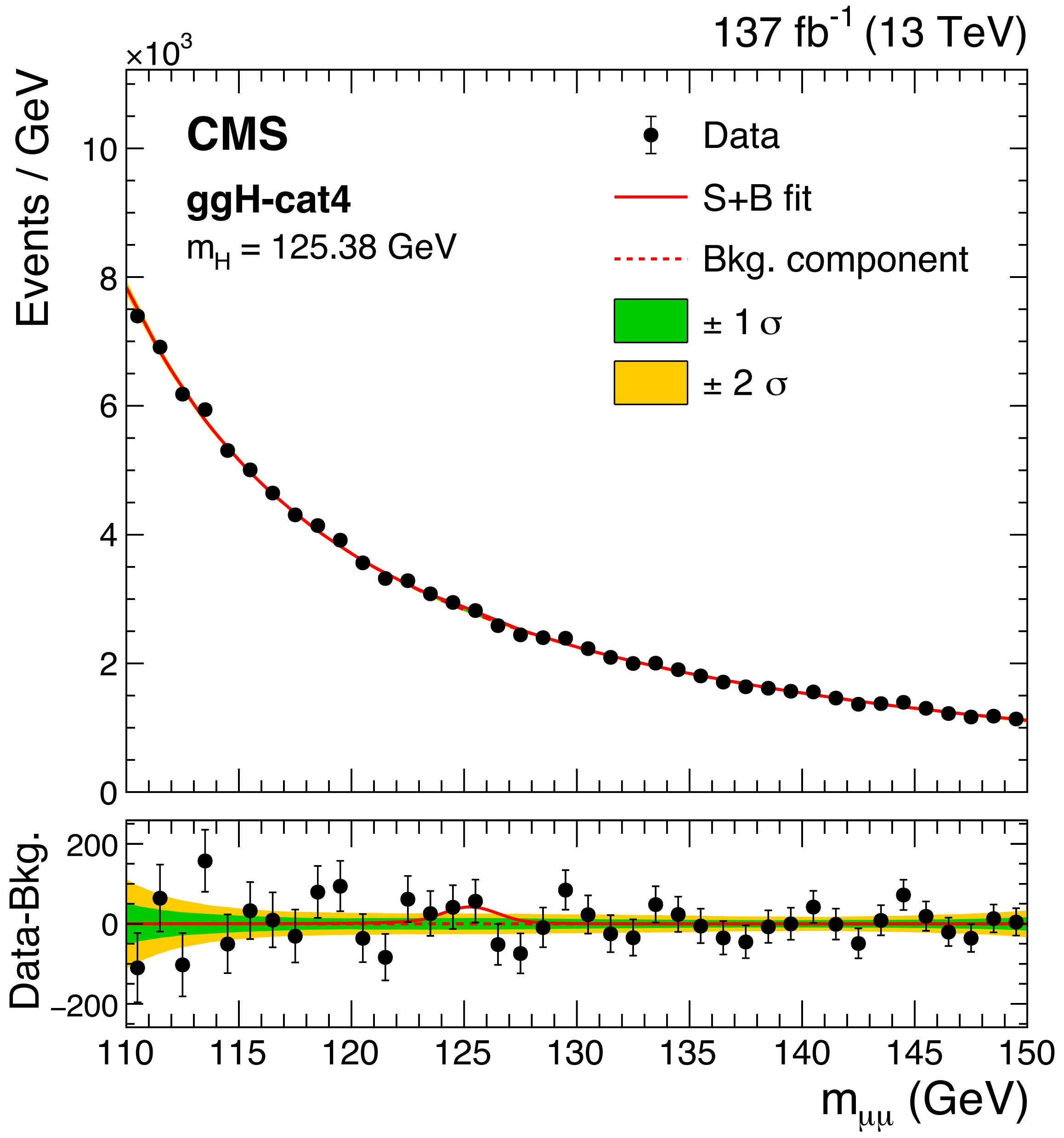

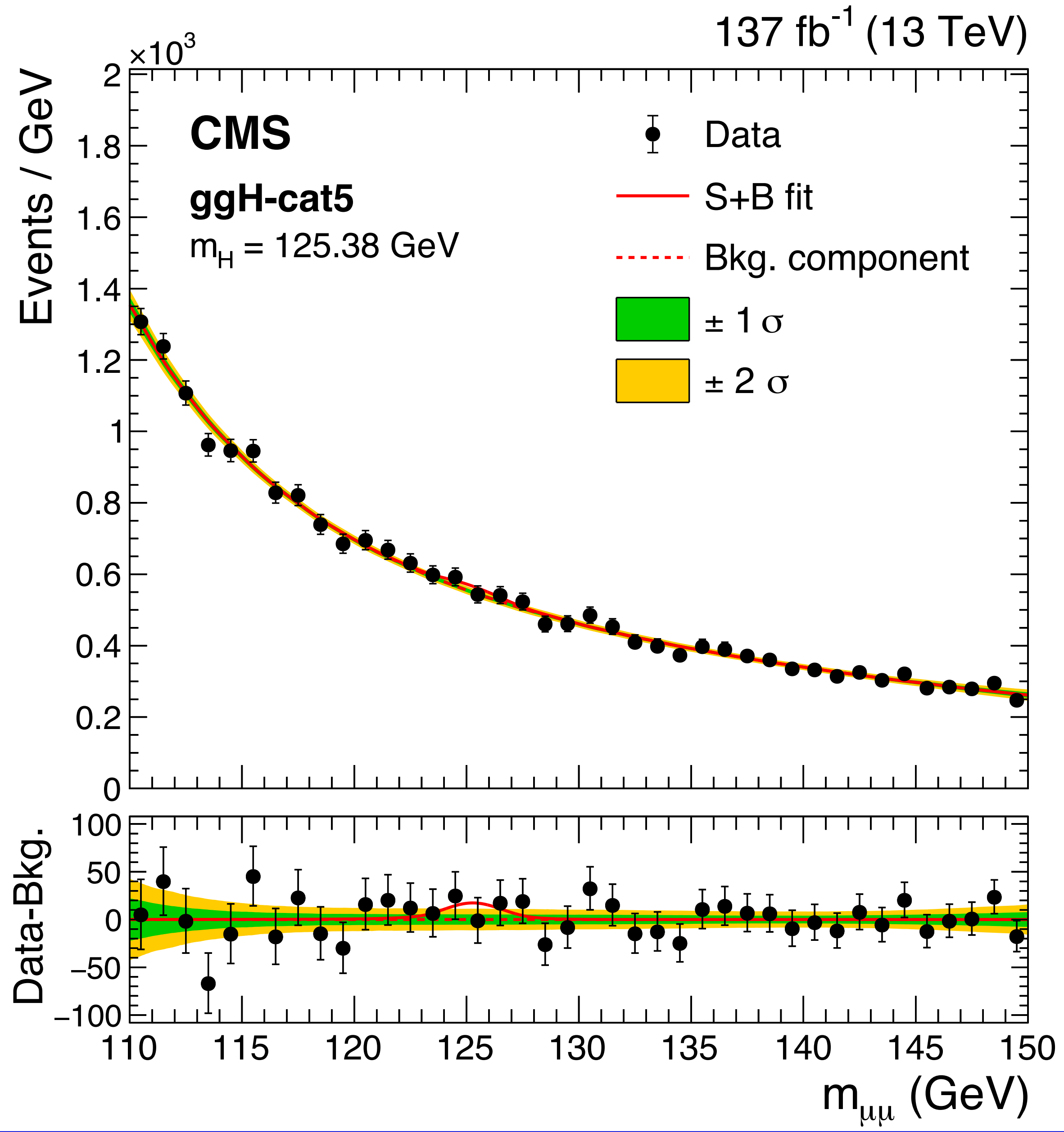

VH analysis

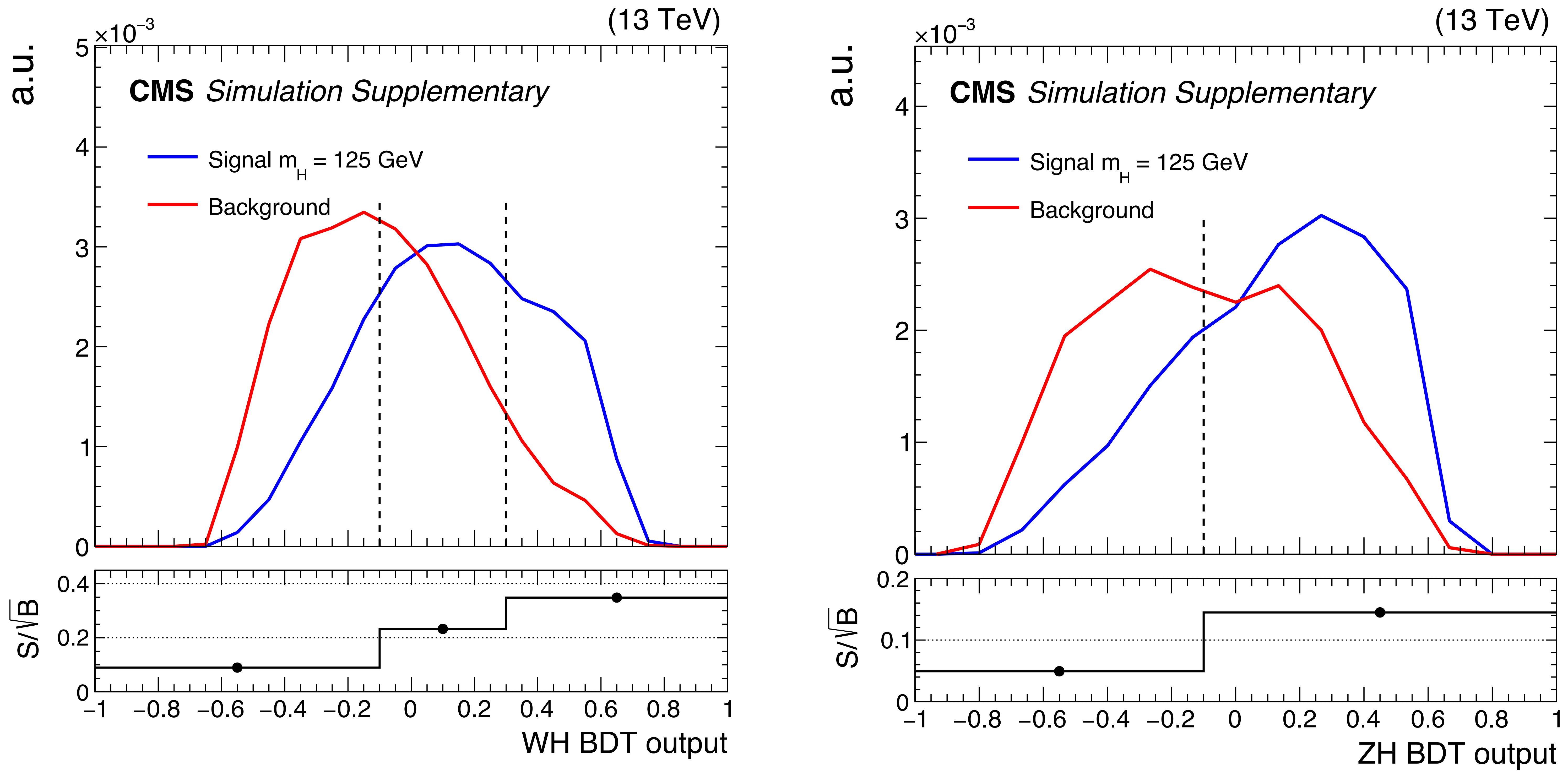

Event category	Total signal	WH (%)	qqZH (%)	ggZH (%)	$t\bar{t}H$+tH (%)	HWHM (GeV)	Bkg. fit function	Bkg. @HWHM	Data @HWHM	S/(S+B) (%) @HWHM	$S/\sqrt{B}$ @HWHM
WH-cat1	0.82	76.2	9.6	1.6	12.6	2.00	BWZγ	32.0	34	1.54	0.09
WH-cat2	1.72	80.1	9.1	1.5	9.3	1.80	BWZ	23.1	27	4.50	0.23
WH-cat3	1.14	85.7	6.7	1.8	4.8	1.90	BWZ	5.48	4	12.6	0.35
ZH-cat1	0.11	—	82.8	17.2	—	2.07	BWZ	2.05	4	3.29	0.05
ZH-cat2	0.31	—	79.6	20.4	—	1.80	BWZ	2.19	4	8.98	0.14

VH mass distributions

Observable	WH leptonic		ZH leptonic	
	$\mu\mu\mu$	$\mu\mu$e	4μ	$2\mu2$e
Number of loose (medium) b-tagged jets	$\leq$1 (0)	$\leq$1 (0)	$\leq$1 (0)	$\leq$1 (0)
Number of selected muons	=3	=2	=4	=2
Number of selected electrons	=0	=1	=0	=2
Lepton charge ($q(\ell)$)	$\sum q(\ell) = \pm 1$		$\sum q(\ell) = 0$	
Low-mass resonance veto	$m_{\ell\ell} > 12\,\mathrm{GeV}$			
N($\mu^+\mu^-$) pairs with $110 < m_{\mu\mu} < 150\,\mathrm{GeV}$	$\geq$1	=1	$\geq$1	=1
N($\mu^+\mu^-$) pairs with $\lvert m_{\mu\mu} - m_Z \rvert < 10\,\mathrm{GeV}$	=0	=0	=1	=0
N(e^+e^-) pairs with $\lvert m_{ee} - m_Z \rvert < 20\,\mathrm{GeV}$	=0	=0	=1	=1

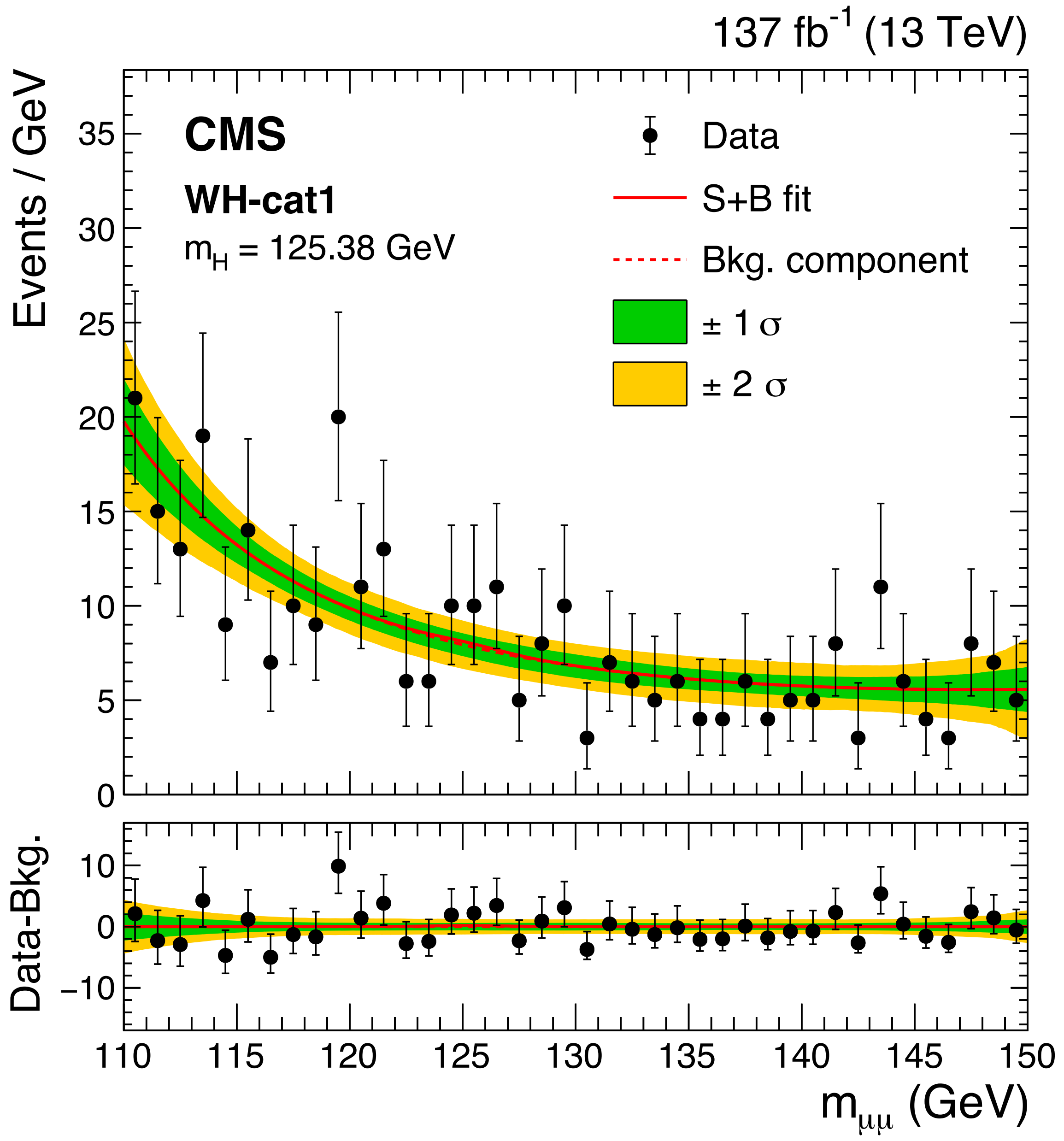

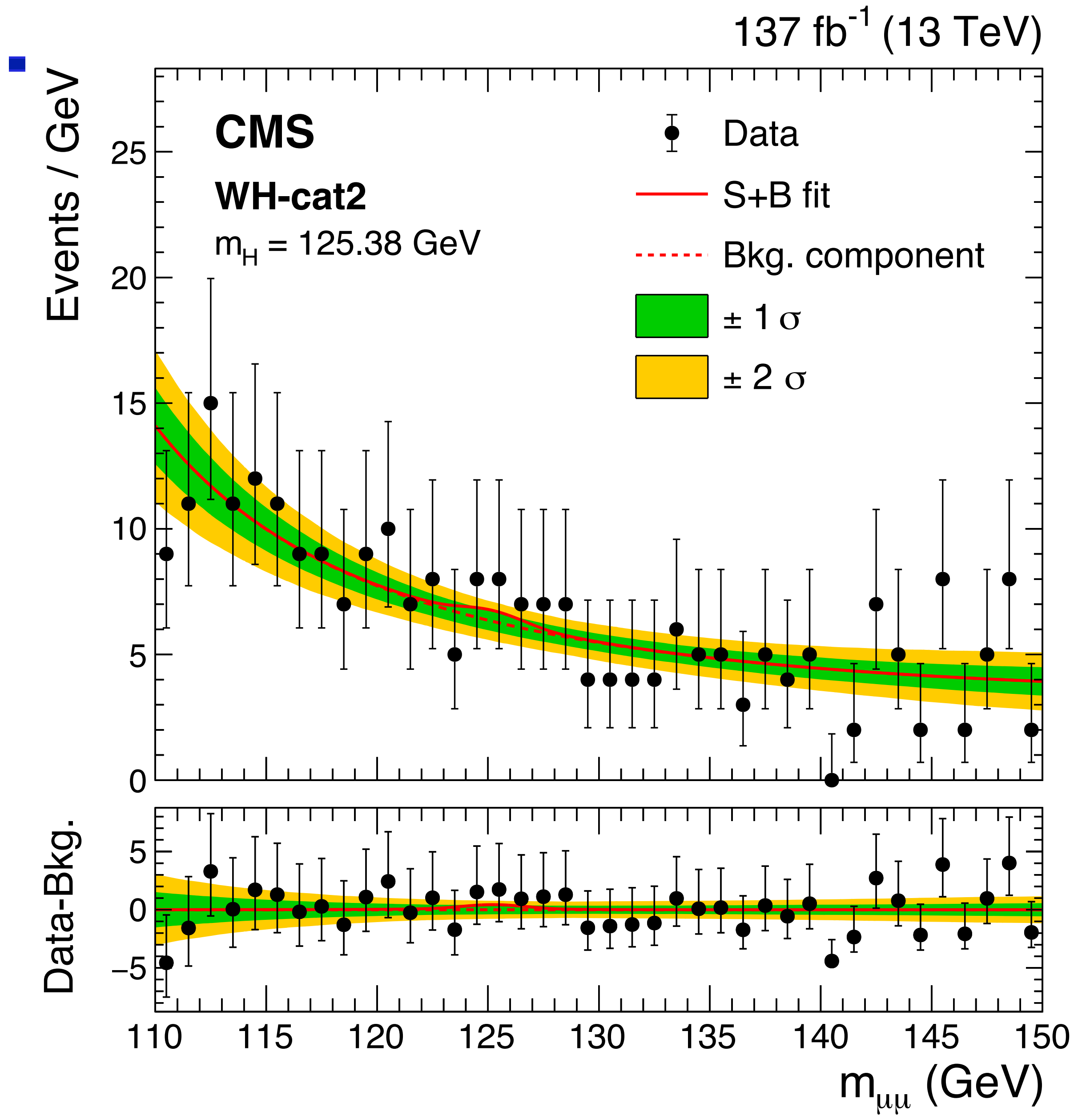

Background model

- BWZγ in WH-cat1

$$\mathrm{BWZ}\gamma(m_{\mu\mu}; a, f, m_Z, \Gamma_Z) = f\,\mathrm{BWZ}(m_{\mu\mu}; a, m_Z, \Gamma_Z) + (1-f)\,\frac{e^{a m_{\mu\mu}}}{m_{\mu\mu}^2}.$$

- BWZ in WH-cat2, WH-cat3 and ZH categories

$$\mathrm{BWZ}(m_{\mu\mu}; a, m_Z, \Gamma_Z) = \frac{\Gamma_Z e^{a m_{\mu\mu}}}{(m_{\mu\mu} - m_Z)^2 + (\Gamma_Z/2)^2}$$

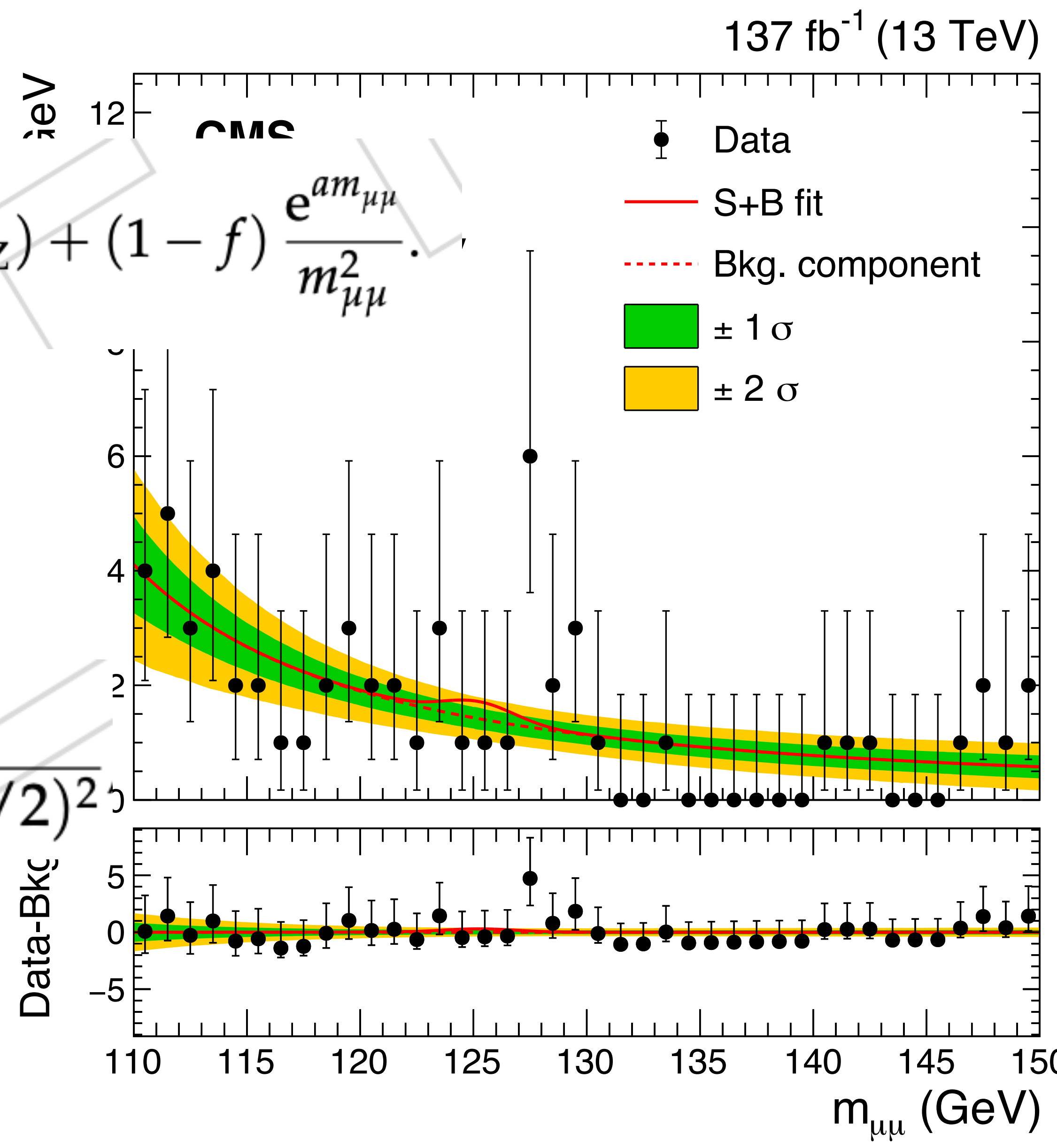

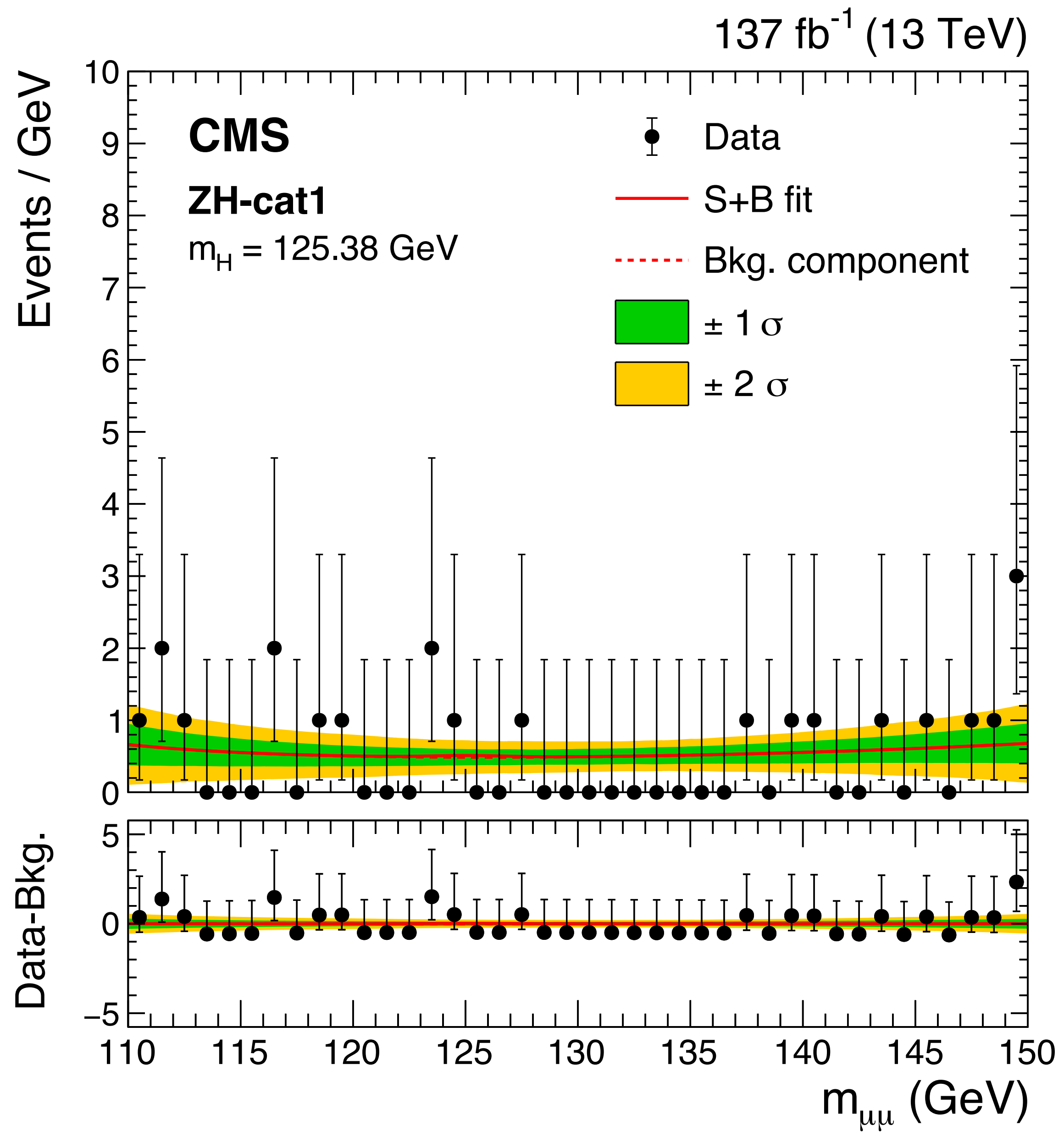

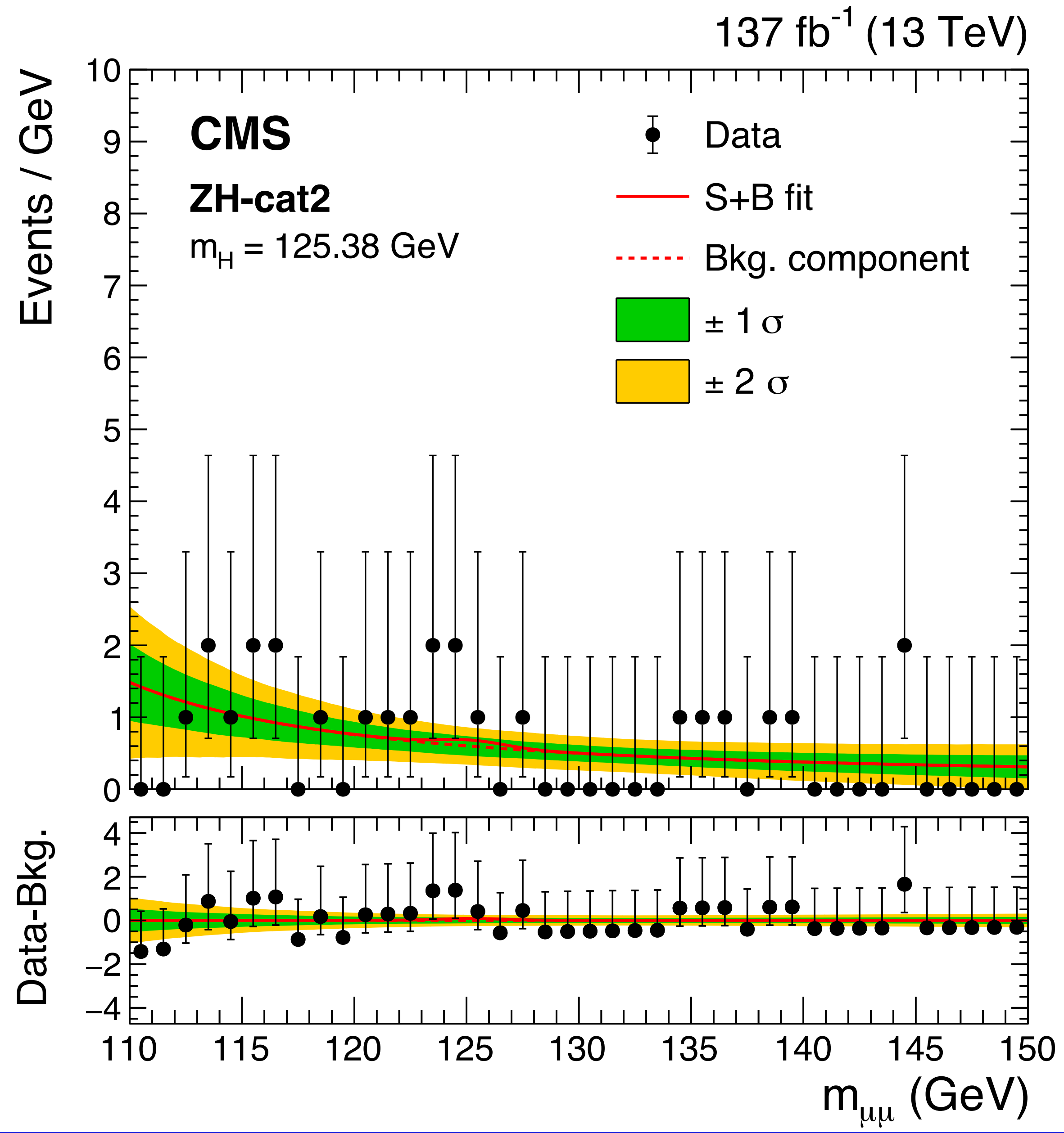

ttH analysis

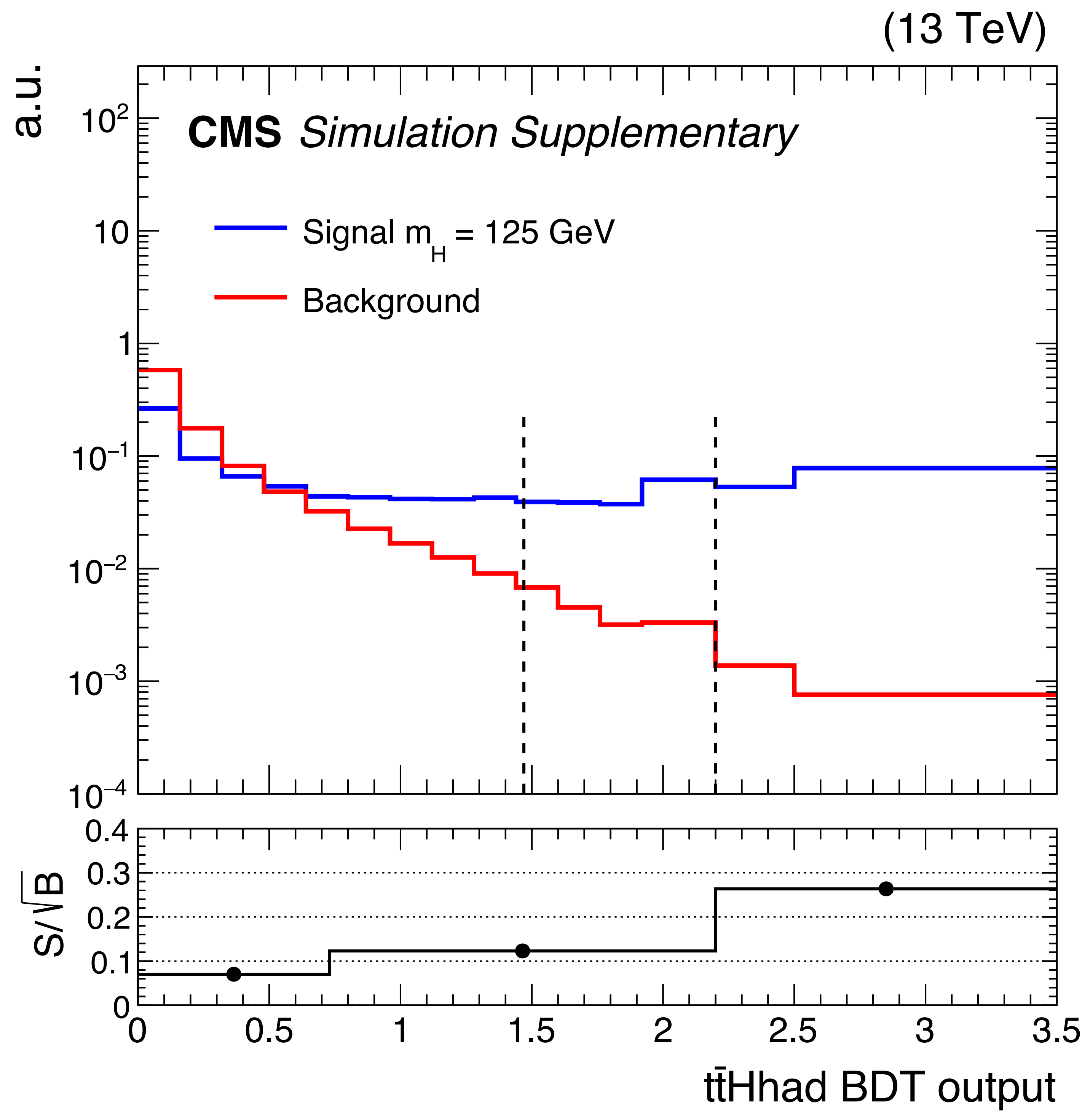

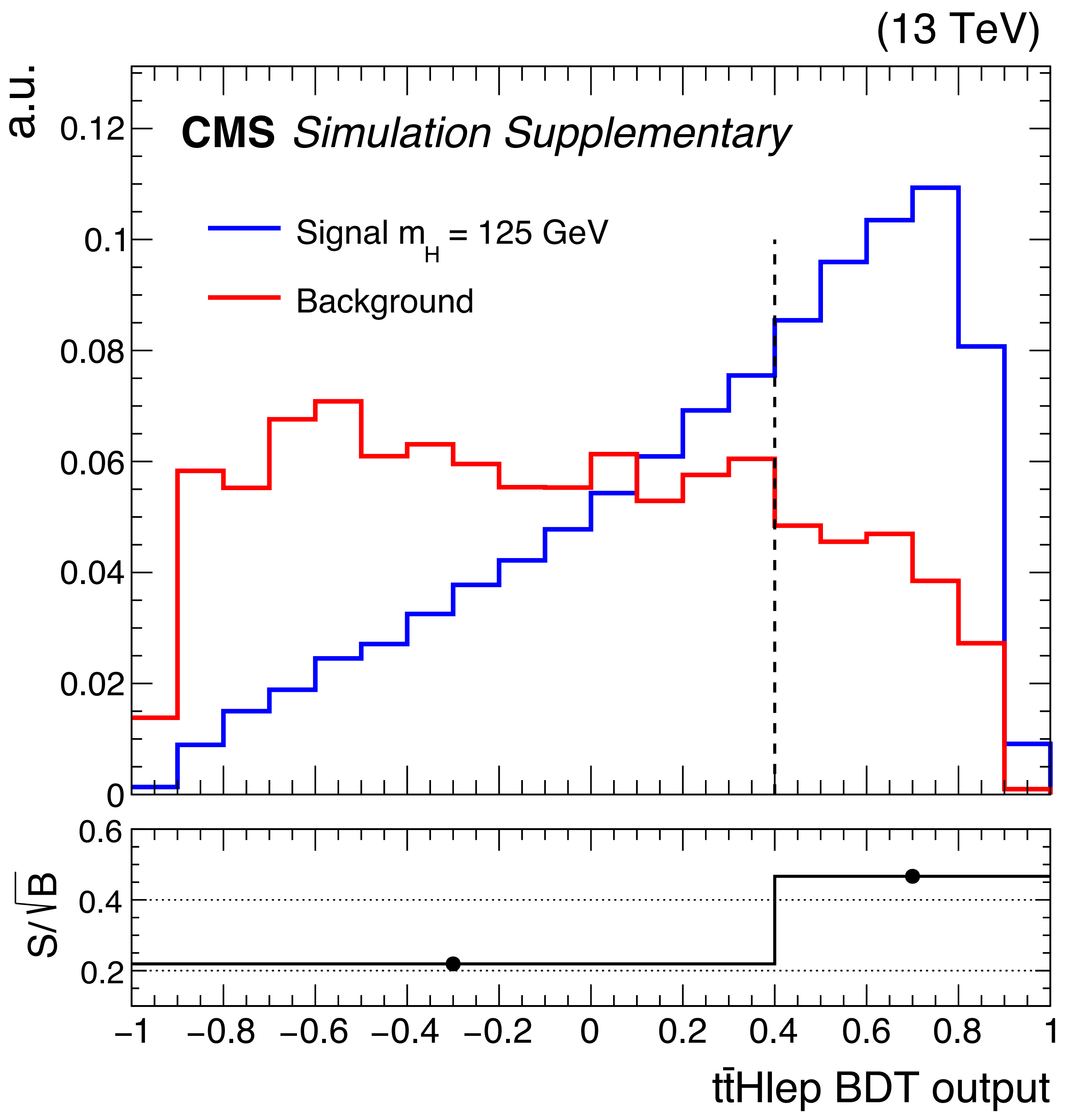

Event category	Total signal	$t\bar{t}H$ (%)	ggH (%)	VH (%)	Other (%)	HWHM (GeV)	Bkg. fit function	Bkg. @HWHM	Data @HWHM	S/(S+B) (%) @HWHM	$S/\sqrt{B}$ @HWHM
$t\bar{t}$Hhad-cat1	6.87	32.3	40.3	17.2	10.2	1.85	Bern(2)	4298	4251	1.07	0.07
$t\bar{t}$Hhad-cat2	1.62	84.3	3.8	5.6	6.2	1.81	Bern(2)	82.0	89	1.32	0.12
$t\bar{t}$Hhad-cat3	1.33	94.0	0.3	1.3	4.4	1.80	S-Exp	12.3	12	6.87	0.26
$t\bar{t}$Hlep-cat1	1.06	85.8	—	4.7	9.5	1.92	Exp	9.00	13	7.09	0.22
$t\bar{t}$Hlep-cat2	0.99	94.7	—	1.0	4.3	1.75	Exp	2.08	4	24.5	0.47

ttH mass distributions

Observable	$t\bar{t}$H hadronic	$t\bar{t}$H leptonic
Number of b quark jets	>0 medium or >1 loose b-tagged jets	
Number of leptons (N($\ell = \mu, e$))	=2	=3 or 4
Lepton charge ($q(\ell)$)	$\sum q(\ell) = 0$	$N(\ell) = 3\ (4) \rightarrow \sum q(\ell) = \pm 1\ (0)$
Jet multiplicity ($p_T > 25$ GeV, $\lvert\eta\rvert < 4.7$)	≥ 3	≥ 2
Leading jet p_T	>50 GeV	>35 GeV
Z boson veto	—	$\lvert m_{\ell\ell} - m_Z \rvert > 10$ GeV
Low-mass resonance veto	—	$m_{\ell\ell} > 12$ GeV
Jet triplet mass	$100 < m_{jjj} < 300$ GeV	—

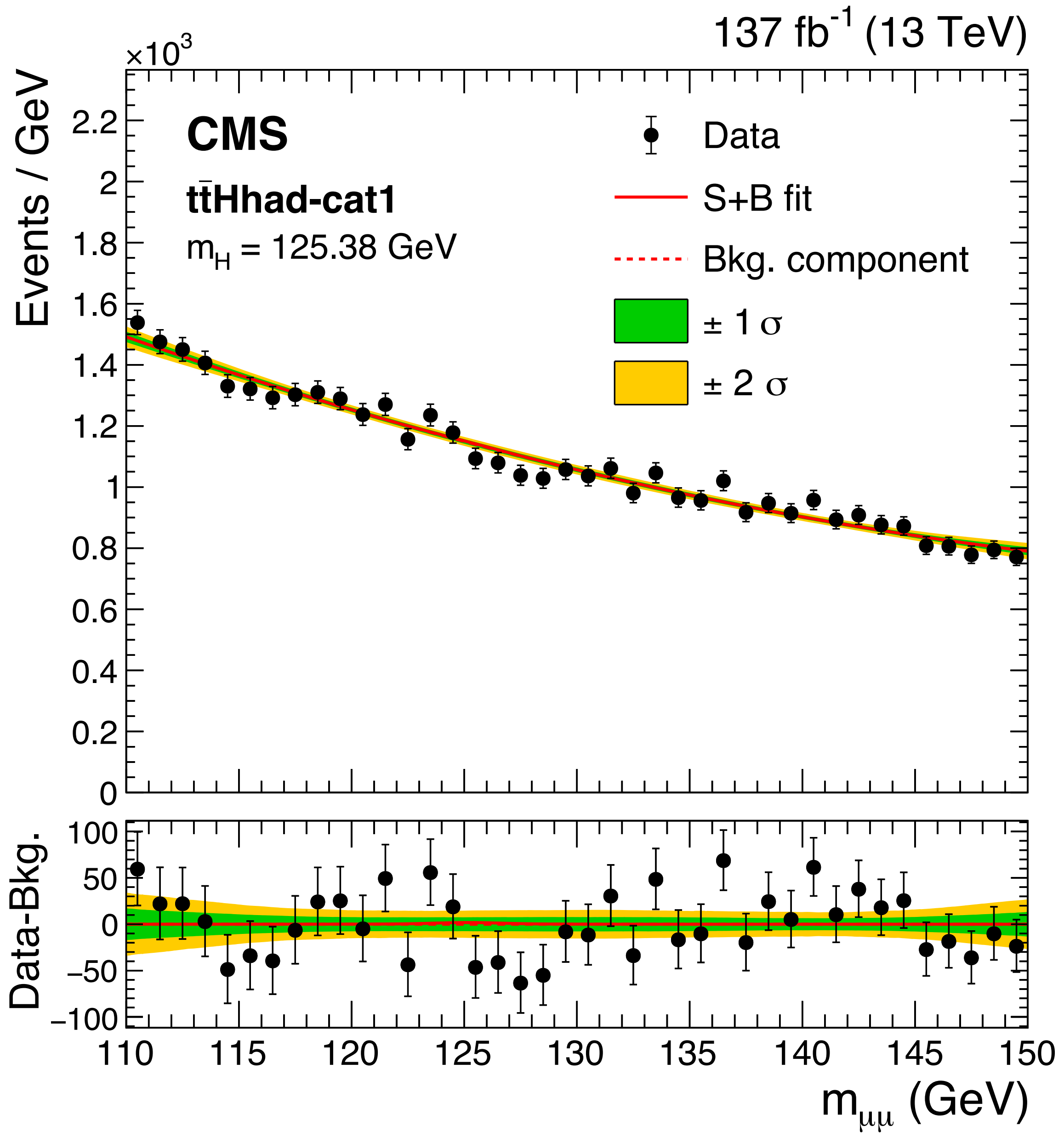

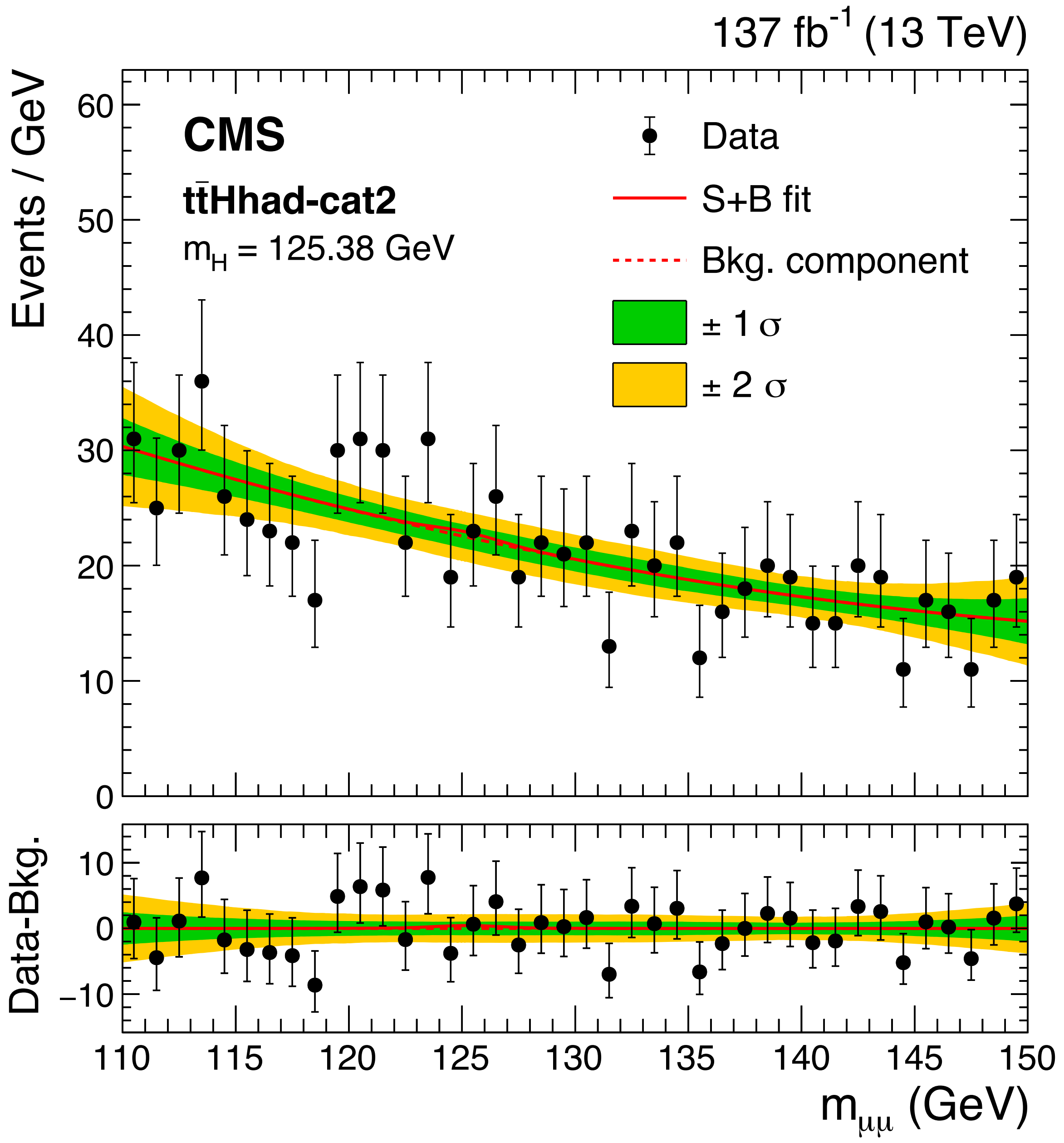

Background model

- ttH-had cat1 and cat2: 2nd order Bernstein polynomial
- ttH-had cat3 sum of two expo
- ttH-leptonic with simple exponential

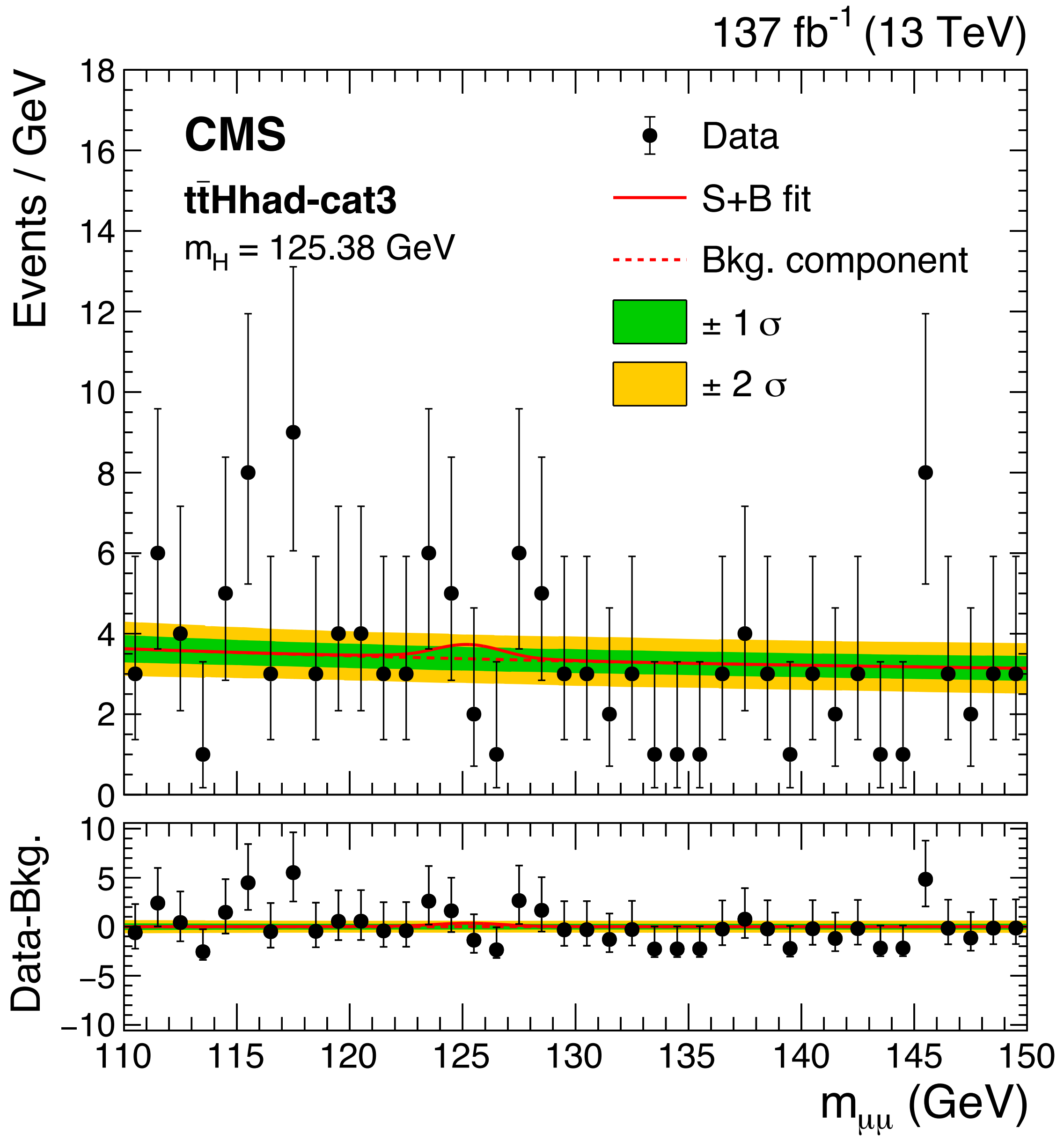

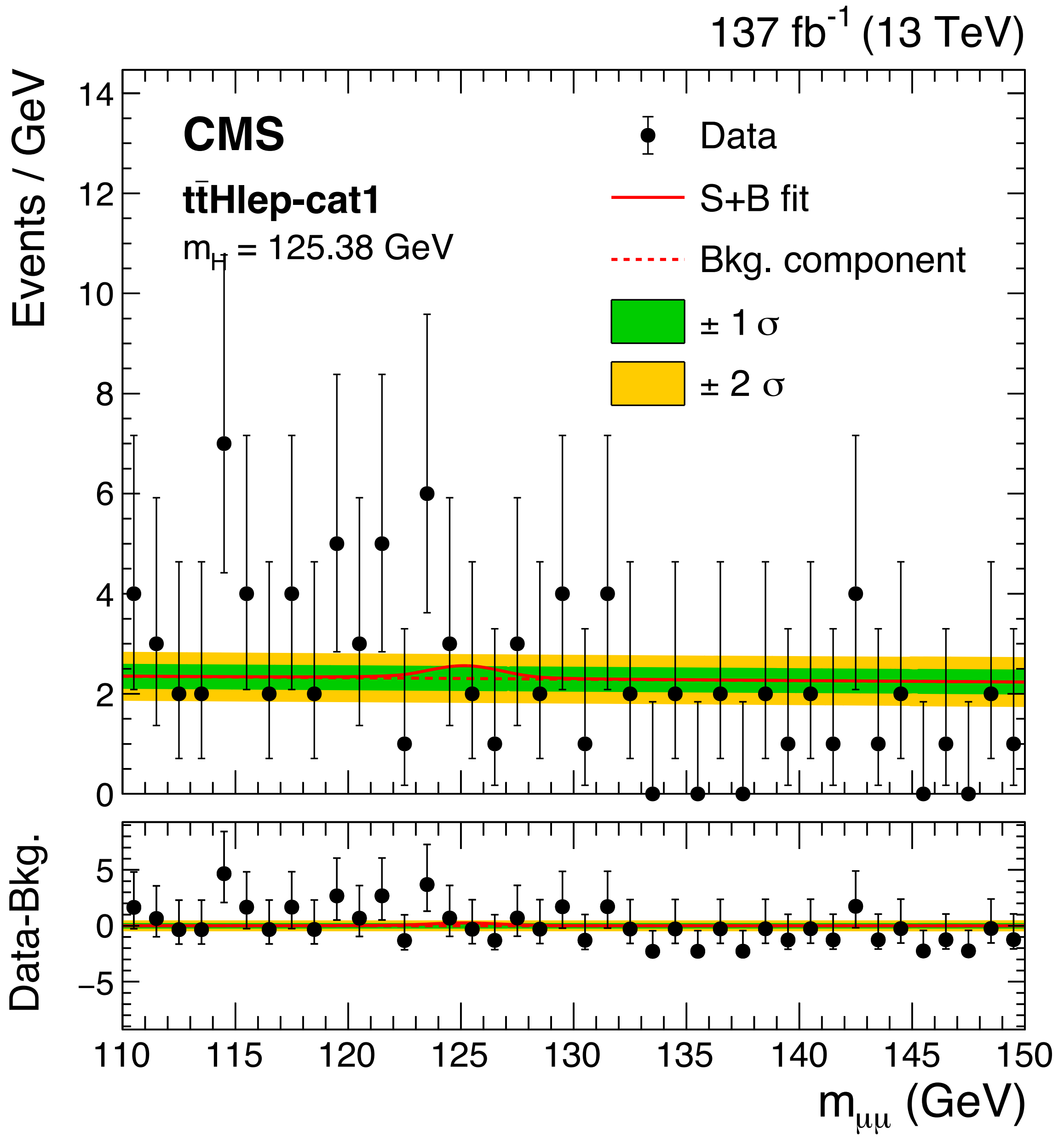

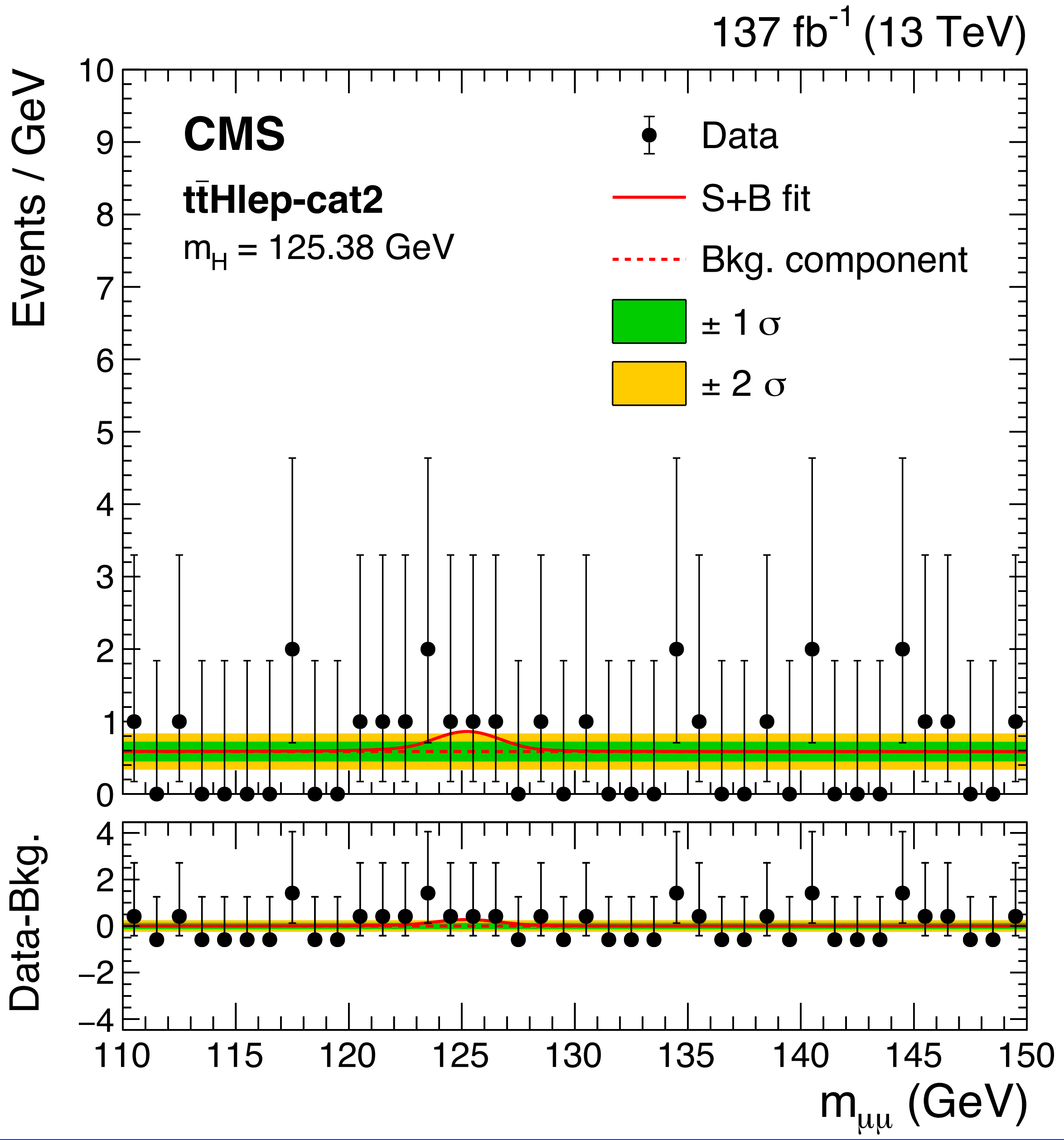

S/(S+B) weighted distributions

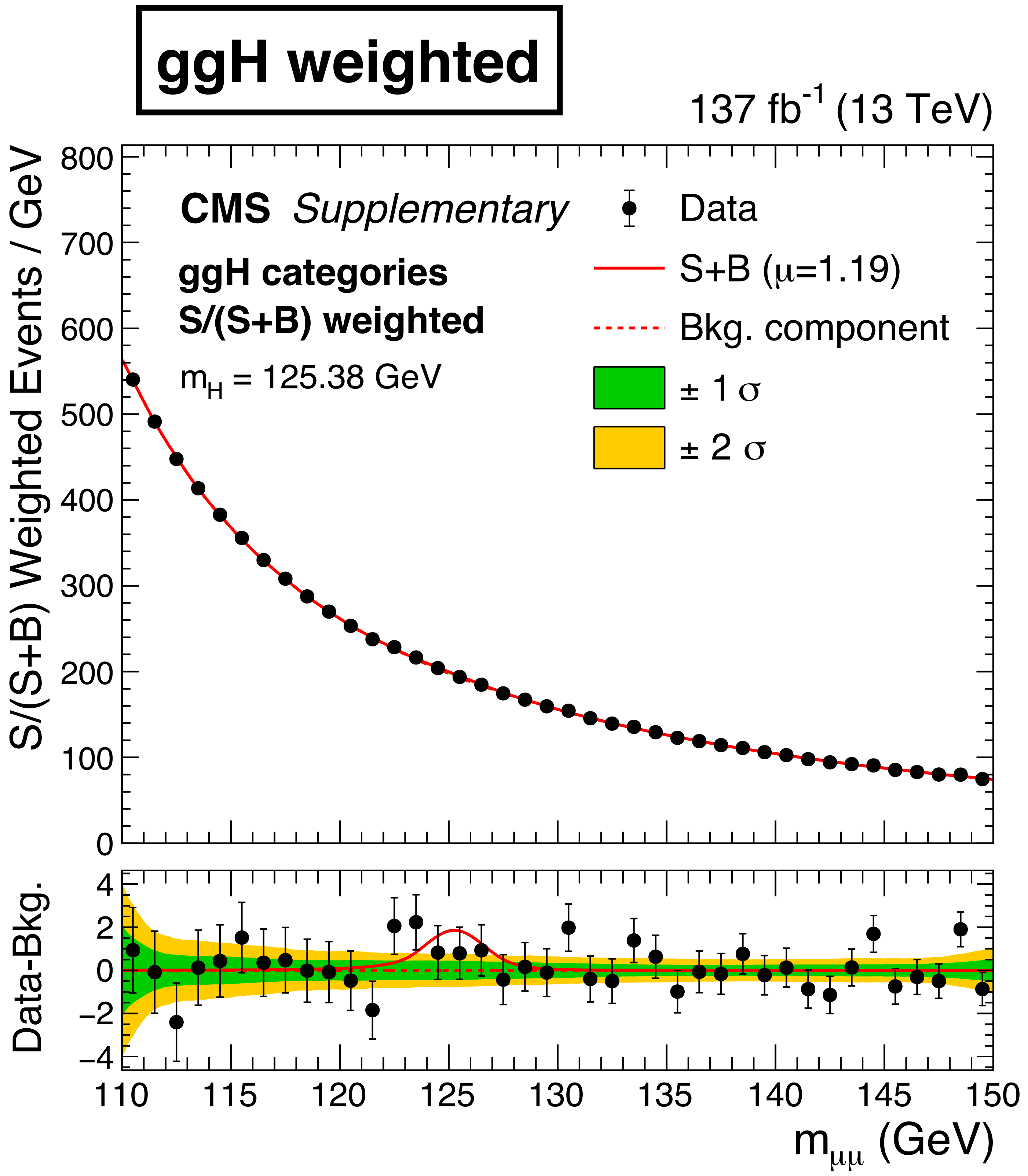

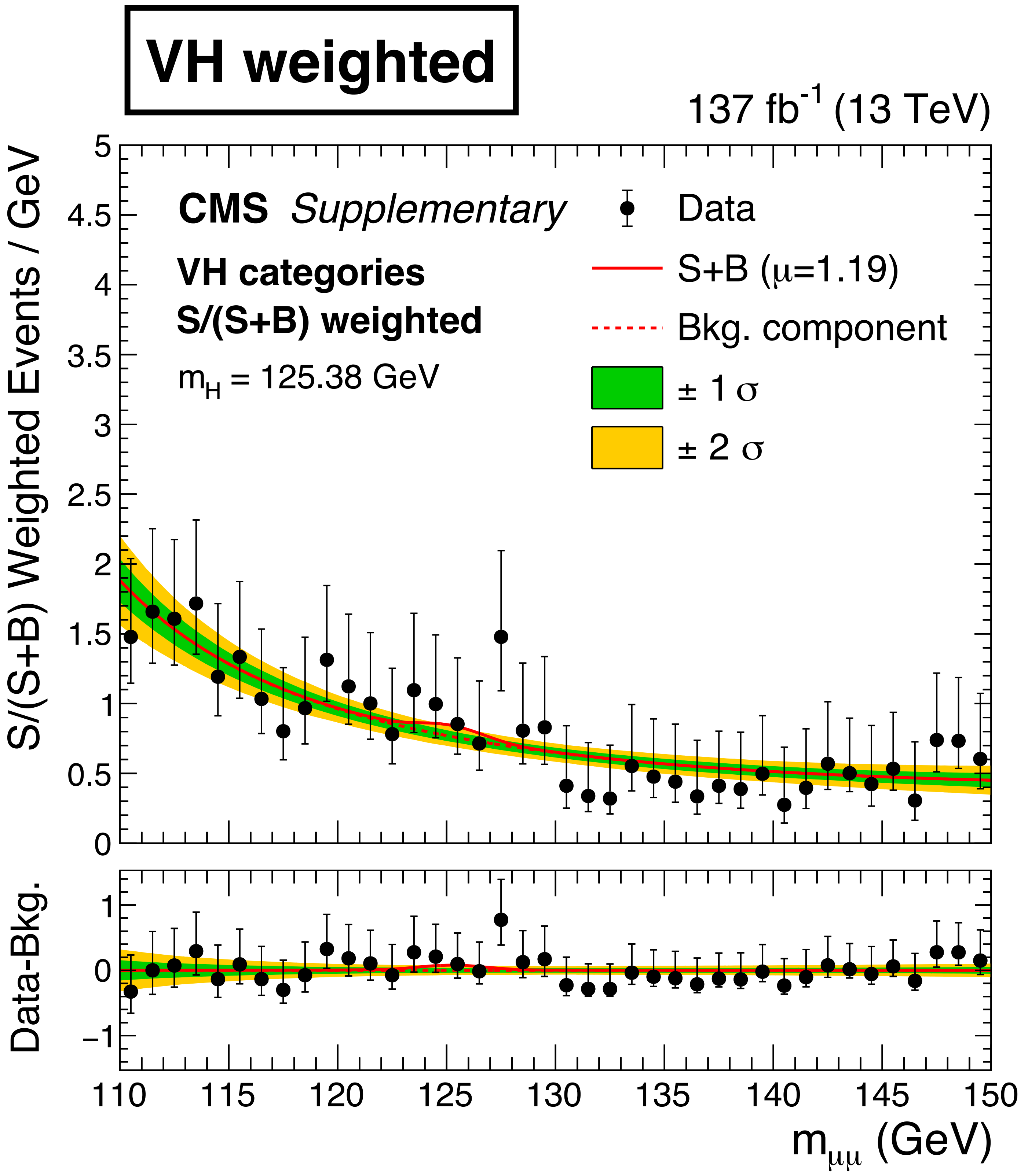

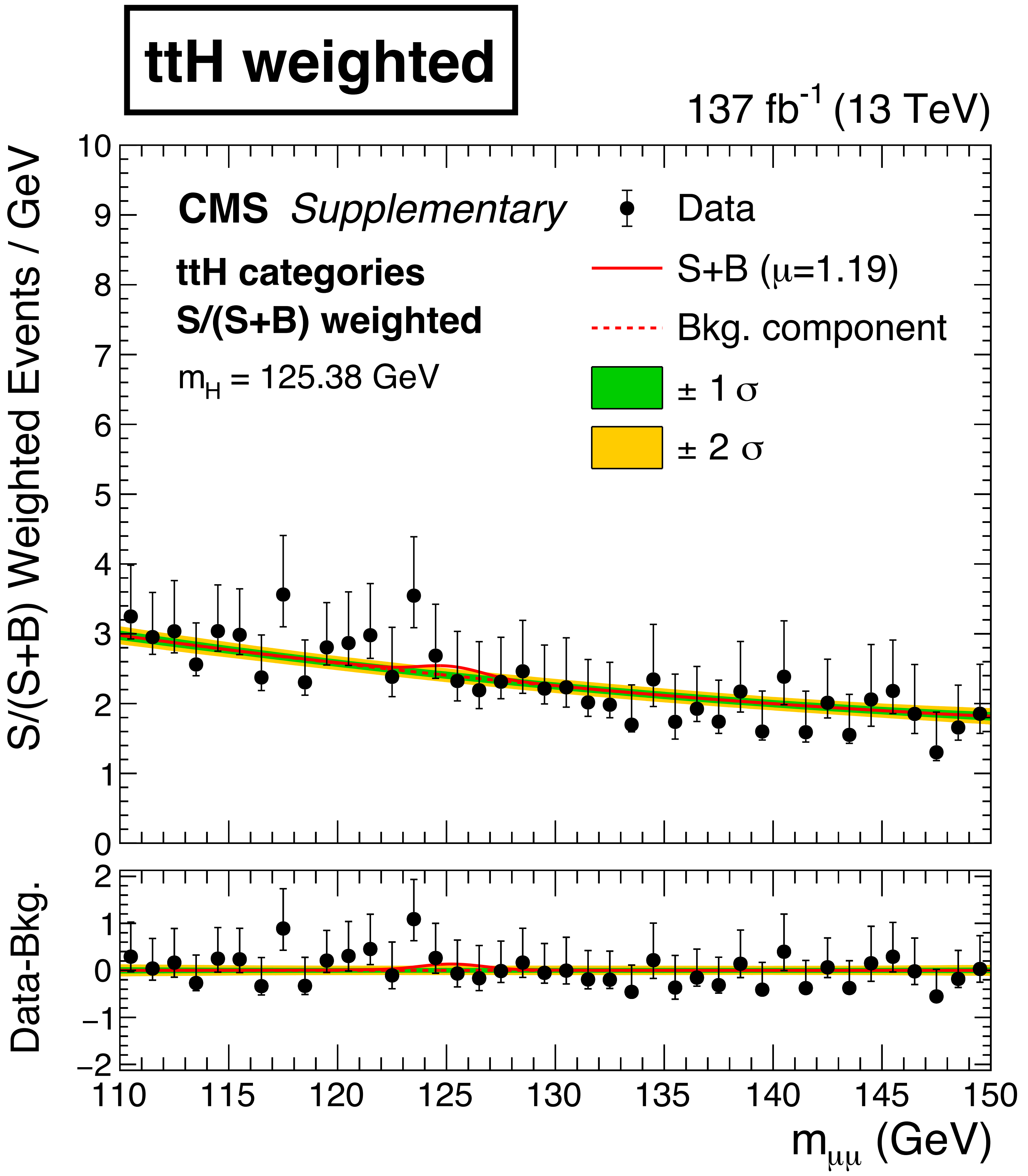

S/(S+B) weighted distributions

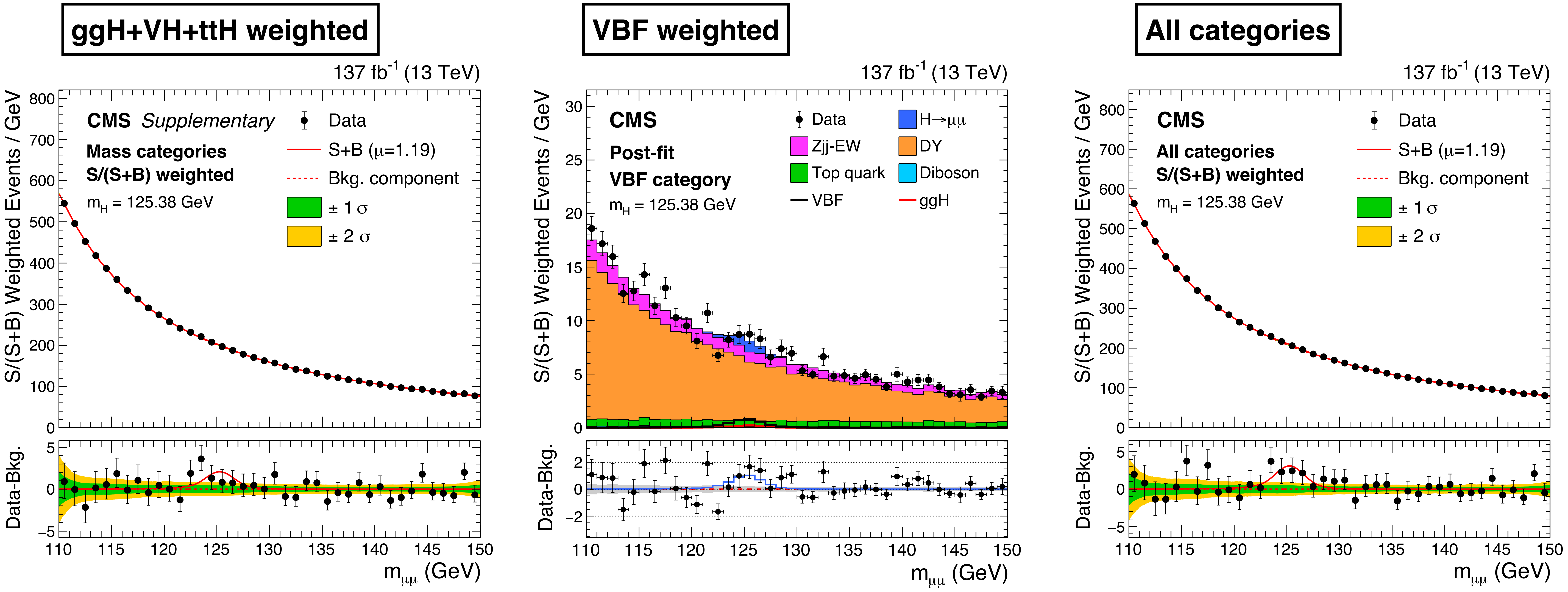

VBF DNN in SR vs m_H hypotheses

m_H = 125.3 GeV

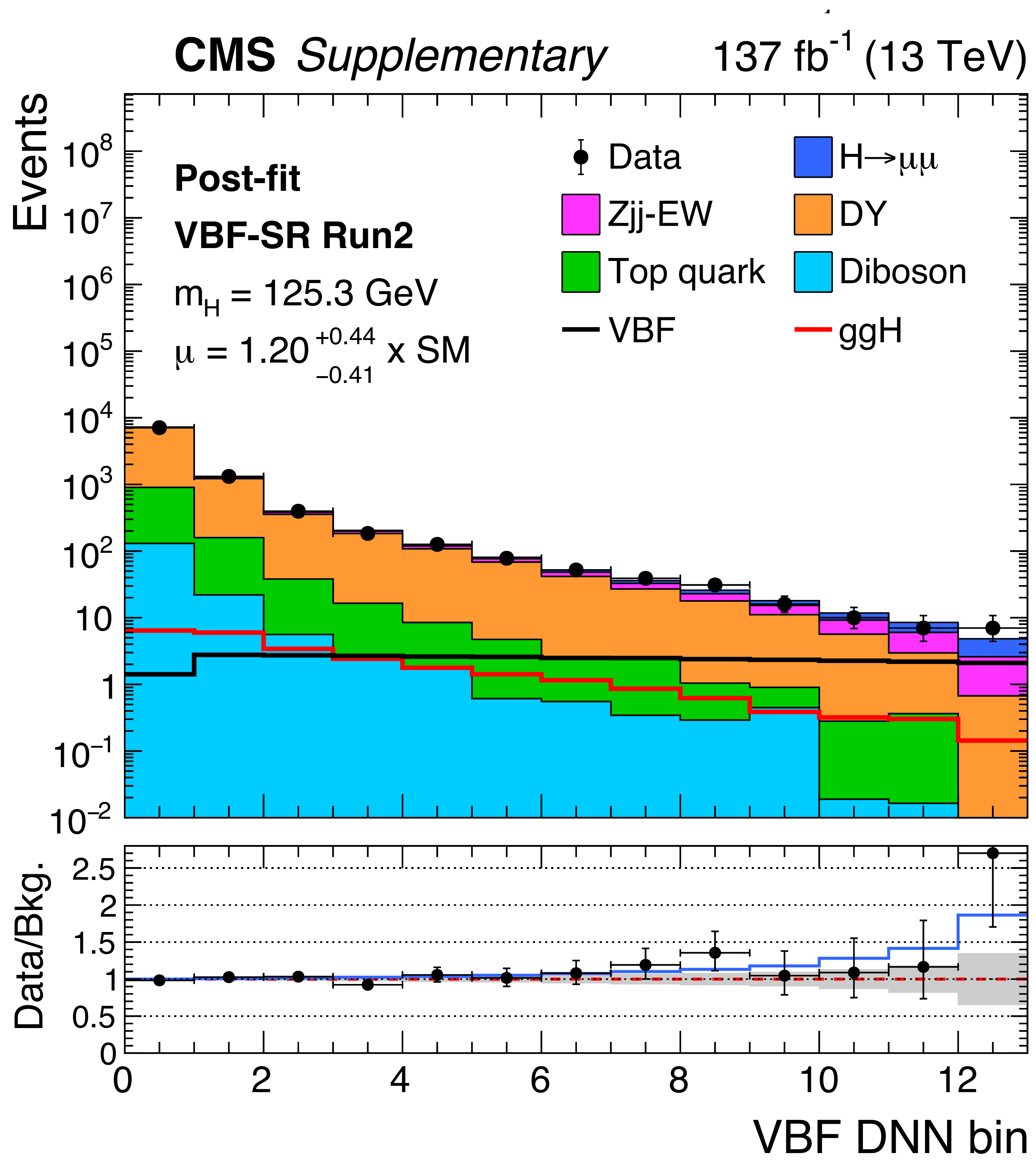

m_H = 125.38 GeV

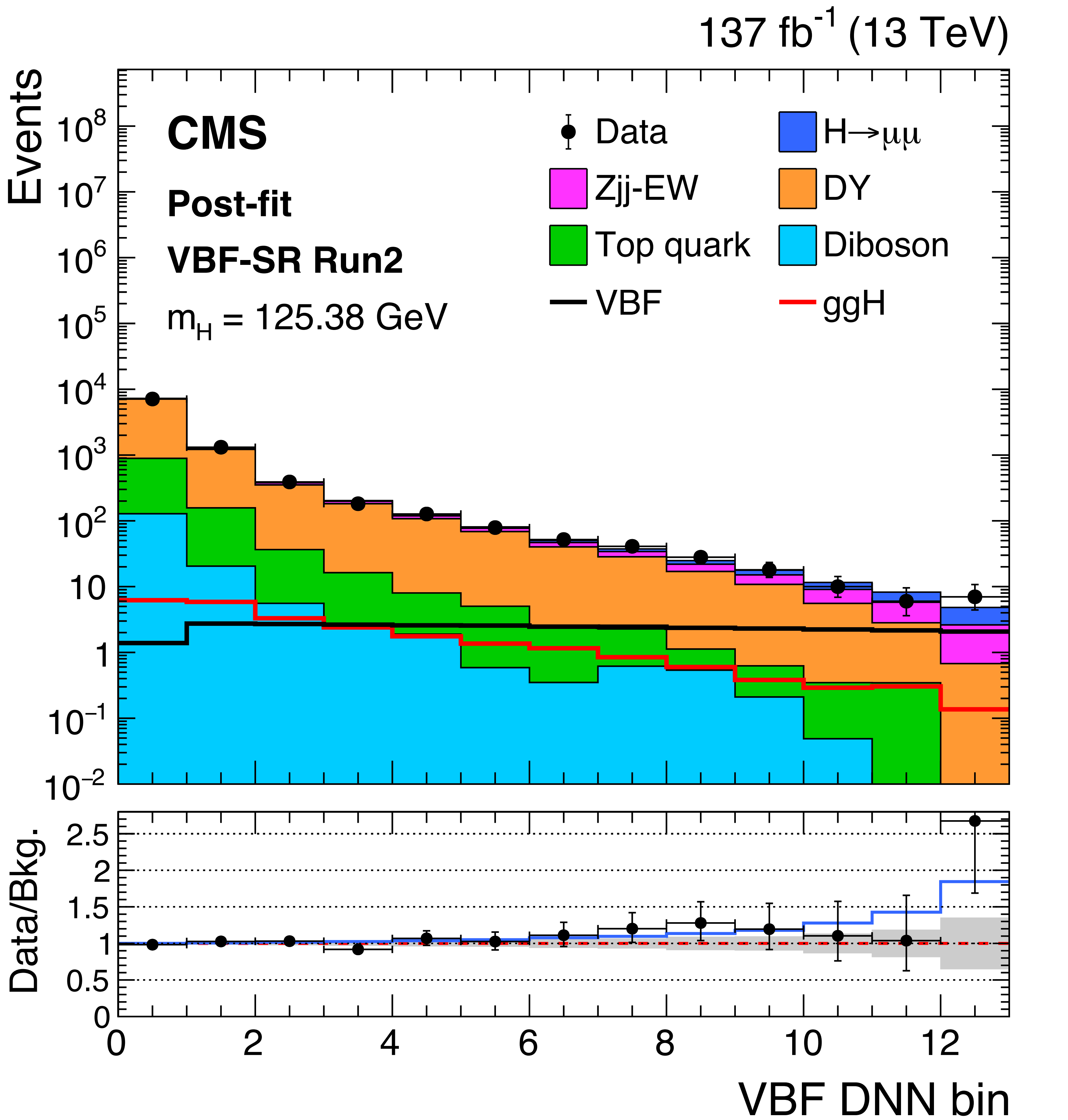

m_H = 125.5 GeV

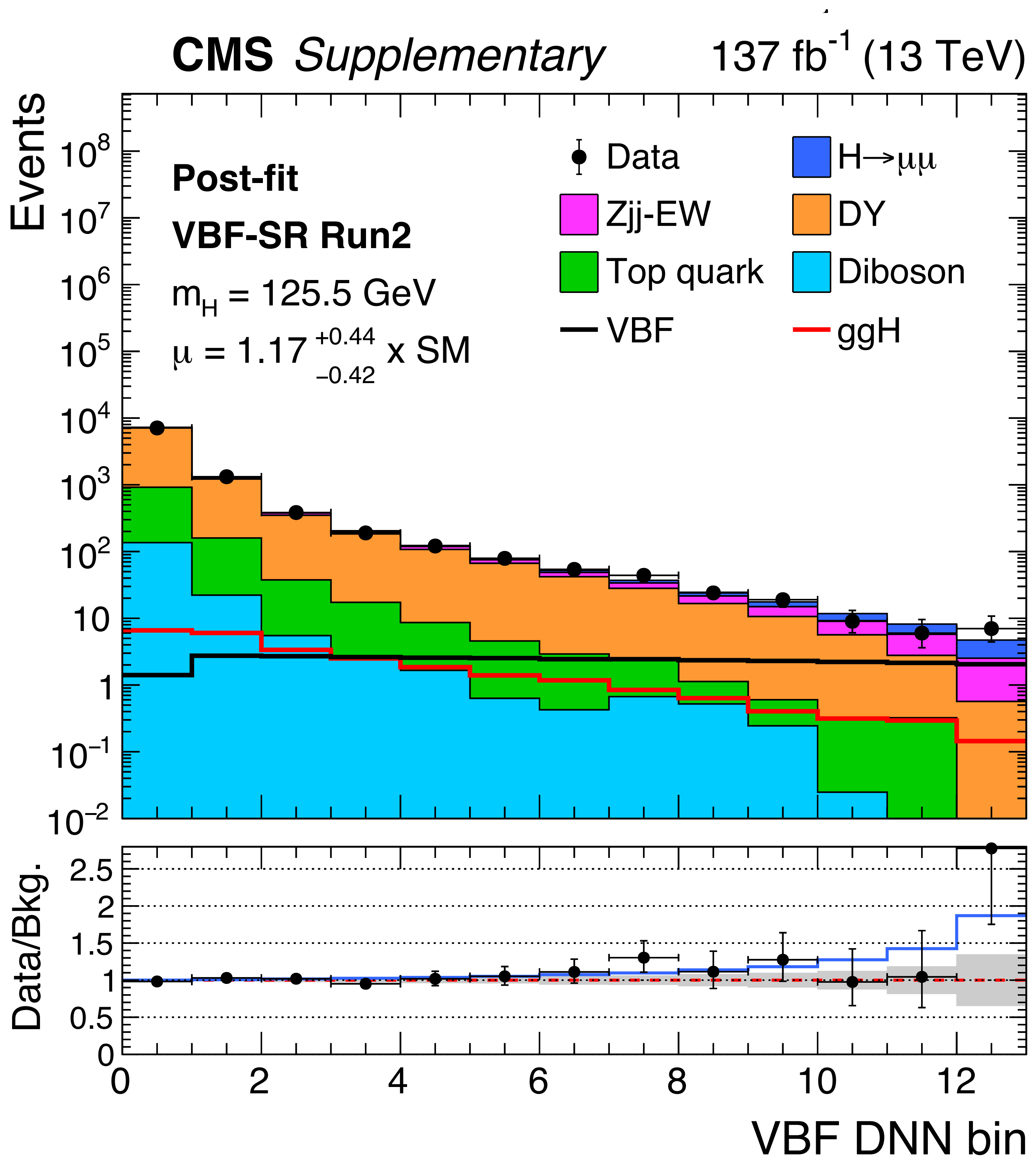

VBF DNN in SR vs m_H hypotheses

m_H = 125.1 GeV

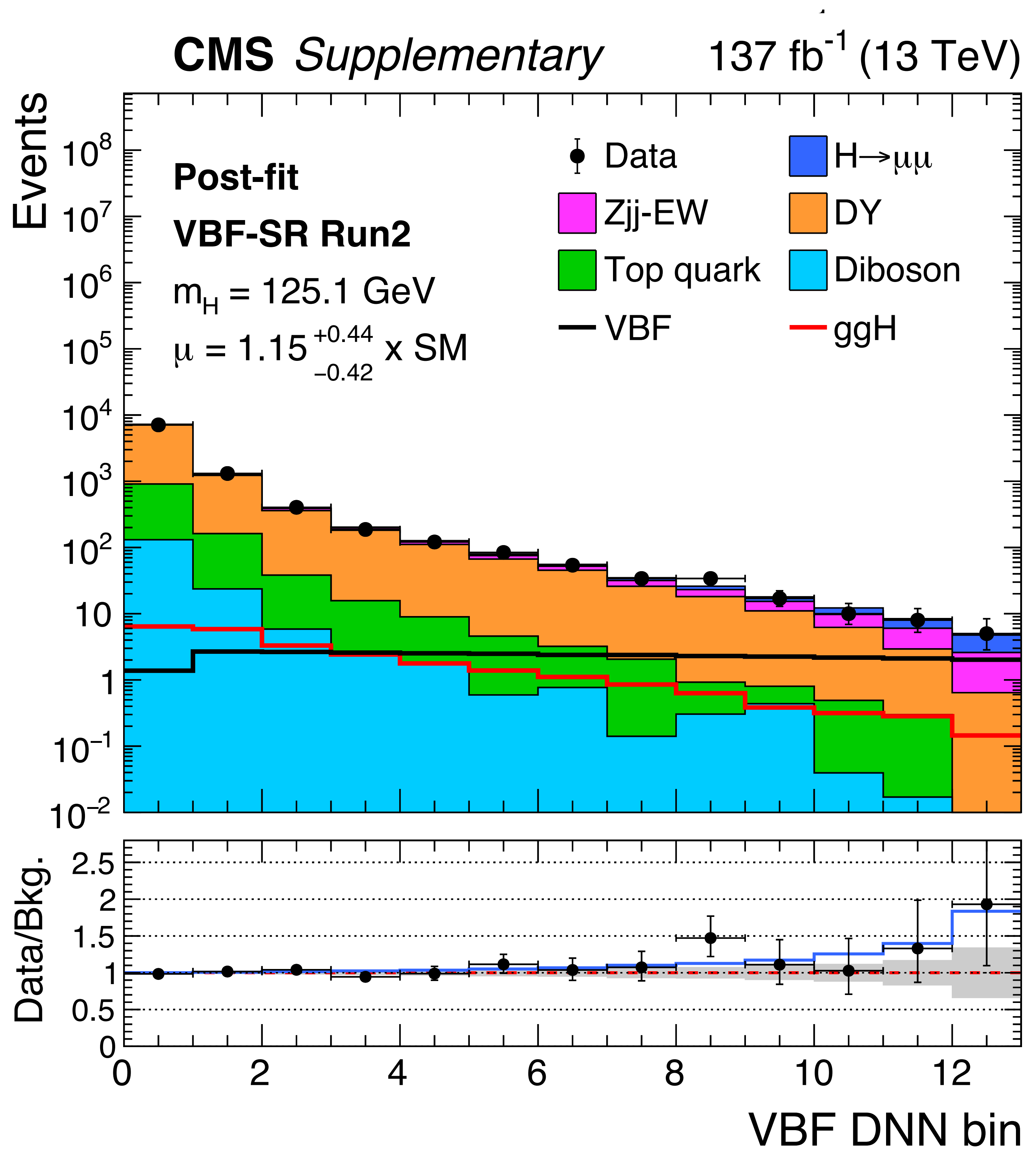

m_H = 125.38 GeV

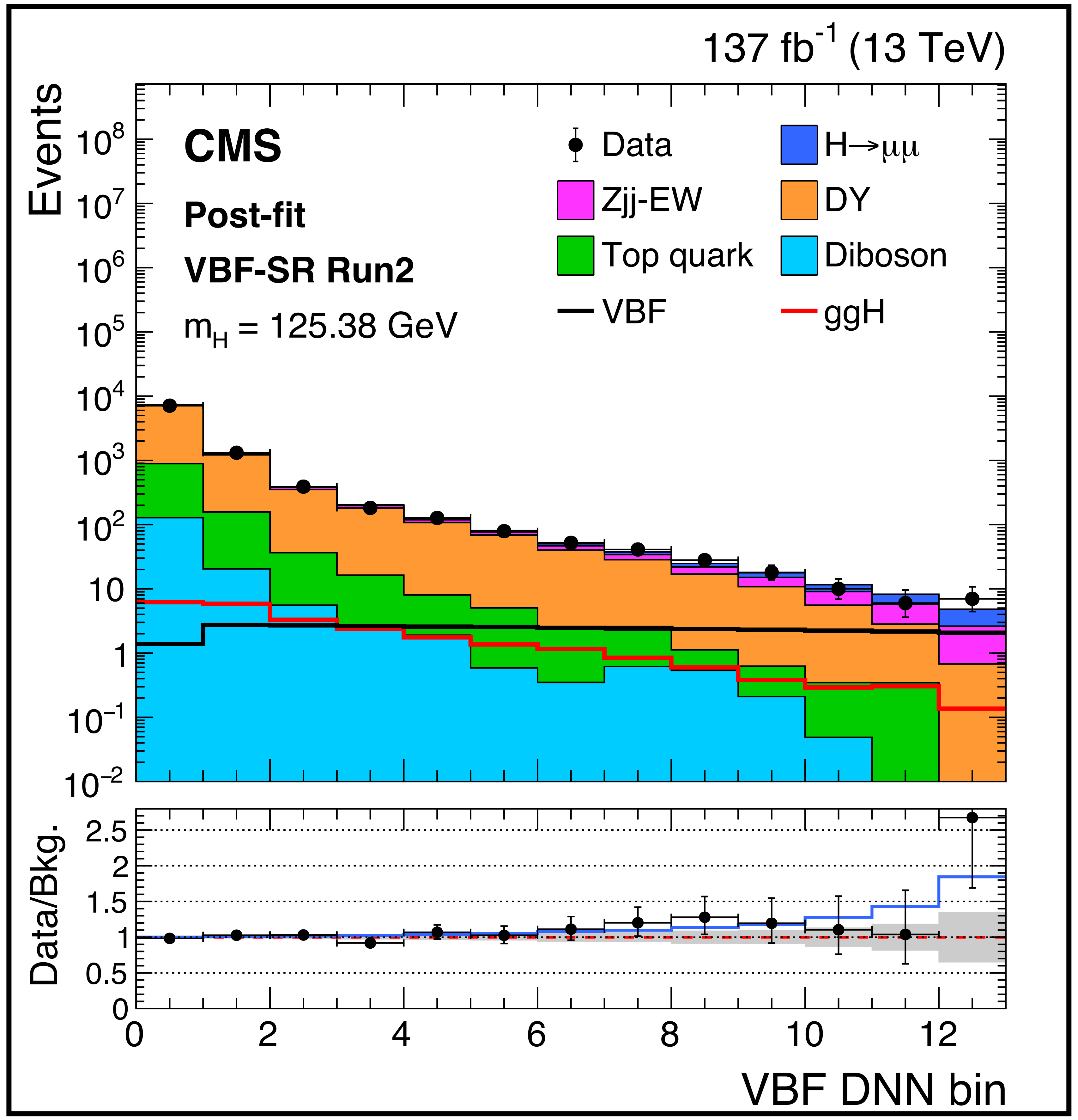

m_H = 125.7 GeV

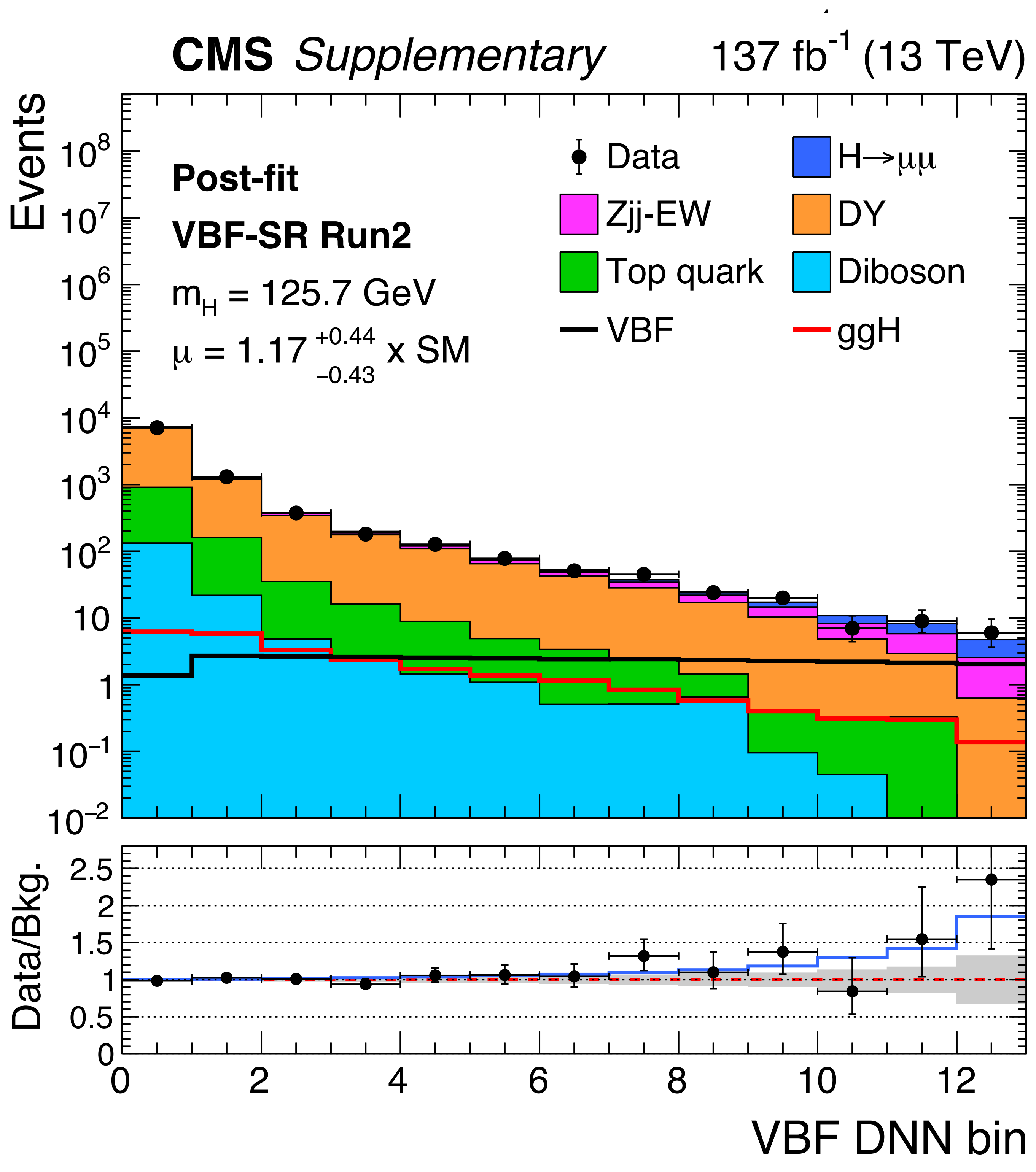

Run1+Run2 combination

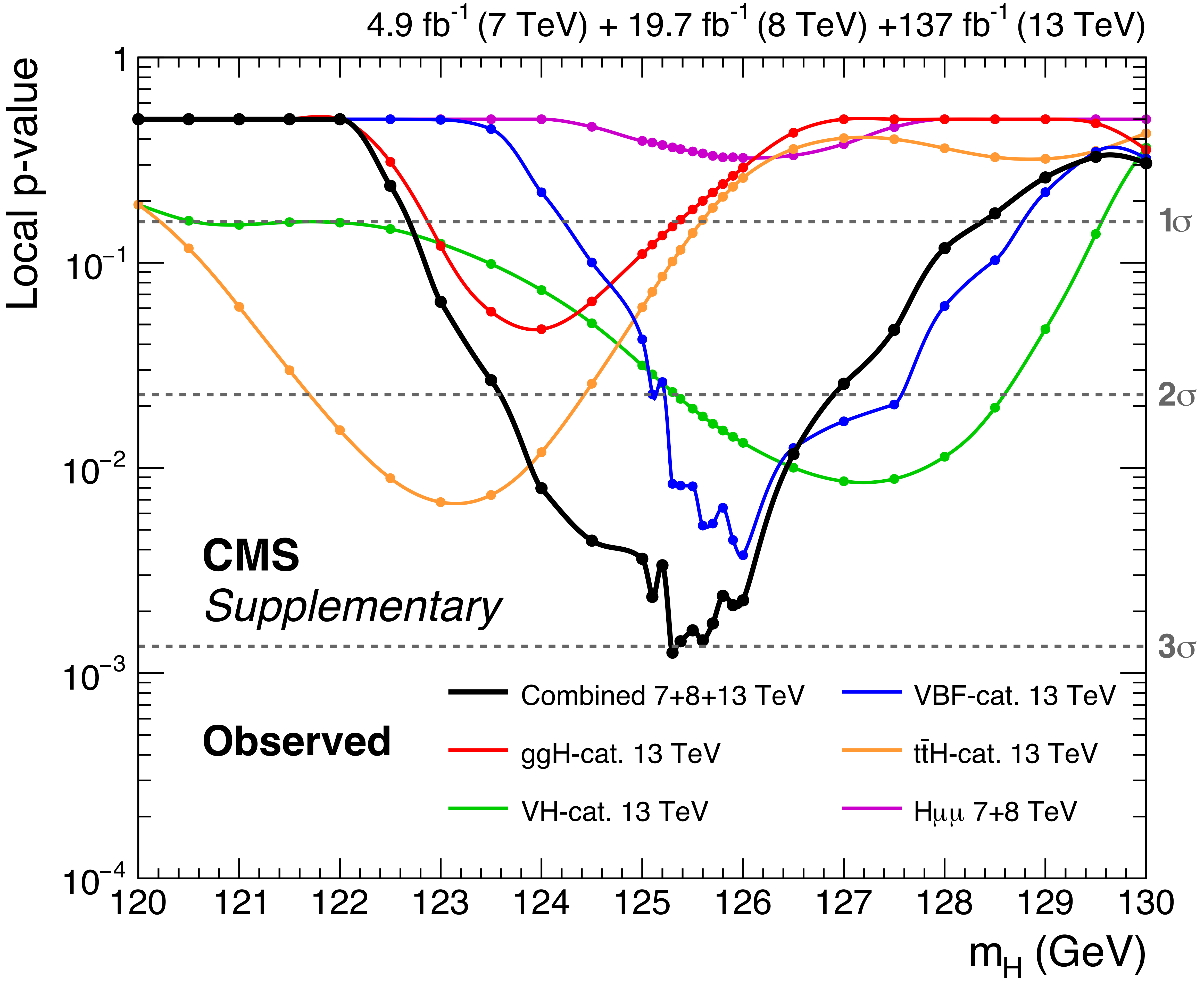

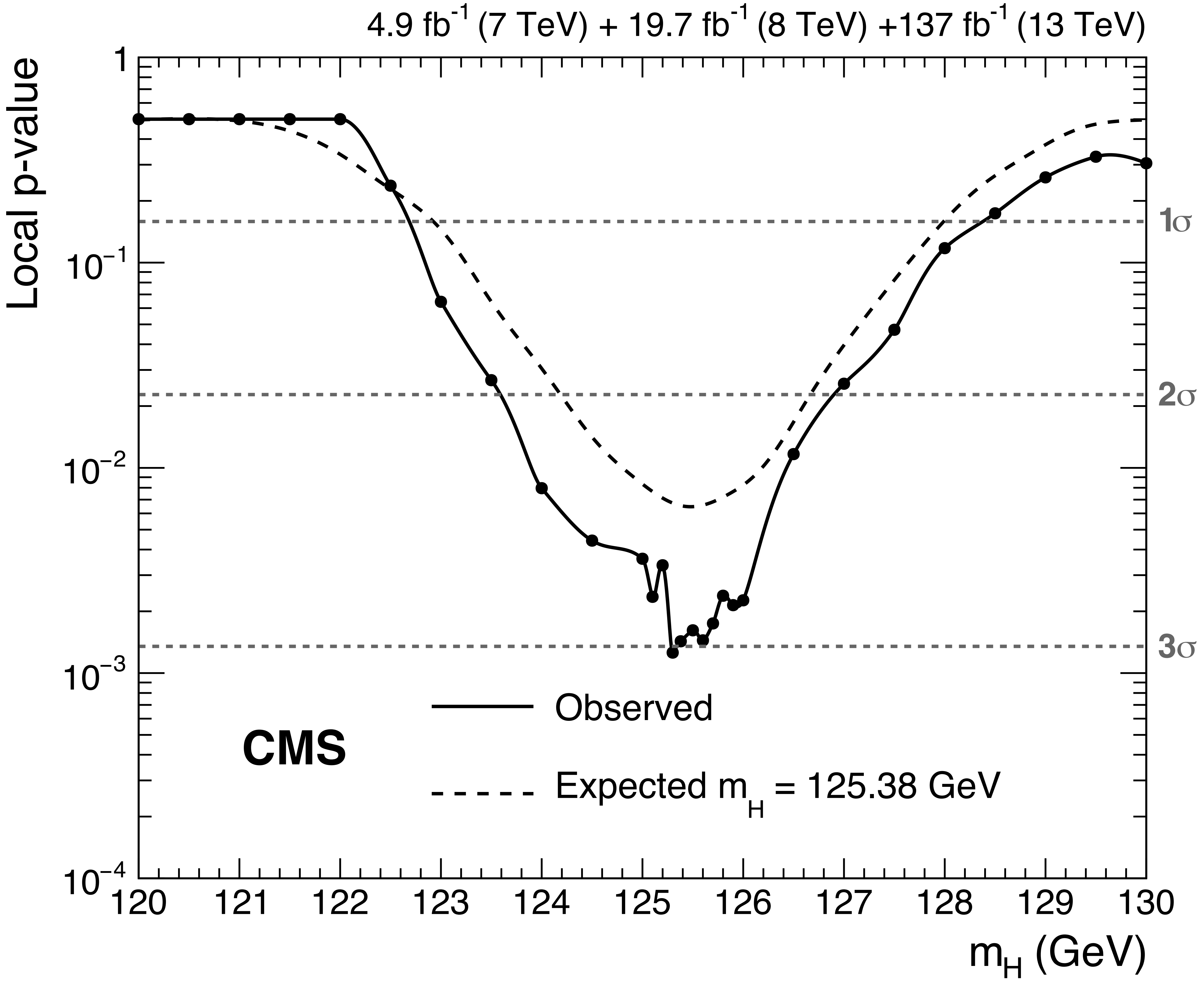

H→μμ signal

Likelihood scans vs μ for m_H = 125.38 GeV

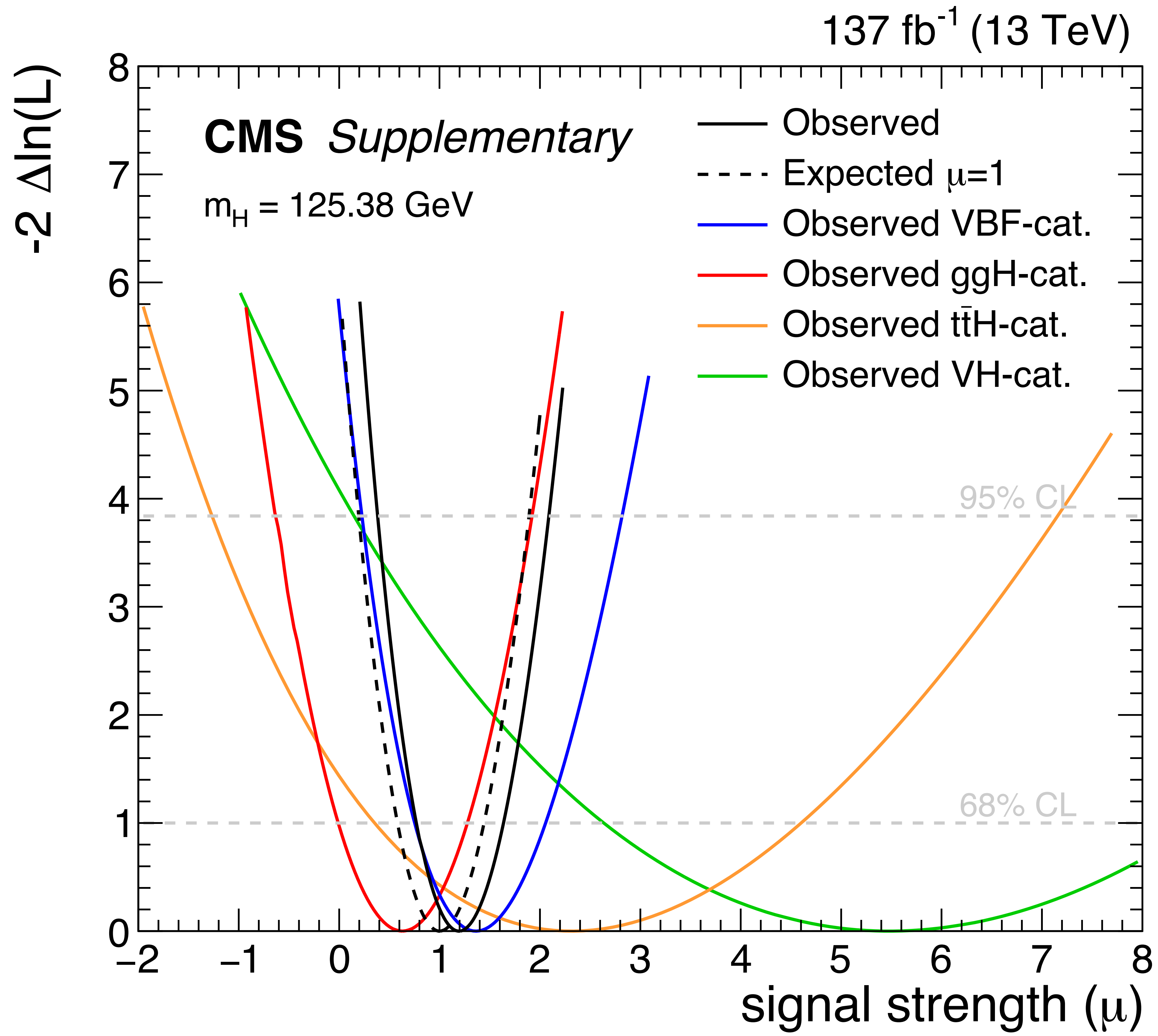

Best fit $\mu = 1.19^{+0.44}_{-0.42}$ → via partial likelihood scans the post-fit uncertainty is breakdown into statistical and systematics

Uncertainty source	$\Delta\mu$	
Post-fit uncertainty	$+0.44$	-0.42
Statistical uncertainty	$+0.41$	-0.40
Systematic uncertainty	$+0.17$	-0.16
Experimental uncertainty	$+0.12$	-0.11
Theoretical uncertainty	$+0.10$	-0.11
Size of simulated samples	$+0.07$	-0.06

H→μμ signal

Likelihood scans vs μ for m_H = 125.38 GeV

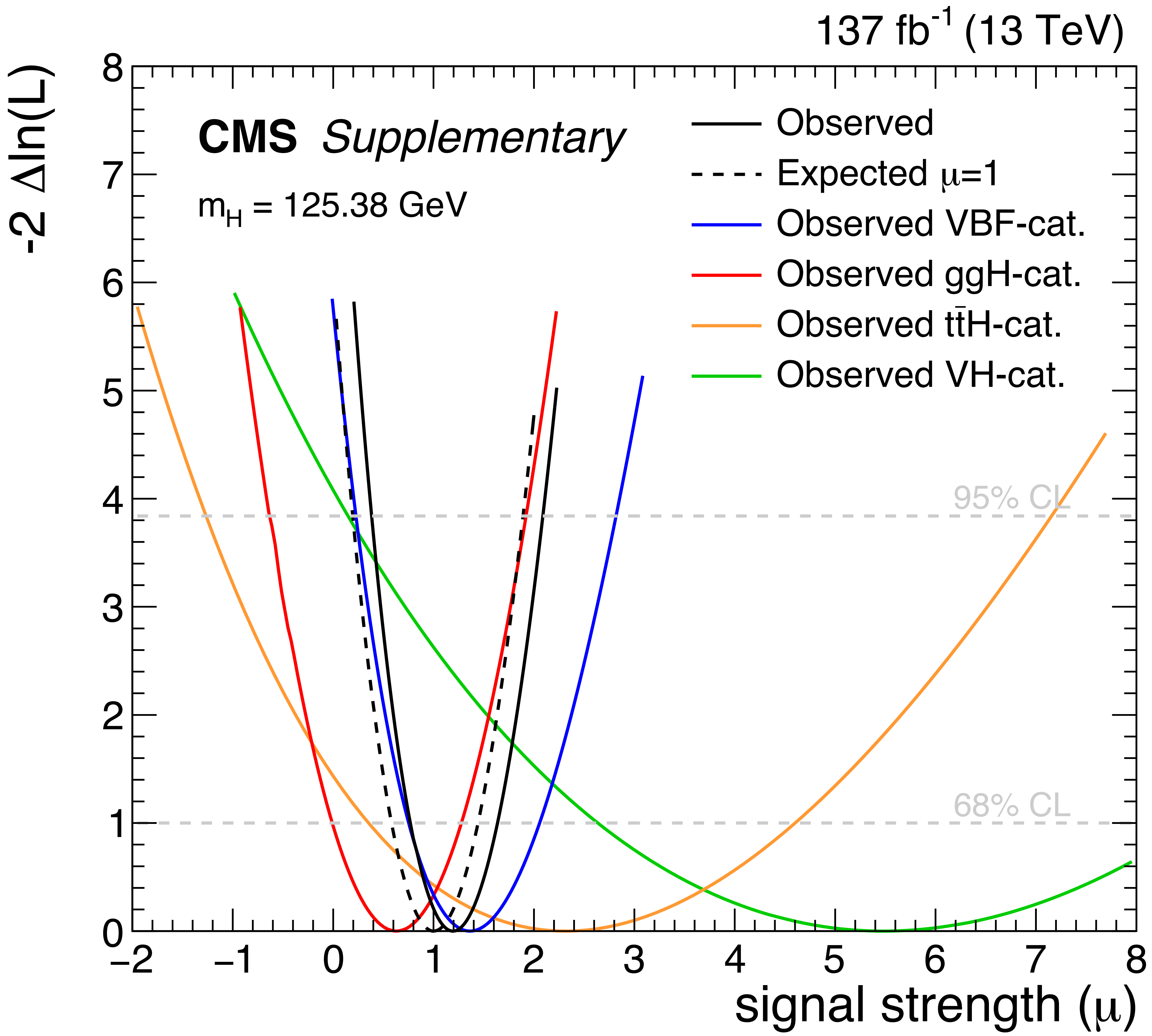

Likelihood scans vs μ_F and μ_V for m_H = 125.38 GeV

- μ_F targets production modes involving Higgs-to-fermions couplings (ggH and ttH)
- μ_V targets production modes involving Higgs-to-vector boson couplings (VBF and VH)

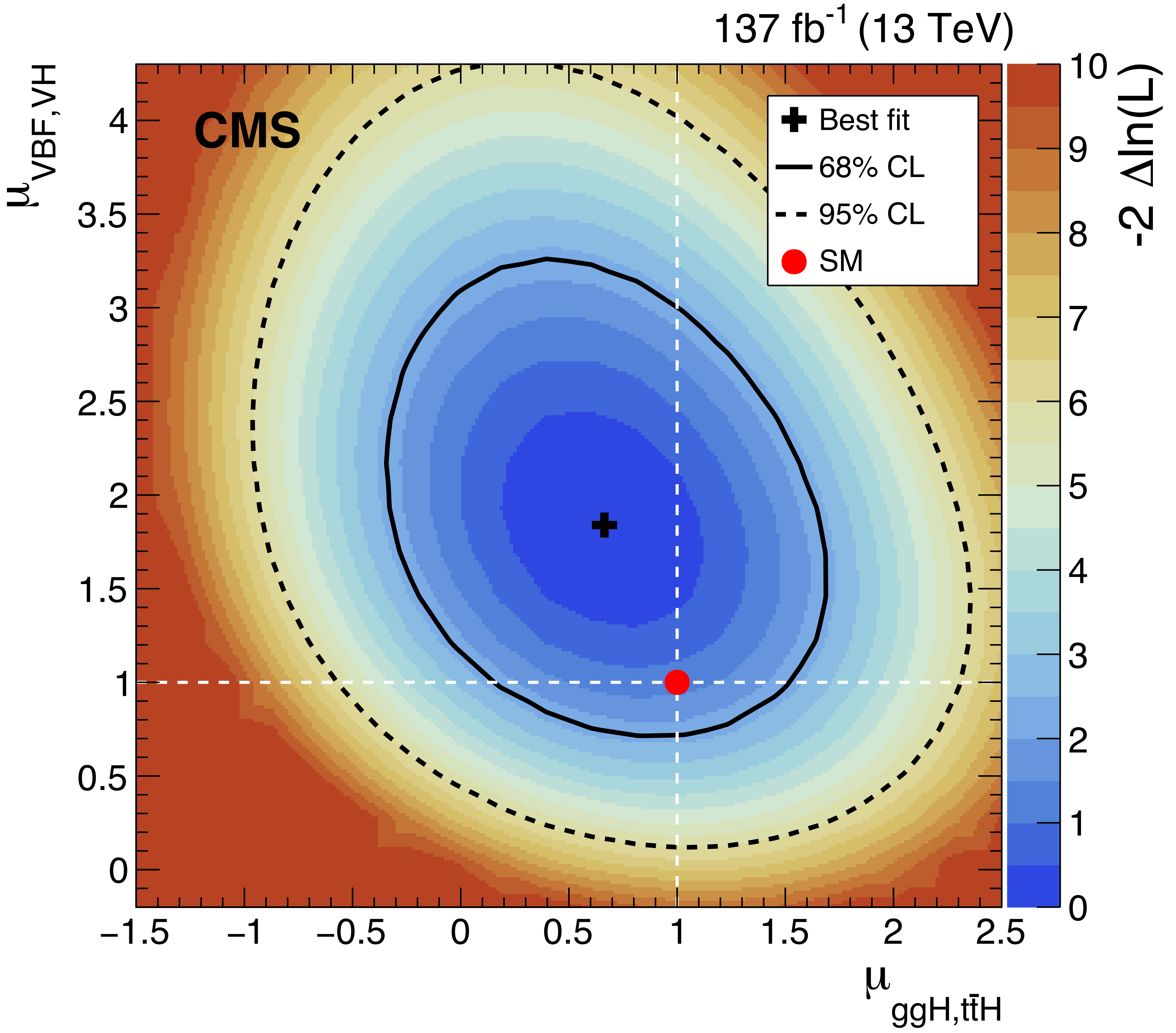

Simulated samples and cross sections

Process	Generator (Perturbative order)	Parton shower	Cross section	Additional corrections
ggH	MADGRAPH5_aMC@NLO (NLO QCD)	PYTHIA	N3LO QCD, NLO EW	p_T(H) from NNLOPS
VBF	POWHEG (NLO QCD)	PYTHIA dipole shower	NNLO QCD, NLO EW	—
qq → VH	POWHEG (NLO QCD)	PYTHIA	NNLO QCD, NLO EW	—
gg → ZH	POWHEG (LO)	PYTHIA	NNLO QCD, NLO EW	—
$t\bar{t}$H	POWHEG (NLO QCD)	PYTHIA	NLO QCD, NLO EW	—
$b\bar{b}$H	POWHEG (NLO QCD)	PYTHIA	NLO QCD	—
tHq	MADGRAPH5_aMC@NLO (LO)	PYTHIA	NLO QCD	—
tHW	MADGRAPH5_aMC@NLO (LO)	PYTHIA	NLO QCD	—
Drell–Yan	MADGRAPH5_aMC@NLO (NLO QCD)	PYTHIA	NNLO QCD, NLO EW	—
Zjj-EW	MADGRAPH5_aMC@NLO (LO)	HERWIG++/HERWIG 7	LO	—
$t\bar{t}$	POWHEG (NLO QCD)	PYTHIA	NNLO QCD	—
Single top quark	POWHEG/MADGRAPH5_aMC@NLO (NLO QCD)	PYTHIA	NLO QCD	—
Diboson (VV)	POWHEG/MADGRAPH5_aMC@NLO (NLO QCD)	PYTHIA	NLO QCD	NNLO/NLO K factors
gg → ZZ	MCFM (LO)	PYTHIA	LO	NNLO/LO K factors
$t\bar{t}$V, $t\bar{t}$VV	MADGRAPH5_aMC@NLO (NLO QCD)	PYTHIA	NLO QCD	—
Triboson (VVV)	MADGRAPH5_aMC@NLO (NLO QCD)	PYTHIA	NLO QCD	—

Systematic uncertainties: correlation

Source of uncertainty	Categories and processes	Type	Correlation vs cat.	Correlation vs year
		Experimental uncertainties		
Integrated luminosity	Sig. in all cat., bkg. in VBF	Rate	Correlated	Partial
Muon efficiency	Sig. in all cat., bkg. in VBF	Rate	Correlated	Correlated
Electron efficiency	Sig. in $t\bar{t}$H and VH	Rate	Correlated	Correlated
Muon trigger	Sig. in all cat., bkg. in VBF	Rate	Correlated	Correlated
Muon p_T scale	Sig. in all cat., bkg. in VBF	Shape in VBF, rate in others	Correlated	Correlated
Nonprompt leptons	Sig. in $t\bar{t}$H and VH	Rate	Correlated	Correlated
Pileup model	Sig. in all cat., bkg. in VBF	Shape in VBF, rate in others	Correlated	Uncorrelated
L1 inefficiency	Sig. in all cat., bkg. in VBF	Shape in VBF, rate in others	Correlated	Uncorrelated
B-tagging efficiency	Sig. in all cat., bkg. in VBF	Shape in VBF, rate in others	Correlated	Correlated
Jet energy scale	Sig. in all cat., bkg. in VBF	Shape in VBF, rate in others	Correlated	Partial
Jet energy resolution	Sig. in all cat., bkg. in VBF	Shape in VBF, rate in others	Correlated	Uncorrelated
		Theoretical uncertainties		
μ_R and μ_F for ggH	ggH in all cat.	Rate	Correlated	Correlated
μ_R and μ_F for VBF	VBF in all cat.	Rate	Correlated	Correlated
μ_R and μ_F for $t\bar{t}$H	$t\bar{t}$H in all cat.	Rate	Correlated	Correlated
μ_R and μ_F for VH	VH in all cat.	Rate	Correlated	Correlated
PDF for ggH	ggH in all cat.	Rate	Correlated	Correlated
PDF for VBF	VBF in all cat.	Rate	Correlated	Correlated
PDF for $t\bar{t}$H	$t\bar{t}$H in all cat.	Rate	Correlated	Correlated
PDF for VH	VH in all cat.	Rate	Correlated	Correlated
ggH accept. vs (p_T(H),N_j,m_{jj})	ggH in all cat.	Shape in VBF, rate in others	Correlated	Correlated
VBF accept. vs (p_T(H),N_j,m_{jj})	VBF in all cat.	Shape in VBF, rate in others	Correlated	Correlated
$t\bar{t}$H accept. from μ_R and μ_F	$t\bar{t}$H in all cat.	Rate	Correlated	Correlated
VH accept. from μ_R and μ_F	VH in all cat.	Rate	Correlated	Correlated
$t\bar{t}$H accept. from PDF	$t\bar{t}$H in all cat.	Rate	Correlated	Correlated
VH accept. from PDF	VH in all cat.	Rate	Correlated	Correlated
PYTHIA ISR and FSR	Sig. in all cat., bkg. in VBF	Shape in VBF, rate in others	Correlated	Correlated
PYTHIA vs HERWIG)	VBF and Zjj-EW in VBF cat.	Shape	Correlated	Correlated
μ_R and μ_F for Drell–Yan	VBF cat.	Shape	Correlated	Correlated
μ_R and μ_F for Zjj-EW	VBF cat.	Shape	Correlated	Correlated
μ_R and μ_F for top bkgs.	VBF cat.	Shape	Correlated	Correlated
μ_R and μ_F for diboson	VBF cat.	Shape	Correlated	Correlated
PDF for Drell–Yan	VBF cat.	Shape	Correlated	Correlated
PDF for Zjj-EW	VBF cat.	Shape	Correlated	Correlated
PDF for top bkgs.	VBF cat.	Shape	Correlated	Correlated
PDF for dibosons	VBF cat.	Shape	Correlated	Correlated
Size of simulated samples	VBF cat.	Bin-by-bin	—	Uncorrelated

Systematic uncertainties: pulls and impacts

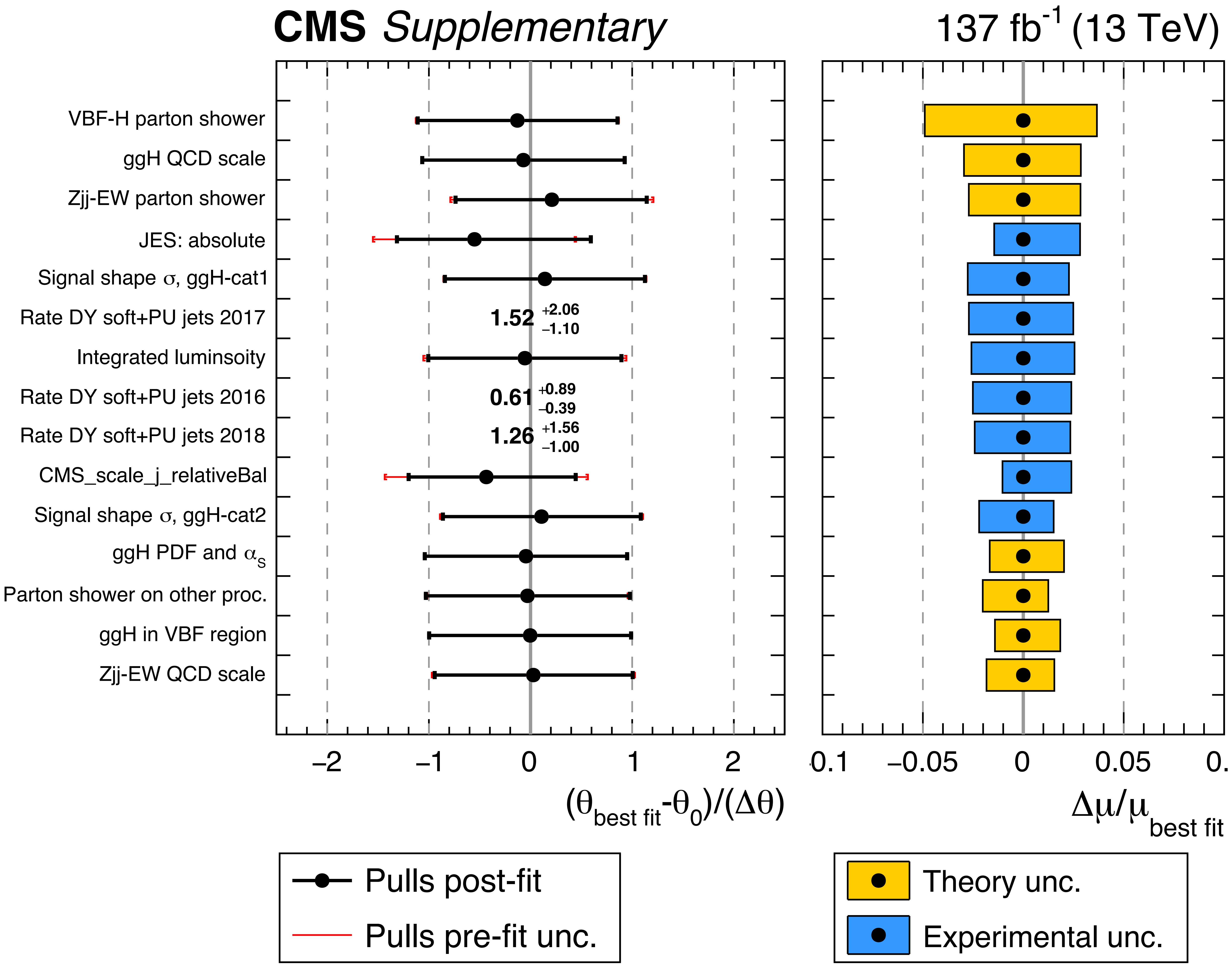

Summary of event categories

- ***H→μμ analysis*** divided in ***exclusive production categories*** targeting ggH, VBF, VH, and ttH modes
- Each of them is further ***divided into subcategories*** optimising the expected significance for H→μμ decays

ggH

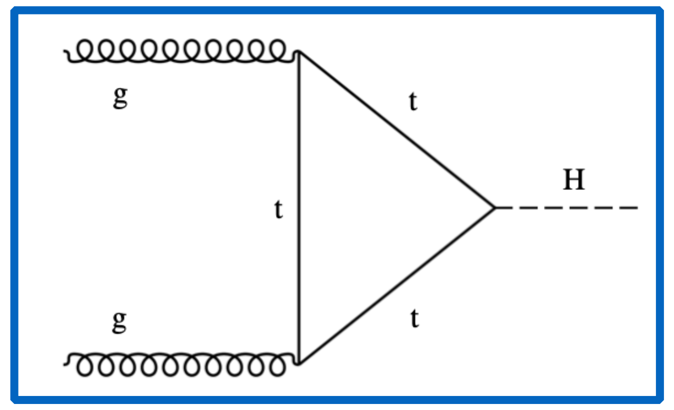

VBF

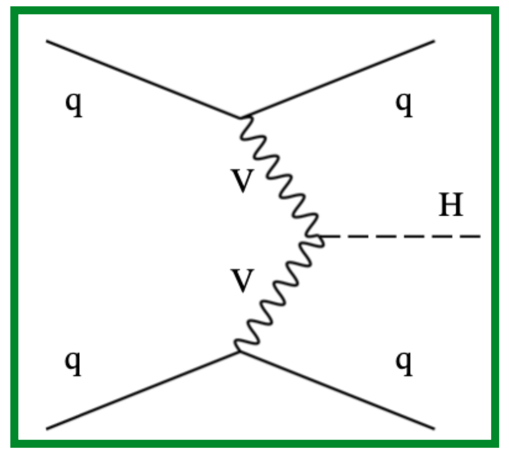

VH

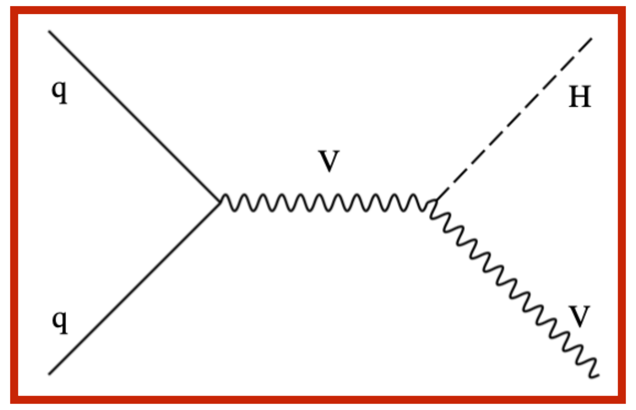

ttH

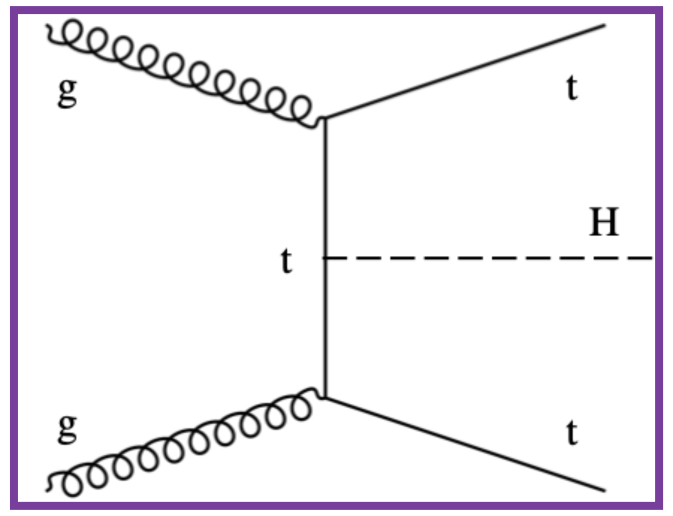

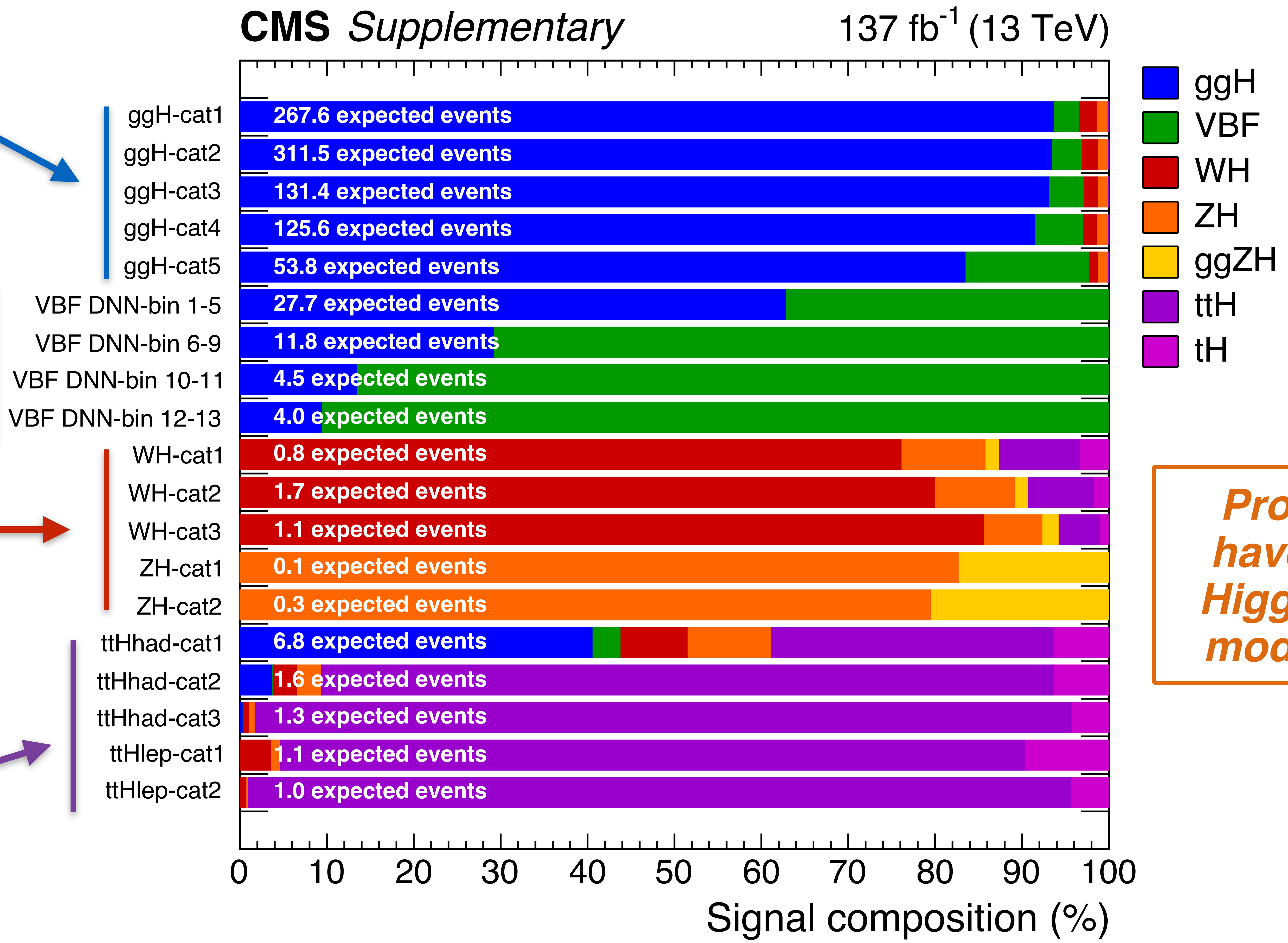

Production categories have good purity in the Higgs boson production mode they are targeting

Coupling fit

Combination with ***CMS-PAS-HIG-19-005***

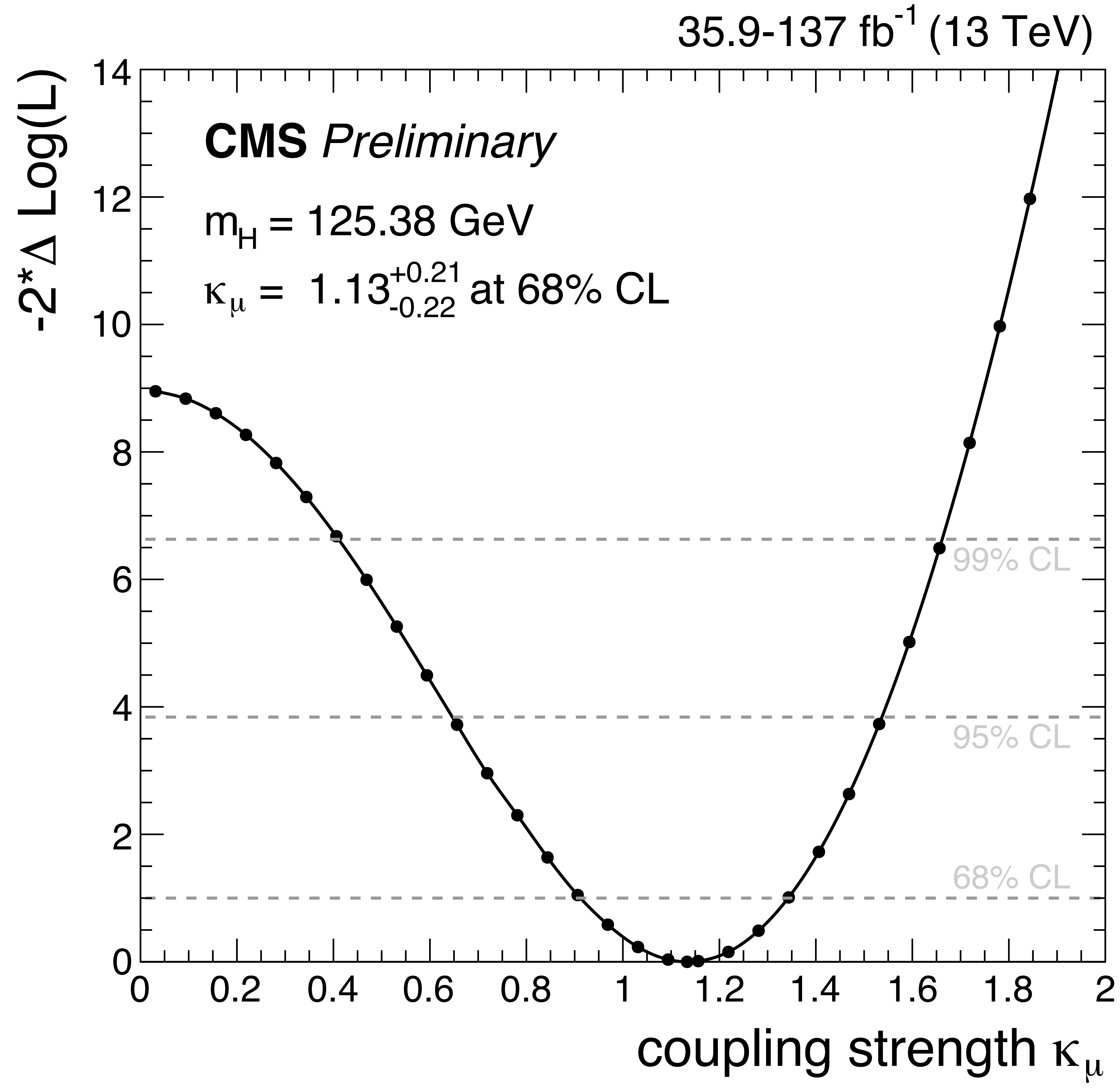

Combination with ***Eur. Phys. J. C 79 (2019) 421***

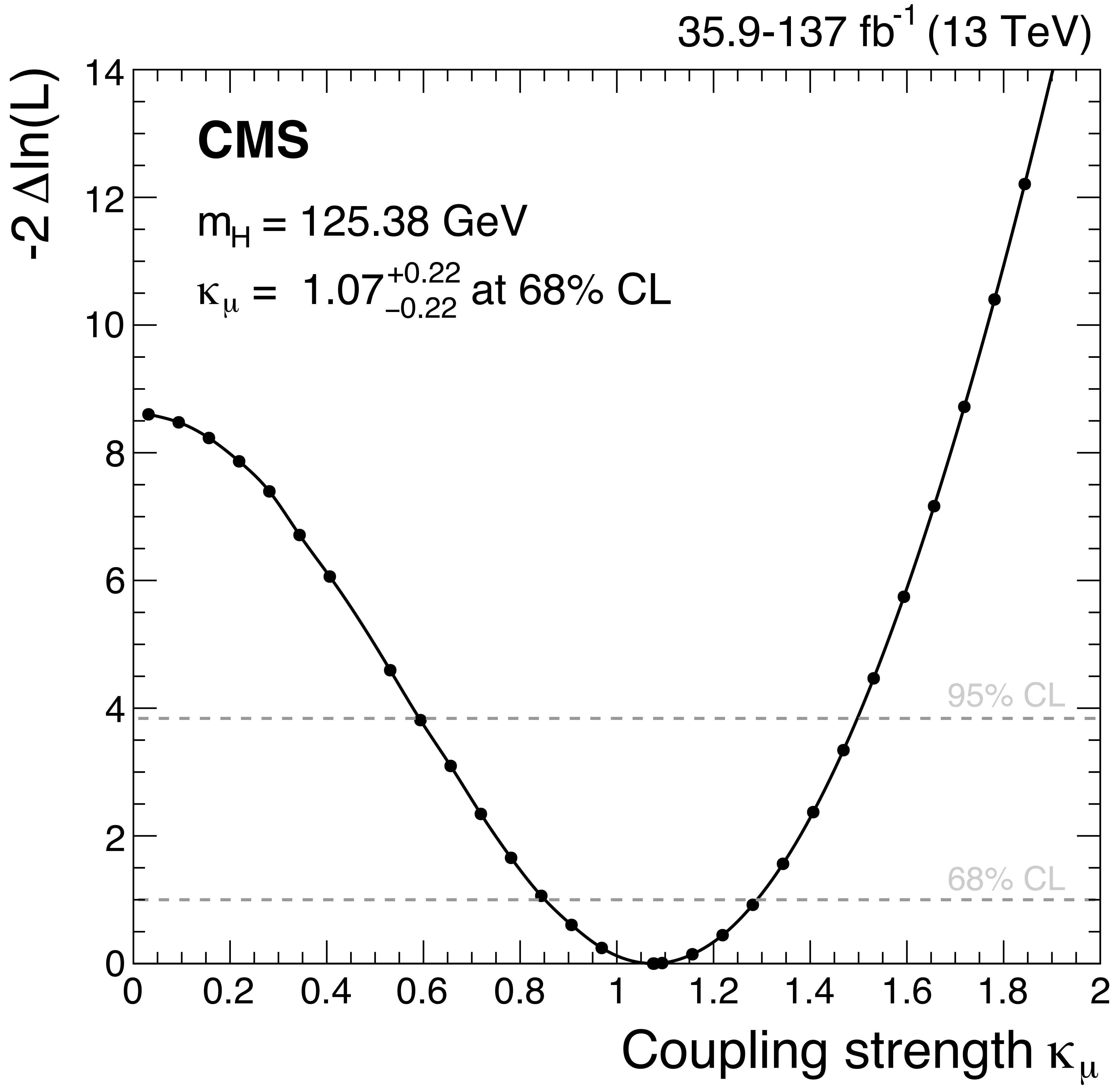

Coupling fit

Combination with ***CMS-PAS-HIG-19-005***

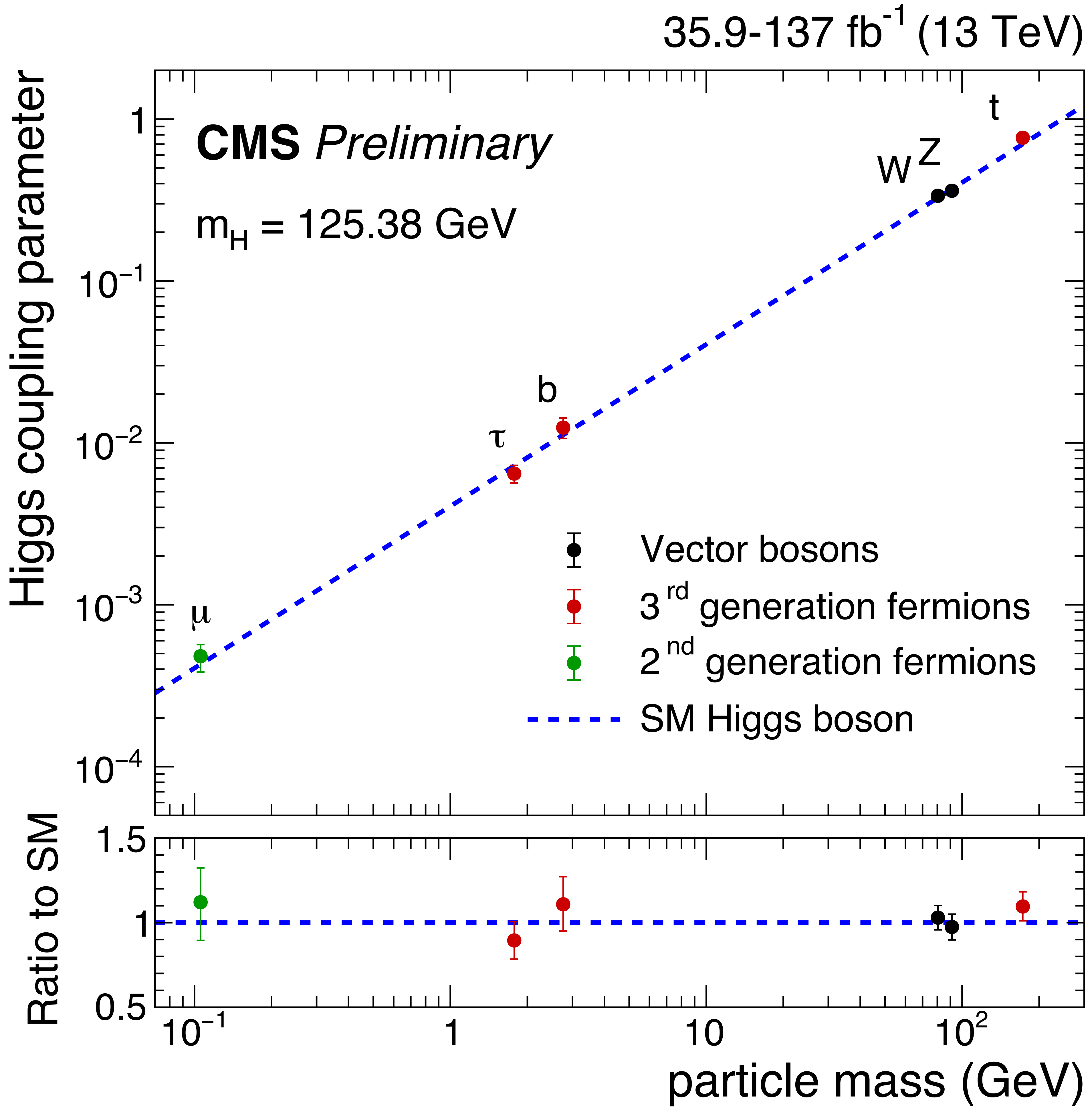

Combination with ***Eur. Phys. J. C 79 (2019) 421***

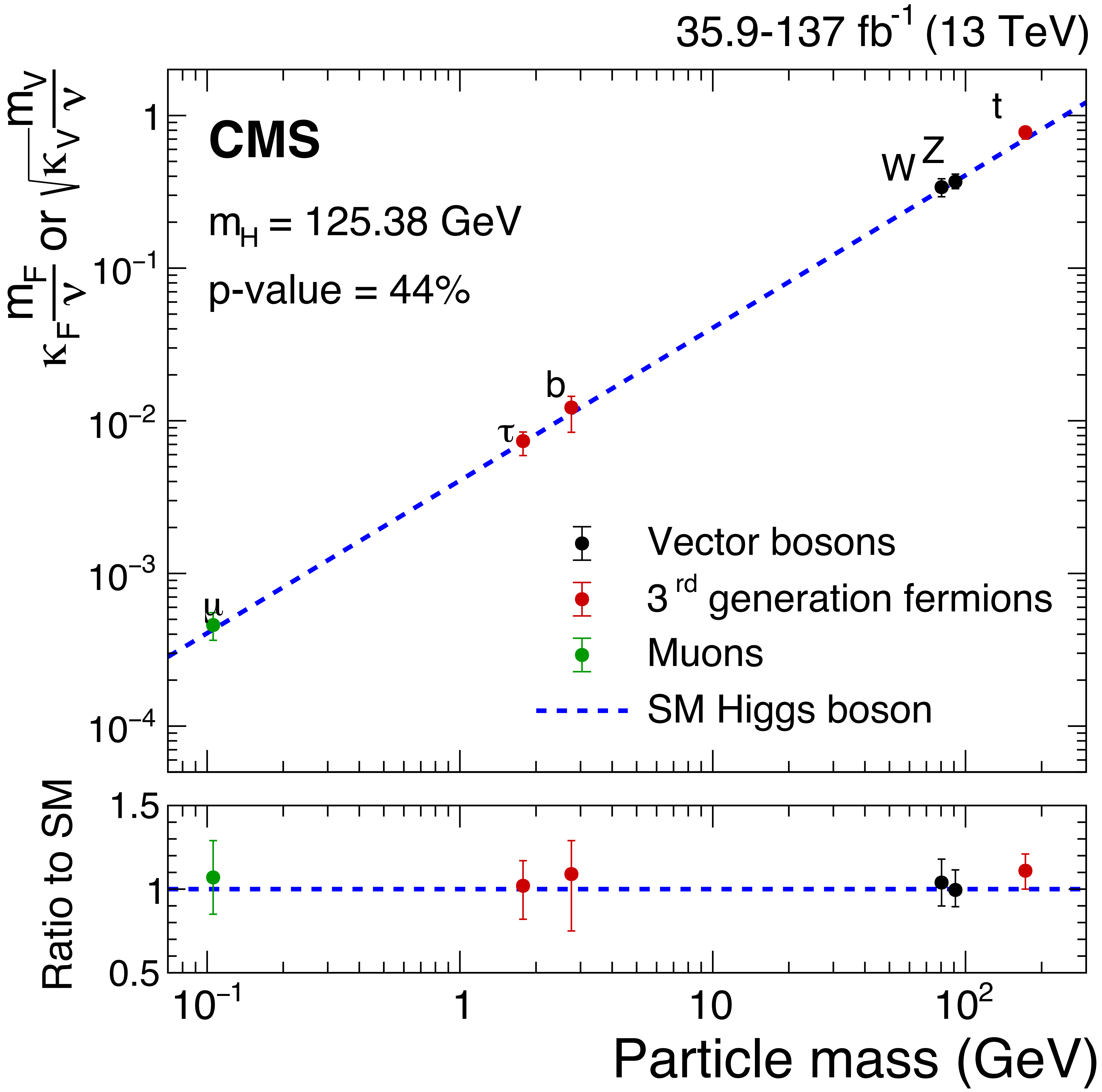

ATLAS and CMS H→μμ result

ATLAS categories

Category	ggF	VBF	WH	ZH	$t\bar{t}H$
VBF Very High	6.6%	93.3%	0.0%	0.0%	0.0%
VBF High	12.8%	87.1%	0.0%	0.0%	0.0%
VBF Medium	21.3%	78.5%	0.1%	0.1%	0.0%
VBF Low	34.8%	64.8%	0.2%	0.2%	0.0%
2-jet Very High	82.0%	15.7%	1.2%	1.0%	0.2%
2-jet High	79.3%	16.0%	2.7%	1.8%	0.3%
2-jet Medium	80.7%	10.4%	5.4%	3.0%	0.5%
2-jet Low	78.2%	6.6%	8.8%	4.9%	1.5%
1-jet Very High	78.2%	21.2%	0.3%	0.3%	0.0%
1-jet High	88.2%	10.4%	0.9%	0.6%	0.0%
1-jet Medium	91.4%	6.1%	1.6%	0.9%	0.0%
1-jet Low	92.4%	3.8%	2.6%	1.2%	0.0%
0-jet Very High	94.1%	2.5%	1.4%	2.0%	0.0%
0-jet High	98.3%	1.0%	0.4%	0.3%	0.0%
0-jet Medium	99.1%	0.6%	0.2%	0.1%	0.0%
0-jet Low	99.5%	0.3%	0.1%	0.1%	0.0%
VH4L	0.0%	0.0%	0.1%	99.5%	0.4%
VH3LH	0.3%	0.1%	96.9%	2.6%	0.1%
VH3LM	4.2%	1.0%	80.8%	8.6%	5.3%
$t\bar{t}H$	0.1%	0.0%	1.5%	0.4%	98.0%

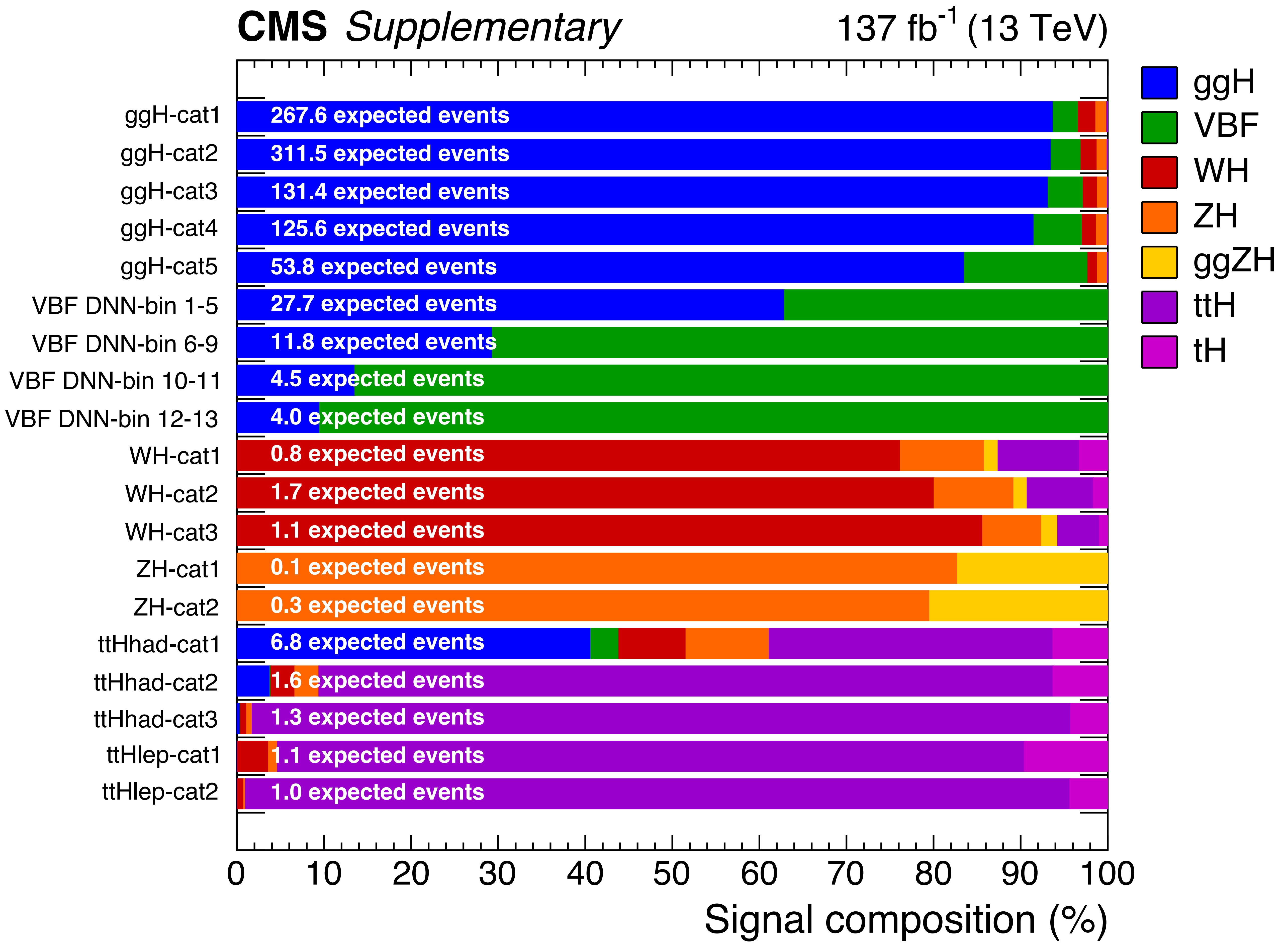

ATLAS and CMS H→μμ result

ATLAS categories

Category	Data	S_{SM}	S	B	$S/\sqrt{B}$	S/B [%]	σ [GeV]
VBF Very High	15	2.81 ± 0.27	3.3 ± 1.7	14.5 ± 2.1	0.86	22.6	3.0
VBF High	39	3.46 ± 0.36	4.0 ± 2.1	32.5 ± 2.9	0.71	12.4	3.0
VBF Medium	112	4.8 ± 0.5	5.6 ± 2.8	85 ± 4	0.61	6.6	2.9
VBF Low	284	7.5 ± 0.9	9 ± 4	273 ± 8	0.53	3.2	3.0
2-jet Very High	1030	17.6 ± 3.3	21 ± 10	1024 ± 22	0.63	2.0	3.1
2-jet High	5433	50 ± 8	58 ± 30	5440 ± 50	0.77	1.0	2.9
2-jet Medium	18 311	79 ± 15	90 ± 50	$18\,320 \pm 90$	0.66	0.5	2.9
2-jet Low	36 409	63 ± 17	70 ± 40	$36\,340 \pm 140$	0.37	0.2	2.9
1-jet Very High	1097	16.5 ± 2.4	19 ± 10	1071 ± 22	0.59	1.8	2.9
1-jet High	6413	46 ± 7	54 ± 28	6320 ± 50	0.69	0.9	2.8
1-jet Medium	24 576	90 ± 11	100 ± 50	$24\,290 \pm 100$	0.67	0.4	2.7
1-jet Low	73 459	125 ± 17	150 ± 70	$73\,480 \pm 190$	0.53	0.2	2.8
0-jet Very High	15 986	59 ± 11	70 ± 40	$16\,090 \pm 90$	0.55	0.4	2.6
0-jet High	46 523	99 ± 13	120 ± 60	$46\,190 \pm 150$	0.54	0.3	2.6
0-jet Medium	91 392	119 ± 14	140 ± 70	$91\,310 \pm 210$	0.46	0.2	2.7
0-jet Low	121 354	79 ± 10	90 ± 50	$121\,310 \pm 280$	0.26	0.1	2.7
VH4L	34	0.53 ± 0.05	0.6 ± 0.3	24 ± 4	0.13	2.6	2.9
VH3LH	41	1.45 ± 0.14	1.7 ± 0.9	41 ± 5	0.27	4.2	3.1
VH3LM	358	2.76 ± 0.24	3.2 ± 1.6	347 ± 15	0.17	0.9	3.0
$t\bar{t}H$	17	1.19 ± 0.13	1.4 ± 0.7	15.1 ± 2.2	0.36	9.2	3.2

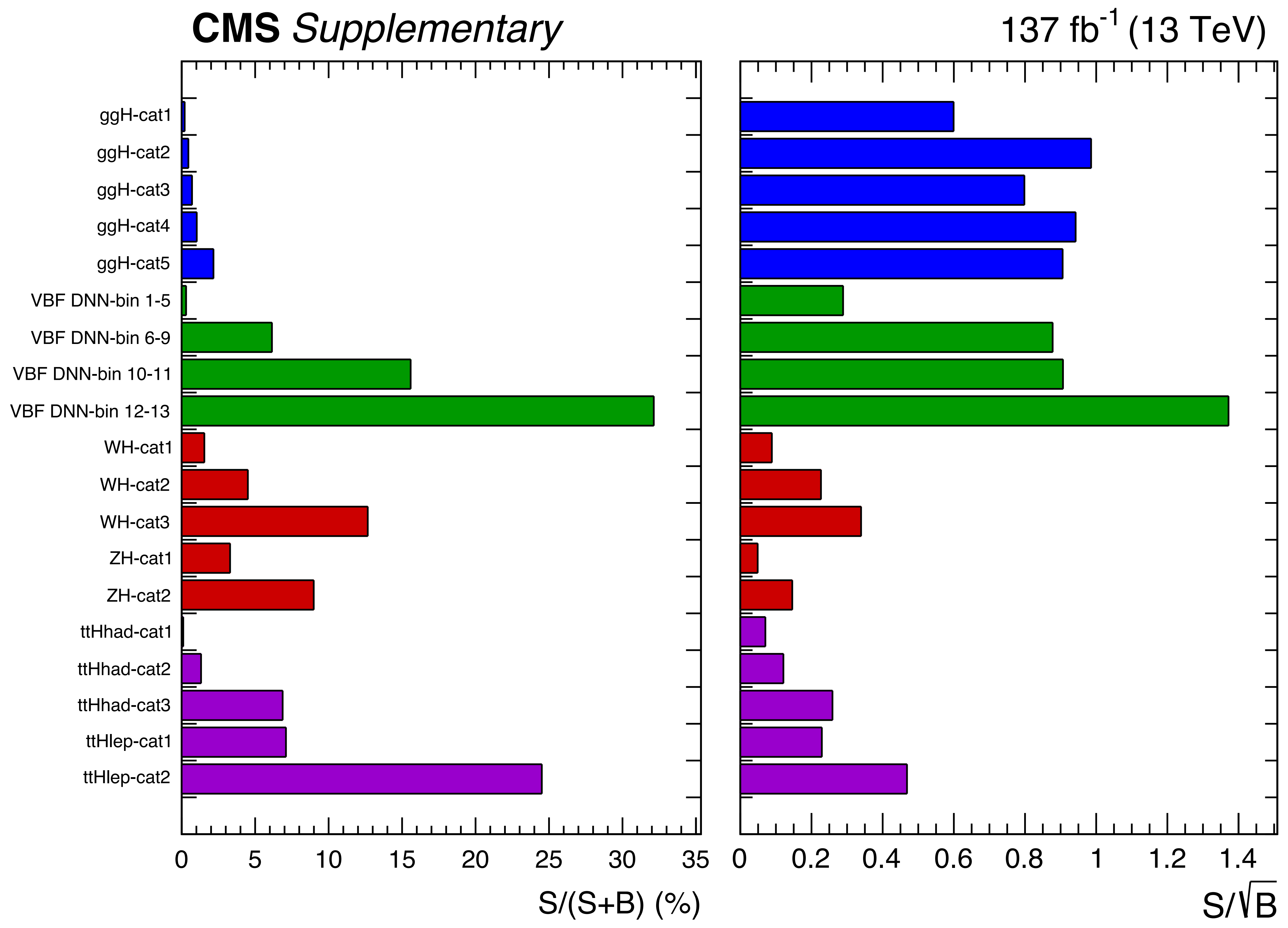

ATLAS and CMS H→μμ result

ATLAS categories

Category	Data	S_{SM}	S	B	$S/\sqrt{B}$	S/B [%]	σ [GeV]
VBF Very High	15	2.81 ± 0.27	3.3 ± 1.7	14.5 ± 2.1	0.86	22.6	3.0
VBF High	39	3.46 ± 0.36	4.0 ± 2.1	32.5 ± 2.9	0.71	12.4	3.0
VBF Medium	112	4.8 ± 0.5	5.6 ± 2.8	85 ± 4	0.61	6.6	2.9
VBF Low	284	7.5 ± 0.9	9 ± 4	273 ± 8	0.53	3.2	3.0
2-jet Very High	1030	17.6 ± 3.3	21 ± 10	1024 ± 22	0.63	2.0	3.1
2-jet High	5433	50 ± 8	58 ± 30	5440 ± 50	0.77	1.0	2.9
2-jet Medium	18 311	79 ± 15	90 ± 50	18 320 ± 90	0.66	0.5	2.9
2-jet Low	36 409	63 ± 17	70 ± 40	36 340 ± 140	0.37	0.2	2.9
1-jet Very High	1097	16.5 ± 2.4	19 ± 10	1071 ± 22	0.59	1.8	2.9
1-jet High	6413	46 ± 7	54 ± 28	6320 ± 50	0.69	0.9	2.8
1-jet Medium	24 576	90 ± 11	100 ± 50	24 290 ± 100	0.67	0.4	2.7
1-jet Low	73 459	125 ± 17	150 ± 70	73 480 ± 190	0.53	0.2	2.8
0-jet Very High	15 986	59 ± 11	70 ± 40	16 090 ± 90	0.55	0.4	2.6
0-jet High	46 523	99 ± 13	120 ± 60	46 190 ± 150	0.54	0.3	2.6
0-jet Medium	91 392	119 ± 14	140 ± 70	91 310 ± 210	0.46	0.2	2.7
0-jet Low	121 354	79 ± 10	90 ± 50	121 310 ± 280	0.26	0.1	2.7
VH4L	34	0.53 ± 0.05	0.6 ± 0.3	24 ± 4	0.13	2.6	2.9
VH3LH	41	1.45 ± 0.14	1.7 ± 0.9	41 ± 5	0.27	4.2	3.1
VH3LM	358	2.76 ± 0.24	3.2 ± 1.6	347 ± 15	0.17	0.9	3.0
$t\bar{t}H$	17	1.19 ± 0.13	1.4 ± 0.7	15.1 ± 2.2	0.36	9.2	3.2

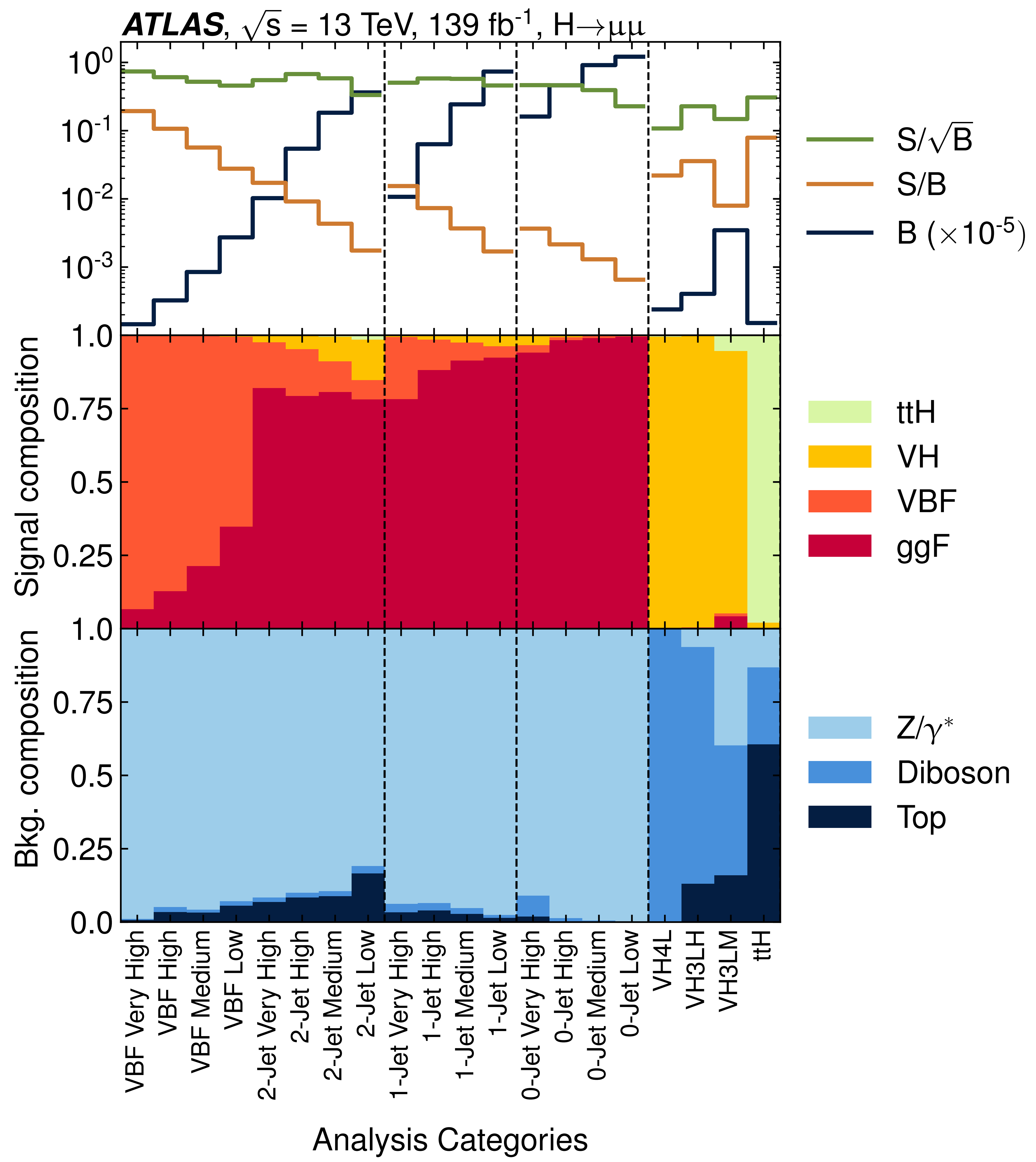

ATLAS H→μμ result

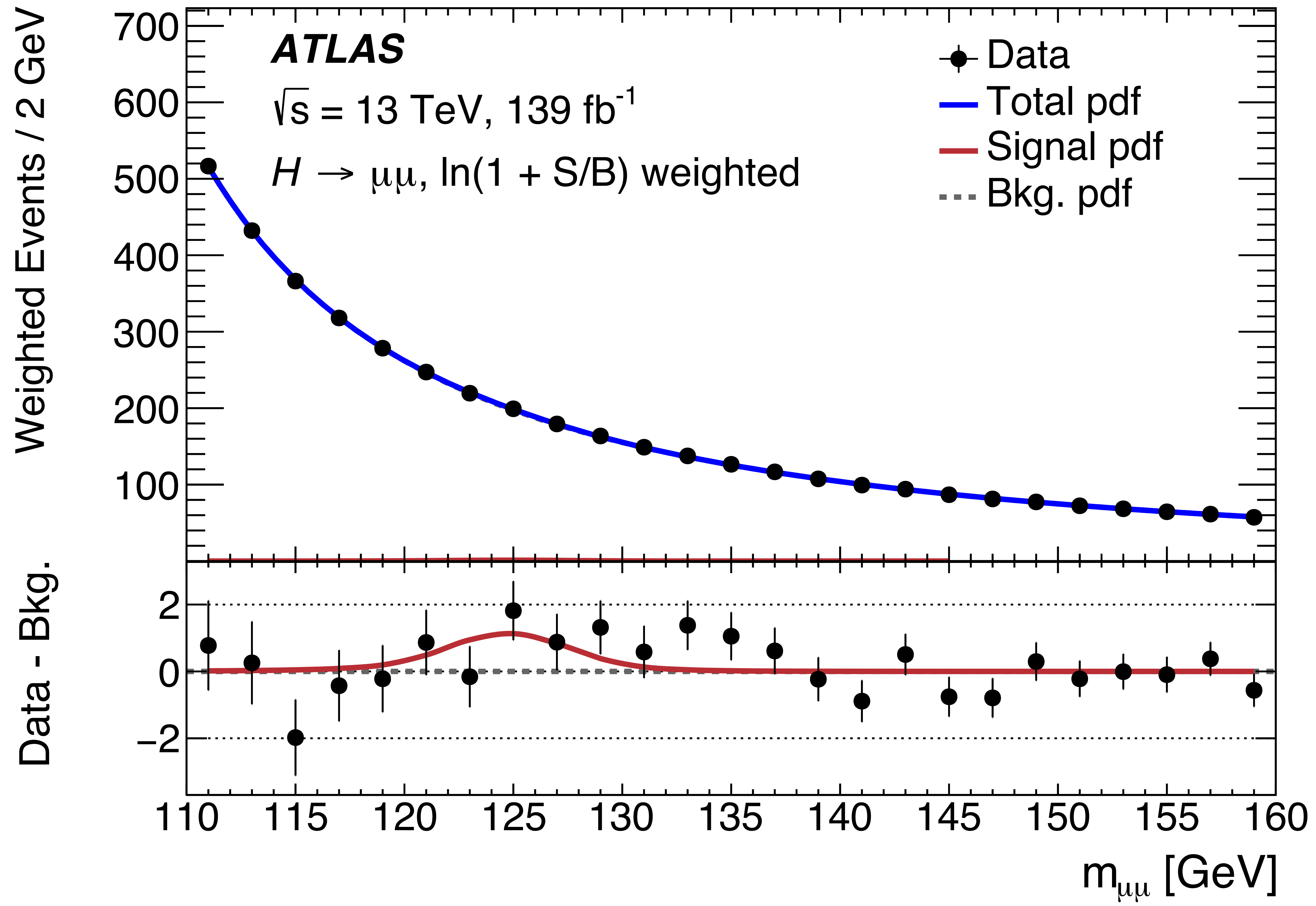

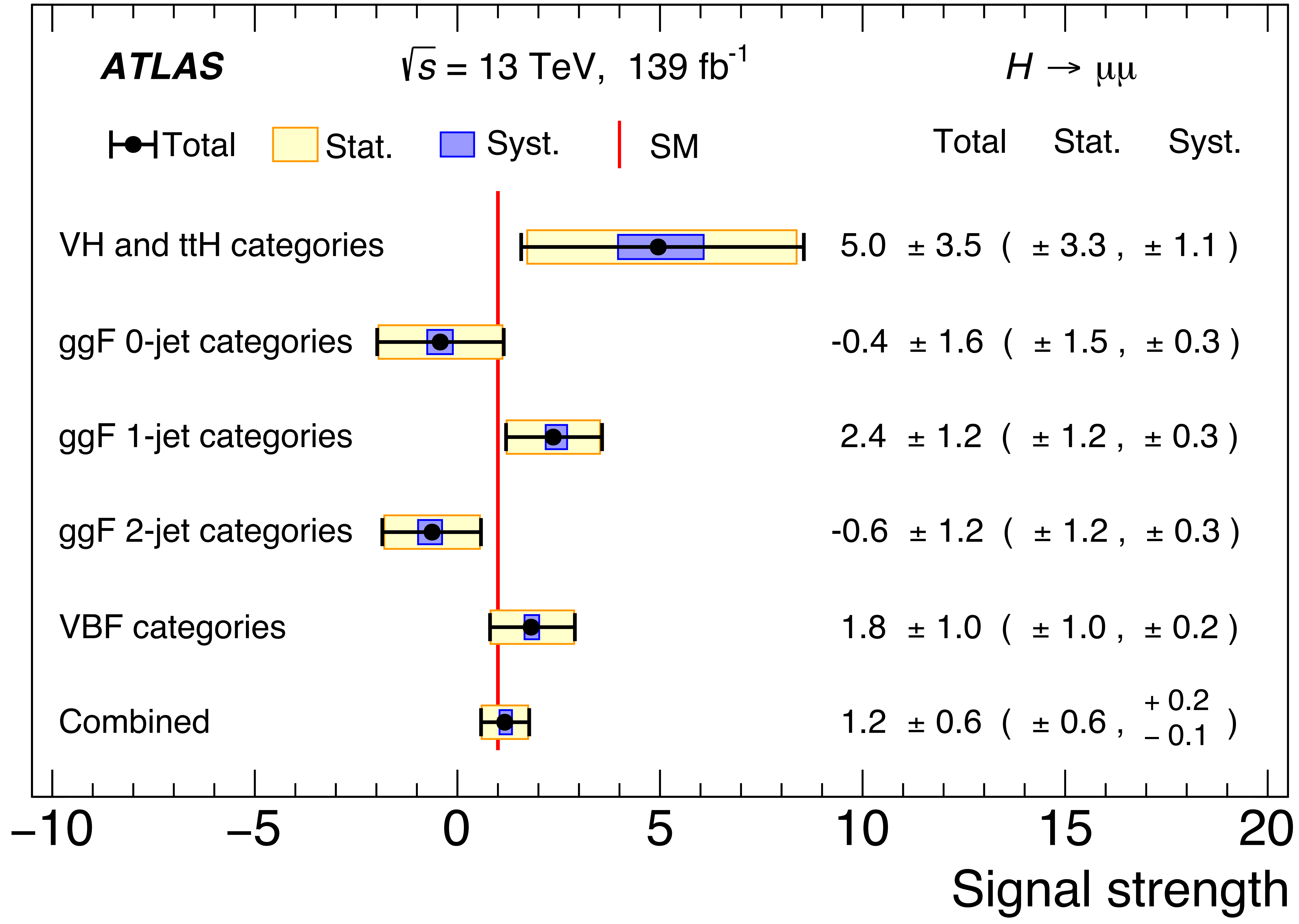

ATLAS vs CMS: results

- Comparison of the final weighted mass distributions as well as fitted signal strength

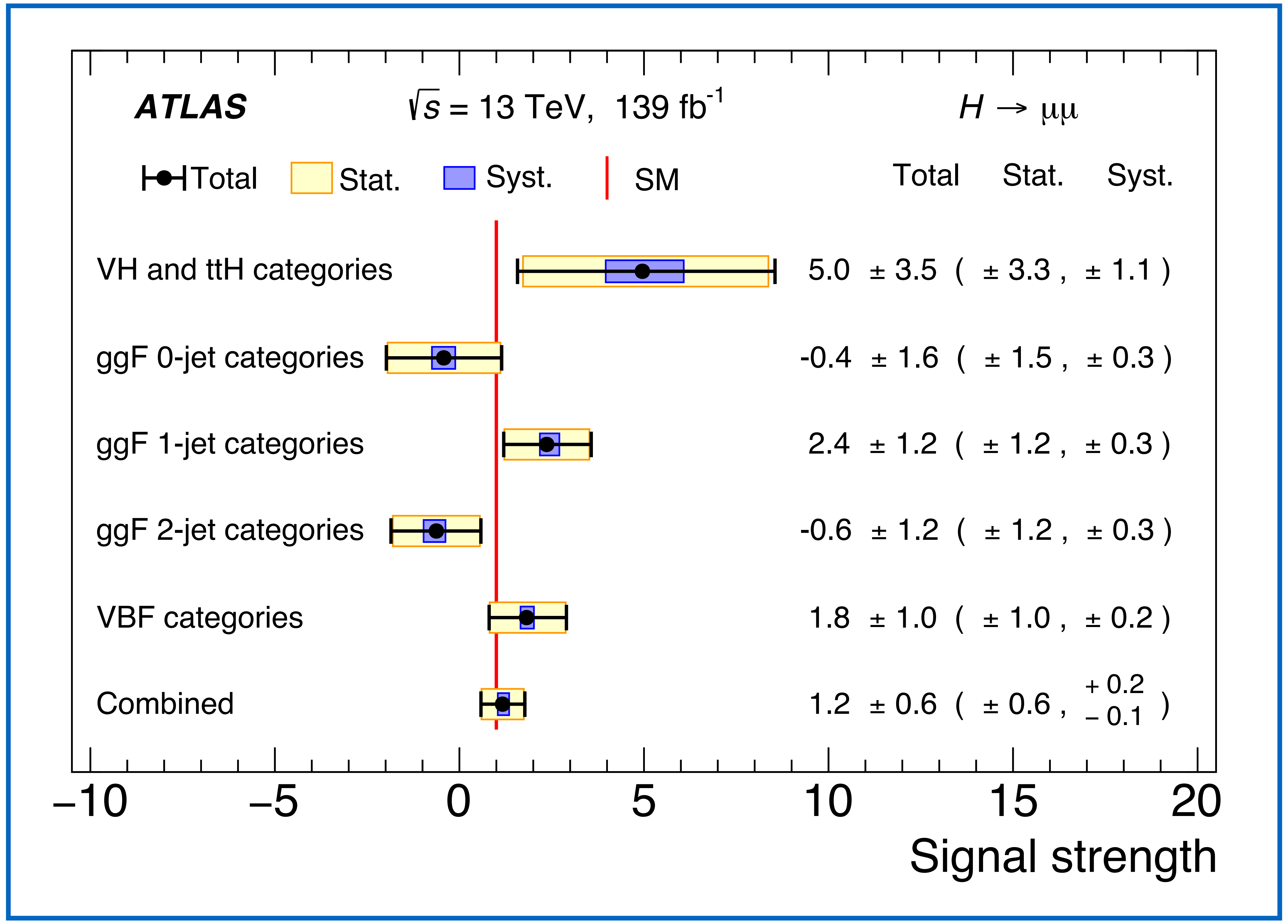

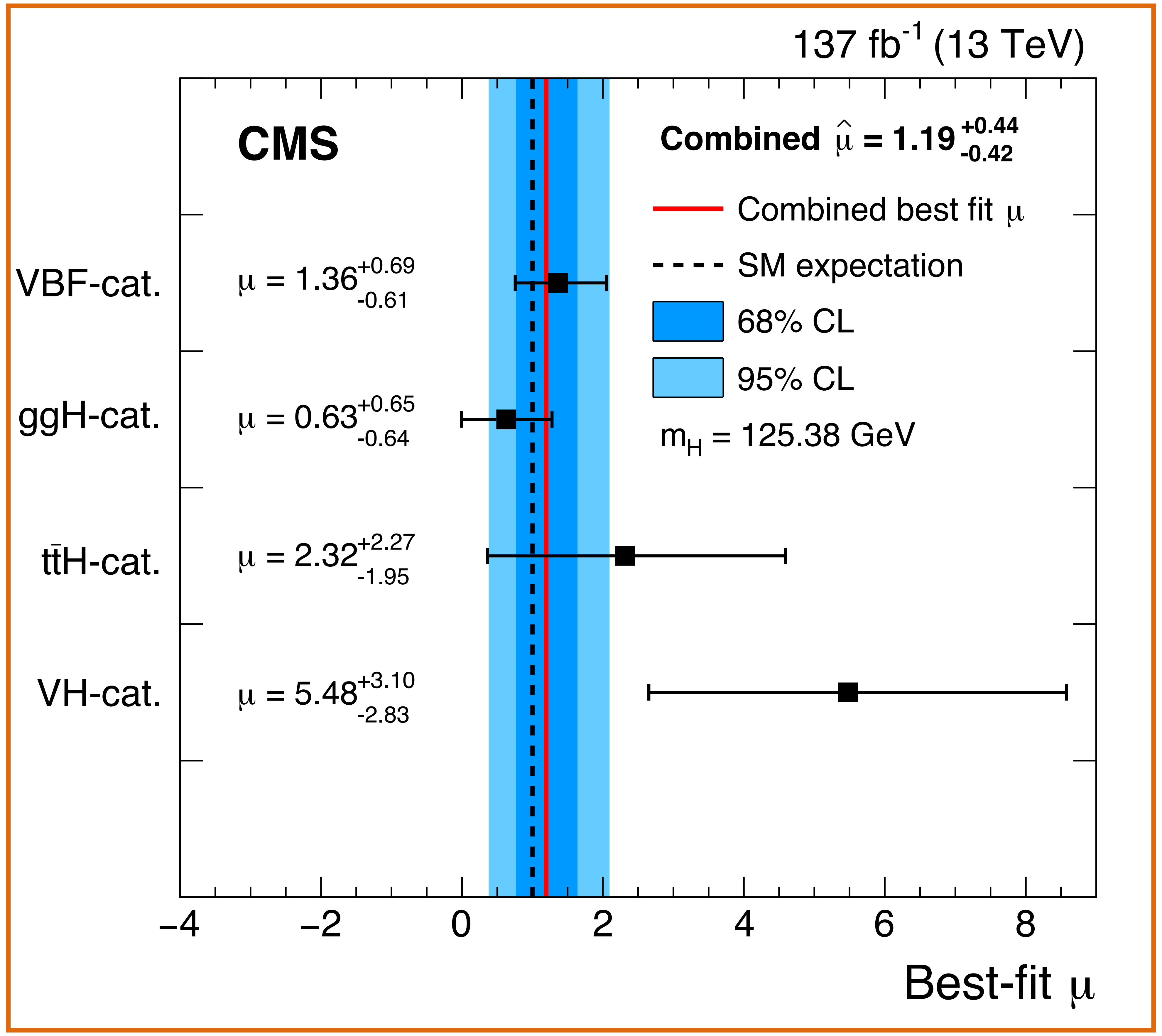

- **ATLAS:** best fit signal strength of 1.2 ± 0.6
- **CMS:** best fit signal strength of 1.19 ± 0.43

ATLAS vs CMS: analysis strategies

Signal prediction

- **ggH simulation:** ATLAS uses NNLOPS, while CMS relies on aMC@NLO reweighed to NNLOP in $p_T(H)$-N_{jet}
- **VBF simulation:** both rely on POWHEG+PYTHIA but CMS uses dipole-shower as in [**arXiv:2003.12435**]

Muon selection

- **Triggers:** both analyses rely on single-muon triggers with similar p_T thresholds but different isolation conditions
  - ATLAS trigger efficiency on $H \to \mu\mu$ events is 91%, CMS one is about 99%
- **FSR recovery:** implemented by both experiments leading to similar gain in m($\mu\mu$) resolution of about 3%
- **Acceptance:** ATLAS (CMS) covers up to $|\eta| < 2.7$ (< 2.4), second muon p_T threshold 15 (20) GeV
- ***Total selection efficiency in the fit region is similar between the two experiments about ~60%***

ttH and VH categories

- In the ttH analysis, ATLAS only targets leptonic final states while CMS has a dedicated ttH-hadronic category
- Thresholds for ***additional leptons*** are looser in ATLAS, while CMS imposes always a 20 GeV cut
- BDT input features are similar between the two experiments

ATLAS vs CMS: analysis strategies

VBF analysis

- In CMS the VBF phase-space defined by selections in m_{jj} and $\Delta\eta_{jj}$, where signal is extracted from a ***fit to a DNN output. Background modelled from simulation.***
- In ATLAS, a ***more "conservative" divide-n-fit*** strategy adopted. Four categories defined along BDT output.
- ***CMS VBF phase-space is more inclusive than the sum of the four categories in ATLAS***

ggH analysis

- In CMS, a ***single BDT*** trained for all events belonging to the ggH category considering several input features
- In ATLAS, ***three dedicated BDT*** trainings for events with $N_{jets} = 0, 1,$ and ≥ 2
- CMS exploits the ***$m_{\mu\mu}$ resolution*** in the training, while ATLAS builds kinematic-only discriminants
- ***Number of categories:*** 5 in CMS and 12 in ATLAS
- ***Fit region:*** 110-150 GeV in CMS, 110-160 GeV in ATLAS
- ***Background model:*** both analyses follow a "core-PDF" method but the technical implementation differs
  - ATLAS selects the bkg. model to be unbiased w.r.t. the MC truth in bias studies
  - CMS selects the bkg. model to be unbiased w.r.t. a variety of analytical functions that can fit the $m_{\mu\mu}$ spectrum